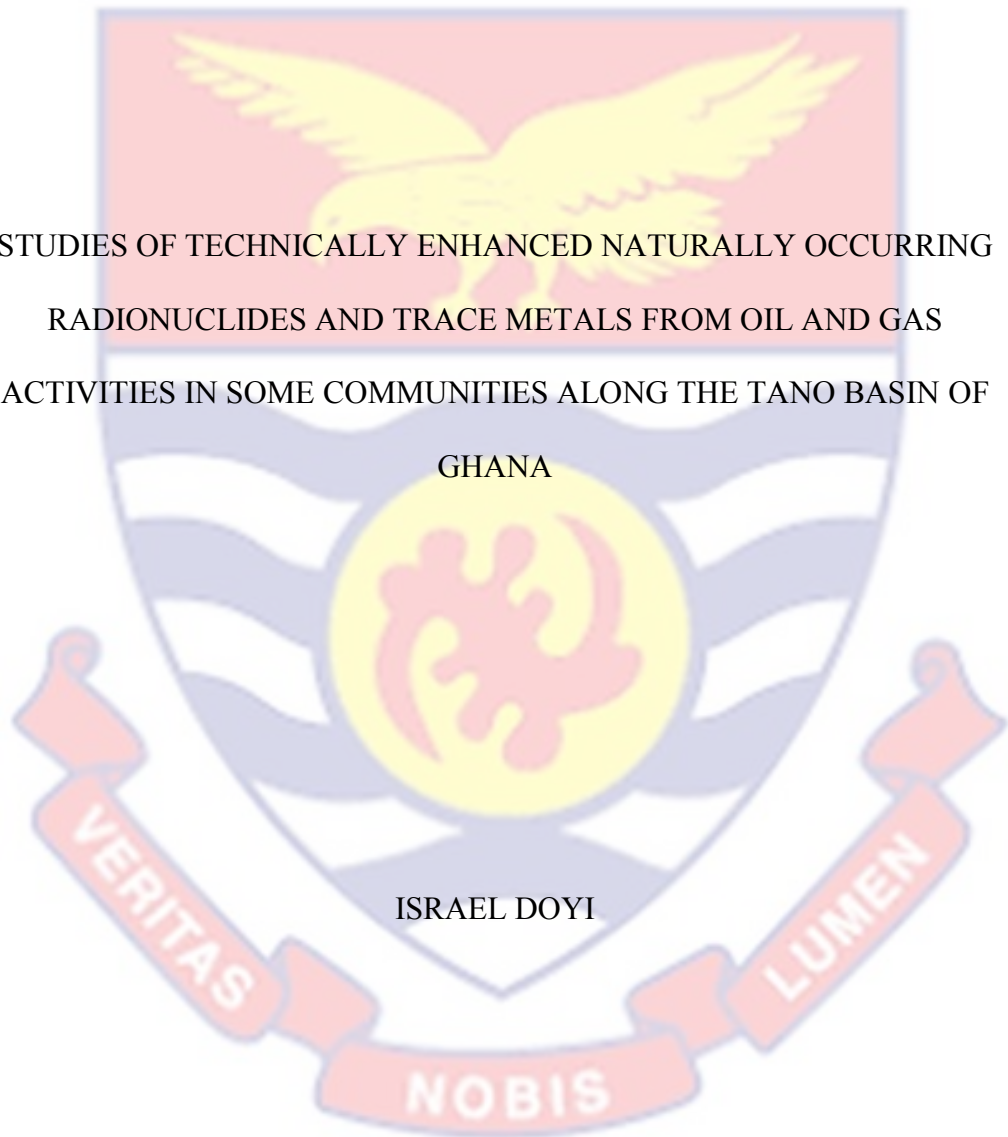UNIVERSITY OF CAPE COAST

STUDIES OF TECHNICALLY ENHANCED NATURALLY OCCURRING

RADIONUCLIDES AND TRACE METALS FROM OIL AND GAS

ACTIVITIES IN SOME COMMUNITIES ALONG THE TANO BASIN OF

GHANA

ISRAEL DOYI

2016

© Israel Doyi

University of Cape Coast

UNIVERSITY OF CAPE COAST

STUDIES OF TECHNICALLY ENHANCED NATURALLY OCCURRING

RADIONUCLIDES AND TRACE METALS FROM OIL AND GAS

ACTIVITIES IN SOME COMMUNITIES ALONG THE TANO BASIN OF
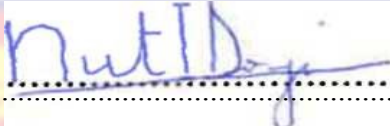
GHANA

BY

ISRAEL DOYI

Thesis submitted to the Department of Chemistry of the School of Physical
Sciences, College of Agriculture and Natural Sciences, University of Cape
Coast, in partial fulfilment of the requirements for the award of Doctor of
Philosophy degree in Chemistry

NOVEMBER 2016

DECLARATION

Candidate's Declaration

I hereby declare that this thesis is the result of my own original research and that no part of it has been presented for another degree in this university or elsewhere.

Candidate's Signature: .... Date: 26-10-2018

Name: Israel Doyi

Supervisors' Declaration

We hereby declare that the preparation and presentation of the thesis were supervised in accordance with the guidelines on supervision of thesis laid down by the University of Cape Coast.

Principal Supervisor's Signature: .... Date: ....

Name: Prof. David Kofi Essumang

Co-Supervisor's Signature: .... Date: ....

Name: Prof. Samuel Boakye Dampare

ABSTRACT

The objective of this study is to determine the background data for the levels of gamma radiation in soil, groundwater sources and food in the communities along the Tano Basin, an oil field in Ghana. The mean activity concentrations measured for ^{238}U, ^{232}Th and ^{40}K in soil samples are 8.65 Bq/kg, 12.51 Bq/kg and 214.11 Bq/kg respectively. The activity concentrations of ^{226}Ra, ^{228}Ra, and ^{40}K in the water obtained were in the range of 0.14±0.01 to 1.38±0.22 Bq/L, 0.18±0.01 to 1.41±0.18 Bq/L and 0.46±0.02 to 5.92±0.10 Bq/L respectively. The total annual effective dose to the public was estimated to be 35.34 µSv per year. Absorbed dose rate, annual effective dose, hazard indices (H_{ex} and H_{in}) were calculated. The absorbed dose rates and annual effective dose were determined and found to be in the range of 7.79 to 37.79 nGyh^{-1} and 9.56 x10^0 to 4.64 x10^1 µSvy-1 respectively. The total annual effective dose were lower than allowable limit set by International Commission on Radiological Protection (ICRP) 1mSvy$^{-1.}$ Hazard indices (H_{ex} and H_{in}) were 0.04 to 0.22 and 0.05 to 0.25 respectively whilst excess lifetime cancer risk (ELCR) were calculated to be in the range 3.35 x 10-5 to 1.62 x10^{-4} and found to be within internationally recommended values. The concentration of metals in soil were in the order Fe > Zn > Cd > Mn > Pb > Ni. The estimated carcinogenic risk to the public from exposure to the metals in soil varies from 3.9 x10^{-9} for Ni to 1.04 x10^{-6} for Cd. The average activity concentrations are 0.70, 52 and 25.63 Bq/kq respectively for ^{238}U, ^{232}Th and ^{40}K in cassava samples. The estimated transfer factors for ^{238}U, ^{232}Th, and ^{40}K are in the range 0.017 – 0.553, 0.003 – 0.078 and 0.019 – 0.057 respectively. The mean transfer factors (TF) are 0.271 (^{238}U), 0.028 (^{232}Th) and 0.033 (^{40}K).

KEY WORDS

Environmental health

Environmental radioactivity

Public health

Radionuclides

Toxicology

Trace metals

ACKNOWLEDGEMENTS

I wish to express my sincere thanks to the almighty God for seeing me through another chapter of my educational ladder.
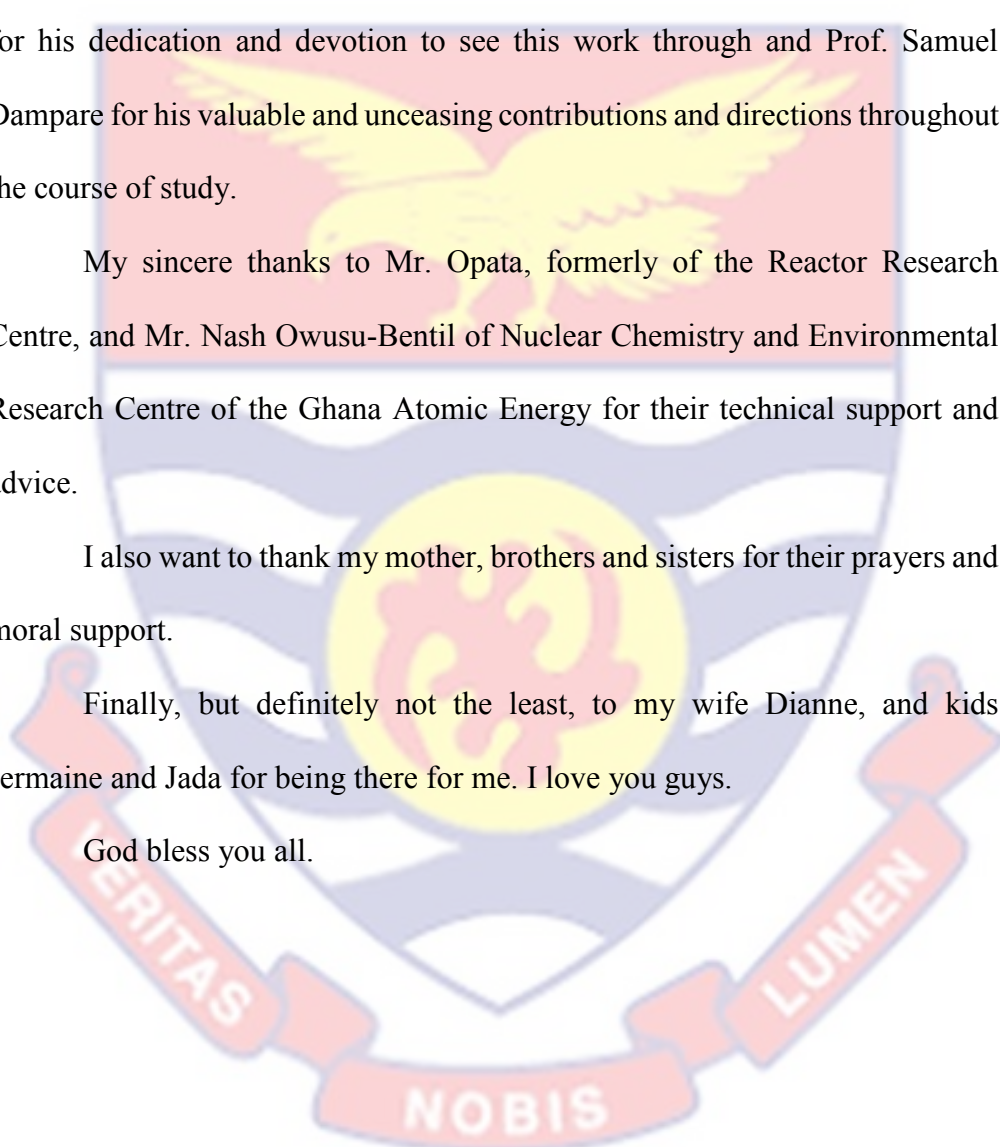
My greatest appreciation also goes to my supervisors, Prof. David Kofi Essumang, who bent backwards in helping actualize this long cherished dream, for his dedication and devotion to see this work through and Prof. Samuel Dampare for his valuable and unceasing contributions and directions throughout the course of study.

My sincere thanks to Mr. Opata, formerly of the Reactor Research Centre, and Mr. Nash Owusu-Bentil of Nuclear Chemistry and Environmental Research Centre of the Ghana Atomic Energy for their technical support and advice.

I also want to thank my mother, brothers and sisters for their prayers and moral support.

Finally, but definitely not the least, to my wife Dianne, and kids Jermaine and Jada for being there for me. I love you guys.

God bless you all.

DEDICATION

Dedicated to my father Mr. Henry Kwame "Emperor" Adjagely-Doyi.

TABLE OF CONTENTS

CHAPTER TWO: LITERATURE REVIEW

LIST OF TABLES

xiv

LIST OF FIGURES

xix

LIST OF ACRONYMS

2-D	–	Two dimensional
3-D	–	Three dimensional
AAS	–	Atomic Absorption Spectroscopy
ABSd	–	Dermal Absorption Factor
AF	–	Adherence Factor
ALARA	–	As low as Reasonably Achievable
ANL	–	Argonne National Laboratory
ANOVA	–	Analysis of Variance
AT	–	Averaging time
ATSDR	–	Agency for Toxic Substances and Disease Registry
BEIR	–	Biological Effects of Ionizing Radiation
BSS	–	Basic Safety Standards
BW	–	Body Weight
C	–	Concentration of Heavy Metals
CA	–	Cluster Analysis
CDI	–	Chronic Daily Intake
CGG	–	Compayne Generale de Geophysique
CN	–	Channel Number
CRPC	–	Canadian Radiation Protection Committee
CSF	–	Chronic Slope Factor
DDREF	–	Dose and Dose Rate Effectiveness Factor
DFS	–	Dermal Soil Contact Factor
DGNAA	–	Delayed Gamma-ray Neutron Activation Analysis
DNA	–	Deoxyribonucleic Acid

ED	–	Exposure Duration
EF	–	Exposure Frequency
EPA	–	Environmental Protection Agency
ED	–	Effective Dose
ET	–	Exposure Time
GHARR-1	–	Ghana Research Reactor 1
HCl	–	Hydrochloric acid
HF	–	Hydrofluoric acid
HI	–	Hazard index
HNO_3	–	Trioxonitrate (V) acid
HPGe	–	High Purity Germanium
HQ	–	Hazard quotient
IAEA	–	International Atomic Energy Agency
ICRP	–	International Commission on Radiological Protection
INAA	–	Instrumental Neutron Activation Analysis
IngR	–	Ingestion Rate
LET	–	Linear Energy Transfer
LOD	–	Limit of Detection
LT	–	Lifetime
MANOVA	–	Multivariate Analysis of Variance
MCA	–	Multi-channel Analyser
MCLG	–	Maximum Containment Level Goal
MDA	–	Minimum Detectable Activity
NAA	–	Neutron Activation Analysis
NORM	–	Naturally Occurring Radioactive Material

NRC	–	Nuclear Regulatory Commission
PCA	–	Principal Component Analysis
PEF	–	Particulate Emission Factor
PGNAA	–	Prompt Gamma-ray Neutron Activation Analysis
pH	–	Power of Hydrogen
QA/QC	–	Quality control/Quality assurance
RfD	–	Chronic Reference Dose
SA	–	Skin Surface Area
SI	–	Standard Internationale
SPSS	–	Statistical Package for the Social Sciences
SSDL	–	Secondary Standard Dosimetry Laboratory
TDS	–	Total Dissolved Solids
TENORM	–	Technologically Enhanced Naturally Occurring Radioactive Material
UNSCEAR	–	United Nations Scientific Committee on the Effects of Atomic Radiation
US	–	United States
USA	–	United States of America
USEPA	–	United States Environmental Protection Agency
USNRC	–	United States Nuclear Regulatory Commission
WIMPS	–	Weakly Interacting Massive Particles
WL	–	Working Level
WLM	–	Working Level Month

RADIONUCLIDES

^{138}La – lanthanum 138

^{142}Ce – cesium 142

^{147}Sm – samarium 147

^{176}Lu – lutenium 176

^{206}Pb – lead 206

^{207}Pb – lead 207

^{208}Tl – thallium 208

^{210}Pb – lead 210

^{210}Po – polonium 210

^{212}Pb – lead 212

^{214}Bi – bismuth 214

^{214}Pb – lead 214

^{214}Po – polonium 214

^{218}Po – polonium 218

^{219}Rn – radon 219

^{220}Rn – radon 220

^{222}Rn – radon 222

^{224}Ra – radium 224

^{224}Th – thorium 224

^{226}Ra – radium 226

^{226}Th – thorium 226

^{227}Th – thorium 227

^{228}Ac – actinium 228

^{228}Ra – radium 228
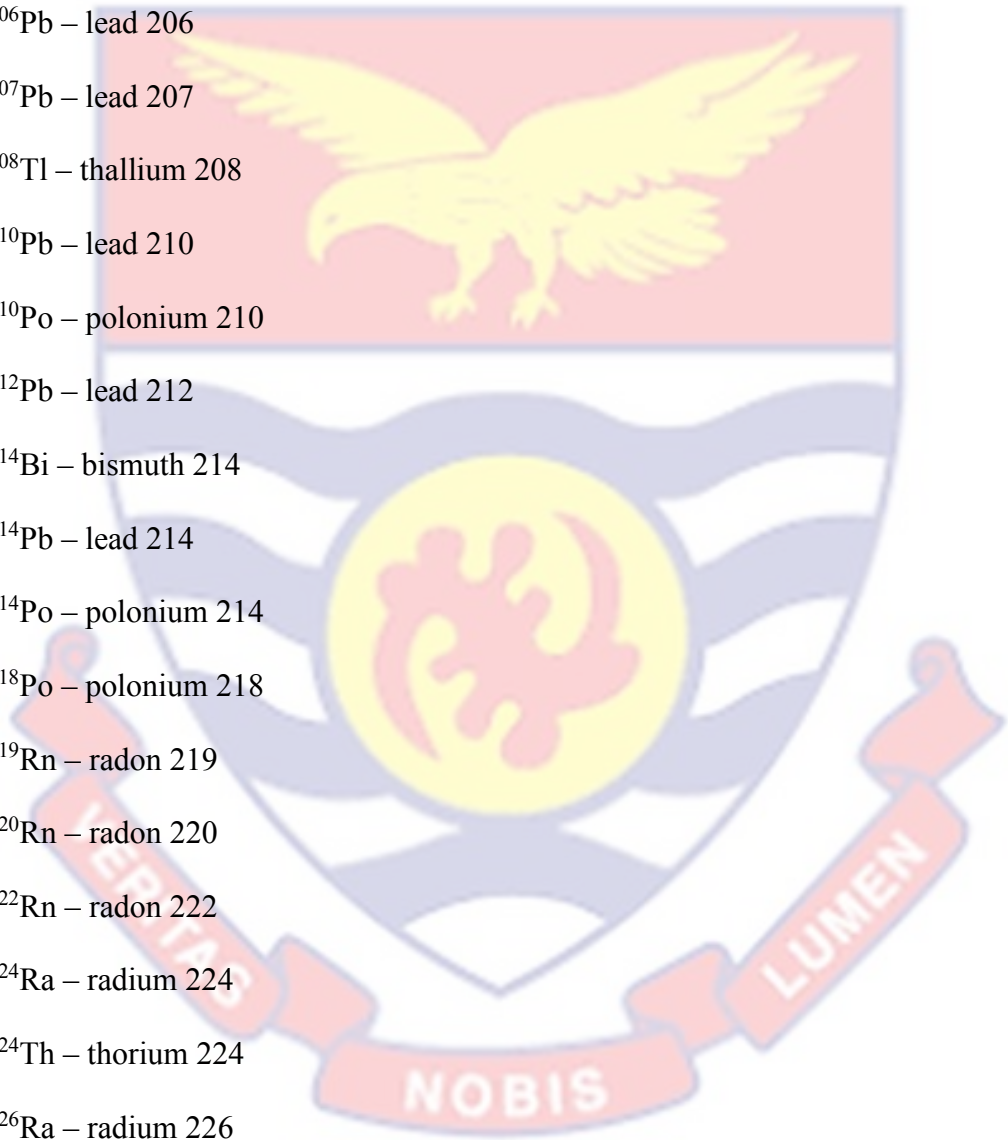
^{228}Th – thorium 228

^{229}Th – thorium 229

^{230}Th – thorium 230

^{231}Pa – protactinium 231

^{231}Th – thorium 231

^{232}Th – thorium 232

^{233}Th – thorium 233

^{234}Pa – protactinium 234

^{234}U – uranium 234

^{235}U – uranium 235

^{238}U – uranium 238

^{40}K – potassium 40

^{87}Pb – lead 87
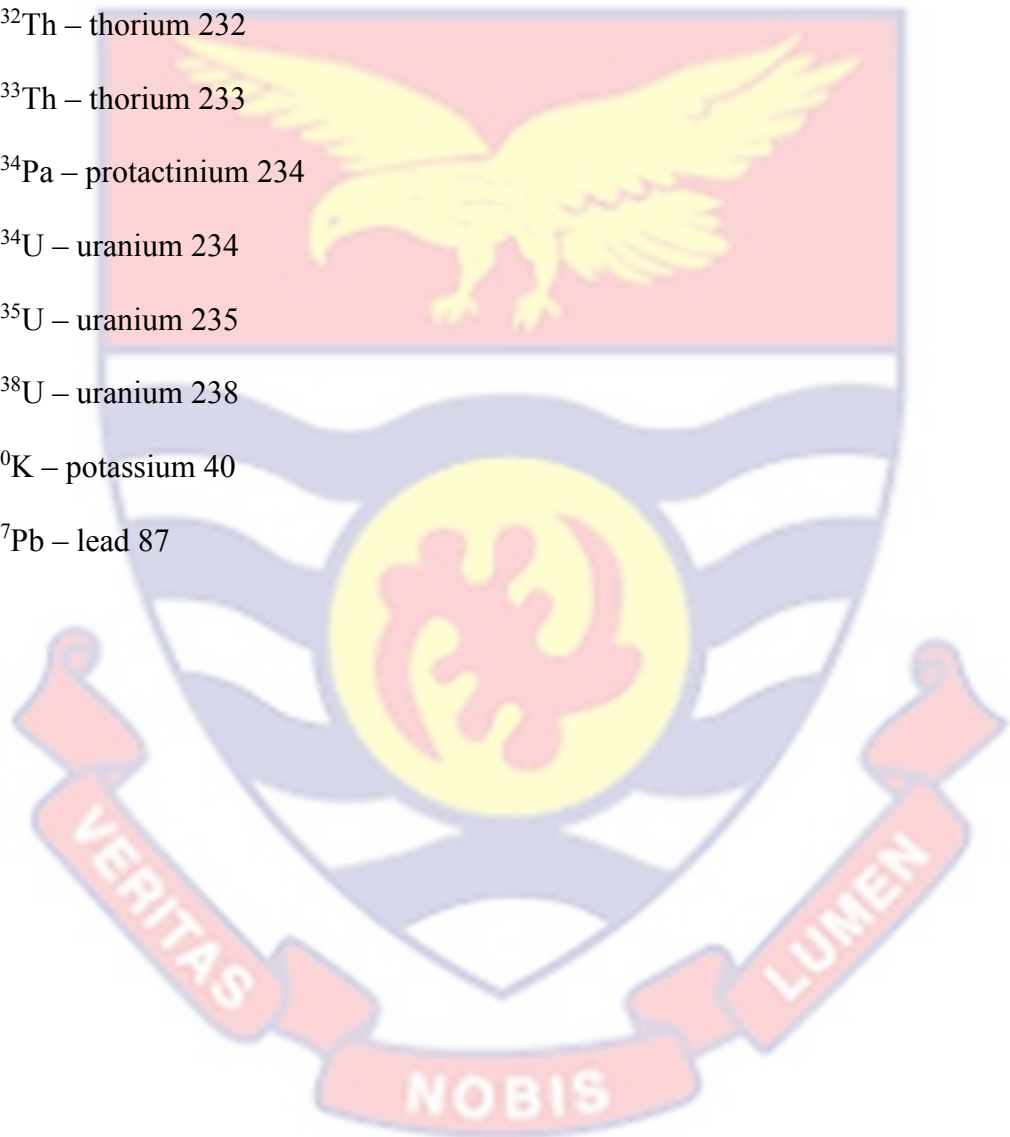
CHAPTER ONE

INTRODUCTION

Based on the knowledge that soil accumulates persistent anthropogenic environmental contaminants, this research was designed to estimate the contamination load, and establish the background pollutant distribution in soil and groundwater. The selected communities were chosen based on their likelihood of being impacted from improper disposal of drilling waste, accidental oil spills, gas flaring and other unforeseen and inadvertent events. Emphasis is placed on radionuclides (^{238}U, ^{232}Th, ^{40}K in soil and ^{226}Ra, ^{228}Ra, ^{40}K in groundwater) and potentially toxic trace metals (As, Cd, Cu, Fe, Mn, Ni, Pb and Zn) as specified in the ATSDR Substance Priority List (ATSDR, 2011). The study aims to profile the contaminants for future referencing on how oil drilling activities have impacted the unit-source industrial area using environmental, nuclear and chemical analytical techniques and statistical analysis. This chapter is a background presentation to the study and environmental contaminants of concern.

Background to the Study

Radiation is part of the natural environment: it is estimated that approximately 80% of all human exposure comes from naturally occurring or background radiation. Certain extractive industries such as mining and oil logging have the potential to increase the risk of radiation exposure to the environment and humans by concentrating the quantities of naturally occurring radiation beyond normal background levels (Azeri, Chirac & Gunashili, 2004).

The International Atomic Energy Agency (IAEA) defines naturally occurring radioactive material (NORM) as a "radioactive material containing

1

no significant amounts of radionuclides other than naturally occurring radionuclides" and includes "materials in which the activity concentrations of the naturally occurring radionuclides have been changed by a process" (IAEA, 2007).

NORMs primarily from the ^{238}U and ^{232}Th series and ^{40}K, is present in the environment: in soils, air and water (Rector, Allard, Jones, Hylard, Lopez, Mitchell, Nickel et al., 2011), geological formations (Peroni, Mulas, Betti, Patata & Ambrosini, 2012) and as a result, exposure to natural sources of radiation is responsible for majority of the total radiation dose received by people every year (Colgan, Organo, Hone & Fenton, 2008)

When these NORMs become concentrated in radionuclides due to human activity, they are referred to as technologically enhance naturally occurring radioactive materials (TENORMs). TENORM waste is produced from several industries such as uranium and metal mining, phosphate ore processing and petroleum industry (Egidi & Hull, 1999).

In the petroleum industry, NORM such as the ones from the ^{232}Th series, as well as ^{40}K are often enhanced as a result of industrial operations, these materials are formally referred to as Technologically Enhanced Naturally Occurring Radioactive Materials (TENORM). (Hrichi, Baccoube & Belgaied, 2013). Being relatively insoluble, both uranium and thorium will not be leached and will remain in the oil formation. In contrast, radium is more soluble, and under certain physical and chemical conditions will be leached from the petroleum reservoir rocks to the formation water, which is present together with the oil in the reservoir (Rajaretnam & Spitz, 2000; Shawky, Amer, Nada, El-Maksoud & Ibraheim, 2001). As oil is pumped to the surface, water will also

come along with it. The produced water extracted with the petroleum contains dissolved mineral salts, some of which may be radioactive, because of the presence of ^{226}Ra and ^{228}Ra and their decay products.

The amount of NORM in an oil-producing field generally increases as the amount of produced water pumped with the oil increases. Radium, the predominant radionuclide brought to the surface with the crude oil and produced water, can either stay in solution in the produced water or co-precipitate with barium in the form of complex compounds of sulfates, carbonates, and silicates found in sludge and scale (Gazineu, de Araujo, Brandao, Hazin & Godoy, 2005). The formation of these hard, very insoluble precipitates is caused by changes in pressure and temperature as the oil/water mixture is pumped to the surface, the amount of precipitate being dependent on the physical-chemical characteristics of the water (Testa, Desideri, Guerra, Meli, Rosselli, Bassignani, Colombo et al., 1994; Rajaretnam & Spitz, 2000).

Scale and sludge, which are the main petroleum wastes are produced by two mechanisms: either incorporation or precipitation onto the production equipment such as pipelines, storage tanks etc. (El Afifi & Awwad, 2005).

The precipitated TENORM wastes around walls of the petroleum pipes reduce the efficiency with which they transport petroleum products and they are then disposed and replaced by new ones periodically (El Afifi, Awwad & Hilal, 2009: Somlai, Jobbagy, Somlai, Kovacs, Nemeth & Kovacs, 2008).

Formation water is another petroleum waste that contains the radium isotopes ^{226}Ra from the ^{238}U series and ^{228}Ra and ^{224}Ra from the ^{232}Th series. All three radium isotopes, but not their parents, thus appear in the formation water co-produced with oil or gas (Zaidan, 2010). Zaidan, 2010 further stated

3

that this causes their precipitation as sulphate and carbonate scales. The mixed stream of oil and water carries the noble gas ^{222}Rn that is generated in the reservoir rock through decay of ^{226}Ra. It appears that the concentrations of ^{226}Ra, ^{228}Ra, and ^{224}Ra in scales and sludge range from less than 0.1Bq/g to 1500Bq/g. The deposition of contaminated scales and sludge in pipes and vessels may produce significant dose rates inside and outside these components.

According to Rood (1998), attention was not given to the health impacts from the uncontrolled release of naturally occurring radioactive wastes which concentrate and accumulate in tubing and surface equipment in the form of scale and sludge.

Abo-Elmagd, Soliman, Salman & El-Masry, (2010) thus concluded that the knowledge of radioactive content and basic radiological parameters in the TENORM waste is very important for purposes of nuclear waste management projects such as:

-setting up the treatment methods for TENORM wastes

-promote the development and/or update of databases on hazardous substances/wastes

-propagate full understanding of nuclear waste status to develop an appropriate action plan for their management.

Geological Setting of Study Area

The Jubilee field discovered in June 2007 is located in the Gulf of Guinea, 60km off the Ghanaian coast. The wells are at a water depth between 1100 and 1300 meters and at a total depth between 3400 and 4200 meters. The field covers 110 km^2, which is about the size of 155 football pitches (Offshore-Technology.com, 2011). In geographical terms, the Jubilee field is a continuous

4

trap with combined hydrocarbon columns in excess of 600 meters (Kastning, 2011).

The West African Transform Margin hosts a series of deeply in-filled sedimentary basins, Tano Basin being one of the most prospective, which is a major part of the Jubilee oil field. In this region, basin formation was as a consequence of the Atlantic rift system which was initiated in the Late Jurassic as the paleo-continents of Southern America and Africa began to break up (CGG, 2012). Continental rifting propagated northwards from the South Atlantic, forming a continuous anoxic seaway in the West African Transform Margin between the Late Albian to Turonian. This led to the deposition and preservation of organic matter which now form the Basin's lacustrine Upper Albian, Cenomanian and Turonian source rocks (CGG, 2012). In the Upper Cretaceous, the Tano Basin became a depositional focus and a thick clastic sequence consisting of fluvial and lacustrine facies. The sequence, in addition to the thin Tertiary section, provided adequate thickness to mature the Cretaceous source rocks in the central and western region of the Tano Basin. Stratigraphically trapped Albian and Cenomanian turbidite sand-stones, from the thick clastic sequence act as the main reservoir within the basin, while marine shales form a seal. As reservoir rocks are predicted to be in close proximity to the source rocks, a minimal hydrocarbon migration pathway is assumed (CGG, 2012). The present study was undertaken in the coastal communities along the Jubilee oil field, Ghana.

5
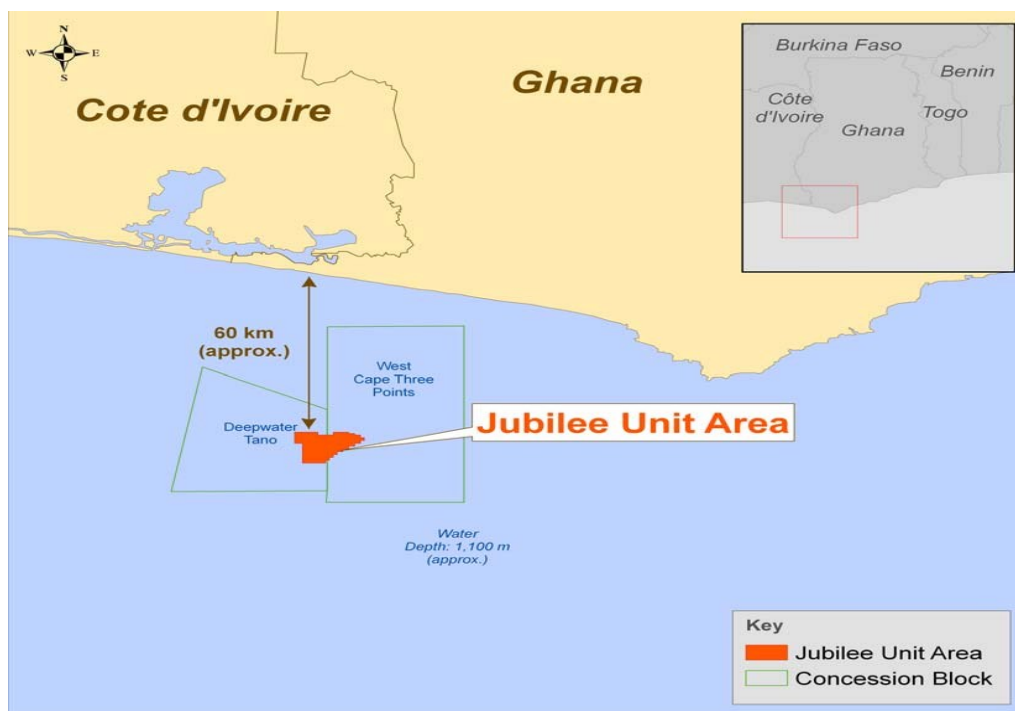
Figure 1: Location of the Jubilee Field, Unit Area.
Tullow Ghana Limited, 2009.

Natural Decay Series

Uranium, radium and thorium occur in three natural decay series, headed by U-238, Th-232 and U-235. In nature the radionuclides in these 3 decay series are approximately in a state of secular equilibrium; in which the activities of all radionuclides within each series are nearly equal. The radionuclides of the uranium-238, thorium-232, and uranium-235 decay series are shown in Tables 2-3, 2-4 and 2-5 (Chapter 2), along with the major mode of radioactive decay for each. Radioactive decay occurs when an unstable (radioactive) isotope transforms to a more stable isotope, generally by emitting a subatomic particle such as an alpha or beta particle. Radionuclides that give rise to alpha and beta particles are shown in these tables, as are those that emit significant gamma radiation.

Gamma radiation is not a mode of radioactive decay (such as alpha and beta decay). Rather, it is a mechanism by which excess energy is emitted from

6

certain radionuclides, i.e., as highly energetic electromagnetic radiation emitted from the nucleus of the atom (ANL, 2005)

Uranium

Uranium of natural isotopic composition consists of three isotopes ^{238}U, ^{235}U and ^{234}U, all of them being radioactive. ^{238}U is an alpha emitter, decaying through the 18-member uranium natural decay series into ^{206}Pb. ^{235}U has a 15 member decay series (the actinouranium series) that decays into ^{207}Pb. This series includes only two long lived (> several days) radioactive members, namely, ^{231}Pa (t½ = 3.28 days) and Ac (t½ = 21.77 days) (Zavodska, Kosorinova, Scerbakova & Jujaj, 2008).

^{234}U occurs as an indirect decay product of ^{238}U. Uranium is a heavy, silvery-white, ductile, weakly radioactive, strongly electropositive and slightly paramagnetic metal exhibiting poor electrical conductivity with an atomic number of 92.

Uranium is a very reactive element readily combining with many elements to form a variety of complexes. The oxygen containing uranium compounds as well as the uranyl ion can combine easily with Cl⁻, Na_3^-, SO_4^{2-} and CO_3^{2-}. Uranium is notorious for its radiological hazard but its chemical toxicity should not be ignored. In general, only dissolved uranium is chemically toxic (Priest, 2001).

Table 1: Decay scheme of Uranium-238

SYMBOL	NUCLIDE	PRINCIPAL MODE OF DECAY	HALF-LIFE	DECAY PRODUCT
U-238	Uranium-218	A	4.46×10^7 yrs	Th-234
Th-234	Thorium-234	B	24.1 days	Pa-234
Pa-234	Proctatinium-234	B	1.17 minutes	U-234
U-234	Uranium-234	A	2.47×10^3 yrs	Th-230
Th-230	Thorium-230	A	8×10^4 years	Ra-226
Ra-226	Radium-226	A	1,602 years	Rn-222
Rn-222	Radon-222	A	3.82 days	Po-218
Po-218	Polonium-218	A	3.05 minutes	Pb-214
Pb-214	Lead-214	B	27 minutes	Bi-214
Bi-214	Bismuth-214	B	19.7 minutes	Po-214
Po-214	Polonium-214	A	1 microsecond	Pb-210
Pb-210	Lead-210	B	22.3 years	Bi-210
Bi-210	Bismuth-210	B	5.01 days	Po-210
Po-210	Polonium-210	B	138.4 days	Pb-206
Pb-206	Lead-206	None	Stable	None

Table 2: Uranium-235 decay scheme

NUCLIDE	PRINCIPAL MODE OF DECAY	HALF-LIFE
Uranium-235	A	7.04×10^8 years
Thorium-231	B	25.5 hours
Proctactnium-231	A	3.25×10^4 years
Actinium-227	B	21.8 years
Thorium-227	A	18.7 days
Radium-223	A	11.4 days
Radon-219	A	3.96 seconds
Polonium-215	A	1.78×10^{-3} seconds
Lead-211	B	36.1 minutes
Bismuth-211	B	2.15 minutes
Polonium-211	A	0.516 seconds
Lead-207	Stable	Stable

Properties of uranium in respect of environmental protection

Environmental uranium is a mixture of three natural isotopes, ^{238}U (99.276%) with $t_{1/2} = 4.5 \times 10^9$ years, ^{235}U (0.718%) having $t_{1/2} = 7.1 \times 10^8$ years and ^{234}U (0.004%) with $t_{1/2} = 2.5 \times 10^5$ years. Uranium is naturally occurring, ubiquitous, lithophilic metal found in various chemical forms including abiotic and biotic environmental forms such as soils, rocks, seas, oceans and microorganisms (Greenwood & Earnshaw, 1984). The dominant uranium valence states that are stable in geologic environments are uraneous (U^{4+}) and uranyl (U^{6+}) states with uranyl being more soluble than the uraneous (NRC,

8

1999). It is further indicated that the transport of uranium occurs generally in oxidizing water and ground water as uranyl ion (UO_2^{2+}) or as uranyl fluoride, phosphate or carbonate complexes. Maximum sorption of uranyl ions on natural materials occurs at pH 5.0 − 8.5. For uranium to be fixed, and thereby accumulate, it requires reduction to U^{4+} by the substrate or by a mobile phase such as H_2S (NRC, 1999).

Uranyl species are less prone to hydrolysis than U^{4+} and consequently colloids play a less significant role in the near surface transport of uranium than thorium. Uranium sulphate and carbonate complexes are soluble and migrate with the groundwater. U^{6+} can be complexed by humic acids associated with peat under acidic to alkaline pH conditions. This may retard U^{6+} migration by adsorption of the complex U^{6+} humic acid onto aquifer material. According to Blantz, Pelayo, Gushwa, Myers & Evan, (1985), investigations of uranium mine waters resulted in knowledge that uranium speciation strongly depends on their pH values. It thus found the following uranium species $Ca_2UO_2(CO_3)_{(aq)}$ at pH 7.1 in carbonate and Ca containing mine water, $UO(CO_3)_3^{4-}$ at pH = 9.8 in carbonate containing and Ca-poor tailing water, $UO_2SO_{4(aq)}$ at pH 2.6 in sulphate-rich mine water.

Radium

Radium is a naturally occurring silvery-white radioactive metal with several isotopes. Radium is an alkali earth metal and occurs in nature only in the +2 oxidation state (divalent cation). Radium is formed when uranium and thorium break down in the environment. Uranium and thorium are formed in small quantities in most rocks and soil. Ra-226 and Ra-228 are the most abundant and longest lived naturally occurring isotopes of Ra. Ra-226 belongs

to the uranium-238 decay series and has a half-life of 1600 years and decays by alpha particle emission to radon-222. Ra-228 belongs to the thorium-232 decay series and has a half-life of 5.75 years, and decays by beta-particle emission (WQA, 2005).

Ingestion of radium is of primary concern as it may cause cancer, kidney damage and birth defects. The US-EPA has set a Maximum Containment Level Goal (MCLG) of zero and a Maximum Containment Level (MCL) of 5 picocuries per litre (pCi/L) for radium

The presence of Ra and Rn in ground water implies the presence of U- and/or Th-bearing minerals within the aquifer. Radium in surface water may be absorbed by plant and may concentrate in aquatic organ isms which consume them. Additionally, surface water radium may undergo various transformations, deposit and migrate in bottom sediments and be incorporated by living organisms, thereby entering the food chain (Atwood, 2013). The transport of radium in waste water depends on the physiochemical forms of radium, the composition of the water, and on the hydrodynamic conditions of the waste water stream. The available information on the physiochemical forms of radium in waste waters is rather limited. It is assumed that the Ra^{2+} ion will be the prevailing dissolved form of radium, except in waste waters containing significant concentration of sulphates, carbonates and some chelating agents. The formation of a solid phase consisting mostly of an insoluble compound of radium is impossible at the concentrations of radium typical of waste waters (Atwood, 2013). However, radium can be co-precipitated with several solids present in waste water such as barium sulphate calcium sulphate and carbonate.

There are two basic forms of radium migration in surface waters: migration in solution and migration in suspended solids (Atwood, 2013).

Radium migrates as a cation competing with other alkaline earth cations for sorption sites in soil systems. Mitchel, Perez –Sanchez & Thorne, (2013) referred to studies by EPA , (2004) which showed that the relative affinity of radium with other elements for ion exchange on clay minerals has been described as $Ra^{2+} > Ba^{2+} > Sr^{2+} > Ca^{2+} > Mg^{2+}$. The EPA, (2004) further reported that radium is readily absorbed to clays and mineral oxides present in soils, especially at pH 7 and above.

Thorium

Thorium is a naturally occurring radioactive element which is a member of the actinide series. Thorium is composed of 27 different isotopes with the common ones being ^{224}Th, ^{226}Th, ^{227}Th, ^{228}Th, ^{229}Th, ^{230}Th, ^{231}Th, ^{232}Th, ^{233}Th, and ^{234}Th (Mahmood & Mohamed, 2010). Although thorium has six naturally occurring isotopes, only ^{232}Th is relatively stable with a half-life of 14.05×10^9 years.

Intake of thorium isotopes by humans occurs mainly through water, cereals, vegetables and animal products. Thorium is widely distributed in small amounts, with an average lithospheric concentration of 8-12 mgg^{-1} in the earth's crust (with an average concentration of 6mgg^{-1} in soil). This is about two or three times as high as the concentration of uranium in the earth's crust. However, thorium is not as soluble as uranium and thus is not mobile as it in the chemical environment, but does move by mechanical processes as discrete resistant mineral grains (Johnson, 1991).

11

Avivar, (2012) stated that the fate and mobility of thorium in water and soil are governed by its chemical and biological behaviours. Acidity and wet conditions enhance the solubility of thorium in soil. Thorium discharged as ThO_2 into surface waters from mining, milling and processing will be present as suspended particles or sediment because of its low solubility. Other soluble ions in water will hydrolize at pH above 5, forming insoluble $Th(OH)_4$ or hydroxyl complexes e.g. $[Th(OH)_2]^{+2}$, $[Th_2(OH)]^{+6}$, $[Th_3(OH)_5]^{+7}$; then, the precipitates or complexes will be absorbed by the particulate matter in water, with the result that the concentration of soluble thorium in water will be very low. In most cases, sediment resuspension and mixing may control the transportation of particle-sorbed thorium in water, but in some cases, the concentration of dissolved thorium in water may increase due to the formation of soluble complexes with carbonate, humic materials or other ligands in the water (Avivar, 2012).

Table 3: Th-232 decay scheme

NUCLIDE	PRINCIPAL MODE OF DECAY	HALF-LIFE
Thorium-232	A	1.4×10^{10} years
Radium-228	B	5.8 years
Actinium-228	B	6.1 hours
Thorium-228	A	1.9 years
Radium-224	A	3.7 days
Radon-220	A	55.6 seconds
Polonium-226	A	0.15 seconds
Lead-212	B	10.6 seconds
Bismuth-212	α 36%	60.5 minutes
	β 64%	
Polonium-212	A	$\times 10^{-7}$ seconds
Talium-208	B	3.1 minutes
Lead-210	Stable	Stable

Potassium

Potassium is a soft, silver-white metal. An important constituent of soil, it is widely distributed in nature and is present in all plant and animal tissues. Potassium-40 is a naturally occurring radioactive isotope of potassium. Two

12

stable (nonradioactive) isotopes of potassium exist, potassium-39 and potassium-41. Potassium-39 comprises most (about 93%) of naturally occurring potassium, and potassium-41 accounts for essentially all the rest. Radioactive postassium-40 comprises a very small fraction (about 0.012%) of naturally occurring potassium. Several radioactive isotopes of potassium exist in addition to potassium-40. These isotopes all have half-lives of less than one day so they are not of concern to this study.

The half-life of potassium-40 is 1.3 billion years, and it decays to calcium-40 by emitting a beta particle with no attendant gamma radiation (89% of the time) and to the gas argon-40 by electron capture with emission of an energetic gamma ray (11% of the time) as shown in Fig. 2.
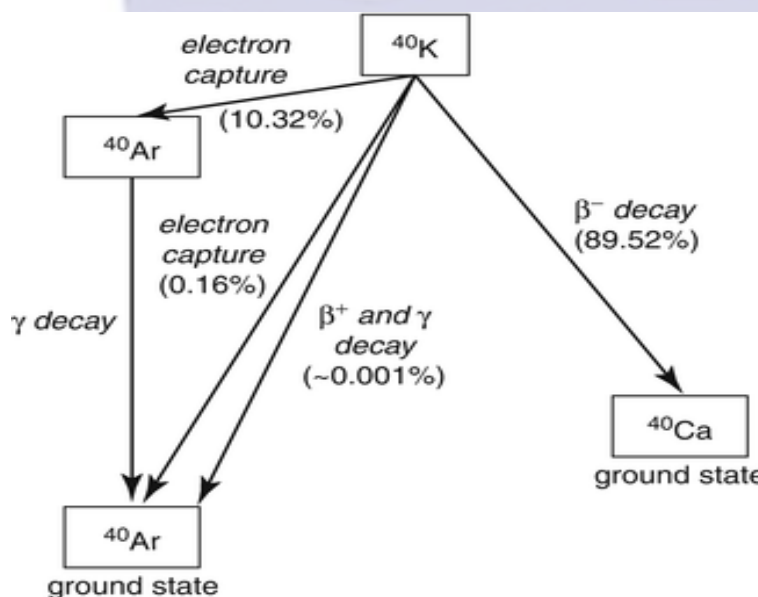
Figure 2: Decay scheme of potassium-40.

Potassium-40 is an important radionuclide in terms of the dose associated with naturally occurring radionuclides. Potassium is present in the earth's crust, oceans, and all organic material. Its concentration in the earth's crust is about 15,000 mg/kg or 1.5%, and its concentration in seawater is about 416 mg/L. Potassium binds preferentially to soil, with the concentration

associated with sandy soil particles estimated to be 15 times higher than in the interstitial water (in pore spaces between soil particles); it binds more tightly to loam and clay soil, so those concentration ratios are higher (above 50). Potassium-40 behaves in the environment the same as other potassium isotopes, being assimilated into the tissues of all plants and animals through normal biological processes. It is the predominant radioactive component in human tissues and in most food. For example, milk contains about 2,000 pCi/L of natural potassium-40. Potassium-40 can present both an external and an internal health hazard.

The strong gamma radiation associated with the electron-capture decay process (which occurs 11% of the time) makes external exposure to this isotope a concern. While in the body, potassium-40 poses a health hazard from both the beta particles and gamma rays. Potassium-40 behaves the same as ordinary potassium, both in the environment and within the human body – it is an essential element for both (ANL, 2005). Hence, what is taken in is readily absorbed into the bloodstream and distributed throughout the body, with homeostatic controls regulating how much is retained or cleared. The health hazard of potassium-40 is associated with cell damage caused by the ionizing radiation that results from radioactive decay, with the general potential for subsequent cancer induction. Lifetime cancer mortality risk coefficients have been calculated for nearly all radionuclides, including potassium-40. While ingestion is generally the most common type of exposure, the risk coefficients for this route are lower than those for inhalation.

As for other radionuclides, the risk coefficient for tap water is about 70% of that for dietary ingestion. In addition to risks from internal exposures, an

external gamma exposure risk also exists for potassium-40. To estimate a lifetime cancer mortality risk, if it is assumed that 100,000 people were continuously exposed to a thick layer of soil with an initial average concentration of 1 pCi/g potassium-40, then 4 of these 100,000 people would be predicted to incur a fatal cancer over their lifetime (Argonne National Laboratory, 2005).

Problem Statement

At the time of the present study, produced water from the Jubilee Oil Field is disposed into the open sea. The only guideline regulating this discharge is the Environmental Protection Agency's guideline of oil-in-water content of 29 mg/L for the discharge of produced water into the ocean (Kpeglo, 2015). Despite this guideline, the produced water may still contain radionuclides and trace metals as these are not regulated in the guideline. Trace metals can be leached into and transported via groundwater, drainage and dust, and incorporated into the food chain (Lin, Xiao, Wu, Ao & Ning, 2012; Lokeshwari & Chandrappa, 2006; Mehrdadi, Nabi, Nasrabadi, Hoveidi, Amjadi & Shojaee 2009). Contamination of soil and water with heavy metals is a potential ecological risk (Siegel, 2002).

Additionally, there was flaring of natural gas from the wells since the inception of oil production in late 2010 to 2014 when the Atuabo gas processing facility was completed. Gas flaring comes with its attendant adverse environmental, economic and health effects (Ajugwo, 2013).

Oil production related activities and TENORM oil drilling waste may generate radiation exposure levels which require attention and continuous monitoring (Attallah, Awwad & Aly, 2012). Radiation workers at the rigs

15

employ basic radiation protection principles of time, distance and shielding but the public may inhale radon gas which is released during drilling raising their risk of lung cancer. In addition, they may be exposed to alpha and gamma radiation released during the decay of radium-226 and the low-energy gamma radiation and beta particles released into the environment by the decay of radium-228. Agbalagba, Avwiri & Chadumoren, (2013) have reported instances where the mean radiation values to the public exceeds the 1.0 mSvy^{-1} recommended by various national and international regulations and guidelines on radiation such as UNSCEAR, 2000 for the general public and non-nuclear environment. Similarly, Rich & Crosby, 2013 presented the potential impact of TENORM to the environment, occupational workers, and the gener al public with the potential health effects of individual radionuclides i.e. cell damage, carcinogenesis, bone marrow damage resulting in anemia among others in a study that analyzed the specific radionuclides present in reserve pits for natural gas mining. The radionuclides present included those from ^{232}Th decay series (^{228}Ra, ^{228}Th, ^{208}Tl) and ^{226}Ra decay series (^{214}Pb, ^{214}Bi, ^{210}Pb) radionuclides.

TENORMs are generally health hazards and will persist long into the future as a component of residual radioactivity in the environment. Analysis of TENORM is therefore critical due to the long radioactive half-lives, high chemical and radiological toxicities and criticality concerns of its isotopes. Additionally, TENORM analysis are necessary for characterization purposes.

Objective and Scope

The general aim of the study is to assess the risk of TENORM exposure to people living in communities along the Jubilee oil field due to oil drilling activities. The main focus of the study was to assess the concentration of

TENORMs of the U/Th decay series and ^{40}K as well as predict their future trends in multimedia environment. Soil, drinking (ground) water and food samples were collected at selected locations within the communities for analysis by gamma spectrometry using high purity germanium (HPGe) detector, neutron activation analysis (NAA) and atomic absorption spectroscopy (AAS). Although the chemical and radiological health hazards of TENORMs are well established (BEIR VI, 1999), the public who are at risk are mostly unaware of their biological effects. This study seeks to propagate the full understanding of the nuclear waste status at the Jubilee oil field and to develop an appropriate action plan for their management. More specifically, the purpose of this study therefore is to:

i. determine the activity concentrations of the radionuclides U/Th series and ^{40}K in the environment

ii. determine the radiation doses from these activity concentrations and compare with international recommended dose limits.

iii. evaluate the potential for exposure to the public and the hazard and risk to the public associated with these dose values.

iv. conduct geochemical studies by quantifying the levels of trace metals as well as the physical parameters in water samples.

v. establish background data on TENORM contamination as a result of oil and gas drilling in Ghana

vi. predict the trends of TENORM concentration in the environment as a result of oil drilling activities.

vii. promote the development and/or the update of databases on hazardous substances/wastes in Ghana

Relevance of Study

There are national and international regulations and guidelines on radiation protection in general and TENORMs in particular. The project is being carried out to safeguard public health and ensure that environmental radioactivity levels in communities along the Jubilee Oil Field conform to provisions in these national and international regulations and guidelines.

Knowledge of how much radiation the public is exposed to as a result of oil logging activities is vital. The oil and gas logging is relatively new in Ghana hence there exists very little data and records on levels of TENORM contamination in this sector. Availability of such information will be helpful in understanding the doses from TENORM waste disposal and other related activities that the public is exposed to, and therefore appropriate actions adopted to reduce exposure. This study is a contribution in this direction by providing enough information that will be the basis for radiation protection, environmental safety enforcement and remediation to safeguard public health and safety in communities of the Jubilee oil field.

The oil wells are important sources of revenue to the Ghana National Petroleum Commission, and therefore an important resource to Ghana. This study therefore aims to provide a road map and establish uniform approaches on TENORM management at the oil fields.

Summary

The background to the study and the contaminants of concern was presented in this chapter. This chapter also included the problem statement, relevance of the study and scope and objectives.

CHAPTER TWO

LITERATURE REVIEW

Introduction

The communities along the Tano basin are mostly rural. The only exceptions are Axim and Half Assini, which are peri-urban. These agrarian communities serve as source of food to urban and local residents. The soil quality in these townships therefore relate to food security. However, the quality of soil in these rural communities may be impacted by the transport of contaminants from nearby industries. At the moment, the main industry capable of impacting the environment in the future is the oil and gas drilling industry offshore the coastal communities. Environmental radionuclide distribution and accumulation is an unstudied and poorly understood aspect of oil and gas drilling in Ghana, and has the potential to increase the radiation exposure of residents living near oil and gas dominated industry activities. This chapter is a presents a review of the environmental concerns of radionuclides and trace metals and potential human health effects from exposure to contaminats from the oil and gas drilling industry.

Overview of TENORM in the Oil and Gas Industry

TENORMs are an inherent part of many geologic materials. Consequently, TENORMs are encountered during geologically related activities. Attallah et al, (2012) reported publications of radioactivity in natural gases in Canada in 1998. Elevated levels of radium were also detected in the Russian oilfields in 1930's. In 1953, the US geological society published a paper on uranium and helium in gas formations. In 1973 US-EPA performed a study on the presence of Rn-222 in natural gas.

19

During the 1980's, elevated concentration of TENORM were found on oil and gas extraction equipment in the North Sea and in the Southern United States (Escott, 1984). This discovery generated concern in the United States and Europe. Elevated TENORM concentration may subject oil and gas workers to unnecessary radiation exposure. Subsequently, elevated radiation concentrations were discovered in 1986 in some oil and gas equipment of the Southern United States (USEPA, 1993). In these cases, the elevated TENORM concentrations in the scales and sludges associated with the equipment were of particular concern. These radioactive wastes represent a significant waste problem for the oil industry and the cleanings from contaminated plant and equipment are either discharged into the sea offshore or through a pipeline onshore. An example is the case of what happened in Aberdeen. The fate and the transport of TENORM in these contaminated scales discharged is not known. The question as to whether the radium remains trapped or migrates out to enter the food chain has never been addressed (Ghoose & Heaton, 2005).

TENORM *Occurrence and Chemistry*

Oil and gas production and processing operations sometimes accumulate TENORM at elevated concentration in the waste stream as by-product. The sources of most of the radioactivity are isotopes of uranium -238 (U-238) and thorium- 232 (Th-232) which are naturally present in subsurface formation from which oil and gas are produced. The primary radionuclide of concern in TENORM wastes are Ra-226 of U-238 decay series and Ra-228 of the Th-232 decay series. Other radionuclides that are of concern include those formed from the decay of Ra-226 and Ra-228 (Veil, Smith, Tamasko, Elcock, Blunt & Gustavious, 1998).

Solid waste, sludge, and produced water are those recipients which are contaminated with residues of natural radionuclides. Radium, which is slightly soluble in water can be mobilized in liquid phases of the formation water stream. Dissolved radium either remains in solution in the produced water or precipitates out in scales or sludges (Veil et al., 1998). The following provides the equation for the formation of alkaline earth carbonates and sulphates.

$$Ca^{+2} + CO_3^{-2} \rightarrow CaCO_3$$

$$Sr^{+2} + SO_4^{-2} \rightarrow SrSO_4$$

$$Ba^{+2} + SO_4^{-2} \rightarrow BaSO_4$$
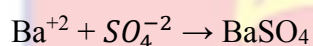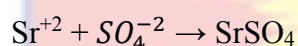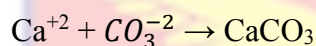
Radium, strontium and barium are chemically similar and radium nuclides co-precipitate together with alkaline earth carbonates and sulphates, replacing calcium, barium or strontium cations in the crystal structures (Bou-Rabee, Al-Zamel, Al-Fares & Bem, 2009). Therefore, the observed levels of activity concentration in both separated sludge and solid scale are usually much higher than those observed from produced water.

The way in which the scales are deposited is connected to the pipes, superficial features, fluid-dynamic phenomena and crystallization kinetics. Variations in sulphates and carbonates solubility can give rise to scale formation, which are affected by some physical and chemical factors, e.g. water chemistry (primarily salinity), temperature variation, pressure changes, pH balance, evaporation in the gas extraction pipes, injection of incompatible sea waters and reinjection of water into the reservoirs (Testa, Desideri, Guerra, Meli & Roselli, 1998 and Veil et al., 1998).

TENORM Management Practices

Underground Injection

Aside discharging into the sea offshore, TENORM contaminated wastes have also been disposed of through underground injection wells. Veil et al., 1998 referred to reports by McArthur, Major, & Lowe, (1995) on a project where two major oil producing companies developed a technology for the injection of TENORM waste in the North Slope Alaska oil field. Accordingly, 100 tons of TENORM solids were cleaned from 3000 oil production pipes and casing and the resulting solids were processed to a particle size of less than 80 µm, slurred with 10000 bbl of water and injected into a class II injection well.

Additionally, two of the four US commercial TENORM disposal companies utilized underground injection. Both facilities reportedly crush, mill and slurry the incoming TENORM waste before its injection.

A mobile TENORM treatment was also developed to dissolve the radioactive component of TENORM into an aqueous solution that can then be disposed of through underground injection. The residual solids no longer contain radioactivity above levels of regulatory concern and can be disposed of as a non-hazardous waste (Capone, Chatterjee, Cleland, Fortunato, Roehrig, Walker & Bush, 1997). Other operators use the process of grinding and milling the waste to a small particle size, slurrying the waste to facilitate pumping and injecting to formations at fracture pressure (Sipple-Srinivassan, Bruno, Bilak, & Danyluk, 1997).

22
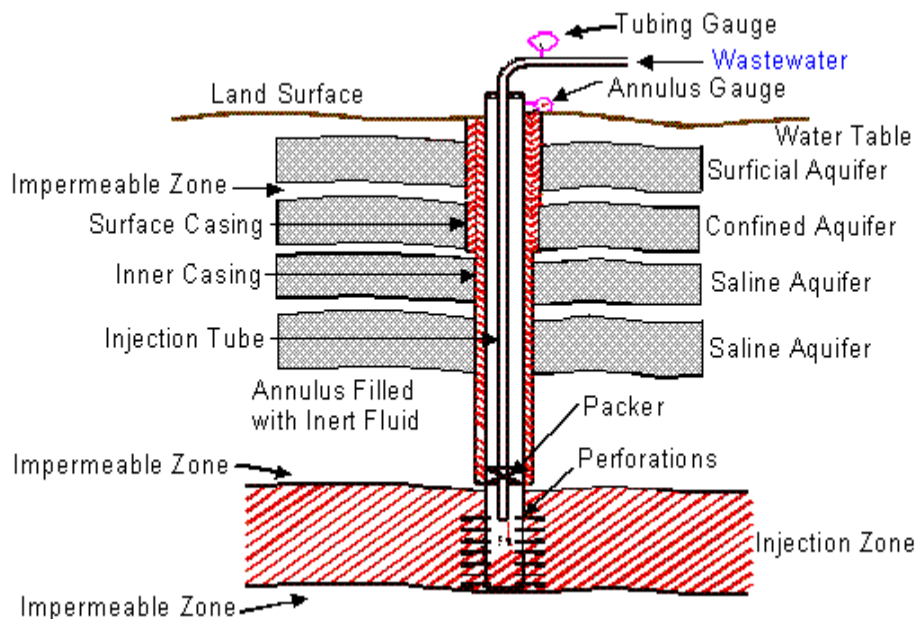
Figure 3: A technical diagram of underground injection of brine water

Landfill Disposal

Other off-site commercial TENORM waste disposal options is bury in landfills. Landfills are primarily designed to handle radioactive wastes other than oil field waste but may be suitable for oil field wastes as well with some modifications

Encapsulation and Downhole Disposal

TENORM waste can also be encapsulated inside a section of a pipe that is then sealed on both ends and lowered into a wellbore or directly in the wellbore. A plug is placed on top of the waste containing zone. Scaife et al., 1994 was referred to by Veil et al., 1998 in a report as being able to do two encapsulation projects in the offshore of Gulf of Mexico. In the first project, TENORM waste was placed into eight joints of casing as the pipe was being lowered into the hole and in the second, 31 drums of TENORM waste were placed into 21 joints of casing on shore and sealed at both ends. The sealed joints were transported offshore and lowered into the well bore. Cement plugs

23

were placed on top of the waste-containing joints in both projects to conceal them.

Land Spreading

The principle of land spreading is to mix TENORM wastes having an activity concentration higher than the action level with clean soil so that the resulting blend has an activity concentration lower than the action level (Veil et al., 1998).

Natural Radiation Exposures

All living organisms are continually exposed to ionizing radiation which has always existed naturally. Some of these exposures according to UNSCEAR, 2000 are fairly constant and uniform for all individuals everywhere, for example the dose from ingestion potassium-40 in foods. Other exposures vary widely depending on location: for example cosmic ray exposures decrease in intensity with depth from the atmosphere and from aircraft altitudes to ground level. The concentration of uranium and thorium are elevated in localized areas as human activities and practices also result in variation in exposures (UNSCEAR, 2000).

Natural background radiation comes from the following three sources

- Cosmic Radiation

- Terrestrial Radiation

i. Building materials and air

ii. Water and foods

- Internal Radiation

Table 4 shows a report by UNSCEAR, 2000 of worldwide annual effective dose from natural sources.

Table 4: Worldwide annual effective dose from natural sources

SOURCE	WORLDWIDE AVERAGE ANNUAL EFFECTIVE DOSE (mSv)	TYPICAL RANGE (mSv)
EXTERNAL DOSE		
COSMIC RAYS	0.4	0.3 – 1.0
TERRESTRIAL GAMMA RAYS	0.5	0.3 – 0.6
INTERNAL DOSE		
INHALATION (MAINLY RADON)	1.2	0.2 – 10
	0.3	0.2 – 0.8
INGESTION	2.4	1.0 – 10
TOTAL		

Source: (UNSCEAR, 2000)

Cosmic Radiation

Cosmic rays can be broadly defined as the massive particles, photons (γ-rays, ×-rays, ultra-violet and infra-red etc.), neutrinos and exotics (WIMPS, axions etc.) striking the earth. Technically, primary cosmic rays are those particles accelerated at astrophysical sources and secondary cosmic rays are those particles produced by the interaction of primary rays with interstellar gas in the atmosphere or in the earth. Thus electrons, protons and helium, as well as carbon, oxygen, ions and other nuclei synthesized in stars are primary rays. Nuclei such as lithium, beryllium and boron are secondary rays. Antiprotons and positrons are also in large part secondary (Gaisser & Stanev, 2007).

The annual average dose worldwide at sea level is estimated to be 320 μSv with directly ionising and indirectly ionising radiation components contributing 270 μSv and 48 μSv respectively. The dominant component of the cosmic ray field at the ground level is muons with energies between 1 and 20 GeV (UNSCEAR, 2000) and thus contribute about 80% of the absorbed dose rate in free air from the directly ionising radiation.

25

Primary cosmic rays usually possess tremendous kinetic energy. These rays are positively charged and gain energy by acceleration within the magnetic fields. In the vacuum of outer space, the charged particles may exist for long periods of time and travel millions of light years. During the flight, they gain high kinetic energies on the order of 2 to 30 GeV [1 GeV = 10^9 eV].

Cosmic ray intensity increases sharply with elevation until a maximum is reached at an altitude of about 20 km. From 20 km to the limit of the atmosphere, the intensity decreases. This pattern is explained by the increased production of secondary cosmic rays resulting from the increasing atmospheric density as one move toward the earth from an altitude of 50 km. Cosmic ray intensity is also related to latitude.

A considerable number of radionuclides are continuously produced in the atmosphere by cosmic ray interaction with matter as shown in Table 5.

Table 5: Radionuclides produced from cosmic rays

RADIONUCLIDE	HALF-LIFE ($t_{1/2}$)	ATMOSPHERIC PRODUCTION RATE (atoms/cm²-sec)
^{10}Be	2.7×10^6 year	4.5×10^{-2}
^{36}Cl	3.1×10^5 year	1.1×10^{-3}
^{14}C	5568 year	1.8
^{32}Si	500 year	1.6×10^{-4}
^3H	12.3 year	0.25
^{22}Na	2.6 year	5.6×10^{-5}
^{35}S	88 day	1.4×10^{-3}
^7Be	53 day	8.1×10^{-2}
^{33}P	25 day	6.8×10^{-4}
^{32}P	14.3	8.2×10^{-4}
^{27}Na	15.1 hr	-
^{38}S	2.9 hr	-
^{39}Cl	55 min	1.6×10^{-3}
^{38}Cl	37 in	

These are mostly produced as fragments but some by activation of stable atoms with neutrons and muons. With the possible exceptions of H-3 and C-14, the radionuclides are normally found in very minute concentrations. Tritium is diluted and mixed with the earth's water and H-2 gas reservoirs while C-14 combines with oxygen to form CO_2.

Terestrial Radiation

Terrestrial radiation is emitted by naturally occurring radioactive materials found in the earth's crust such as uranium, thorium, and potassium and any of their decay products, such as radium and radon. These radionuclides are ubiquitous and present in very low concentrations. These radionuclides, which appeared on Earth at the time of formation of the Earth are termed "primordial".

Of the primordial radionuclides that are still detectable, three are of overwhelming significance. These are K-40, U-238 and Th-232. Uranium and thorium each initiate a chain of radioactive progeny, which are nearly always found in the presence of the parent radionuclide.

Other primordial long-lived radionuclides which occur in nature but of very low concentrations are Rb-87, La-138, Ce-142, Sm-147 and Lu-176 etc. The main reservoir of natural radioactivity is the lithosphere. However, existing variations associated with specific types of formation and certain minerals, or regional with little correlation to types of rocks and minerals exist.
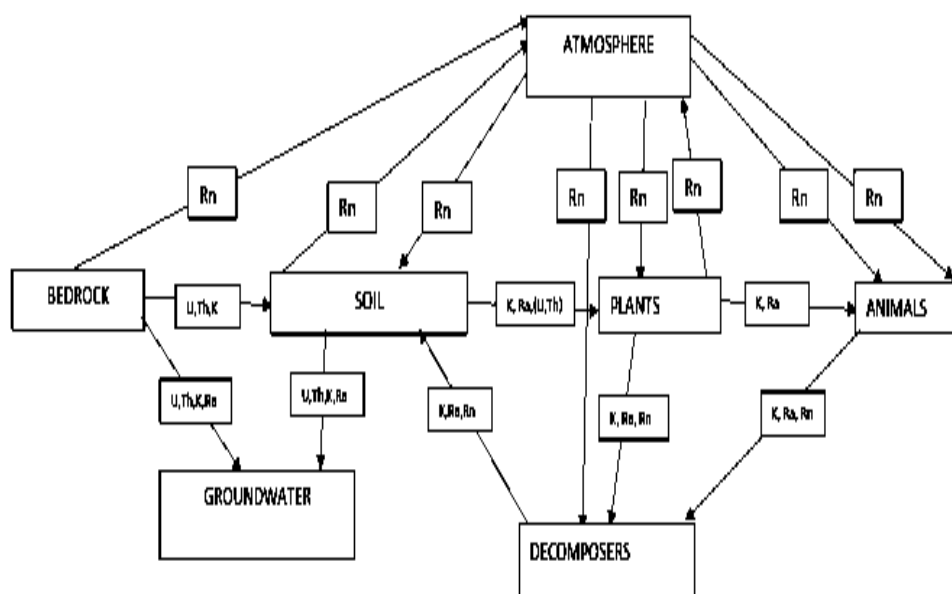
Figure 4: Major pathways of primordial radionuclides and important progeny in terrestrial ecosystem (Rania, 2014)

Chemical properties of radionuclides, physical factors of the ecosystem, physiological and ecological attributes of the biota are some of the factors that influence the distribution of primordial radionuclides and their progeny in the natural ecosystem.

Radon

Radon is a naturally occurring radionuclide. The largest source of radon in the environment is due to the ambient levels produced by the widespread distribution of uranium, thorium and their decay products in the soil. Radon has three natural isotopes; Actinon (^{219}Rn) from the ^{235}U decay series; Thoron (^{220}Rn) from the ^{232}Th decay series; and Radon (^{222}Rn) from the ^{238}U decay series (UNSCEAR, 1993).

Radon is an inert noble gas that does not interact chemically with other elements. All isotopes of radon are radioactive and their decay results in formation of new elements. ^{219}Rn usually is not considered in the evaluation of

28

radon-induced health effects because it is not abundant in the environment and has extremely short half –life of 4 seconds. The average rate of production of ^{220} Rn is about the same as ^{222} Rn, but ^{220}Rn has a short half-life of 56 seconds, decaying rapidly into polonium that most ^{220} Rn does not reach the atmosphere (ATSDR, 2012). All discussions of radon in this study therefore refer to ^{222} Rn unless otherwise stated.

The primary route of exposure of radon and its decay particles are through inhalation. The radon progeny are present in air either as free atoms or attached with aerosols (Tufail, Ahmad, Khan, Zafar & Khan, 1992). The radon progeny present in ambient air constitute significant radioactive hazards to human lungs. Radon decays by alpha emission hence the radon progeny are positively charged and so electrostatically attach to particulates in air (Doyi, Oppon, Glover, Gbeddy & Kokroko, 2013). Charged ions can easily bind to surfaces like dust, droplets, walls, etc., further, these ions can be inhaled by humans and can attach to the respiratory epithelium. 90% of the inhaled radon absorbed is exhaled. Remaining 10% decay into alpha particles and cause radioactive effects on lung parenchyma and cause cancer. The United States Environmental Protection Agency (EPA, 2013) estimates radon as the second most frequent cause of lung cancer, behind cigarette smoking. Combined cigarette smoking and exposure to radon have a synergistic effect.

Potential for Human Exposure

The ultimate fate for radon is transformation through radioactive decay. There are no sinks for radon, since its radioactive half-life is 3.8 days (O'Neil, Heckelman & Koch, 2006). In soil, alpha recoil is the mechanism by which radon is released into the pore space, its ultimate release into ambient air as a

function of the soil porosity, soil moisture content and meteorological factors such as precipitation, atmospheric pressure and the temperature versus altitude profile. Once radon is released to ambient air its dispersion is primarily determined by atmospheric stability, including vertical temperature gradients and effects of wind.

In groundwater, radon moves by diffusion and primarily by the mechanical flow of water. Radon solubility in water is relatively low and with radioactive half-life of 3.825 days much of it will decay before it released from groundwater.

Radon levels in ambient air vary with the type of soil and underlying bedrock of the area. The average outdoor radon concentration in United State is 14.8 Bq/m^3 with Steck, Field & Lynch (1999) quoting 22.2 -30.3 Bq/m^3 for Iowa and Minnesota (ATSDR, 2012).

The primary human exposure to radon is inhalation of [222]Rn and its decay products present in air from all sources, but daily intake of radon originating from drinking water only is estimated at 3.7-22.2 Bq/ day both from ingestion of drinking water and inhalation of radon released from drinking water (Cothern, Lappenbusch & Michel, 1986).

Several exposure pathways therefore need to be taken into account to determine the total annual effective dose. The annual effective dose can be calculated from the measured radon concentration in air as follows;

$$D_{Rn} = K(Rn)_A.\text{F}.C_{Rn}.t_{exp,} \tag{1}$$

where:

K (Rn)$_A$ is the dose coefficient pertaining to the dose convention following ICRP publication 65 in mSv per Bq.h /m^3

F is the equilibrium factor of 0.4 or 0.6 indoor and outdoor occupancy respectively.

t_{exp} is the annual exposure time (h)

C_{Rn} is the Rn concentration (Bqm^{-3})

Internal Radiation

In addition to cosmic and terrestrial sources, all people also have radioactive potassium-40, carbon-14, lead-210 and other isotopes inside their bodies from birth. The variation in dose form one person to another is not as great as the variation in dose from cosmic and terrestrial sources. The average annual dose to a person from internal radioactive material is about 4 millirems/year (USNRC Technical Training Center, 2014).

Potential TENORM Producing Industries

The idea of the phenomenon of enhanced natural radionuclide concentrations in materials as part of industrial activities dates back to the early 20th century when Elster & Geitel, (1904) discovered an enrichment of radioactive substances in thermal brines. It was the same year when radon was found in petroleum by Himstedt (Karsten, 2007). With time, some more substances of other industrial types were found to contain enhanced levels of natural radionuclides with the Canadian Radiation Protection Committee (CRPC, 2000) proposing a classification system for TENORM industries by summarizing them in six groups (Karsten, 2007). This summary is the basis for this classification as follows:

1.   Metal ore processing and metal recycling

Mining, transportation and processing of metals, the consequent emissions of radionuclides to air and water bodies could lead to potential

exposure of humans (UNSCEAR, 2000). Apart from the ores themselves, generated sludge and scales are the main contaminated materials. The following metal industries are concerned:

a.   Tin

b.   Niobium

c.   Aluminium

d.   Iron and steel

e.   Zinc

f.   Copper

g.   Molybdenum

h.   Vanadium

i.   Hafnium

j.   Lead

2.   Metal extraction and processing

Elevated levels of radionuclide concentrations may occur when minerals or sand are mined and/or processed. The following industries are concerned:

a.   Uranium mining

b.   Zircon sands

c.   Fertiliser industry

d.   Rare earth element industry

e.   Abrasive and refractory industry

f.   Thorium compound industry

g.   Titaniumdioxide pigment industry

3.   Organic material processing

32

Enhanced natural radionuclide concentrations may occur when crude oil or natural gas is extracted to the surface. Scales in technical installations as well as sludge are the most important materials. The following types of industries are concerned:

a.   Oil and gas extraction

b.   Hard coal mining

4.   Thermal-electric production

When hard coal is combusted, contaminated ashes remaining in the combustion vessels may lead to enhanced natural radionuclide concentration. The industry type concerned is

a.   Hard coal power plants

5.   Water treatment facilities

When fresh or waste water is treated by adsorptive media or ion exchange resins to remove minerals and other impurities can lead to elevated levels of natural radioactivity. For geothermal production of drinking water, the radionuclide concentration depends on the geological formation the ground water is extracted from. The types of industries concerned are

a.   Waterworks

b.   Waste water treatment plants

c.   Geothermal installations.

6.   Tunneling and underground workings

Enhanced natural radionuclide concentrations may occur in areas where galleries are installed in rocks containing radioactive minerals or releasing radon/thoron due to their porosity or cracks. From the definition in this study, this group is not part of TENORM but NORM. The installations concerned are:

    a.   Underground caverns

    b.   Underground radon-spas

    c.   Electric vaults

    d.   Tunnels

    e.   Sewer system

Pathways and Scenarios

According to O'brien & Copper, (1998), the pathways by which TENORM can reach humans is quite complex, thus significant approach to establish the pathways that contribute significantly to human exposure is essential. Penfold, Degrange, Mobbs & Schneider, (1999) described five pathways and connected them with situations that workers and the general public are most exposed

    1.   Inhalation of dust

Most exposed situation: dusty conditions with little respiratory protection.

The sources of inhaled radioactive materials include debris from atmospheric nuclear weapon testing; nuclear reactor and medical gaseous waste; radioactive materials manufacturing; diagnostic medical radionuclide use; coal- and gas-burning power plants; airborne soil; and naturally emanating gases. The radionuclides (and their average concentrations) commonly found in the atmosphere include: ^{210}Pb (0.01 pCi/m^3); ^{210}Po (0.001 pCi/m^3); ^{238}U (12×10-5 pCi/m^3); ^{232}Th (2×10-5 pCi/m^3); ^{230}Th (4.5×10-5 pCi/m^3); ^{228}Th (3×10-5 pCi/m^3); ^{222}Rn and ^{220}Rn (270 pCi/m^3 or 10 MBq/m^3); ^{14}C, ^{3}H. In addition, smokers are exposed to radiation from the radionuclide ^{210}Po, which

is found in tobacco; the resulting dose to the bronchial epithelium can be as high as 0.2 mSv per year (NCRP 1984; Shapiro 1990; UNSCEAR 1993).

2.   Ingestion of dirt/dust

Most exposed situation: dirty and dusty areas with little protective clothing

The sources of radionuclides that contribute to radiation exposure by ingestion include nuclear weapons testing, the accidental or intentional release of radioactivity from nuclear reactors, the release of medical or experimental radionuclides into sanitary sewers, and naturally occurring radionuclides (which normally represent the source of highest oral dose). There is a small probability of radionuclide ingestion because of the potential for surface water and groundwater contamination and uptake by plants and animals following erosion of ground cover from a contaminated site. Among the naturally occurring radionuclides, uranium, ^{40}K, and ^{226}Ra are found in soils and fertilizers; as a result, they are incorporated into foods consumed by animals and humans. The practice of using phosphate fertilizers has resulted in uranium concentrations in food at levels up to 8 ng/g, resulting in an estimated average annual intake of uranium from dietary sources of 10 Bq; as a result, the average skeletal content of uranium is estimated to be 25 μg, which is equivalent to approximately 17 pCi (Eisenbud, 1987; UNSCEAR, 1993).

3.   External irradiation

Most exposed situation: close to large amounts of material with little shielding

35

4.   Inhalation of radon

Most exposed situation: in rooms with large amounts of material and little ventilation.

The largest dose of radiation from natural sources comes from the inhalation of ^{222}Rn and ^{220}Rn (thoron) gases. These colorless and odorless gases, which are in the uranium and thorium transformation chains respectively, are continuously released from the soil. Worldwide, the total emanation rate of radon is estimated to be 50 Ci/sec (2 TBq/sec); the total atmospheric content is estimated to be 25 MCi (1 EBq). The main factors controlling the rate of radon release and subsequent exposure are: ground porosity, ground cover, temperature, meteorological conditions, and the type of construction and ventilation properties of dwellings. The rate of radon emanation from soil is thought to increase with diminished atmospheric pressure and to decrease during periods of, or in areas of, elevated moisture, while the atmospheric concentration of radon tends to increase during temperature inversions and as the humidity decreases.

5.   Dermal/Skin contamination

Dermal exposure to radionuclides refers to exposures from a radionuclide placed in direct contact with skin surface. Dermal exposure is typically a minor route of internal and external exposure. In general, depending on the specific physical properties of the radionuclide that may reside on the skin, the percutaneous absorption of radionuclides from particles is negligible, especially if the skin is thoroughly washed immediately after exposure. The long-term biological effects of dermally absorbed radionuclides are limited to the level of the epidermis and dermis (and its vasculature). More soluble forms

of the radionuclides may result in a small percentage of the nuclide being absorbed if it is not removed from the skin's surface, for example tritium is readily absorbed into the body through the skin. Generally, the skin is an effective barrier against absorption of radionuclide into the body (ATSDR, 1999).

Environmental Concerns Associated with Tenorms from Oil and Gas Industry

Oil-gas-water is brought to the surface through the well tubing. TENORM is brought to the surface through the downhole tubing as part of the oil-gas-water mixture. Hard scales also precipitate from the formation water onto the downhole tubing in response to changes in temperature, pressure, and salinity as the water is brought to the surface. The scale is typically a mixture of carbonate and sulphate minerals.

During the separation process of the oil-gas-water mixture, different radionuclides are separated. In the separation process, the deposits tend to be in the form of soft scales, sludges or films. Radium sludges tend to accumulate on oil and water side of the separation process (IAEA, 2003). Similarly, radon and it's progeny can be found in the gas and in films on the inside of the gas handling equipment (Gessel, 1975).

There are also additional TENORM containing residues or contaminated soils from the water discharges produced. Another residue is the formation water that has been separated from the oil-gas-water mixture. Studies of large quantities of water produced from wells of oil and natural gas drilling and production sites have indicated that a number of wells yielded water with an average radium concentrations in excess of 1.85 Bq/L (White, 1992). The IAEA

in 2003 further cites reports by Spaite & Smithson (1992) that suggests that average radium concentrations in water from some wells can be as high as 111 Bq/L.

Separated water is often re-injected into the oil bearing formation which is often considered a sound waste management approach posing minimal potential impacts to human health, provided that there is no hydraulic connection to usable underground resources. Once the well is abandoned, the casing is properly cemented to prevent leakage into these aquifers. In many cases however, the water is discharged into holding surface ponds (onshore) or discharged directly into the sea (offshore) thus posing a potential environmental, health and radiological concerns.

The largest concern in terms of radionuclide activity concentrations for TENORM in the oil and gas industry involves hard scales which form in the inside of the downhole tubing which must be removed occasionally. In terms of exposure, scales with the average radionuclide concentrations of 1000 – 100 000 Bq/kg tend to be relatively insoluble, thus the radionuclide would only be released slowly into the environment (Raabe, 1996).

Sludges that accumulate in tanks and other settling areas within the production equipment tend to have less enhancement of TENORM than the scales; however, the concentrations can still be a concern. Radionuclide concentrations range from background to roughly 1×10^4 to 4×10^4 Bq/kg (Gray, 1993).

The radionuclides in sludges are more available for release into the environment than the case for the scales. Thus although radionuclide activity

concentrations are less than those of scales, potential exposures via the food chain and radon pathways are more likely (IAEA, 2003).

Biological Effects of Ionising Radiation

High doses of ionizing radiation can lead to acute effects, such as skin burns, hair loss, birth defects, illness, cancer, and death. The basic principle of toxicology, "the dose determines poison," applies to the toxicology of ionizing radiation as well as to all other branches of toxicology. In the case of threshold effects ("deterministic effects" in the language of radiation toxicology), such as skin burns, hair loss, sterility, nausea, and cataracts, a certain minimum dose (the threshold dose), usually in the order of hundreds or thousands of rad, must be exceeded in order for the effect to be expressed. An increase above the threshold dose will increase the severity of the effect (ATSDR, 1999).

Chronic exposure to TENORMs however results in delayed effects such as the development of certain forms of cancer namely leukemia, cancers of the lung, stomach, esophagus, bone, thyroid, the brain and nervous system. For cancer induction, increasing the radiation dose does not increase the severity of the cancer; instead it increases the chance of cancer induction (ATSDR, 1999). In the case of carcinogens generally, whether chemical or radiological, safety standards are based on a postulated zero threshold (i.e., any increment of carcinogen, no matter how small, is assumed to carry with it a corresponding increase in the chance of causing cancer). Increasing the size of the dose increases the probability of inducing a cancer with that carcinogen. Cancers that are, in fact, caused by radiation are completely indistinguishable from those that seem to occur spontaneously or are caused by other known or suspected carcinogens (ATSDR, 1999).

Ionising radiation has the ability to affect the chemical state of a material and so cause changes which are biologically important. Damage to a cells genetic material, particularly the DNA is believed to be the major cause of harmful effects of radiation leading to cell killing and mutations (cancer).

All biological damage effects begin with the consequence of radiation interactions with the atoms forming the cells resulting in deterministic or stochastic effect. There are two mechanisms by which the radiation ultimately affects cells. These two mechanisms are direct or indirect effect/action.

Direct Effect

When radiation interacts with the atoms of the DNA molecule, or some other cellular component critical to the survival of the cell, it is direct effect or direct action (USNRC, 2014). Direct action or interaction may affect the ability of the cell to reproduce and thus survive. If enough atoms are affected such that the chromosomes do not replicate properly, or if there is significant alteration in the information carried by the DNA molecule, then the cell may be

i-   Repaired: DNA repair system may correctly repair radiation lesions; however no repair system is completely error free and lesions may be converted to mutations (UNSCEAR, 2012).

ii-   Cell death: the cell can die like millions of cells do naturally

iii-   Mutation: in a very small number of events, a damaged cell may exhibit a change in the cell's reproductive structure allowing the cell to regenerate as a potentially pre-cancerous cell. Over a period of many years or decades, this may result in a full blown, malignant cancer (USNRC, 2014).

Direct action is the predominant process with high linear energy transfer (LET) radiation (e.g. α-particles, proton, and neutrons) primarily because the ionization track is very dense. Direct action is associated with radiation effects for which a zero threshold dose is postulated. In this scenario, damage may be transmitted to succeeding generations of cells, making the damage in this instance cumulative with radiation dose.

Indirect Effect

The adult body is composed of 70% water. When ionizing radiation interacts with the body, electrons are ripped from water molecules leading to the production of free radicals that are chemically toxic (Cember, 1996).

The reactions are described by

$H_2O \rightleftharpoons H_2O + e^-$

$H_2O^+ \rightleftharpoons H^+ + OH^.$

$O_2 \rightleftharpoons O^- + O^+$
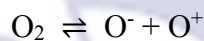
The hydroxyl radical ($OH^.$) is the major oxidizing agent resulting from ionization of water. Although free radicals are extremely reactive, most of the reactions recombine to form oxygen and water in about 10^{-5} seconds without causing any biological effects. However biological effects may occur if these free radicals interact with other chemical compounds which diffuse far enough to the damage critical cell components. Free radicals may act as oxidizing or reducing agents and form peroxides when they react with water, these may inactivate cellular mechanisms or interact with genetic material in the cell.

$OH^. + OH^. \rightleftharpoons H_2O_2$

[Roentgen, 2013].

Similarly, the free radicals combine to form gaseous hydrogen

41

$$H^+ + H^+ \longrightarrow H_2$$
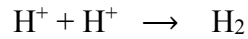
If the irradiated water contains dissolved oxygen, the free H^+ radical may combine with oxygen to form Hydroperoxyl radical

$$H^+ + O_2 \longrightarrow HO_2$$

The hydroperoxyl formed is not very reactive and has a longer lifetime than free $OH^.$ radical and is able to combine with free H^+ radical leading to the formation of H_2O_2.

$$HO_2 + H^+ \longrightarrow H_2O_2 \qquad \text{(Faanu, 2011)}.$$
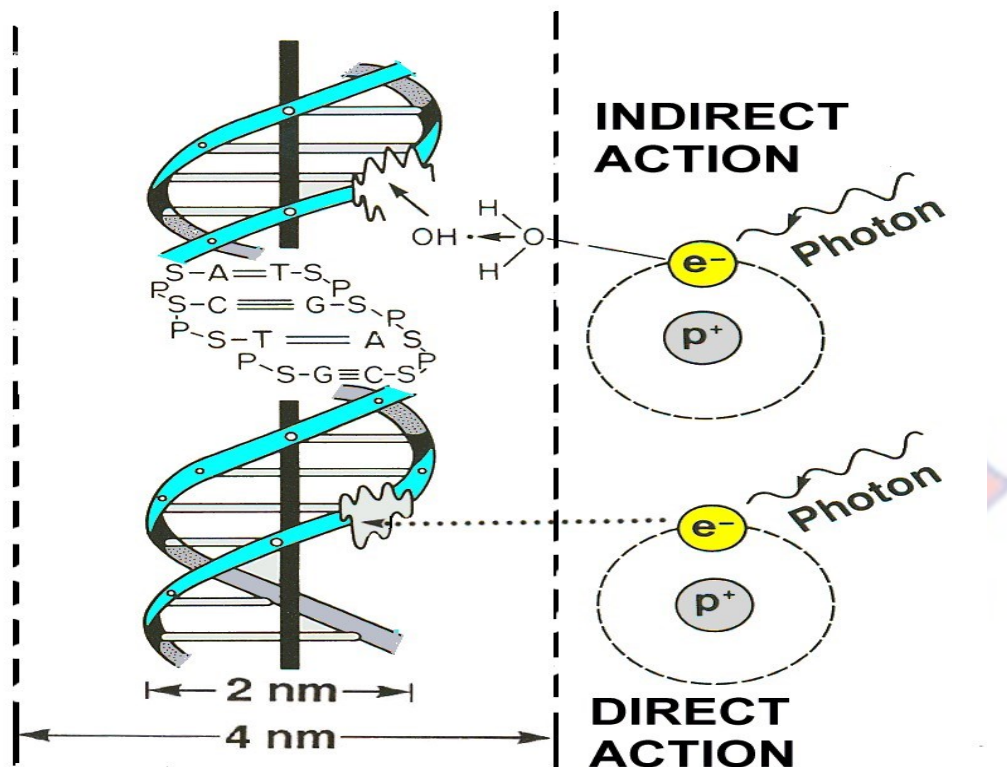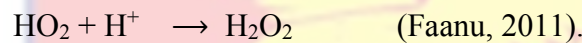
Figure 5: Mechanisms of direct and indirect actions on DNA helix

Trace Metals

Heavy/trace metal(loid)s hereto refered to as trace metals occur naturally in rocks and soils. Increasingly, higher levels of trace metals are being released into the environment due to human activities. The mobility and

42

bioavailability of metals to living organisms is due to their chemically reactive nature in the environment (Zovka & Romić, 2011).

Trace metals constitute an ill-defined group of inorganic chemical hazards. Trace metals that predominantly contaminate the environment are lead (Pb), chromium (Cr), arsenic (As), zinc (Zn), cadmium (Cd), copper (Cu), mercury (Hg), and nickel (Ni) (GWRTAC, 1997). Soils act as a major repository and as a source of pollution and medium of transfer of pollutants to ground water and the food chain, and then to human and/or animals (Khan, Rehman, Khan, Khan & Shah, 2010; Wuana & Okieimen, 2011). Most metals do not undergo microbial or chemical degradation (Kirpichtchikova, Manceau, Spadini, Panfili, Marcus & Jacquet, 2006), and their total concentration in soils persists for a long time after their introduction into the environment (Adriano, 2003). Changes in their chemical forms (speciation) and bioavailability are, however, possible (Wuana & Okieimen, 2011).

The risks and hazards to humans and the ecosystem from trace metal contaminated soil are through direct ingestion or contact with contaminated soil, the food chain (soil-plant-human or soil-plant-animal-human), drinking of contaminated ground water, reduction in food quality (safety and marketability) via phytotoxicity, reduction in land usability for agricultural production causing food insecurity, and land tenure problems (Ling, Shen, Gao, Gu, & Yan, 2007; McLaughlin, Zarcinas, Stevens & Cook, 2000a; McLaughlin, Hamon, McLaren, Speir &Rogers, 2000b).

Trace metals are a major component of environment. The ubiquity and pervasiveness of metals (e.g. Pb) is due, in part, to their widespread use in fuel, paint, manufacturing and refining (Caussy, Gochfeld, Gurzau, Neagu & Ruedel,

2003; Hivert, Coquet, Glorennc & Bard, 2002). Due to their non bio-degradable nature, their residence time in soil can be thousands of years (Ogunbanjo, Onawumi, Gbadamosi, Adejoke & Anselm, 2016; Semlali, Dessogne, Monna, Bolte, Azimi, Navarro, Denaix et al., 2004). To ensure public health, a better understanding of their distribution and potential health risks are of utmost importance (Ogunbanjo et al., 2016). Metal exposure in humans has been linked to a range of adverse health outcomes including carcinogenic, neurotoxic, hepatotoxic, genotoxic and mutagenic diseases (Jaishankar, Tseten, Anbalagan, Mathew & Beeregowda, 2014; Tchounwou, Yedjou, Patlolla & Sutton, 2012). They are typically systemic toxicants that induce a range of diseases, even at lower levels of exposure (Tchounwou et al. 2012). Lead, for example, has been demonstrated to lead to neurological damage, decreased cognitive function, increased blood pressure, seizures, coma and even death. Children are particularly susceptible to Pb exposure, with effects typically expressing as diminished educational outcomes, widening socio-economic achievement gap and inequalities that span across generations (Evens, Hryhorczuk, Lanphear, Rankin, Lewis, Forst & Rosenberg, 2015; Gould, 2009; McLaine, Navas-Acien, Lee, Simon, Diener-West & Agnew, 2013; Miranda, Kim, Reiter, Galeano & Maxson, 2009; NCHH, 2015; Reuben, Caspi, Belsky, Broadbent, Harrington, Sugden, Houts et al., 2017; Zhang, Baker, Tufts, Raymomd, Salihu & Elliott, 2013).

Neutron Activation Analysis

Neutron Activation Analysis (NAA) is a nuclear process used for determining the concentration of elements in a vast amount of materials. It allows the precise identification and quantification of the elements, above all of

44

the trace element in the sample. NAA has applications in Chemistry but also other research fields such as geology, archaeology, medicine, environmental monitoring and forensic science (Hamidatou, Slamene, Akhal & Zhouranen, 2013).

The sequence of events occurring during the most common type of nuclear reaction used for NAA, namely the neutron capture or (n, gamma) reaction is illustration by

$$n + {}^{A}Z \rightarrow {}^{A+1}Z^{*} \rightarrow {}^{A+1}Z + \gamma$$
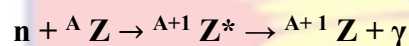
where ; ${}^{A}Z$ is the target nucleus

${}^{A+1}Z^{*}$ is a compound nucleus in an excited state which de-excite with the emission of   gamma ray called prompt gamma

${}^{A+1}Z$ is the product after irradiating the target nucleus which is radioactive

The radioactivity produced after irradiation is governed by the usual decay equation and generally represented by;

$$R = N \int \sigma\ (E)\ \phi\ (E)\ \delta E \qquad\qquad (2)$$

(Landsberger, 1994).

Where

R is the reaction rate, $\phi(E)\ \delta E$ is the neutron flux of neutrons with kinetic energy between E and $E + \delta E$ in $n \cdot cm^{-2}s^{-1}$, $\sigma\ (E)$ is the neutron capture cross-section in cm^{2} defined as the probability of a radioactive capture reaction occurring in a collision between a neutron and a nucleus given in terms of area and dependent on the energy of the incident neutron, N is the number of atoms of the element in the sample.

45

During neutron irradiations, the dominant reaction rates are the thermal and epithermal components and because the neutron cross-section of the fast neutrons (R_{fast}) is negligible the reaction rate of the fast neutron is small.

The activity of an element in a sample is given by the following general expression:

$$A = \sigma\phi\left(\frac{m}{M}\right)N_A SDC\theta P_\gamma\eta \qquad (3)$$

where;

A is the measured activity in Bq from a product of an expected reaction.

σ is the activation cross-section of the reaction in cm^2

ϕ is the activity neutron flux in $n\cdot cm^{-2}s^{-1}$

m is the mass of the element in g

M is the atomic weight of the element to be determined in $gmol^{-1}$

S is the saturation factor which is given by $S=[1-\exp(-\lambda t_1)]$, λ is the constant of the reactive product and t_1 is the duration of irradiation.

D is the decay factor and it is given by $D=\exp(-\lambda t_d)$ and t_d is the duration of decay.

C is the correction factor for nuclide decay during the counting time given by $C= [1-\exp(-\lambda t_c)]$ and t_c is the duration of counting.

N_A is the Avogrado's constant, which is 6.0228×10^{23} atoms/mol

θ is the relative natural isotropic abundance of the activated isotope.

P_γ is the probability of emission of photon with energy E and

η is the detector efficiency for the measured gamma radiation energy.

By using terms D & C and normalising, weights between standards and sample and performing irradiations, decay and counting times are normally

fixed for all samples and standards such that time dependent factors cancel. Other terms such as N, M, δ, ϕ, σ, S all cancel.

The overall equation becomes

$$C_{sam} = C_{std} \left(\frac{A_{sam}}{A_{std}}\right)\left(\frac{A_{std}}{D_{sam}}\right)\left(\frac{C_{std}}{A_{sam}}\right)\left(\frac{W_{std}}{W_{sam}}\right),$$

(4)

where W_{sam} and W_{std} are the weights of the sample and standard respectively.

C_{sam} is the unknown concentration of the element in the sample.

C_{std} is the known concentration of the element in the standard.

A_{sam} is the activity of the sample.

A_{std} is the activity of the standard

By the comparator method using the same geometry and equal weights of both sample and standard, the equation is simplified to

$$C_{sam} = C_{std} \left(\frac{A_{sam}}{A_{std}}\right)$$

(5)

Absolute Method

The absolute method uses the basic neutron activation equation and the accuracy of measurement in this mode is reliant on the accuracy of the nuclear constants, the accurate knowledge of the efficiency of the detector, the neutron flux, the counting statistics and source to detector geometry. For most elements, the errors in nuclear constants are less than 5% (IAEA - TECDOC – 564, 1990).

The nuclear constants are M, f, σ, Θ, λ and N_A. Equation (3) may be expressed in a simple form as (Osae, 1988):

$$m_i = \frac{D_i C_i}{\phi \delta_{(E)} B_i}$$

(6)

$$D_i = \frac{\lambda_i M_i}{\sigma_i \Theta_i N_A f_i G}$$

47

D_i is a constant, it is obtained for any element by using nuclear constants. Using D, ϕ, $\delta_{(E)}$, and B_i and analysing for C, the amount of the element, m_i, can be evaluated with Equation (6). To reduce the overall error, the Absolute Method is standardized (Osae, 1988; Osei, 2003). The Standardization of this procedure is to irradiate known standard reference material (SRM) of the element of interest and then determine the experimentally measured value using Equation (6) (Osei, 2003).

The correction factor, F, for the measured value is:

$$F = \frac{m_e}{m_{std}},$$

where m_e is the experimentally measured value and m_{std} is the known concentration

Single Relative Standardization Method

For stable neutron sources once the specific activities (sensitivities) of the elements of interest have been determined, samples can be irradiated without standards. As a precaution for unseen changes, it is a good practice to monitor the neutron flux within a series of experiments to check if the neutron flux is indeed stable. If conditions do not change with time, then the standardization can be done once.

Equation (5) can be re-arranged as

$$\frac{C_{sam}}{m_{sam}} = \frac{C_{std}}{m_{std}} = S.A \qquad (7)$$

where S.A is the specific activity or sensitivity of the element with regards to INAA

From Equation (7)

$$S.A = \frac{C_{sam}}{m_{sam}} \qquad (8)$$

The number of counts under a photo peak area and the specific activity of the element are used to determine the amount of the element in the sample using equation 8 (Osei, 2003).

Techniques

With respect to the time of measurement, NAA falls into two categories;

- Prompt gamma-ray neutron activation analysis (PGNAA) where measurements take place during irradiation.
- Delayed gamma-ray neutron activation analysis (DGNAA) where measurements follow radioactive decay (Hamidatou et al, 2013).

PGNAA technique is generally performed by using a beam of neutron extracted through a reactor beam part. Fluxes on samples irradiated in beams are in the order one million times lower than on samples inside a reactor but detectors can be placed very close to the sample compensating for much of the loss of sensitivity due to flux (Hamidatou et al, 2013). The PGNAA technique is most applicable to elements with extremely high neutron capture cross-sections (B, Cd, Sm and Gd); elements which decay too rapidly to be measured by DGNAA; elements that produce only stable isotopes (e.g. light elements); or elements with weak decay gamma-ray intensities, 2D, 3D-analysis of (main) elements distribution can be performed by PGNAA (Hamidatou et al, 2013).

DGNAA (convectional NAA) is useful for the vast majority of elements that produce radioactive nuclides. The technique is flexible with respect to time such that the sensitivity for a long-lived radionuclide that suffers from interference by a short-lived radionuclide can be improved by waiting for the short-lived radionuclide to decay or quite the contrary, the sensitivity for short-lived isotopes can be improved by reducing the time of irradiation to minimize

the interference of long-lived isotopes. The sensitivity is a key advantage of DGNAA over other analytical methods (Hamidatou et al, 2013). DGNAA was used in this study.

Concepts

Hamidatou et al., 2013 also reported that in the majority of INAA procedures, thermal reactor neutrons are used for the activation: neutrons in thermal equilibrium with their environment. Materials can be activated in any physical state, viz. solid, liquid or gaseous (Hamidatou et al, 2013).

The analytical procedure is based on four steps;

Step 1: Sample preparation; most cases only heating or freeze during crushing or pulverization, fractionating, evaporation or pre-concentration, sieving, homogenization, weighing, check of impurities (blank test), encapsulation and sealing irradiation vial (capsule) , as well as the selection of the best analytical process and the preparation of the standards (Hamidatou et al, 2013).

Step 2: Irradiation of samples can be taken from the various types of neutron sources according to need and availability. For INAA, short irradiations are done in Pneumatic Transfer System A of the Ghana Research Reactor-1 at a pressure of 45 to 50 kPa. The irradiation time was chosen according to the half-lives of the elements of interest (Hamidatou et al, 2013). For short-lived elements with half-lives up to 20 minutes, irradiation time of 30 seconds was chosen. For the medium-lived elements, that is, those with half-lives between 20 minutes and 3 days the irradiation times were between 10 and 60 minutes. For the long-lived elements, that is, those with half-lives greater than 3 days, the irradiation time was 6 hours (Osei, 2003).

50

Step 3: After irradiation, the capsule is taken from the reactor and allowed to decay until the level of activity was within the acceptable limit for handling. The irradiated samples are then removed from the capsule for counting. The irradiated samples are placed on the detector and the counts accumulated for a pre-selected time to obtain the spectra intensities. For short irradiation counting time of 600 s was found to be adequate (Hamidatou et al, 2013). For the medium and long irradiation, counting times are 1800 s and 3600 s, respectively. Quantitative and qualitative analysis are done using a PC based gamma spectrometry system consisting of HPGe detector and a multichannel analyzer (MCA) that convert the analog signals to digital and sort them according to their incoming energies (Serfor-Armah, Nyarko, Carboo, Osae, Anim-Sarpong & Akaho, 2000; Osei, 2003). In NAA, nearly exclusively the (energy of the) gamma radiation is measured because of its higher penetration power of this type of radiation and the selectivity can be obtained from distinct energies of the photons-differently from beta radiation which is a radiation which is a continuous energy distribution. The interaction of gamma and X-radiation with matter results among others in ionization processes and subsequent generation of electrical signals that can be detected and recorded.

Step 4: Measurement, evaluation and calculation involve taking gamma spectra and then calculating trace element concentration of sample and preparation of the NAA report.

Instrumentation

The instrumentation used to measure gamma rays from radioactive samples generally consists of a semiconductor detector, associated electronics

and a computer-based multi-channel analyzer (MCA/computer) (Hamidatou et al, 2013).

Most NAA laboratories operate one or more high purity germanium (HPGe) detectors, which operate at liquid nitrogen temperature (77.0 K). Although HPGe detectors come in different shapes and sizes, the most common shape is coaxial (Hamidatou et al, 2013). These detectors are very useful for the measurement of gamma rays with energies in the range from about 60 KeV to 3.0 MeV. The two most important characteristics of an HPGe detector are its resolution and efficiency. Other characteristics to consider are peak shapes, peak-to-Compton ratio, pulse rise time, crystal dimensions or shape and price (Hamidatou et al, 2013).
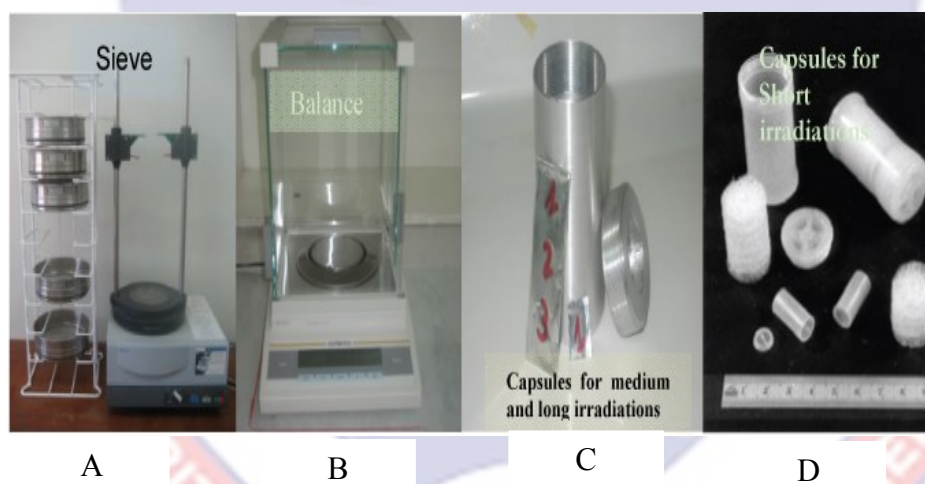
Figure 6: Instruments (A & B) and materials (C & D) used for the sample Preparation.
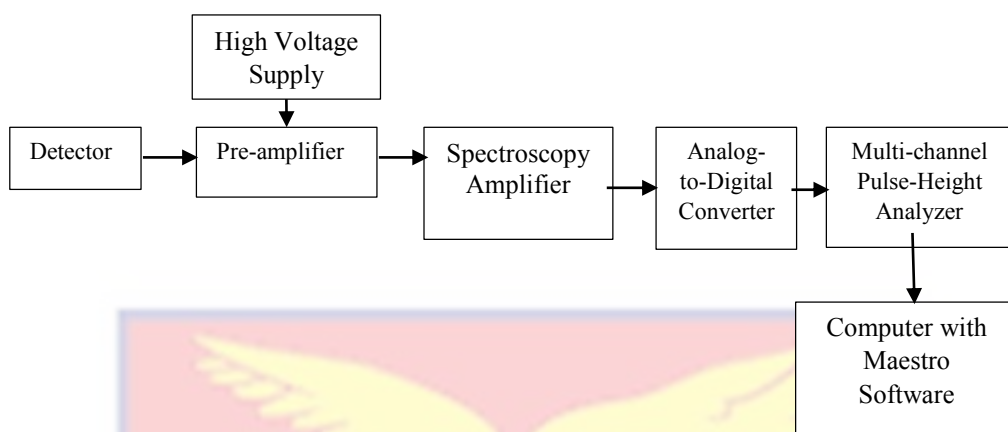
Figure 7: Schematic diagram of the gamma spectrometry system at GHARR-1 used for this study.

Figure 8: Detector system at GHARR-1 used in this study.

Summary

This chapter is a review of the literature on radionuclides, trace metals from oil and gas drilling activities past, and present, their influence on the environment to emphasize their relevance for environmental contamination studies

CHAPTER THREE

METHODOLOGY

Introduction

Areas associated with significant oil and gas exploration and drilling activities are most likely to experience challenges with radionuclides and heavy metals due to the generation and release of contaminated produced water and solid wastes (Christie, 2012). The Tano Basin in Ghana is one such area with high level of commercial oil and gas industry since 2007 (Dailly, Henderson, Hudgens, Kanschat & Lowry, 2012). This chapter presents the multi-step procedure comprising data collection, exposure assessment, toxicity assessment and risk characterization that was adopted to analyse the environmental contaminant of concern. Environmental analytical methods (including atomic abdorption spectroscopy, neutron activation analysis, and gamma-ray spectrometry) were utilised in the study and the data informed contaminant exposure studies. Trace metal data were explored using GIS, allowing spatial and temporal trends to be investigated.

Methods

This chapter is a description of the location and geology of the study area, sampling protocol, sample preparation and analysis. It also entails detailed description of the methodology adopted for the calculation of concentration of radionuclides and hence estimation of effective doses to the public. Determination of heavy metals both in water and soil samples as well as physical parameters of water samples are also described. First sampling was undertaken in June, 2014 and the second sampling in February, 2015 to account for both wet and dry seasons.
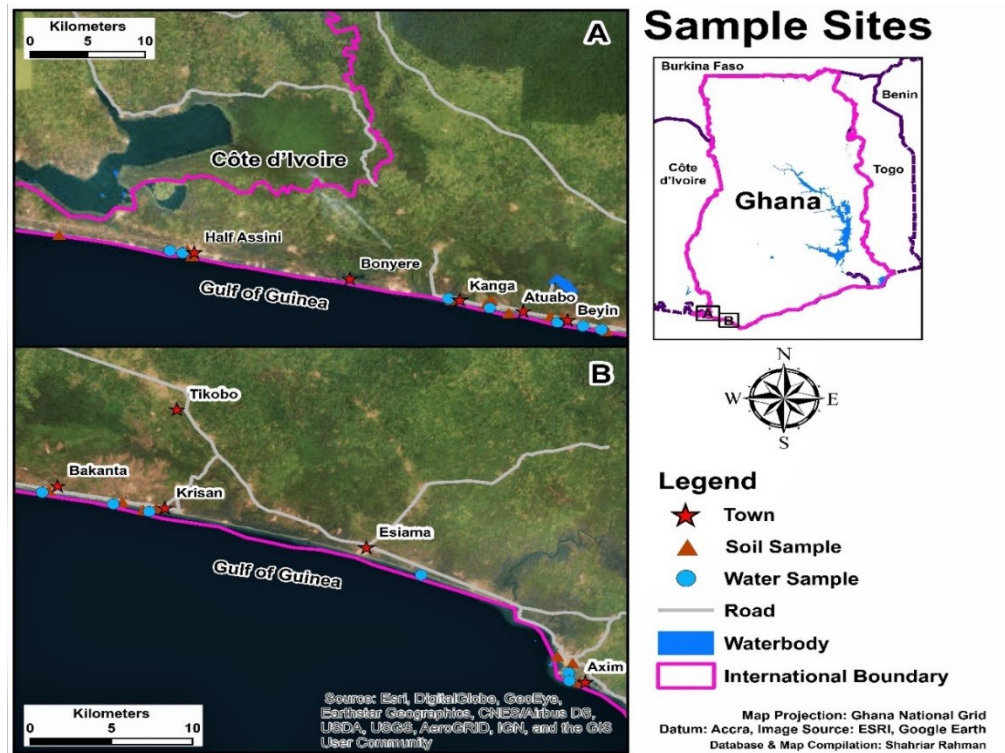
Figure 9: Map of Sampling Locations in the Communities.

Study Area

The study was carried out in the coastal communities along the Jubilee oil field of Ghana. The selected Districts are the coastal Districts of Ezema East, Ellembelle and Jomoro with Axim, Atuabo, Nyale Kplole, Ekebaku, Beyin, Ellonyi, Kengen, Krisan, Twerene, and Half Assini as selected coastal towns and villages.

Table 6: A table of the communities' population distribution along the Jubilee oil field

No.	TOWN	LOCATION COORDINATES	DISTRICT	DISTRCT POPULATION FOR 2010
1	Axim	4º 52' 6" N 2º 14' 29" W	Nzema East	60,828
2	Atuabo	5º 3' 0" N 2º 52' 60" W	Ellembelle	87,501
3	Nyale Kplole	4º 57' 60" N 2º 28' 47" W	Ellembelle	87,501
4	Ekebaku		Ellembelle	87,501
5	Beyin	4º 59' 6" N 2º 35' 13" W	Jomoro	150,10
6	Ellonyi		Jomoro	150,10
7	Kengen	4º 59' 53" N 2º 38' 40" W	Jomoro	150,10
8	Krisan	4º96'	Ellembelle	87,501
9	Twerene		Jomoro	150,10
10	Half Assini	5º 3' 0" N 2º 53' 0" W	Jomoro	150,10
11	Newtown	5º 6' 60 N 3º 4' 60" W	Jomoro	150,10

Source: Field work, 2016

Geology of the Study Area

The Tano-Cape Three Points Basin is a Cretaceous wrench modified pull-apart basin bounded by the Saltpond Basin in the East and the St. Paul Fracture Zone in the West. The basin is the eastern extension of the Cote d'Ivoire-Ghana Basin and formed as a result of trans-tensional movement during the separation of Africa and South America, and the opening of the Atlantic Ocean in the Albian. Active rifting and subsidence during this period resulted in the formation of a deep basin. Prevailing conditions at the time were ideal for the deposition of shales, thus thick organic rich shale was deposited in the Cenomanian and Turonian.

Several river systems contributed significant clastics into the deep basin and led to deposition of large turbidite fan/channel complexes. The working play type is the Cretaceous Play, which consists of Cenomanian-Turonian and

Albian shales as source rocks with Turonian slope fan turbidite sandstones and Albian sandstones in tilted fault blocks as reservoirs. Trapping is both stratigraphic and structural (Petroleum Commission of Ghana, 2014). In the Upper Cretaceous, the Tano basin became a depositional focus, and a thick clastic sequence consisting of fluvial and lacustrine facies was deposited. This sequence, in addition to the thin Tertiary section, provided adequate thickness to mature the Cretaceous source rocks in the central and western region of the Tano Basin.

Rapid drowning of the West African Transform Margin created ideal conditions for deposition of thick rich source rock in the Cenomanian. Creation of a deep basin with significant river systems onshore, led to the deposition of large turbidite fan/channel complexes (forming stratigraphic traps for oil) in deep water(Atta-Peters & Garrey, 2014). The basin (Cretaceous to Eocene) forms part of the broad Apollonian Formation occupying the southwest corner of Ghana and larger portion of southeast Côte d'Ivoire (Atta-Peters & Garrey, 2014). The rocks onshore consist of alternating sands, clays and limestones with gentle dips overlying the Precambrian metamorphosed Birimian System composed of schist, phyllite and greywackes (Atta-Peters & Garrey, 2014).

At depth, the sands and clays are more compact and pass into sandstones and shales. The basin comprises a thick Upper Cretaceous drift section which is dominated by basin floor fans, stratigraphic traps and channel systems (Adda, 2013). The rift section comprises shallow marine to continental deposits. The working play type is the Cretaceous Play, which consists of Cenomanian and Albian shales as source rocks with Turonian slope fan turbidite sandstones and Albian sandstones in tilted fault blocks as reservoirs. Trapping is both

stratigraphic and structural (Adda, 2013). As reservoir rocks are predicted to be in close proximity to the source rocks, a minimal hydrocarbon migration pathway is assumed. The prolific Tano Basin is thus the results of

- an exceptionally favourable coincidence of regional geological factors

- rich source rocks deposited and matured for oil

- tectonics and structural geology establishing framework for focusing charge

- world class turbidite reservoirs deposited in giant statigraphic traps

- highly effective seals preserving oil and gas for discovery and development (Atta-Peters & Garrey, 2014).

Meteorological Data of the Study Area

The Jubilee Oil Field is located offshore the Western Region of Ghana. The meteorological data presented were obtained from Tullow Ghana Limited, 2009. Figure 9 shows the location of communities along the Jubilee oil field and where sampling was carried out. Table 6 shows the communities and their population distribution along the oil field. The major community is Axim. Subsistence farming is the main occupation of the people. Axim is the only coastal town with long term climatic data within the vicinity of the Jubilee Field and study area. Axim experiences rainfall throughout the year. A bi-modal pattern is observed with peaks in May-June and October. The mean peak value for Axim is about 460 mm, normally in June. Axim experiences lowest rainfall of 51 mm in January. Rainfall over the sea is similar to that over land with the months of highest observed rainfall in May-June and September-October (Tullow Ghana Limited, 2009).
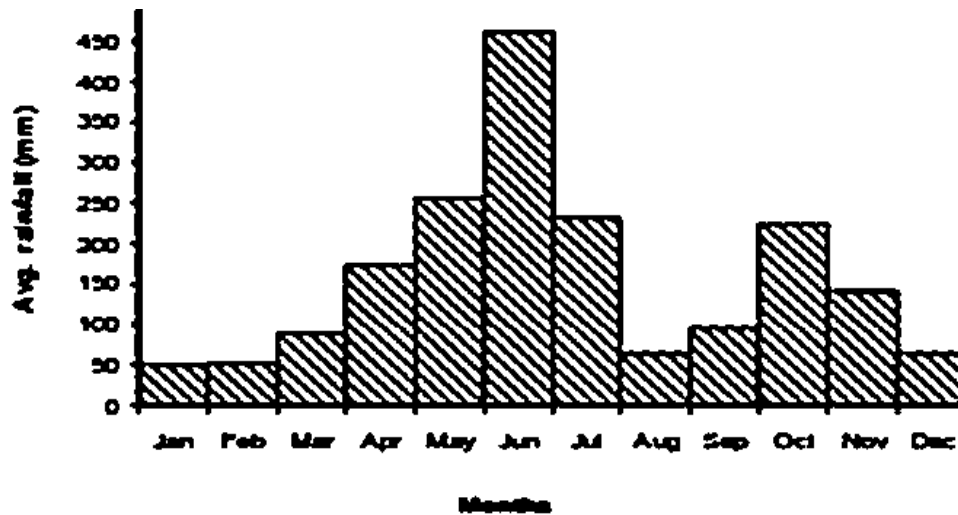
Figure 10: Precipitation Data for Axim from 1999 to 2008
Source: Tullow Ghana Limited, 2009.

Annual temperature pattern in Axim generally range between 24 and 30°C. Temperature is generally high from February to May and from November to December with peak temperatures recorded in March. Lower temperatures were recorded between June and October with the coolest month usually being August. The 10 year average for Axim was 28.3°C between 1998 and 2008.
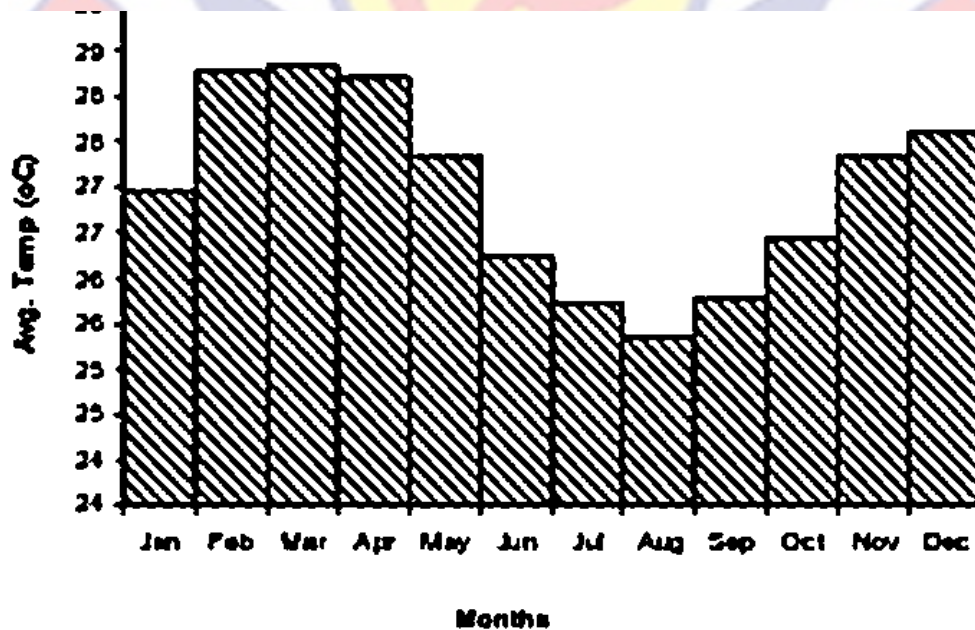
Figure 11: Temperature data for Axim from 1999 to 2008
Source: Tullow Ghana Limited, 2009.

59

Sampling

Soil

In each community, the community was divided into four (4) zones after the initial survey using a Geographical Positioning System (GPS). The sampling strategy that was adopted for the soil samples was random (IAEA, 2004; Faanu, 2011). Samples were randomly collected within defined boundaries of the area of concern within each area earmarked for sampling. Each sampling point was selected independent of the location of all other sampling points. All locations within the area of concern had equal chance of being sampled using this procedure. The soil samples were taken using a plastic trowel to a depth of 5 to 10 cm. This is the normal depth at which human beings will be exposed directly and also is the average depth the tubers of cassava will grow. Sampling locations were selected based on accessibility to the public especially children. Soil samples were collected using a plastic trowel that was wiped clean each time prior to sampling using KimWipes and deionised water. Before sampling commenced, the trowel was passed through soils immediately adjacent to the sample site to remove any possible effects associated with the previous sample site. A minimum of ten soil samples were taken from each geological zone (n = 26) in hermetically sealed non-coloured polyethylene ziplock bags and transported to the laboratory, dried, sieved and homogenized into a composite sample.

Water

The groundwater samples were taken from the drinking water sources in the communities such as boreholes, taps and mechanized pipes. The samples were collected using the normal process used by the community into labelled

60

500 mL plastic bottles. The bottles were acid washed with concentrated HNO_3 and treated with methylated spirit prior to sampling (Faanu, 2011). This is to ensure that radionuclides remain in solution rather than adhering to the walls of the container and to remove anions from the container. The bottles were rinsed with deionized water and equally rinsed with water to be sampled before being filled to the brim without any head space to prevent the escape of radon and CO_2 being trapped in the water. The pH of the water samples were measured insitu using pH meter model WTW pH 3110 in conjunction with a glass electrode with a calomel reference electrode. The pH meter was calibrated with standard buffer solutions with pH 4.01, 7.0 and 9.21. The TDS and conductivity was measured using conductivity meter WTW cond. 3210. The equipment was calibrated with the following standard solutions, 0.01M KCl with absorbance of 1413 μs/cm and 0.1M KCl with absorbance of 12880 μs/cm.

Figure 12: The Sampled Boreholes at Ellonyi.

Figure 13: One of the Sampled Wells at Beyin.

Food Sampling

About 3kg of cassava tubers were sampled from farms in the different communities. Cassava was selected because it is the food crop that is common to all the sampled communities and is a major staple. Samples were randomly collected within defined boundaries of the area of concern within each area earmarked for soil sampling. The samples were transported in non-coloured hermetically sealed zipper lock bags to the laboratory.

Sample Preparation for Gamma Spectrometry

Soil

The soil samples were air dried in trays for 2 weeks and the oven dried at a temperature of 105°C for 3 to 4 minutes until the samples were well dried. The samples were milled into fine powder using Laboratory Mortar Grinder (Pulverisette-2) at the A. Chatt Chemical Laboratory of the Ghana Atomic Energy Commission. The milled samples were sieved through a 2 mm pore size mesh, homogenized and 1 kg of each composite sample weighed into 1 L

Marinelli beakers. The beakers were covered and sealed with a paper tape to prevent the escape of the gaseous radionuclides in the sample. The samples were stored for at least 30 days to allow for secular equilibrium between the log-lived parent radionuclides and their short-lived progeny radionuclides in the ^{238}U and ^{232}Th decay series. The samples were counted on a high purity germanium (HPGe) detector for 36000 s (10 hours).

The method of the γ-ray analysis reported in published research works (Darko, Tetteh & Akaho, 2005 and Ademola, 2011) was adopted for this study. The gamma spectrometer used for the analysis consists of an ORTEC GEM Coaxial n-type HPGe gamma-ray detector with ORTEC Multichannel Analyzer (MCA) and MAESTRO-32 evaluation software for spectrum acquisition and processing. The relative efficiency of the detector was 28.5 % with energy resolution of 1.8 keV at gamma ray energy of 1332 keV of ^{60}Co. ^{238}U was determined from average of 295.25 keV peak of ^{214}Pb and 1764.5 keV peak of ^{214}Bi. The gamma lines 583.19 keV and 2614.53 keV of ^{208}Tl were used to determine ^{232}Th and that of ^{40}K was determined from the gamma line of 1460.83 keV.

Water

Water samples were filtered to remove all suspended particles. One (1) litre of each water sample was measured into Marinelli beaker and counted on an HPGE detector for 36000 s. The activity concentration of ^{226}Ra, ^{228}Ra and ^{40}K were then determined. The Marinelli beakers were decontaminated by cleaning them well using diluted hydrochloric acid solution and de-ionized water. The beakers were then dried using a temperature controlled oven and filled with appropriate amount of water sample. The caps of the filled Marinelli

beakers were then firmly closed and wrapped with thick vinyl tape around their necks and kept for 4 weeks for achieving the secular equilibrium between gaseous and non-gaseous decay products of naturally occurring radionuclide series before being counted.

Food

The sampled cassava were thoroughly cleaned and the edible portions chopped and air dried for a week. The samples were freeze dried using freeze drier model CHRIST Gamma 2 – 16 LSC. The samples were ground into fine powder using Laboratory Mortar Grinder (Pulverisette-2) at the A. Chatt Chemical Laboratory of the Ghana Atomic Energy Commission and sieved through 2mm mesh. 300 g of the sieved cassava samples were weighed into a 1 L Marinelli beaker. The samples were counted using an HPGe detector for 36000 s and the activity concentration of ^{238}U, ^{232}Th and ^{40}K determined.

Sample Analysis, Instrument Calibration and Measurements

The activity concentrations of the radionuclides in the samples were measured using a High Purity Germanium Detector (HPGE) detector. Gamma rays of soil, water and food samples were measured by direct instrumental analysis without pre-treatment. The gamma spectrometry system consists of an n-type HPGE detector (ORTEC) coupled to a computer based multi-channel analyser (MCA) mounted in a cylindrical lead shield (100 mm thick) and cooled in liquid nitrogen. The relative efficiency of the detector was 20 % with energy resolution of 1.8 keV at gamma ray energy of 1332 keV of ^{60}Co. The radionuclides were identified using gamma ray spectrum analysis software, ORTEC MAESTRO-32.

The background spectra were determined using an empty Marinelli beaker and used to correct the net peak area of gamma rays of measured isotopes. The energy and efficiency calibration were performed using multi gamma solid water standard in a 1 litre Marinelli beaker in the energy range of 60 keV to ~2000 keV. The standard radionuclides are uniformly distributed in solid water with volume and density of 1000ml and 1.0 g/m^3 respectively (source number, NW146) and manufactured by QSA Global GmbH, Germany. The gamma emitting radionuclides used for the calibration in the Marinelli beaker geometry were: ^{57}Co (122 keV), ^{137}Cs (662 keV), ^{60}Co (1173 and 1333 keV) and ^{88}Y (1838 keV) with certified uncertainties ≤3 %.

Calibration of the Gamma Spectrometry System

Prior to the measurements, the detector and measuring assembly were calibrated for energy and efficiency to enable both qualitative and quantitative analysis of the samples to be performed. The energy and efficiency calibrations were performed using mixed radionuclide calibration standard homogenously distributed in the form of solid water, serial number NW 146 with approximate volume 1000 mL and density 1.0 g cm^{-3} in a 1.0 L Marinelli beaker. The standard was supplied by Deutscher Kalibrierdienst (DKD-3), QSA Global GmBH, Germany and contains radionuclides with known energies (^{241}Am (59.54 keV), ^{109}Cd (88.03 keV), ^{57}Co (122.06 keV), ^{139}Ce (165.86 keV), ^{203}Hg (279.20 keV), ^{113}Sn (391.69 keV), ^{85}Sr (514.01 keV), ^{137}Cs (661.66 keV), ^{60}Co (1173.2 keV and 1332.5 keV) and ^{88}Y (898.04 keV and 1836.1 keV) and activities in a 1000 ml Marinelli beaker was used.

Energy Calibration

The energy calibration was performed by matching the principal gamma rays observed in the spectrum of the standard to the channel numbers. The formula relating the energy and the channel number was expressed as

$$E = A_0 + A_1 \cdot CN \tag{9}$$

Where E is the energy, CN is the channel number for a given radionuclide, and A_0 and A_1 are calibration constants for a given geometry. A graph of energy against channel number was plotted as shown in Figure 14 (page 121).

From the energy calibration curve the following expression was obtained:

$$E = 15.33 + 1.265\, CN \tag{10}$$

Efficiency Calibration

The efficiency calibration was performed by acquiring a spectrum of the standard until the count rate of total absorption could be calculated with a statistical uncertainty of <1% at a confidence level of 95%. The net count rate was determined at the photo peaks for all the energies to be used for the calculation of the efficiency. The efficiency was then related to the count rate and the activity of the standard by

$$\eta = \frac{N_T - N_B}{P_E \cdot A_{STD} \cdot T_{STD}} \tag{11}$$

Where P_E is the gamma ray emission probability for the energy E,

$\eta(E)$ is the efficiency of the detector,

N_T is the total count under a photopeak in a peak range,

N_B is the background counts,

66

A_{STD} is the activity of the calibration standard for a given radionuclide in Bq at the time of measurement and

T_{STD} is the counting time of the standard.

The efficiency is related to the energy by the expression.

$$\ln \eta(E) = B_0 + B_1\ln E + B_2(\ln E)^2 \qquad (12)$$

Where, B_0, B_1, B_2 are calibration constants for a given geometry and the other symbols have the usual meaning given earlier in the passage. The efficiency calibration curve is shown in Figure 15. From the efficiency calibration curve the following expression was obtained:

$$\ln\eta = 3.202 - 0.88\ln E_\gamma \qquad (13)$$

$$\text{for } E_\gamma > 100 \text{ keV}$$

Validation of Analytical Method

The applicability of the analytical system as well as the method quality control was cross checked using certified reference materials containing concentrations comparable to NORM values. The certified reference material with Source no. 146 and certificate provided in Tables 7 and 57 (Apendix I) were within 95% of confidence level prepared in the powder matrix containing ^{238}U, ^{232}Th and ^{40}K in secular equilibrium and were used. The reference materials were placed in 1.0 L Marinelli beaker sealed and then left undisturbed for at least 3 weeks in order to establish radioactive equilibrium in ^{226}Ra decay chain segment prior to being measured. ^{238}U was determined from average of 295.25 keV peak of ^{214}Pb and 1764.5 keV peak of ^{214}Bi. The gamma lines 583.19 keV and 2614.53 keV of ^{208}Tl were used to determine ^{232}Th and that of ^{40}K was determined from the gamma line of 1460.83 keV. The activity concentrations of the reference materials were then evaluated using equation 15

67

as reported in this study and compared to the certified material activity. The results had an overall relative discrepancy of less than 5% among certified central values.

Table 7: Analytical results (mg/kg) of IAEA Certifed Reference Material used for calibrating the gamma spectrometry system

Nuclide	Certified Activity	Observed Activity
Americium-241	2.97E03	2.99E03
Cadmiun-109	1.69E04	1.67E04
Cobalt-57	8.84E02	8.84E02
Cerium-139	9.66E02	9.71E02
Mercury-203	2.56E03	2.56E03
Tin-113	3.18E03	3.20E03
Strontium-85	3.89E03	3.89E03
Caecium-137	2.78E03	2.75E03
Yitrium-88	6.62E03	6.65E03
Cobalt-60	3.40E03	3.42E03
Cobalt-60	3.40E03	3.40E03
Yitrium-88	6.62E03	6.60E03

Source no. : NW 146

Determination of Minimum Detectable Activity

Minimum detectable activity (MDA) is defined as the smallest quantity of radioactivity that could be measured under specified conditions. The MDA is an important concept in low level counting particularly in environmental level systems where the count rate of a sample is almost the same as the count rate of the background. Under these conditions, the background is counted with a blank, such as sample holder, and everything else that may be counted with an actual sample. In this work, 1liter Marinelli beaker filled with distilled water was counted for 36000s and the average background peaks used to determine MDA (Cember, 1996). For (^{238}U decay series), the minimum detectable activity was determined using average peak areas of the daughter gamma ray lines 295.2, 351.9 keV of ^{214}Pb and 609.31, 1764.5 keV of ^{214}Bi. The daughter gamma ray lines of 238.63 keV of 212Pb, 583.2 and 2614.53 keV of ^{208}Tl and 911.21keV of ^{228}Ac keV were used to determine the MDA of ^{232}Th. The MDA

68

of 40 using the gamma ray line at 1460.8 keV. The minimum detectable activities (MDA) were calculated according to formula

$$MDA = \frac{\delta\sqrt{B}}{\eta.P.T.W} \ (Bq/kg) \tag{14}$$

where;

is the statistical coverage factor equal to 1.645(confidence level 95%),

B is the background for the region of interest of each radionuclide,

T is the counting time in seconds,

P is the gamma emission probability (gamma yield) of each radionuclide,

W is the weight of the sample container, and

η is the detector efficiency for the measured gamma ray energy.

Determination of Activity Concentrations

The activity concentrations of ^{238}U, ^{232}Th and ^{40}K was determined in the soil and water samples were calculated using the following analytical expression as shown in equation (ASTM, 2005; Darko, Faanu, Razak, Emi-Reynolds, Yeboah & Oppon, 2010).

$$A_{sp} = \frac{N_D e^{\lambda_p T_d}}{p.T_c.\eta.m} \tag{15}$$

Where;

N is the net counts of the radionuclide in the samples,

Td is the delay time between sampling and counting,

P is the gamma emission probability (gamma yield),

η is the absolute counting efficiency of the detector system,

Tc is the sample counting time,

m is the mass of the sample (kg) or volume (l),

$e^{\lambda_p T_d}$ is the decay correction factor for delay between time of sampling and counting, and

p is the decay constant of the parent radionuclide.

Calculation of Annual Effective Dose from External Gamma Dose Rate Measurements

At each sampling location, outdoor external gamma dose rates were measured using a digital environmental gamma survey meter (RADEYE, G-10, Germany). The dose rate meter was calibrated at the Secondary Standard Dosimetry Laboratory (SSDL) of the Radiation Protection Institute of Ghana Atomic Energy Commission with a calibration factor provided. At each location, five measurements were made at 1 meter above the ground and the average value taken in μGy/h. The annual effective dose ($E_{\gamma, ext}$) was then estimated from the measured average outdoor external gamma dose rate from the equation below:

$$E_{\gamma,\ ext} = D_{\gamma,ext}\, T_{exp} DCF_{ext} \tag{16}$$

where;

$D_{\gamma, ext}$ is the average outdoor external gamma dose rate μGy/h,

T_{exp} is the exposure duration per year, 8760 hours (365 days) and applying an outdoor occupancy factor of 0.2,

DCF_{ext} is the effective dose to absorbed dose conversion factor of 0.7 Sv/Gy for environmental exposure to gamma rays (UNSCEAR, 2000).

70

Calculation of Absorbed Dose Rate and Annual Effective Dose due to

Radioactivity in Soil Samples

The activity concentrations of ^{238}U in soil samples was calculated from the average energies of 295.21 and 351.92 of ^{214}Pb and 609.31, 1764.49 keV of ^{214}Bi. The activity concentrations of ^{214}Pb and ^{214}Bi in secular equilibrium with their parents were assumed to represent ^{238}U activity concentration. The activity concentrations of ^{232}Th was determined from the average energies of 238.63keV of ^{212}Pb, 583.19 and 2614.53 keV of ^{208}Tl and 911.21 keV for ^{228}Ac respectively. The activity concentrations of ^{208}Tl and ^{228}Ac in equilibrium with their parents were also assumed to represent the activity concentration of ^{232}Th. The activity concentration of ^{40}K was determined from the energy of 1460.83 keV. The external gamma dose rate from the samples was calculated from the activity concentrations of the relevant radionuclides from equation

$$D\ (nGyh^{-1}) = 0.041A_K + 0.462A_U + 0.604A_{Th} \qquad (17)$$

where

A_K, A_U and A_{Th} are the activity concentrations of ^{40}K, ^{238}U and ^{232}Th respectively. Table 8 is table of dose conversion factors of ^{40}K, ^{238}U, and ^{232}Th.

Table 8: Activity to dose rate conversion factors

Radionuclide	Dose Coefficient (nGy/h per Bq/kg)
^{40}K	0.0417
^{238}U	0.462
^{232}Th	0.604

Source: (UNSCEAR, 2000)

The absorbed dose rate in air however translates to the annual effective dose rate indoors for individuals using the values of the absorbed dose rate in

indoor air, $D(nGy.h^{-1})$, the indoor occupancy time and the absorbed dose to the effective dose conversion factor($0.7\ Sv.Gy^{-1}$).

The annual effective dose in unit of mSv/y was derived by converting the total absorbed dose in nGy/h and multiplying by time T of one year using the equation

$$H_E = D(nGyh^{-1}) \times T(hy^{-1}) \times F(\mu Svy^{-1}) \qquad (18)$$

where

D is the calculated dose rate,

T is time in hours for a year given for a factor of exposure 0.20 per day throughout the year i.e. $T = 0.20(24)\left(365 + \frac{1}{4}\right)\ hy^{-1} \qquad (19)$

F is the conversion factor given as $0.7\text{x}\ 10^{-3}\mu Sv/y$ (UNSCEAR, 1993; 2000), Fasasi, Oyawale, Mokobia, Tchokossa & Ajayi, 2003).

Equations 17 to 19 were implemented in EXCEL spreadsheet with the concentrations of Table 8 for calculating absorbed and annual effective doses (Table 19).

In the case of the water samples, the committed effective doses ($H_{E,ing}$) were estimated from the activity concentrations of each individual radionuclide and applying the yearly water consumption rate for adults of 730 L/year (2 L/day multiplied by 365 days). The dose conversion factors of ^{228}Ra, ^{226}Ra and ^{40}K taken from the BSS and UNSCEAR report, (IAEA, 1996 and UNSCEAR, 2000) using equation

$$\text{HE}, \gamma_{ing}(w) = A_{sp}(w).I(w).\Sigma DCF_{Ing}\ (^{226}\text{Ra},\ ^{228}\text{Ra},\ ^{40}\text{K}) \qquad (20)$$

where,

Asp (w) is the activity concentration of the radionuclides in a sample in Bq/L,

I (w) is intake of water in litres per year, and

DCF$_{Ing}$ is the ingestion dose coefficient in Sv/Bq taken from the BSS (IAEA, 1996).

The committed effective dose is the arithmetic summation of the effective dose of the three radionuclide measured.

Table 9: Committed effective dose conversion factor (Sv/Bq) for members of the public

Radionuclide	Infant ≤ 1year	Children 1 – 12 years	Teenagers 13 – 17 years	Adults >17 years
^{226}Ra	4.7 E-06	6.2 E-07	1.5E-06	2.8E-07
^{228}Ra	3.0 E-05	3.4 E-06	5.3 E-06	6.2 E-07
^{40}K	6.2 E-08	2.1 E-08	7.6 E-09	6.2 E-09
Volume of Water/L/day	0.5	1.0	2.0	2.0

Source: (WHO, 2008 and IAEA, 1996)

The estimated annual effective dose by ingestion of radon was calculated because of habitual consumption of water by dwellers. It was computed using the formula below:

$$H_{E,ing} \text{ (Rn)} = Cw \cdot CRw \cdot Dcw \qquad (21)$$

where

$H_{E,ing}$ (Rn) is the annual effective dose (μSvy^{-1}) due to ingestion of radon from the consumption of water;

Cw is the concentration of Rn-222 in the ingested drinking water (Bq l^{-1});

CRw is the annual intake of drinking water (1 y^{-1}), and

Dcw is the ingested dose conversion factor for ^{222}Rn (SvBq^{-1}).

A dose conversion factor of 5 x 10^{-9} Sv Bq^{-1} was used as suggested by the United Nations Scientific Committee on the Effects of Atomic Radiation (UNSCEAR). Annual effective dose due to intake of ^{222}Rn from drinking water is calculated considering that an adult. An average of 730 L water was estimated annually for an adult (Age > 18y) (Cevik, Damla & Karahan, 2006).

73

For the food samples, annual effective dose was calculated by applying the consumption rate of root crop of 170 kg/year, the activity concentrations of ^{238}U, ^{232}Th and ^{40}K and their dose conversion factors.

$$E_{ing}(f) = A_{sp}(f).I(f).\Sigma DCF_{Ing} \ (^{238}\mathbf{U}, \ ^{232}\mathbf{Th}, \ ^{40}\mathbf{K}) \qquad (22)$$

Where,

Asp (f) is the activity concentration of the radionuclides in a sample in Bq/kg,

I (f) is intake of foodstuff in kg per year, and

DCF_{Ing} is the ingestion dose coefficient for the public were 4.5 x 10^{-5}, 7.2×10^{-5}, 6.2×10^{-6} for ^{238}U, ^{232}Th, and ^{40}K respectively.

The annual consumption rate of root tubers was calculated to be 170 kg /year (ICRP, 2007; BSS IAEA, 1996).

Determination of the concentration of metals in soil and water samples by NAA

Soil samples were prepared by weighing 0.1 g of the finely ground powder into a polyethylene film, sealed using a soldering rod and labelled with the sample code. The sample was then placed in a polyethylene capsule and sealed again before the samples were irradiated. For the water samples, 0.5 g of each sample was prepared into a polyethylene vial of 1.2 cm diameter and 2.3 cm height for irradiation. In order to ensure the sample is maintained intact during the irradiation, the sample was doubly encapsulated by placing the smaller polyethylene vial into a bigger capsule of diameter 1.6 cm and height of 5.5 cm. The IAEA-SOIL-7 reference material was used for the validation and analysis of Cu, Fe and Zn. The concentration of the metals was quantified by comparator method using the same geometry, equal weights of both sample and

standard, with the same irradiation, decay and counting times as follows (Landsberger, 1994).

$$C_{sam} = C_{std}\left(\frac{A_{sam}}{A_{std}}\right)$$ (23)

Where;

C_{sam} is the unknown concentration of the element in the sample,

C_{std} is the known concentration of the element in the standard,

A_{sam} is the activity of the sample and

A_{std} is the activity of the standard.

Quality Assurance and Quality Control

In order to assess the accuracy of the results obtained by the NAA analytical method in this study, the NAA method was used to measure Cu, Fe and Zn concentrations in the IAEA-SOIL-7 reference material in triplicate. The results of the observed metal concentrations were within the 95% confidence interval of the certified values as presented in Table 10.

Table 10: Analytical results (mg/kg) of IAEA-SOIL-7 certified reference material

Element	Certified values, mg/kg	Observed values, mg/kg
Cu	11	12
Fe	25700	25525
Zn	104	111

Source: Laboratory work, 2016

Measurement of Airborne Radon Activity Concentrations and

Calculation of Inhalation Dose

Air borne radon activity concentrations were measured directly with a Genitron Alpha Guard, Model PQ 2000/mp50. The measurements were carried out indoor in residential areas. The Alpha Guard is provided with a large surface

glass fibre filter, which allows only the gaseous Rn to pass through whilst the radon progeny are prevented from entering the ionisation chamber. The filter also protects the interior of the chamber from contamination by dusty particles. The data was evaluated using Alpha View/Expert Software, which automatically transforms radon daughter concentrations from working level (WL) to equilibrium equivalent concentration (ECC) in Bqm^{-3}. The annual effective dose from radon gas in air was estimated from equation

$$E_{inh}(Rn) = DCF_{Rn}.F_{Rn}.C_{Rn}.T_{exp} \tag{24}$$

Where

$E_{inh}(Rn)$ is the annual effective dose from inhalation of radon,

DCF_{Rn} is the dose per unit intake of radon via inhalation in $nSv/Bqhm^{-3}$ (9 $nSv/Bqhm^{-3}$) (UNSCEAR, 2000),

F_{Rn} is equilibrium factor for indoor occupancy of 0.4 (UNSCEAR, 2000),

C_{Rn} is the radon activity concentration in Bqm^{-3}

T_{exp} is the exposure period of one year for outdoor occupancy, which is 1760 hours using outdoor occupancy factor of 0.2.

Calculation of Total Annual Effective Dose

The total annual effective dose (ET) to members of the public was calculated using ICRP dose calculation method (ICRP, 1991). The analytical expression for the total annual effective dose is determined by summing all the individual equivalent doses for the exposure pathways considered in this study. These include:

- External gamma irradiation from the gamma emitting radionuclides in the soil samples ($E\gamma$(^{228}Ra, ^{226}Ra, ^{40}K);

- Committed dose from ingestion of water containing ^{228}Ra, ^{226}Ra, ^{40}K $E_{ing}(W)$;

- Inhalation of radon gas from soil, $E_{inh}(Rn)$

Thus:

$$E_T = E_\gamma (^{238}U, ^{232}Th, ^{40}K) + E_{ing}(W) + E_{inh}(Rn) + E_{ing}(F) \qquad (25)$$

Where

E_T is the total annual effective dose in Sievert,

$E_\gamma(^{228}Ra, ^{226}Ra, ^{40}K)$ is the external gamma ray annual effective dose from the soil,

$E_{ing}(W)$ is the committed effective dose from consumption of water,

$E_{inh}(Rn)$ is the annual effective dose from the inhalation of radon gas in air,

$E_{ing}(F)$ is the annual effective dose from ingestion of food

Determination of Radium Equivalence Index

The radium equivalent activity, Ra_{eq}, concept allows a single index or number to describe the gamma output from different mixtures of ^{238}U (^{226}Ra), ^{232}Th, and ^{40}K in material (Frame, 2006). Ra_{eq}, the most frequently used indicators for the assessment of the gamma-ray radiation hazard to humans from environmental samples in Bq/kg is defined in the formula proposed by UNSCEAR (Yasir, Ab Majid, Yahaya, 2007).

$$Ra_{eq} = C_U + \frac{10}{7}C_{Th} + \frac{10}{130}C_K \qquad (26)$$

Where C_{Ra}, C_{Th}, and C_K are the activity concentrations of ^{238}U, ^{232}Th, ^{40}K respectively. In the definition of Ra_{eq}, it is assumed that 370Bq/kg of ^{226}Ra 259Bq/kg of ^{232}Th and 4810Bq/kg of ^{40}K produce the same gamma ray dose rate. The above criterion only considers the external hazard due to gamma rays

77

in building materials. The maximum recommended value of Ra$_{eq}$ raw building materials and products must be less than 370 Bq/kg for safe use. This means that the external gamma dose must be less than 1.5 mSv/year.

Determination of Radiological Hazard Indicators

Following the measurement of the radionuclide concentrations in the samples and the determination of the radium equivalent activity (Ra_{eq}), external hazard index (H_{ex}) and internal hazard index (H_{in}) are used as radiological indicators to estimate the radiological implications of the use of the soil samples as building materials. Assuming secular equilibrium between ^{40}K, ^{232}Th and ^{238}U and their progenies, these indices are used to estimate the level of Y-radiation hazard associated with the natural radionuclides in grains samples. The external hazard index (H$_{ex}$) commonly used to evaluate the indoor radiation dose rate due to external exposure to gamma radiation from natural radionuclides building materials can be calculated from the expression (Tufail et al., 2000):

$$H_{ex} = \frac{1}{370}C_U + \frac{1}{259}C_{Th} + \frac{1}{4810}C_K \leq 1 \qquad (27)$$

Where C$_K$, C$_{Th}$ and C$_K$ are the activity concentrations of ^{238}U, ^{232}Th and ^{40}K respectively. This expression indicates that the value of the external hazard index must be less than unity for the external gamma radiation hazard to be considered negligible or insignificant. Thus, the maximum values of H_{ex} equal to unity correspond to the upper limit of Ra_{eq} being 370 Bq/kg. Considering the hazardous nature of internal exposure to ^{222}Rn and its decay products to the lungs and other respiratory organ, and the fact that reducing the ^{226}Ra to half of its maximum acceptable limit for external exposure only will make H_{in} the

internal hazard index less than unity. Thus the internal hazard index, H_{in}, was calculated using the following equation

$$H_{in} = \frac{1}{185}C_U + \frac{1}{259}C_{Th} + \frac{1}{4810}C_K \qquad (28)$$

Excess Lifetime Cancer Risk (ELCR) was calculated using the equation

$$ELCR = E \times DL \times RF \qquad (29)$$

Where

E is the Annual Effective Dose

DL is the average duration of life (estimated to 70 years)

RF is the Risk Factor (Sv-1) i.e. fatal cancer risk per Sievert. For stochastic effects, ICRP uses RF as 0.05 for public (Taskin, Karavus, Topuzoglu, Hindiroglu & Karahan, 2009).

The cancer and hereditary risks due to low doses without threshold dose known as stochastic effect were estimated using the ICRP cancer risk assessment methodology (ICRP, 1991 & 2007). In its 1990 recommendations, risks from radiation induced cancers were derived from observations of people exposed to high doses using a dose and dose rate effectiveness factor (DDREF). Risk estimates based on the observations of people exposed to low doses has associated large uncertainties and therefore will contribute to quantitative risks estimates (ICRP, 1991). The lifetime risks of fatal cancer recommended in the 1990 recommendations by the ICRP are 5×10^{-2} for the members of the public (ICRP, 1991). In its latest recommendations of 2007, the Commission has retained its fundamental hypothesis for the induction of stochastic effects of linearity of dose and effect without threshold and a dose and dose-rate effectiveness factor (DDREF) of 2 to derive the nominal risk coefficients for low doses and low dose rates. In its latest recommendations, the system of

79

regulations for radiological protection based on the 1990 recommendations has not changed (ICRP, 2007). A new set of nominal risk coefficient has been derived to be used for the estimation of fatal cancer as well as hereditary effects.

The recommended nominal risk coefficients in its 2007 recommendations are given in Table 11. The new nominal risk coefficients were derived based upon data on cancer incidence weighted for lethality and life impairment whereas the 1990 values were based upon fatal cancer risk weighted for non-fatal cancer, relative life years lost for fatal cancers and life impairment for non-fatal cancer. However the combined detriment from stochastic effects in the new values has remained unchanged at around 5 % Sv^{-1} (ICRP, 2007).

Table 11: Detriment-adjusted nominal risk coefficients for stochastic effects after exposure to radiation at low dose rate (10^{-2}).

Exposed Population	Cancer		Heritable effects		Total detriment	
	2007	1990	2007	1990	2007	1990
Whole	5.5	6.0	0.2	1.3	5.7	7.3
Adult	4.1	4.8	0.1	0.8	4.2	5.6

Source: (ICRP, 2007)

The risk of exposure to low doses and dose rates of radiation to members of the public in the communities along the Jubilee oil field were estimated as using the 2007 recommended risk coefficients (ICRP, 2007) and an assumed 70 years lifetime of continuous exposure of the population to low level radiation.

Fatality cancer risk = total annual effective dose (Sv) x cancer nominal risk factor (30)

Hereditary effect = total annual effective dose (Sv) x hereditary nominal effect factor (31)

The total annual effective dose estimated from the study area from the potential pathways of exposure of members of the public to ionising radiation was 35.34μSv/y. The basic approaches to radiation protection all over the world are consistent with the recommendations of ICRP publications (ICRP, 1991; 2007). The recommendations are that, all exposures above the natural background radiation should be kept as low as reasonably achievable (ALARA) and below the individual dose limits of occupationally exposed workers of 20 mSv per year average over 5 years and for members of the public of 1 mSv per year. It is also important to note that, studies so far has not established the effect of radiation in the low dose rate range. A factor of 3-10 lower is required to satisfy most regulations (Faanu, 2011).

Uncertainty Estimation

Every measurement or test has an error of measurement. If repeated, a test or measurement often gives different result, even though it usually is very similar to the original result. A test result therefore gives the approximation of the true value of the quantity to be measured. A measurement or test is only complete when accompanied by a quantitative statement of its uncertainty. The uncertainty is required in order to decide whether the result is adequate for its intended purpose and to ascertain if it is consistent with other similar results (IAEA, 2004). Accordingly, in the present study, the uncertainty of all activity concentrations for any radionuclide is determined through the expression

$$A_{sp} = \frac{N.\ e^{\lambda.T_d}}{\eta.\ P.M.T_c} \tag{32}$$

Where A_{sp} = specific activity in Bq/kg

N = background corrected net peak area

= the absolute detection efficiency

81

P = gamma ray yield

T_c = counting time of the sample

= decay constant of respective radionuclide

T_d = time between sampling and time of counting

Some of the uncertainties identified for the quantification of the uncertainty in the determination of the specific activity concentration include

- net peak area

- detection efficiency

- sample mass

- counting time.

The overall uncertainty in the determination of the activity concentration was obtained from

$$dA_{sp} = A_{sp} * [(\frac{dN}{N})^2 + (\frac{d\eta}{\eta})^2 + (\frac{dM}{M})^2]^{\frac{1}{2}} \qquad (33)$$

dN is determined from the uncertainty in the integration of the peak area of each energy event.

dM is the standard uncertainty in the weighing balance used to weigh the samples and the standard uncertainty was quoted as 0.1 mg.

d is the uncertainty in the efficiency calibration counting system (Faanu, 2011).

Determination of Physical Parameters and Trace Metals Concentration

The geochemical studies were carried out by determining the following parameters: pH; Total Dissolved Solids (TDS); Conductivity. The concentrations of trace metals such as cadmium (Cd), iron (Fe), zinc (Zn), copper (Cu), manganese (Mn), arsenic (As), chromium (Cr), and lead (Pb) were also investigated in water samples within the communities.

82

pH, Conductivity and Total Dissolved Solids (TDS) Determination

The pH values of the water samples were measured using pH meter model WTW pH 3110 in conjunction with a glass electrode with a calomel reference electrode. The pH meter was calibrated with standard buffer solutions with pH 4.01, 7.0 and 9.21. The TDS and conductivity were measured using conductivity meter WTW cond. 3210. The equipment was calibrated with the following standard solutions, 0.01M KCl with absorbance of 1413 µs/cm and 0.1 M KCl with absorbance of 12880 µs/cm.

Trace Metals Determination

Water samples

The trace metals in the water samples were determined using Atomic Absorption Spectrophotometer (AAS). The water samples were digested by adding 6 mL HNO_3 (65%), 3 mL of HCl (37%) and 0.25ml of H_2O_2 (30%) were added to 5 mL of the water sample in Teflon digestion tubes; the tubes were closed tightly and placed in the ETHOS 900 microwave digester. The digested samples were allowed to cool, and then transferred into clean 25 mL volumetric flask and diluted to 20 ml with deionized water. Lead (Pb), arsenic (As), nickel (Ni), manganese (Mn) and cadmium (Cd) in the digested samples were determined using AA240 FS atomic absorption spectrometer as per Table 12. Acetylene gas and air were used as fuel and oxidant, respectively. The flow rates for acetylene and air, 2 and 13.5 L/min, respectively, were kept constant for the analysis of the metals. The flow rates for acetylene and air, 2 and 13.5 L/min, respectively, were kept constant for the analysis of the metals.

Soil Samples

Soil samples were air-dried, and all dead roots, leaves, crumbs, and any other foreign matter were hand-picked while wearing hand gloves. The air-dried soil samples were ground in a mortar to obtain homogenates and then passed through a 250 μm sieve to remove coarse particles. The powdered soil samples were digested by adding 6 mL (65 % HNO_3) and 3 mL (HCl) to 0.25 g of the powdered samples in a Teflon beaker and digested per the digestion code 308 (Milestone acid digestion cookbook, 1996). The digests were diluted and analyzed for Pb, As, Ni, Mn and Cd similarly as described in section 3.13.2.1 for the water samples.

Table 12: Operating parameters for the determination of metals using atomic absorption spectrometer of AAS (Varian AA240FS Atomic Absorption Spectrometer)

Parameter	Pb	As	Ni	Mn	Cd	Co	Hg
Wavelength, nm	224.8	193.7	232	279.5	228.8	240.7	253.7
Slit width, nm	0.2	0.5	0.2	0.2	0.5	0.2	0.2
Lamp current, mA	5.0	10.0	4.0	5.0	4.0	7.0	4.0
Background correction	ON	OFF	ON	OFF	OFF	OFF	OFF
Precision, %	0.6-1.0	0.02-0.08	0.5-1.3	0.02-1.0	0.2-0.9	0.3-1.0	0.02-0.9
Fuel	Acetylene	Acetylene	Acetylene	Acetylene	Acetylene	Acetylene	Acetylene
Support	Nitrous oxide	Nitrous oxide	Nitrous oxide	Nitrous oxide	Nitrous oxide	Nitrous oxide	Nitrous oxide

Source: Laboratory work, 2016

Quality Assurance

Strict QA/QC measures were adopted to ensure reliability of the results. All chemicals and reagents used were of high purity. Glassware used were cleaned thoroughly with detergent and rinsed several times using deionized water. Deionized water was used for all dilution purposes. For the purposes of detection and quantification limits of the AAS, a blank solution was read 25 times, and the standard deviations were calculated for the noise levels generated

for each of the elements of interest. The detection limit (LOD) for each element was achieved as follows:

$$LOD = \frac{3*S}{m} \qquad\qquad (34)$$

Where S is the standard deviation of the blank readings and m represents the gradient of the calibration curve for each element. The limit of quantification was calculated using 10 s/m. The accuracy and reproducibility of the analytical procedure was determined by spiking and homogenizing three replicates of each of three samples selected at random. Triplicate of each sample was spiked with three different concentrations of the element of interest as follows: Pb (2.0, 5.0, and 10.0 mg/l), Co (2.0, 5.0, and 8.0 mg/l), As (0.02, 0.04, 0.06), Hg (0.02,0.04, 0.06), Ni (2.0, 5.0, and 10.0 mg/l), Mn (1.0, 2.0, 5.0), and Cd (0.5, 2.0, and 3.0 mg/l) and treated in a similar manner as the samples. The recoveries obtained for each of the elements are shown in Table 13. The absorbances measured by the AAS were converted to concentrations using standard calibration curves. One thousand milligrams per liter single element standards of the elements of interest, obtained from Fluka Analytical (Sigma Aldrich Chemie GmbH, Switzerland), were diluted using 10 % HNO_3 and used to generate the calibration curves for the AAS analysis. The regression data of the calibration curves for AAS is shown on Table 14.

Table 13: Recoveries of spiked samples

Metal	Spike	Recovery	% Recovery	% Deviation
Pb	2.00	2.06	103	3.0
	5.00	5.10	102	2.0
	10.0	9.86	98.60	1.4
Co	2.00	1.98	99.0	1.0
	5.00	4.96	99.2	0.8
	8.00	7.79	97.4	2.6
As	0.02	0.018	90	10.0
	0.04	0.036	90	10.0
	0.06	0.061	101.7	8.3
Hg	0.02	0.021	105	5.0
	0.04	0.042	105	5.0
	0.06	0.062	103.3	3.3
Ni	2.00	2.03	101.5	1.5
	5.00	4.89	97.80	2.2
	10.0	9.97	99.70	0.3
Mn	1.00	1.003	100.3	0.3
	2.00	1.993	99.70	0.3
	5.00	5.00	100.0	0.0
Cd	0.50	0.48	96	4
	2.00	2.01	100.5	0.5
	3.00	2.96	98.67	1.33

Source: Laboratory work, 2016

Table 14: Regression data of calibration curves

Parameter	Technique	Equation	r^2
Pb	AAS	y= 0.0379X + 0.0007	0.9997
As	AAS		
Ni	AAS	y= 0.0945X – 0.0179	0.9961
Mn	AAS		
Cd	AAS	y= 0.205X + 0.0152	0.997

Determination of Hazard Indices for Ingestion of Heavy Metals in Soil

Plain data on the metal content of soil is sometimes insufficient to describe the full risk that arises from the exposure of humans, both children and adults, to different heavy metals from rocks/soil, particularly in the case when more details on human health risk are required.

Exposure of humans to rocks/soil actually is through dust exposure that comprises (i) inhalation exposure and/or (ii) oral exposure (ingestion). For such exposition, EPA guidance recommends daily rates of 20 mg/h for children and 10 mg/h for adults (USEPA, 1997; De Miguel Iribaren, Chacon, Ordonez &

86

Charlesworth, 2007). For the purposes of this study, risk characterization comprises calculations of carcinogenic and non-carcinogenic risk for ingestion and inhalation.

Basic formulas used for the calculation of dose received through the different pathways from soil are presented as Chronic Daily Intake (CDI):

$$\text{CDI}_{\text{ingestion}} = C \times \frac{IngR \times EF \times ED}{BW \times AT} \times 10^{-6} \qquad (35)$$

$$\text{CDI}_{\text{inhalation}} = C \times \frac{InhR \times EF \times ET \times ED}{PEF \times BW \times AT} \qquad (36)$$

$$\text{CDI}_{\text{dermal}} = C \times \frac{SA \times SL \times ABS \times EF \times ED}{BW \times AT} \times 10^{-6} \qquad (37)$$

As carcinogenic substances, Pb, Cd, and Ni were selected to assess the carcinogenic hazard risk (Total Risk) using equations 38 – 43.

$$\text{CDI}_{\text{ing-ca}} = C \times \frac{IR \times EF}{AT_{ca}} \times 10^{-6} \qquad (38)$$

where

$$IR = \frac{ED_{child} \times IngR_{child}}{BW_{child}} + \frac{(ED_{adult} - ED_{child}) \times IngR_{adult}}{BW_{adult}} \qquad (39)$$

$$\text{CDI}_{\text{inh-ca}} = C \times \frac{EF \times ET \times ED}{PEF \times 24 \times AT_{ca}} \times 10^{3} \qquad (40)$$

$$\text{CDI}_{\text{derm-ca}} = C \times \frac{ABS_d \times EF \times DFS_{adj}}{AT_{ca}} \times 10^{-6} \qquad (41)$$

where CDI_{ing}, CDI_{inh}, CDI_{dermal} are the chronic daily intake or dose contacted through oral ingestion(mgkg^{-1}d^{-1}), inhalation (mgm^{-3} for non-cancer and μgm^{-3} for cancer) and dermal contact with soil particles (mgkg^{-1}d^{-1}), respectively. *RfD* was the reference dose, *CSF* was the chronic slope factor (USEPA, 1997; De Miguel et al., 2007). The definitions and values of other parameters used for the calculation of ingestion, inhalation and dermal of soil are presented in Tables 15 and 16.

Risk Characterisation

The basic equation for calculating non-carcinogenic hazard for a single element is expressed as the hazard quotient:

$$\text{HQ} = \frac{CDI}{R_f},$$ (42)

where the non-cancer hazard quotient is a unitless number defined as the probability of a person experiencing an adverse effect. The greater is the value of CDI/RfD above unity, the greater is the level of concern. CDI is the chronic daily intake of a toxicant expressed in $mgkg^{-1}day^{-1}$ and RfD is the chronic reference dose for the toxicant expressed in $mgkg^{-1}d^{-1}$. (USEPA, 1997; De Miguel et al., 2007).

$$\text{HI} = \sum\text{HQ} = \text{HQ}_{ing} + \text{HQ}_{inh} + \text{HQ}_{derm}$$ (43)

For each chronic non-carcinogenic exposure, the separate chronic hazard index (HI) should first be calculated from the ratios of the chronic daily intake (CDI) to the chronic reference dose (RfD) for the individual chemicals and then the obtained results summed as described in the equation.

For each chronic non-carcinogenic exposure, the separate chronic hazard index (HI) should first be calculated from the ratios of the chronic daily intake (CDI) to the chronic reference dose (RfD) for the individual chemicals and then the obtained results summed as described in the equation:

$$\text{HI} = \sum\text{HQ} = \text{HQ}_{ing} + \text{HQ}_{inh} + \text{HQ}_{derm}$$ (44)

$$HI = \sum_{k-1}^{n} CDI_k / R_f D_k,$$

where the hazard index is a unitless number defined as the probability of a person experiencing an adverse effect. Generally, the greater the value of CDI/RfD above unity, the greater is the level of concern. It is the summation of

88

the hazard quotients for different contaminants and/or different exposure pathways, CDI_k is the chronic daily intake of the kth toxicant in mg/kg/day and RfD_k is the chronic reference dose for the kth toxicant in $mgkg^{-1}day^{-1}$ (USEPA, 1997; De Miguel et al., 2007).

The values for the non-carcinogenic hazard index and carcinogenic lifetime risk for individual elements, the cumulative risk for different exposure pathways for individual elements and the cumulative risk for all elements are reported in Table 31.

For carcinogens, the risks are estimated as the incremental probability of a person developing cancer over a lifetime as a result of exposure to the potential carcinogen. The basic equation for calculating the excess lifetime cancer risk is:

$$Risk = CDI_{ca} \times CSF \tag{45}$$

where "Risk" is a unitless probability of a person experiencing cancer over a lifetime; CDI is the chronic daily intake or dose $(mgkg^{-1}day^{-1)}$; SF is the slope factor, expressed in $(mgkg^{-1}day^{-1})$.

$$\textbf{Total Risk} = Risk_{ing} + Risk_{inh} + Risk_{dermal} \tag{46}$$

All risks are cumulative, hence it is possible to calculate the cumulative cancer risk expressed as the total cancer risk, or non-carcinogenic hazard expressed as the hazard index.

The cancer risk equation which describes estimates of incremental individual lifetime cancer risk for the simultaneous exposure to several carcinogens is as follows

$$Total\ Cancer\ Risk = \sum_{k=1}^{x} CDI_k \times CSF \tag{47}$$

where CDI_k is the chronic daily intake or dose (mg/kg/day) for substance k, SF_k is the slope factor, expressed in $(mgkg^{-1}day^{-1})$, for substance k and $CDI_k \times SF_k$ is the risk estimate for the kth substance.

Table 15: Values of Variables for Human Health Risk Assessment

Parameters	Unit	Definition	Value	
			Child	Adult
C	mg/kg	heavy metal concentration		
ABS_d	--	dermal absorption factor	0.03	0.001
SL/AF	mg/cm^2	Soil-to-skin adherence factor	0.2	0.07
BW	Kg	body weight	16.2	61.8
ED	Year	exposure duration	6	30
EF	d/year	exposure frequency	350	350
ET	h/d	exposure time	24	24
IngR	mg/d	soil ingestion rate	200	100
SA	cm^2	skin surface area available for exposure	2800	5700
InR	m^3d^{-1}	Inhalation Rate	20	
AT_{nc}	D	averaging time for non-carcinogenic	$ED \times 365$	
AT	D	averaging time for carcinogenic	$LT \times 365$	
DFS_{adj}	$mg \times year/kg/d$	soil dermal contact factor-age-adjusted	362.4	
IR	$mg \times year/kg/d$	soil ingestion rate age-adjusted	113	
LT	Year	Lifetime	72	
PEF	m^3/kg	Soil-to-air particulate emission factor	1.36×10^9	

Source: Laboratory work, 2016

Table 16: Toxicological Parameters for Different Heavy Metals of Health Risk Assessment

Elements	RfD_{ing} $(mgkg^{-1}d^{-1})$	RfC_{inh} (mgm^{-3})	ABS_{GI}	CSF_{ing} $(mgkg^{-1}d^{-1})$	IUR (μm^{-3})
Cd	1.0×10^{-3}	1.0×10^{-5}	0.025	--	1.8×10^{-3}
Ni	2.0×10^{-2}	9.0×10^{-5}	0.04	--	2.6×10^{-4}
Pb	3.5×10^{-3}	--	1	8.5×10^{-3}	1.2×10^{-5}
Zn	3.0×10^{-1}	--	1	--	--

Source: Laboratory work, 2016

Data processing of Heavy Metals

SPSS version 20.0 for Windows was used for the statistical evaluation of the data obtained from heavy metal analysis. Principal Component Analysis (PCA) was used to deduce the hypothetical source of heavy metals being anthropogenic or natural. The PCA was done using Direct Obliman Rotation

due to the fact that it is a direct approach to produce oblique factor rotation and the factors can therefore correlate with each other. Cluster Analysis (CA) was used to classify the geochemical groups, clustering the samples with comparable trace metal contents. CA was expressed according to the Ward-algorithmic Method, and squared Euclidean distance was employed for quantifying the distance between clusters of identical metal contents.Microsoft Excel 2010 was used to process all the physicochemical analytical data on soil and groundwater samples. StatistiXL Version 1.8 and XYChartLabeler Add-Inns for Microsoft Excel were used for principal component analysis (PCA) whilst Visual PROMETHEE Academic Edition Version 1.4.0.0 was used for PROMETHEE-GAIA multi-criteria decision making (MCDM).

Multivariate Data Analysis

The application of multivariate data analysis techniques in environmental pollution investigation has been necessitated by the increasing complexities in environmental data. The application of these techniques in environmental research is still evolving and the potentials are enormous. Multivariate analysis techniques essentially maximise relevant pollutant information whilst reducing inherent complexities in observed data (Miller & Miller, 2010). In this regard, multivariate analysis is indispensable in characterizing pollutant behaviour patterns, source apportionment and ranking (Ayoko, Bonire, Abdulkadir, Olurinola, Ehinmidu, 2007) of study sites.

Principal Component Analysis (PCA) was used to deduce the hypothetical source of heavy metals being anthropogenic or natural. The PCA was done using Direct Obliman Rotation due to the fact that it is a direct approach to produce oblique factor rotation and the factors can therefore

correlate with each other. Cluster Analysis (CA) was used to classify the geochemical groups, clustering the samples with comparable trace metal contents. CA was expressed according to the Ward-algorithmic Method, and squared Euclidean distance was employed for quantifying the distance between clusters of identical metal contents.

The physicochemical properties of groundwater samples were analysed using multivariate parametric method principal component analysis (PCA) and non-parametric multi-criteria decision-making methods, Preference Ranking Organisation Method for Enrichment Evaluation (PROMETHEE) and Geometrical Analysis for Interactive Aid (GAIA). PCA is highly useful technique in reducing the amount of data when a multivariate data has correlation. The original variables in the observed multivariate data is linear transformed into new principal components such that the eventual selected principal components during the analysis accounts for the largest variations where the first principal component (PC1) accounts most of the variation compared to the second (PC2) and so on. Further details on PCA can be found in Miller& Miller (2010). The detailed procedures for PROMETHEE-GAIA have been outlined by various publications (Ayoko et al., 2007; Behzadian, Kazemzadeh, Albadvi & Aghdasi, 2010; Espinasse, Picolet, & Chouraqi, 1997; Khalil, Goonetilleke, Kokot & Carrol, 2004).

Basically, PROMETHEE computes the degree of preference of one object compared with another for each variable based on various modelling scenarios such as the choice of relevant preference function, whether low (minimized) or high (maximized) variable values are preferred, weightings assigned to each variable and whether partial (PROMETHEE I) or complete

(PROMETHEE II) ranking is preferred. GAIA on the other hand displays the PROMETHEE results as biplots analogous to PCA thereby enabling the interpretation of the relevance of various variables under investigation. However, GAIA has an added feature of a decision axis called pi (π) which enables the interpretation of the global performance of each object with respect to the decision vector.

Relevant chemical information in the data matrix such as clustering of criteria or actions and characterisation of outliers can be derived from GAIA biplots. PROMETHEE essentially serves as a data pre-treatment process for GAIA. As a result standardization, mean centering, normalization and other forms of data pre-treatment may not be required which may be considered a key advantage compared to other forms of multivariate analyses (Ayoko et al., 2003). In this study, complete ranking information highly relevant to selecting one community in preference to all others for monitoring of heavy metals pollution in the immediate future was obtained and the relationships between the heavy metals content of soil and groundwater were also determined. This information is critical in assessing the potential future impact of Ghana's emerging oil and gas industry on the ecosystem and public health of the communities in the immediate offshore vicinity of the Tano Basin.

Geospatial Distribution of Heavy Metals

The geospatial distribution of each heavy metal analyte was done using Minitab version 17.2.1 Contour Plot. The contour plot examines the relationship between response variable (heavy metals, Z) and two predictor variables (longitude (X) and latitude (Y)) by viewing discrete contours of the predicted response variable (Minitab, 2015).

93

Analysis of Radon Concentration in Groundwater

Radon concentrations in the groundwater which serves as a source of drinking water and other domestic uses for the inhabitants of the communities were measured with RAD7, an electronic radon detector connected to a RAD-H_2O accessory (Durridge co., USA) for a period of one month. The RAD7 detector was used for measuring radon in water by connecting it with a bubbling kit which enables it to degas radon from a water sample into the air in a closed loop. A sample of water was measured into a radon-tight reagent bottle of 250 mL capacity connected in a close circuit with a zinc sulphate coated detection chamber which acts as a scintillator to detect alpha activity and a glass bulb containing hygroscopic substance (silica gel/calcium chloride) to absorb the moisture. Air was then circulated in a closed circuit for a period of 5-10 minutes until the radon was uniformly mixed with the air and the resulting alpha activity was recorded and it directly gives the radon concentration.

Statistical Analysis of Samples

In this study, Paired Sample t-test statistical technique was used to compare the Means of the radionuclides concentrations in the soil and water samples for the first batch samples of June, 2014 and second batch samples of February, 2015. If the probability value P is greater than the significance level at 5 % (P>0.05), then it implies that the paired sample Means are insignificant or the Mean of the two paired samples are equal. On the other hand if the P-value is less than the significance level at 5 % (P<0.05) then there is a significant difference between the means of the two sets of data. The paired sample t-test computes the difference between two variables for each case, and tests to find

94

out if the average difference is significantly different from zero at 95 % Confidence level.

The paired sample t-test is calculated from the expression below:

$$T = \frac{\bar{d}}{s_d/\sqrt{n}} \qquad \qquad (48)$$

Where d is this the Mean difference between two samples,

s_d is the standard deviation,

n is the sample size and

t is a paired sample t-test with

n-1 being the degrees of freedom.

Soil-to-Plant Transfer of Radionuclides

Radionuclides are taken up by food crops from soil and incorporated into the human food-chain giving rise to radiological exposure. In radiological risk assessments, soil-to-plant transfer factor (TF) is a key parameterused to estimate the activity concentration in food crops from activity concentration in soils. The TF is a "lumped" parameter that encapsulates in an implicit way many processes and is defined as the ratio between activity concentration in a given tissue of the plant and in the soil at harvest (Hegazy & Emam, 2010; Tome, Rodriguez & Lazano, 2003).

$$TF = \frac{\text{activity concentration of radionuclide in plant } (Bq/kg\ dry\ weight)}{\text{activity concentration of radionuclide in soil } (Bq/kg\ dry\ weight)} \qquad (49)$$

The concentration of a nuclide in a plant or plant part, Cv, i (in Bq/kg, dry weight), is taken to be linearly related to its concentration in soil within the rooting zone, Cs, i (also in Bq/kg, dry weight) (Asaduzzaman, Khandaker, Amin, Bradley, Mahat & Nor, 2014). To estimate the uptake from soil by edible portions of cassava, we assumed that the foliar absorption is negligible and that the uptake from soil to plant is mainly by the root (Mazzilli & Saueia, 2011).

Computational Activity Concentration Assessment

Newton's forward interpolation equation is a formula designed for reconstruction of functions whose value will increase or remain constant with an independent variable (Ripa, 2010). It is therefore useful for activity and dose reconstruction, against an independent variable, time. Refer to (Ripa, 2010) for more information on the theory of Newton's forward interpolation formula.

The activity concentrations of radionuclides were reconstructed by the Forward Different Interpolation Method. This was achieved by expressing the term "$e^{-\lambda t}$" of the radionuclide decay equation "$A = A_0 e^{-\lambda t}$" into a 4th order Taylor polynomial form. The decay factor $e^{-\lambda t}$ was approximated to a polynomial form by the following analysis

$$P_n(\lambda t) = P_n(z)$$

Since $P_n(z) = e^{-\lambda t} = e^{-z}$; this yields the polynomial of

$$e^{-z} = P_n(z) = a_0 + a_1(z - z_0) + a_2(z - z_0)(z - z_1) + a_3(z - z_0)(z - z_1)(z - z_2 + \cdots +$$

$$a_n(z - z_0)(z - z_1)(z - z_2) \dots (z - z_{n-1})$$

And the fourth order of this can be written as

$$e^{-z} = P_n(z) = a_0 + a_1(z - z_0) + a_2(z - z_0)(z - z_1) + a_3(z - z_0)(z - z_1)(z - z_2) + a_4(z - z_0)(z - z_1)(z - z_1)(z - z_2)(z - z_3)$$

Where $\qquad a_0 = y_0 = P_0(z_0)$

$$a_1 = \frac{y_1 - y_0}{h} = \frac{\Delta y_0}{h}$$

$$a_2 = \frac{y_2 - 2y_1 + y_0}{2h^2} = \frac{\Delta^2 y_0}{2h^2}$$

$$a_3 = \frac{y_3 - 3y_1 + 3y_1 - y_0}{2!h^3}$$

96

$$a_4 = \frac{y_4 - 4y_3 + 6y_2 - 4y_1 + y_0}{4! h^4}$$

Such that

$$P_n(z) = az^4 + bz^3 + cz^2 + dz + e$$

And

$a = a_4$

$b = a_3 - a_4(z_0 + z_1 + z_2 + z_3$

$c = a_2 - a_3(z_0 + z_1 + z_2) + a_4(z_0 z_1 + z_0 z_2 + z_0 z_3 + z_1 z_2 + z_1 z_3 + z_2 z_3)$

$d = a_1 - a_2(z_0 + z_1) + a_3(z_0 z_1 + z_0 z_2 + z_0 z_3) + a_4(z_0 z_1 z_2 + z_0 z_1 z_3$

$\qquad + z_0 z_2 z_3 + z_1 z_2 z_3)$

$e = a_0 - a_1(z_0) + a_2(z_0 z_1) - a_3(z_0 z_1 z_2) + a_4(z_0 z_1 z_2 z_3)$ (Taapopi,

2015).

The 2013 version of Microsoft Excel was used to evaluate the above relations to obtain the coefficients *a, b, c, d and e* and the polynomial equals to e^{-z} was obtained.

$$e^{-z} = 0.0067z^2 - 0.0820z^3 + 0.3993z^2 - 0.9560 + 1 \qquad \textbf{(50)}$$

Based on the assumption that radionuclides activity concentrations in the soils are uniform, an MATLAB R2013 script was written to estimate the concentration of the radionuclides ^{238}U, ^{232}Th and ^{40}K using their respective half-lives.

Summary

This chapter is a presentation of the analytical methodologies adopted for evaluating contaminants of concern in soil, groundwater and food samples. The methods of human risk assessment and data analysis were also outlined.

CHAPTER FOUR

RESULTS AND DISCUSSION

Introduction

The present study encompasses the analysis of ^{238}U (^{226}Ra), ^{232}Th (^{228}Ra), ^{40}K and trace metals in fifty one (51) composite samples each, for the two periods of sampling in selected communities along the coast bordering the Jubilee oil field. This included 26 soil samples, 20 water samples. Five (5) composite cassava samples were also taken from five farms in some of the communities along the shore approximately 60km from the Jubilee oil fields. The results obtained from the in-situ and laboratory measurements are summarised in Tables 18 to 56 and Figures 14 to 42.

Quality Control and Quality Assurance

Quality control and validation of results were carried out in order to ascertain the quality and the reliability of measurements by the calibration of the HPGE detector with respect to energy and efficiency using standard radionuclides in a one (1) litre Marinelli beaker with solid water as the matrix. For the soil, water and food samples, the mixed radionuclide standard source in solid water matrix was also used for the efficiency calibration. The standard radionuclides that were used for the energy and efficiency calibrations are shown in the appendix section for the solid water matrix. The corresponding energy and efficiency calibration curves obtained for 1.0 litre Marinelli beaker geometry are shown in Figures 14 and 15 respectively. The resolution of the high purity germanium detector was evaluated using ^{60}Co at the energy of 1332 keV and the results are shown in Figure 16 with an estimated value of 0.19 %.
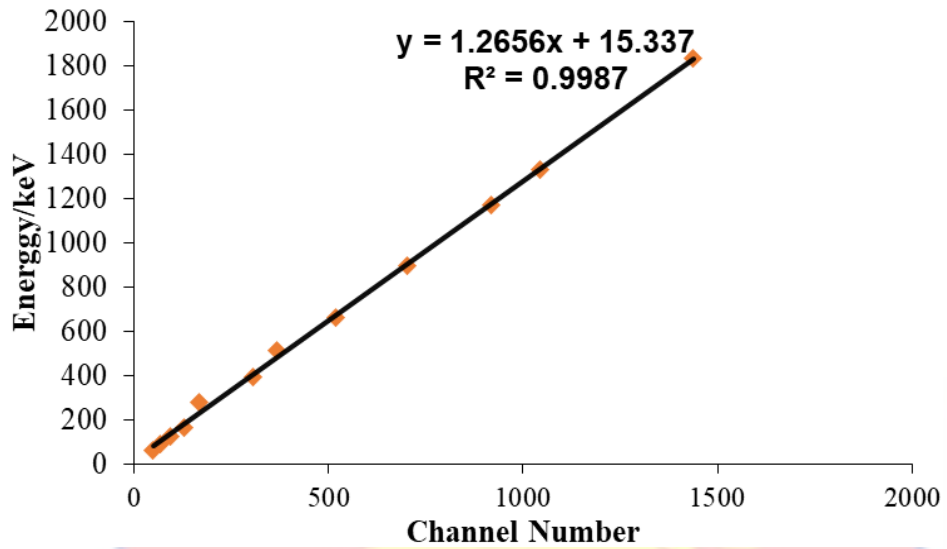
Figure 14: Energy Calibration Curve using mixed standard radionuclides in a one litre Marinelli beaker
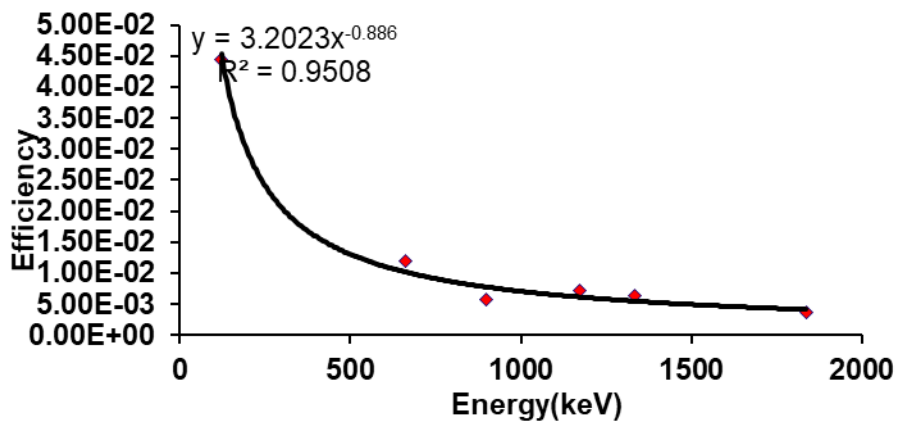
Figure 15: Efficiency Calibration Curve as a function of energy for mixed radionuclides standard in a one litre Marinelli beaker.
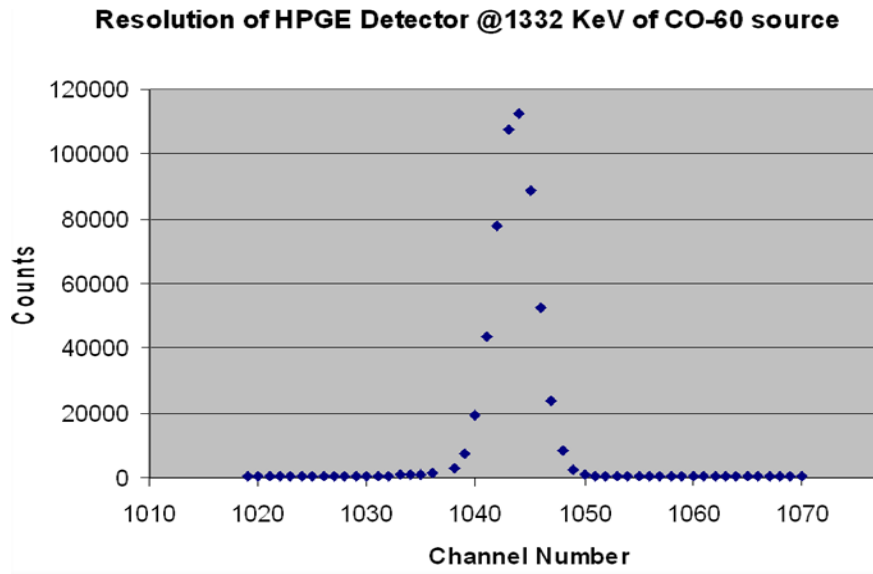
Figure 16: Energy Resolution of the HPGE detector at 1332 keV of ^{60}Co.

$Resolution = \frac{1045 - 1043}{1044} = 0.19\%$

The resolution of the detector measured at 1332 keV of ^{60}Co source was 0.19 %.

The Minimum Detectable Activities for ^{238}U (^{226}Ra), ^{232}Th (^{228}Ra) and ^{40}K are shown in Table 17 with estimated values of 0.05, 0.04 and 0.10 Bq/kg respectively.

Table 17: The Minimum Detectable Activity concentrations of ^{238}U, ^{232}Th, ^{40}K

Radionuclide	Minimum Detectable Activity, Bq/kg
^{238}U	0.05
^{232}Th	0.04
^{40}K	0.10

Source: Laboratory work, 2016

Activity Concentration

Soil

The estimated average activity concentrations of ^{238}U, ^{232}Th and ^{40}K in the soil are presented in Table 18. ^{238}U is in the range of 1.60 to 21.34 B/kg with

100

an average of 8.65 Bq/kg. The range and average values for ^{232}Th and ^{40}K are 2.78 - 32.24 Bq/kg averaging 12.51 Bq/kg and 110.56 - 527.63 Bq/kg averaging 214.11 Bq/kg.

Table 18: Activity Concentrations of Radionuclides in Soil

Community	Activity Concentration, Bq/m³		
	^{238}U	^{232}Th	^{40}K
ABH	8.96 ± 1.54	9.12 ±1.16	298.27 ± 44.74
ABH 2	6.25 ± 0.39	19.64 ±1.56	226.41 ± 33.96
ABH 3	9.32 ± 1.40	10.11±1.52	301.61 ± 45.24
ALIS	4.15 ± 0.62	6.22 ± 0.93	132.15 ± 18.82
Axim Castle	12.90 ±1.07	8.06 ± 1.50	352.87 ± 52.93
Krisan 1	1.60 ± 0.36	3.09 ± 0.30	124.43 +1.48
Krisan 2	14.45 ± 2.17	16.34 ± 2.45	263.41 ± 39.15
Krisan 3	12.71 ± 1.91	8.13 ± 1.22	134.26 ± 20.14
Beyin 1	13.38 ±5.36	29.75 ± 2.82	169.99 ± 25.50
Beyin 2	3.240 ± 0.21	3.01 ± 0.24	127.28 ± 1.29
Ellonyi	21.34 ± 1.40	26.03 ±0.98	146.52 ± 21.98
Kengen 1	5.92 ± 0.81	15.16 ± 1.88	142.33 ± 4.21
Kengen 2	7.90 ± 0.35	3.81 ± 0.36	128.91 ± 1.33
Twenen	5.20 ± 0.78	7.43 ± 1.11	189.23 ± 28.14
Nyale Kplole	8.96 ±1.99	32.24 ± 1.84	340.04 ± 51.01
Nyale Kplole 2	4.62 ± 0.31	3.84 ± 0.31	128.66 ± 61.39
Nyale Kplole 3	9.26 ±2.33	19.24 ±1.20	231.70 ± 34.76
Anokyi 1	8.87 ± 1.13	17.12 ± 2.44	354 ± 13.90
Anokyi 2	4.56 ± 0.61	20.33± 1.62	273 ± 7.41
Atuabo 2	13.95 ± 0.24	12.91 ± 0.25	136.30 ± 0.42
Kikam	10.69 ± 0.15	17.66 ± 0.92	213±8.73
Half-Assini 1	8.36 ± 0.81	6.55 ± 0.77	174+3.47
Half-Assini 2	5.59 ± 0.84	2.78 ± 0.42	527.63 ± 79.14
Half-Assini 3	6.08 ± 0.91	9.27 ± 1.39	110.56 ± 1.54
Half-Assini 4	9.05 ± 2.32	6.01 ±1.95	204.70 ± 30.71
Newtown	7.45 ± 0.37	11.35 ± 1.45	135.478+1.47
Range	1.60 - 21.34	2.78 - 32.24	110.56 - 527.63
Average	8.65	12.51	214.11

Source: Laboratory work, 2016

Table 18 presents the level of ^{238}U, ^{232}Th, ^{40}K in soil samples in some communities along the Tano basin in Ghana. The level of ^{238}U, ^{232}Th, and ^{40}K ranged from (1.60 ± 0.36 to 21.34 ± 1.40), (2.78 ± 0.42 to 32.24 ± 1.84) and (110.56 ± 1.54 to 527.63 ± 79.14) with average values of 8.65+1.17 Bqkg^{-1}, 12.51+1.25 Bqkg^{-1} and 214.11+24.34 Bqkg^{-1} respectively. The average levels of ^{238}U, ^{232}Th and ^{40}K are lower than international data 35, 30 and 400Bq kg^{-1},

respectively published by UNSCEAR 2000. Ellonyi has the highest concentration of ^{238}U. The highest value of ^{232}Th was recorded in Nyale Kplole whilst the highest level of ^{40}K was observed in Half-Assini 2 when compared with the concentrations of all the other samples. The reason could be attributed to differences in their geological nature. Comparing the range of ^{238}U, ^{232}Th and ^{40}K levels with data from Sudan (18.94 to 26.53 Bqkg^{-1}), (19.08 to 31.41 Bqkg^{-1}), (187.57 to 385.56 Bqkg^{-1}); India (8.89 to 56.71 Bqkg^{-1}), (137.32 to 334.47 Bqkg^{-1}),(823.62 to1064.97 Bqkg^{-1}); Palestine (9.7 - 83.5 Bqkg^{-1}), (5.3 - 44.8 Bqkg^{-1}) and (10.2 - 404.0 Bqkg^{-1}); Nigeria (2.87± 0.15 to 7.14 ±0.14 Bqkg^{-1}), (1.29±0.02 to 5.53±0.02 Bqkg^{-1}), (2.73±0.03 to 66.52±0.81 Bqkg^{-1}) (Fadol, Salih, Idriss, Elfaki & Sam, 2015: Mehra, Badhan, Sonkawade, Kansal & Singh, 2010; Thabayneh & Jazzar, 2011; Avwiri, Onunogbo & Nwokeoji, 2014). The levels of radionuclide concentration from the present study seem to be normal.

A comparison of activity concentration ^{238}U, ^{232}Th and ^{40}K in soil with published data are shown in Table 19. The current study recorded an annual averages of 9 Bq/kg, 3 Bq/kg and 214 Bq/kg which are all lower than the worldwide averages of 35 Bq/kg, 30 Bq/kg and 400 Bq/kq for ^{238}U, ^{232}Th and ^{40}K respectively (UNSCEAR, 2000).

Table 19: Comparison of activity concentrations of ^{238}U, ^{232}Th and ^{40}K in soil in the study area and published data

| Country | Concentration in soil, Bq/kg | | | | | | Absorbed Dose Rate, nGy/h | | Reference |
| | ^{238}U | | ^{232}Th | | ^{40}K | | | | |
	Range	Av.	Range	Av.	Range	Av.	Range	Av.	
Egypt	2-51		1-32		17-99		2-47		Yousef et al., 2007
Pakistan	26-32		51-55		500-610		63-73		Akhtar et al., 2005
	30-39		51-64		560-636		68-83		
Palestine	10-84	35	5-45	24	10-404	120	12-83	36	Thabayneh et al., 2012
Egypt	5-64	17	2-96	18	29-650	320	20-133	32	UNSCEAR, 2000
China	2-440	32	1-360	41	9-1800	440	2-340	62	UNSCEAR, 2000
USA	8-160	40	4-130	35	100-700	370	14-118	47	UNSCEAR, 2000
India	7-81	29	14-160	64	38-760	400	20-110	56	UNSCEAR, 2000
Japan	6-98	33	2-88	28	15-990	310	21-77	53	UNSCEAR, 2000
Malaysia	38-94	67	63-110	82	170-430	310	55-130	92	UNSCEAR, 2000
Iran	8-55	28	5-42	22	250-980	640	36-130	71	UNSCEAR, 2000
Denmark	9-29	17	8-30	19	240-610	460	35-70	52	UNSCEAR, 2000
Ghana	2-47	9	3-72	3	111-528	214	8-38	20	This study
Worldwide	17-60	35	11-64	30	140-850	400	18-93	55	UNSCEAR, 2000

Source: Laboratory work, 2016

The correlation analysis using Pearson Correlation Matrix Method was also used to assess the correlation between ^{238}U, ^{232}Th and ^{40}K due to soil samples Table 20).

Table 20: Correlation analysis using Pearson Correlation Matrix Method used to assess the correlation between ^{238}U, ^{232}Th and ^{40}K respectively due to soil samples.

Radionuclide	^{238}U	^{232}Th	^{40}K
^{238}U	1	0.501**	0.049
^{232}Th	0.501**	1	0.133
^{40}K	0.049	0.133	1

** Correlation is significant at 0.01 level (2-tailed)

The results showed a strong positive correlation between that ^{232}U and ^{232}Th with a correlation coefficient of 0.501. This implies ^{238}U that ^{232}Th exist together in minerals. A weak positive correlation existed ^{232}Th and ^{40}K in the soil samples with a correlation coefficient of 0.133 and between between ^{40}K and ^{238}U in soil samples with a correlation coefficient of 0.049. This implies potassium and thorium seems to co-exist well as compared to potassium and uranium in the samples.
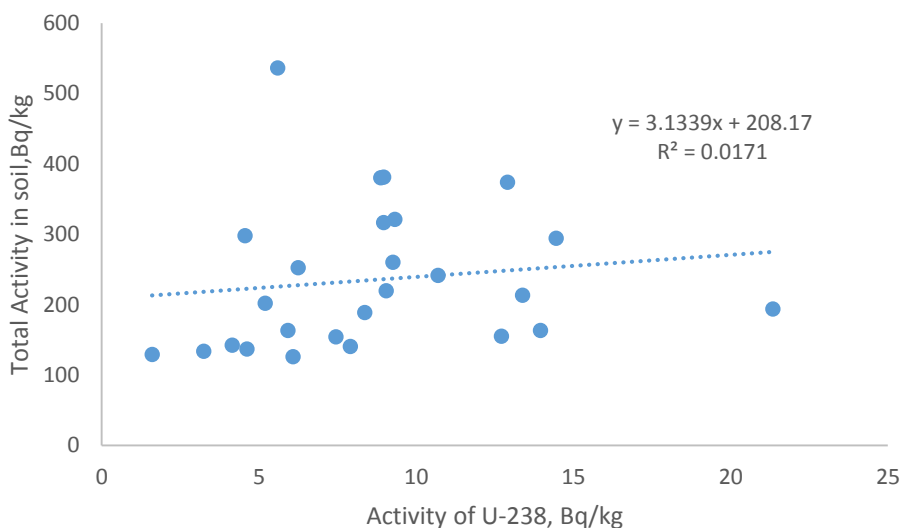
Figure 17: A comparison of the total activity of the radionuclides in the soil sample with the concentration of U-238.

104
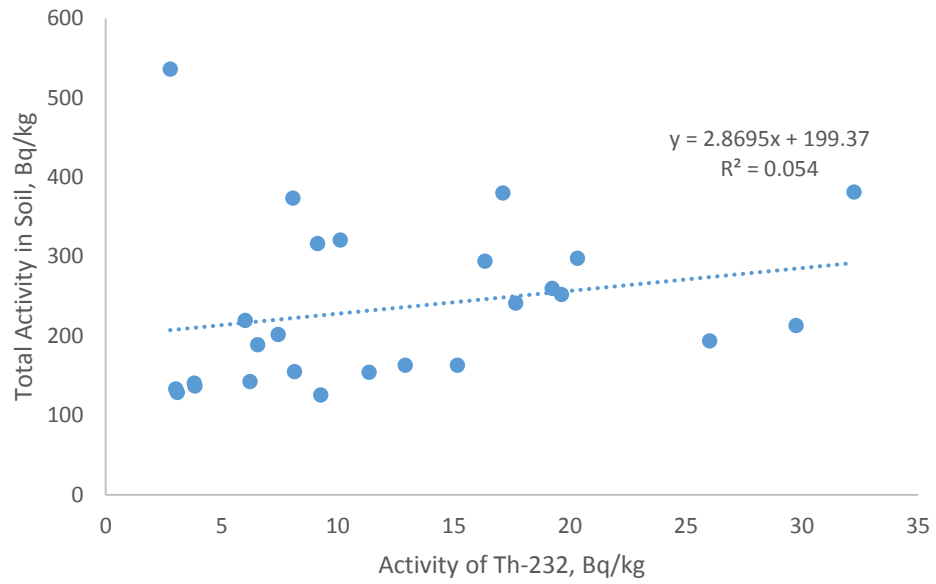
Figure 18: A comparison of the total activity of the radionuclides in the soil sample with the concentration of Th-232.
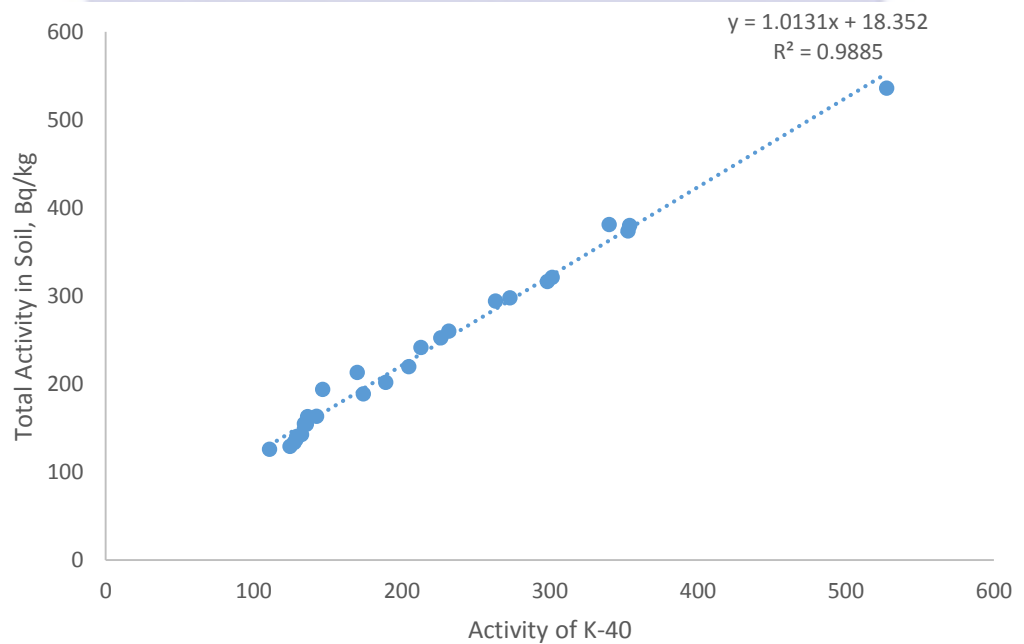
Figure 19: A comparison of the total activity of the radionuclides in the soil sample with the concentration of K-40.

The comparison of the total activity concentration of the radionuclides in soil with the activity concentration of ^{238}U is presentation as Figure 17 with those of ^{232}Th and ^{40}K as Figures 18 and 19.

105

In Figure 19, a good correlation $R^2 = 0.9885$ exists between ^{40}K activity concentrations and the total activity concentration due to ^{238}U, ^{232}Th and ^{40}K in the soil samples. In Figures 17 and 18 a poor correlation $R^2 = 0.0171$ and $R^2 = 0.054$ respectively exists between ^{238}U and ^{232}Th and the total activity concentrations.
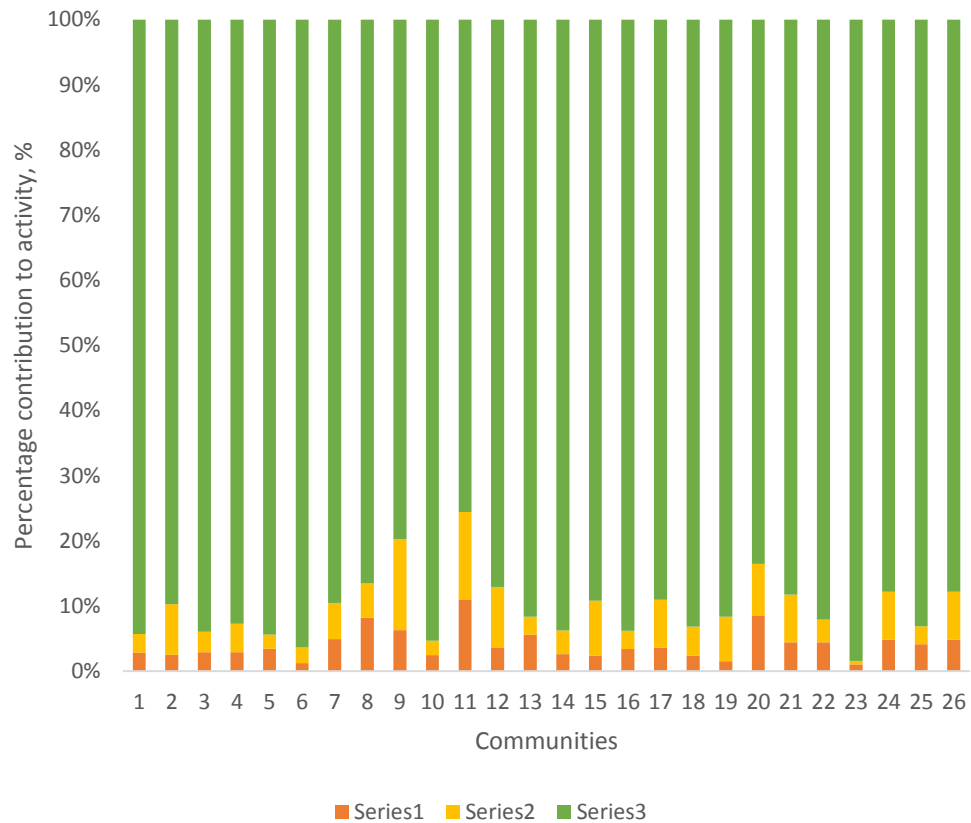
Figure 20: Percentage contribution of ^{238}U, ^{232}Th and ^{40}K in the soil samples to the total activity concentrations in the study communities.

Figure 20 is a presentation of the percentage contributions of each radionuclide in soil to the total activity concentrations in the study area. ^{40}K contributes significantly more to the total activity among the three radionuclides in the soil samples than ^{238}U and ^{232}Th (Faanu, 2011).

The results of the activity concentrations of the first and second sampling are presented in Table 21 as way of comparing the seasonal variations

106

in the activity concentrations as both samplings took place in the rainy and dry seasons respectively.

Table 21: Comparison between the mean activity concentrations of ^{238}U, ^{232}Th and ^{40}K for the first and second batch samples

Community	^{238}U		^{232}Th		^{40}K	
	1st	2nd	1st	2nd	1st	2nd
ABH	8.99	8.93	10.04	8.20	275. 08	321.46
ABH 2	7.01	5.49	17.51	21.77	242.72	210.62
ABH 3	9.11	9.53	10.24	9.98	313.10	290.12
ALIS	4.52	3.78	6.45	5.99	115.24	149.06
Axim Castle	13.41	12.39	7.81	8.31	361.43	344.31
Krisan 1	1.52	1.68	2.93	3.25	109.66	139.20
Krisan 2	14.01	14.46	16.11	16.47	251.82	275.00
Krisan 3	12.84	12.58	9.01	7.25	126.05	142.47
Beyin 1	12.96	13.80	28.37	31.13	182.43	157.55
Beyin 2	3.11	3.37	2.90	3.12	136.24	118.32
Ellonyi	23.10	19.58	24.70	27.36	138.71	154.33
Kengen 1	5.86	5.98	16.32	14.00	154.80	129.86
Kengen 2	8.12	7.68	3.57	4.05	117.67	140.15
Twenen	5.31	5.09	7.51	7.35	204.13	174.33
Nyale Kplole	8.83	9.09	34.18	31.16	326.92	353.16
Nyale Kplole 2	4.40	4.84	4.13	3.55	147.75	109.57
Nyale Kplole 3	9.46	9.06	18.06	20.42	251.48	211.92
Anokyi 1	8.63	9.11	19.13	15.11	339.67	368.33
Anokyi 2	4.40	4.72	23.31	17.02	284.93	261.07
Atuabo 2	13.24	14.66	11.98	13.84	139.01	133.59
Kikam	10.81	10.57	16.04	19.28	187.82	238.18
Half-Assini 1	8.24	8.48	6.38	6.72	162.36	185.64
Half-Assini 2	5.49	5.69	2.56	3.00	541.77	513.49
Half-Assini 3	5.81	6.35	7.84	10.70	99.86	121.26
Half-Assini 4	8.86	9.24	4.57	7.45	187.25	222.15
Newtown	7.71	7.19	12.79	9.91	131.41	139.55

Source: Laboratory work, 2016

For comparative analysis, the activity concentrations for the two batches of the samples taken at two different periods (Table 21). The results of the activity concentrations of ^{238}U, ^{232}Th and ^{40}K for the two periods did not vary significantly with p-values of 0.980, 0.950 and 0.794 respectively as shown in Table 42 (page 135). This implies that, the soil systems are more stable and secular equilibrium are easily achieved thus accounting for the insignificant difference for the two periods.

Water

The estimated average activity concentrations of ^{226}Ra, ^{228}Ra and ^{40}K in ground water samples are presented in Table 22. ^{226}Ra is in the range of 0.14 ± 0.01 to 1.62 ± 0.30Bq/L with an average of 0.58 ± 0.061 Bq/L. The range and average values for ^{228}Ra and ^{40}K are 0.18 ± 0.01 to 1.42 ± 0.21 Bq/L averaging 0.84 ± 0.09 Bq/L and 0.46 ± 0.02 to 5.92 ± 0.10 Bq/L averaging 2.51 ± 0.15 Bq/L.

Table 22: Activity concentrations of ^{226}Ra, ^{228}Ra and ^{40}K in groundwater

Community	ACTIVITY CONCENTRATION, Bq/L		
	^{226}Ra	^{228}Ra	^{40}K
Axim 1	0.24 ± 0.06	0.54 ± 0.11	3.55 ± 0.58
ABH	0.82 ± 0.03	0.73 ± 0.02	1.02 ± 0.10
ALIS	0.35 ± 0.02	0.88 ± 0.02	3.92 ± 0.10
Krisan	1.38 ± 0.22	1.12 ± 0.20	4.74 ± 0.52
Nyale Kplole 1	0.56 ± 0.03	0.95 ± 0.02	3.03 ± 0.22
Nyale Kplole 2	0.18 ± 0.01	0.85 ± 0.03	0.92 ± 0.10
Nyale Kplole 3	0.36 ± 0.02	0.78 ± 0.06	3.88 ± 0.09
Atuabo 1	0.25 ± 0.01	1.42 ± 0.21	2.32 ± 0.14
Atuabo 2	0.46 ± 0.07	0.89 ± 0.18	1.42 ± 0.15
Ekebaku	0.14 ± 0.01	1.02 ± 0.03	5.92 ± 0.10
Beyin 1	0.37 ± 0.06	1.41 ± 0.18	4.64 ± 0.21
Beyin 2	0.15 ± 0.01	0.19 ± 0.02	0.78 ± 0.12
Kikam	0.61 ± 0.02	0.37 ± 0.04	2.61 ± 0.09
Kengen 1	1.13 ± 0.12	0.79 ± 0.02	1.37 ± 0.11
Kengen 2	0.22 ± 0.04	0.43 ± 0.05	0.84 ± 0.15
Anokyi	0.73 ± 0.08	0.98 ± 0.10	2.33 ± 0.05
Twenen	0.21 ± 0.02	0.18 ± 0.01	0.46 ± 0.02
Half-Assini 1	1.62 ± 0.30	1.36 ± 0.20	0.68 ± 0.02
Half-Assini 2	0.16 ± 0.01	0.74 ± 0.08	3.85 ± 0.08
Half-Assini 3	1.03 ± 0.08	1.20 ± 0.22	1.84 ± 0.05
Minimum	**0.14 ± 0.01**	**0.18 ± 0.01**	**0.46 ± 0.02**
Maximum	**1.62 ± 0.30**	**1.42 ± 0.21**	**5.92 ± 0.10**
Average	**0.58 ± 0.061**	**0.84 ± 0.09**	**2.51 ± 0.15**

Source: Laboratory work, 2016

Produced water which contains some level of radioactivity generated from oil drilling activities are released into the open environment, therefore the determination of naturally occurring radionuclides in groundwater is useful as

108

a direct input to environmental and public health studies (Isam, Pettersson & Lund, 2002).

According to Agbalagba et al., 2013 several naturally occurring alpha and beta emitting radionuclides such as ^{238}U, ^{226}Ra, ^{216}Pb, ^{222}Rn and others are frequently dissolved in ground water supplies and their concentrations vary over an extremely wide range, mainly depending upon the amount of radioelement present in bedrock and soil with which the water comes in contact. Considering the carcinogenicity of ^{222}Rn (US EPA, 2003) and high radiotoxicity of ^{226}Ra and ^{228}Ra, their presence in water and the associated health risks require particular attention. The presence of these radioelements in water depends on the water's origin, geochemical characteristic which is a function of the Th and U contents in the aquifer, the geochemical properties of the aquifer solids, and the half-lives of each isotope (Gascoyne, 1989; ICRP, 1993). As the background concentration of natural radioactivity in groundwater in most parts of Ghana is not known, the levels of ^{226}Ra, ^{228}Ra and ^{40}K were investigated in representative groundwater to assess the radiological risk resulting from the consumption of this water.

The concentrations of ^{226}Ra, ^{228}Ra, and ^{40}K varied from 0.14 ± 0.01 to 1.62 ± 0.30 Bq/L, 0.18 ± 0.01 to 1.42 ± 0.21 and from 0.46 ± 0.02 to 2.51 ± 0.15 Bq/L. The values of ^{226}Ra in groundwater samples from Krisan (1.38 Bq/L), Kengen 1 (1.13 Bq/L), Half-Assini 1&3 (1.62 and 1.03 Bq/L) are close to the maximum contaminant levels of 1.85 mBq/L proposed in the USA (US EPA, 1999) for drinking water. ^{226}Ra and ^{40}K average activity concentrations were also well below the WHO recommended permissible level for drinking water of 1.0 and 10.0 Bq/L for ^{226}Ra and ^{40}K respectively (WHO, 2008). Only ^{228}Ra

average activity concentration recorded a value of 0.84, which is higher than the WHO recommended value of 0.1 Bq/L.

The generally low activity concentrations for ^{226}Ra and ^{232}Th for water samples of studied areas can be good indicator for the low radioactivity levels in the aquifer rocks. Because radionuclide concentrations in ground waters depend on the minerals derived from aquifer rocks, the communities have Birimian formation composed of schists, phyllite and greywacks rocks (Attah-Peters & Garrey, 2014). The concentrations of radionuclide's ^{226}Ra, ^{228}Ra and ^{40}K in water samples are in the narrow range, this probably is due to the fact that the sites studied cover an area with similar aquifer lithologies and consequently no large differences in radionuclide solubilities and mobilities. The relatively high abundance of ^{40}K activity observed may be due to agricultural activities going on in the area that involve the use of potassium fertilizers which may have been transported to the groundwater, given that ^{40}K is a highly soluble element. The average concentrations of ^{228}Ra of 0.084 ± 0.09 is higher than that of ^{226}Ra of 0.58 ± 0.06. This does not reflects the fact that ^{226}Ra which is a progeny of ^{238}U is more soluble in water than ^{228}Ra, a progeny of ^{232}Th (Focazio, Szabo, Kraemer, Mullin, Barringer & DePaul, 1998).

The activity concentrations of radionuclides were slightly higher in the second batch of samples than the first even though the water samples were near neutral conditions. However, the differences are not significant. The estimated mean annual effective doses for the first and second batch samples were 0.21 and 0.27 mSv respectively. The results of the activity concentrations of the two sets of water samples were not significantly different with p-values greater than

0.05 as shown in Table 23. To test if there were significant difference in the mean concentrations of ^{226}Ra, ^{228}Ra and ^{40}K, ANOVA was used.

Table 23: Comparison between mean values of the activity concentrations of ^{226}Ra, ^{228}Ra and ^{40}K in ground water samples for the two sets of data.

First and second batch results	^{226}Ra activity concentration, Bq/kg	^{228}Ra activity concentration, Bq/kg	^{40}K activity concentration, Bq/kg	Annual Effective dose, μSv
Probability value	0.986**	0.635**	0.993**	0.12

** Correlation is significant at 0.01 level (2-tailed)

The analysis indicated that there were significant differences in the means at 5% significant level. Further, multiple comparison tests was conducted and the results are given in Table 24. The mean concentrations of ^{226}Ra and ^{40}K and ^{228}Ra and ^{40}K are significantly different whereas ^{226}Ra and ^{228}Ra are not. This implies that ^{226}Ra and ^{228}Th may exist together in varying concentrations in different types of rocks and water samples (Faanu, 2011).

Table 24: Correlation analysis using Pearson Correlation Matrix Method used to assess the correlation between ^{226}Ra, ^{228}Ra and ^{40}K respectively due to groundwater samples.

Radionuclide	^{226}Ra	^{228}Ra	^{40}K
^{226}Ra	1	0.423	-0.149
^{228}Ra	0.423	1	0.353
^{40}K	-0.149	0.353	1

Source: Laboratory work, 2016

The average activity concentrations of ^{226}Ra, ^{228}Ra and ^{40}K obtained from the present study was compared to literature for groundwater from other parts of the world and observed to be below the averages reported in Nigeria (Nwankwo, 2012 & 2013) and (Ononugbo, Avwiri & Egieya, 2013); Iran (Ehsanpour, Abdi, Mojtaba & Hashem, 2014); Yemen (Harb, El-Kamel, Zahran, Abbady & Ahmed, 2014).

111

Comparisons of the activity concentrations of ^{226}Ra, ^{228}Ra and ^{40}K and published data are presented in Table 25. The average values of 0.55 Bq/L for ^{226}Ra, 0.84 Bq/L for ^{228}Ra and 2.51 Bq/L for ^{40}K obtained for this study are below the values obtained from other parts of the world.

Table 25: Comparison of activity concentrations of ^{226}Ra, ^{228}Ra and ^{40}K in groundwater in the study area and published data.

Country	Concentration in drinking water, Bq/L						
	^{226}Ra/^{238}U		^{228}Ra/^{232}Th		^{40}K		
	Range	average	Range	Average	Range	Average	Reference
Nigeria	0.02-7.35	4.04	0.009-3.98	0.77	0.45-30.14	4.81	Nwankwo, 2012,
Nigeria		9.22		8.46		44.27	Ononugbo et al. 2013
Nigeria	0.81-7.40	3.70	1.80-5.60	3.60			Nwankwo, 2013
Iran	≤0.5-9701		≤0.2-28215		MDA-10332		Ehsanpour et al., 2014
Yemen	0.22-2.67	1.44	0.15-3.06	1.2	7.87-26.02	18.34	Harb et al., 2014
Ghana			0.25-1.20	0.57	0.88-8.86	3.67	Nguelem et al., 2013
Ghana			0.17-0.65	0.59	0.72-6.92	2.59	Nguelem et al. 2013
Ghana	0.18-1.62	0.55	0.18-1.42	0.84	0.68-4.74	2.51	This study

Source: Field work, 2016

Activity concentration of K-40 compared to WHO standard
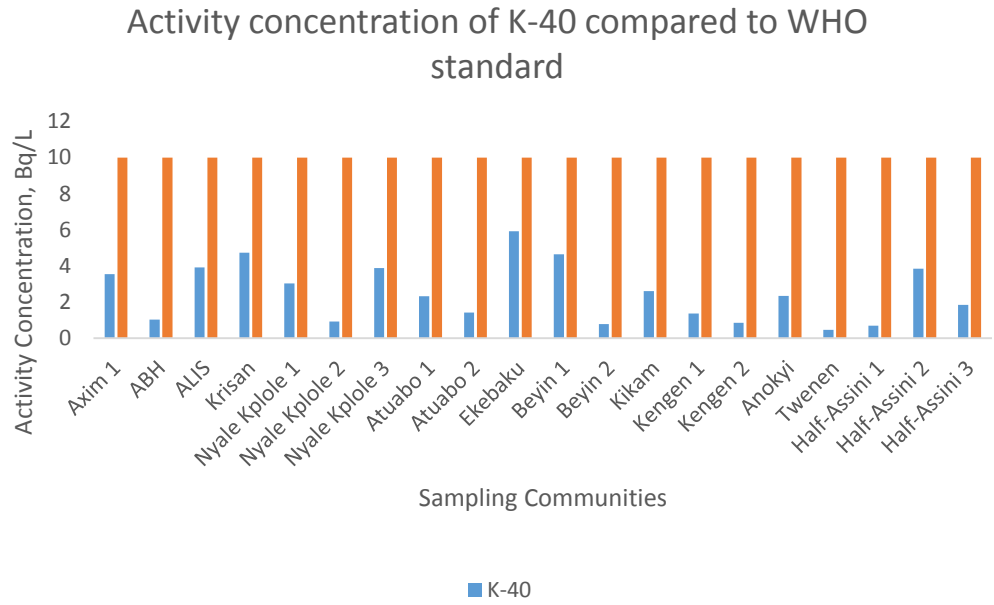
Figure 21: Comparison of Specific Activity of K-40 in groundwater samples with WHO, 2008 Standard

Activity concentration of Ra-228 (Bq/L) and WHO standard
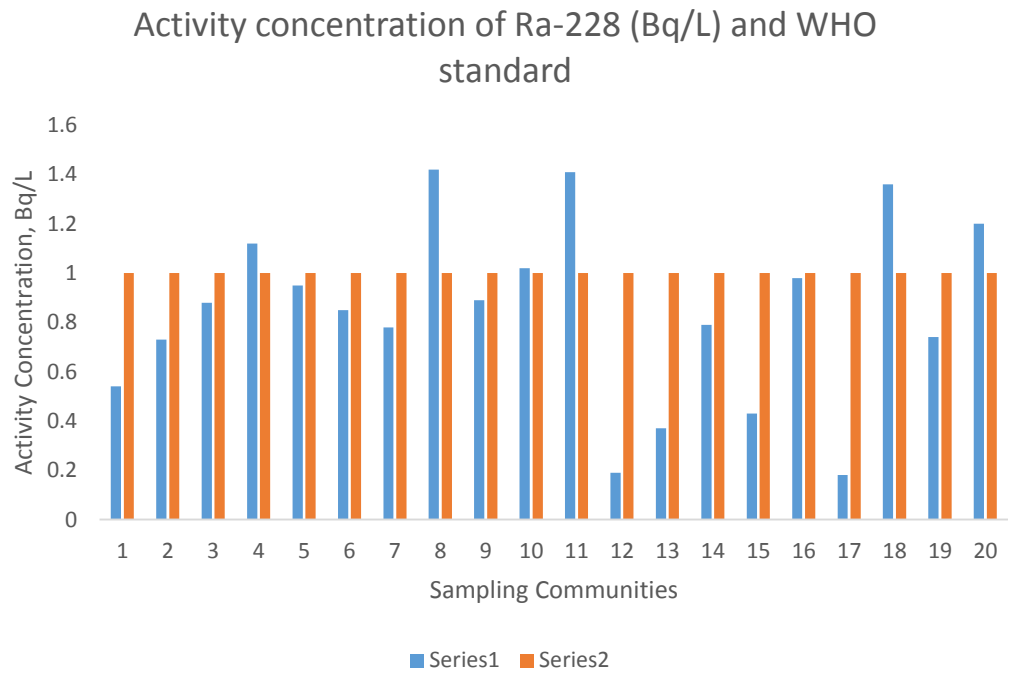
Figure 22: Comparison of Specific Activity of Ra-228 in groundwater samples with WHO, 2008 Standard

113

Activity concentration (Bq/L) of Ra-226 and WHO standard
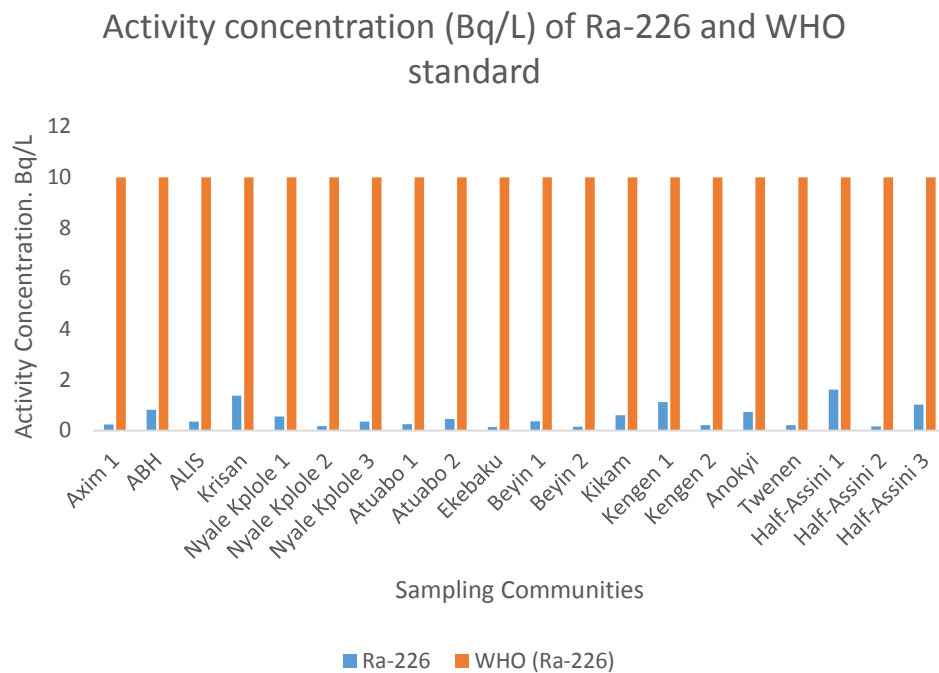
Figure 23: Comparison of Specific Activity of Ra-226 in groundwater samples with WHO, 2008 Standard

Comparisons of the specific activities of K-40, Ra-228 and Ra-226 with their corresponding WHO, 2008 standards are presented in Figures 21, 22 and 23 respectively.

Radon

Radon in Water

Radon-222 activity concentration in water is within the range 35 ± 5 to 177 ± 22 Bq/L averaging at 90.05 ± 10.6 Bq/L (Table 26). The annual effective dose from ^{222}Rn due to the ingestion of groundwater ranges from 0.13 ± 0.018 to 0.65 ± 0.08 mSv with an average of 0.33 ± 0.04 mSv.

Table 26: Rn-222 concentration in water and the estimated annual effective doses

Community	Water ^{222}Rn, Bq/L	Groundwater ^{222}Rn annual effective dose, (ingestion) mSv
Axim 1	91 ± 8	0.33 ± 0.03
ABH	83 ± 11	0.30 ± 0.04
ALIS	132 ± 15	0.48 ± 0.06
Krisan	173 ± 17	0.63 ± 0.06
Nyale Kplole 1	88 ± 11	0.32± 0.04
Nyale Kplole 2	56 ± 12	0.20 ± 0.04
Nyale Kplole 3	75 ± 7	0.27 ± 0.03
Atuabo 1	35 ± 5	0.13 ± 0.02
Atuabo 2	43 ± 7	0.16 ± 0.03
Ekebaku	177 ± 22	0.65 ± 0.08
Beyin 1	156 ± 14	0.57 ± 0.05
Beyin 2	118 ± 15	0.43 ± 0.06
Kikam	67 ± 6	0.24 ± 0.02
Kengen 1	94 ± 13	0.34 ± 0.05
Kengen 2	71 ± 5	0.26 ± 0.02
Anokyi	52 ± 6	0.19 ± 0.02
Twenen	62 ± 7	0.23 ± 0.03
Half-Assini 1	79 ± 12	0.29 ± 0.04
Half-Assini 2	50 ± 11	0.18 ± 0.04
Half-Assini 3	99 ± 8	0.36 ± 0.03
Range	**35 ± 5 - 177 ± 22**	**0.13 ± 0.018 - 0.65 ± 0.08**
Mean	**90.05 ± 10.6**	**0.33 ± 0.04**

Source: Laboratory work, 2016

Rn-222 concentrations obtained for the groundwater samples from the coastal communities along the Tano Basin using RAD7 electronic detector are presented in Table 20. The radon concentrations obtained ranged from 35 ± 5 to 177 ± 22 Bq/L with a mean of 90.05 ± 10.6 Bq/L. The highest radon concentration levels recorded from this study i.e. Ekebaku (177 ± 22 Bq/L), Krisan (173 ± 17 Bq/L), and Beyin 1 (156 ± 14 Bq/L) sites have their radon concentrations exceeding U.S maximum contamination level (MCL) which is 11.1 Bq/L (Auvinen, Salomen, Pekkanen, Pukkala, Ilus & Kurttio, 2005). The values are however well below the European Union reference level of 1000 Bq/L. 100% of all samples monitored exceeded the limit of U.S Environment Protection Agency proposed limit of 11 Bq/L. This is very alarming, since

115

dwellers mostly store water for household activities indoors which in such cases contributes to indoor radon gas.

The variations in the concentration of radon from the different investigatory sites could be an indication of higher content of radioactivity in geological setting in communities registering higher values than those with lower values because bedrock, soil and groundwater system are in interaction with each other. As a result of this interaction, some natural radionuclides may dissolve into groundwater from bedrock system and soil during their infiltration from surface into aquifer (Yuce, Didem, Alimeju, Turgay, Muset, Mert & Sakir, 2009).

These generally low concentration levels of radon in groundwater as compared to the European Union reference level of 1000 Bq/L could be explained from the geological context of the surrounding rocks. The deepest layer in the studied areas are dolomite, followed by limestone and then chalky stones near the surface. This geological structure is similar for almost all the studied locations. Indeed, uranium and radon are found in small amount in all the types of rocks. However, some types of rocks have more concentration of uranium and radon than others. These include light-colored volcanic rocks, granites, dark shales, sedimentary rocks that contain phosphate, and metamorphic rocks derived from these rocks. Dolomite and limestone are sedimentary stones but they are composed of calcium not phosphate which may explain the low concentration values obtained in the study.

Another possible explanation is the depth of the wells. Usually radon concentration increases as the depth in earth increases (CDC, 2010). Some studies, however, found a relation between high radon concentration in water,

116

soil and air and seismic activities and earth quake. Indeed, the exhalation rate of radon are found to increase near the faults (Gregoric, Zmazek & Vaupotic, 2008; Singh, Kumah, Singh, Mahajan, Kumar & Dhar, 2010; US EPA, 2006).

As there is no absolute safe value of radiation from radon on general public (Auvinen et al., 2005), each country had its suggested target safe limit. Although there are a number of studies on radon level in the outdoor and indoor air in Ghana (Ansre, Miyittah, Andam & Dodor, 2017; Faanu, 2011), no water radon level reference has been established and therefore, there has been no specific safe limit value for radon. There are no standard reference level developed in the neighbouring countries as well and they still depend on the U.S or European standard safe levels.

The results of the comparison of radon concentration in groundwater with published data are also given in Table 27. Compared to other countries, the range for ground water in Sweden was found to be 1200 – 15200 Bq/L, Poland 1200 – 32000 Bq/L and India 2560 – 7750 Bg/L (Knutsson & Olofosson, 2002: Karpinska, Kapala, Mnich & Szpak, 2010; Badham, Mehra & Sonkawade, 2010). These were far higher than the study values. The ranges from this study were however very close to the range of values from Ghana of 5 - 47 Bq/L (Asumadu-Sakyi, Oppon, Quarshie, Adjei, Akortia, Nsiah-Akoto & Appiah, 2012) and much similar to that in Romania 1- 129 Bq/L (Cosma, Moldovan, Dicu & Kovacs, 2008). This does not suggest an intrusion of radon from oil logging activities but rather from natural sources.

Table 27: Comparison of radon concentrations of in groundwater in the study
area and published data

Country	Water ^{222}Rn, Bq/L	Reference
Ghana	35-177	This study
Sweden	1200-15200	Knutsson et al., 2002.
Poland	1200-32000	Karpinska et al., 2010
Ghana	5-47	Asumadu-Sakyi et al., 2012
India	2560-7750	Badham et al., 2010
China	8-49	Wu et al., 2014.
Mexico	Background – 4	Vázquez-López et al., 2011
India	1–5	Duggal et al., 2013.
Romania	1–129	Cosma et al., 2008
Turkey	1–54	Akar et al., 2012
Poland	0.42–11	Bem et al., 2013

Source: Laboratory work, 2016

Radon in Air

Table 28 shows the results of airborne radon concentrations as well as
the estimated annual effective dose. Airborne radon concentration ranged from
15.43±2.67 to 30.00±5.58 Bq/L as theannual effective dose is from 1.96E-02 to
3.80E-02 µSvy^{-1}.

Table 28: Rn-222 concentration in air and the corresponding estimated
airborne annual effective doses

Community	Radon concentration Airborne ^{222}Rn, Bq/m^3	Airborne ^{222}Rn annual effective dose, µSvy^{-1}
Axim 1	22.50±2.18	2.85E-02
ABH	15.46±2.20	1.96E-02
ALIS	18.68±4.64	2.37E-02
Krisan	21.16±3.53	2.68E-02
Nyale Kplole 1	30.00±5.58	3.80E-02
Nyale Kplole 2	26.47±2.91	3.35E-02
Atuabo 1	15.80±2.22	2.00E-02
Ekebaku	29.30±3.78	3.71E-02
Beyin 1	15.43±2.67	1.96E-02
Beyin 2	17.90±1.33	2.27E-02
Kengen 1	23.70±4.88	3.00E-02
Kengen 2	15.66±4.31	1.98E-02
Twenen	18.80±3.29	2.38E-02
Half-Assini 1	15.60±2.74	1.98E-02
Half-Assini 2	18.85±2.40	2.39E-02
Half-Assini 3	19.50±2.53	2.47E-02
Min	**15.43±2.67**	**1.96E-02**
Max	**30.00±5.58**	**3.80E-02**
Average	**20.30±2.85**	**2.57E-02**

Source: Laboratory work, 2016

Radon gas which is considered as a dangerous radioactive gas, as it decays by alpha particles which is characterized by high ionizing power (OGP, 2008) and known to contribute about 50% to the average annual radiation exposure from natural sources was also determined. The results varied in a range of $15.43 \pm 2.67 - 30.00 \pm 5.58$ with a mean value of 20.30 ± 2.85 Bq/m³. The calculated annual effective dose from inhalation ranged from 1.96E-02 to 3.8E-02 mSv/y with a mean value of 2.57E-02 mSv/y (Table 28).

The results in this study compared well with results published in UNSCEAR, 1996 & 2000 reports for normal areas around the world with values in a range of 2-30 Bq/min air (UNSCEAR, 2000). The results are also below the action level of radon concentration in air of 1000 Bq/m intervention is required. The corresponding annual effective dose is 6 mSv/year using an assumed outdoor occupancy of 1760 hours per year (ICRP, 1991 and UNSCEAR, 1993 & 2000). This means that the oil drilling activities in the area studied does not have significant impact on the levels of ^{222}Rn gas.

Food

The cassava samples harvested from gardens within the study area were characterised to quantify the activity concentrations of ^{238}U, ^{232}Th and ^{40}K dry weight in Bq/kg. The activity concentrations of ^{238}U, ^{232}Th, and ^{40}K are in the range of 0.41 ± 0.14 to 1.04 ± 0.44 Bq/kq, 0.10 ± 0.004 to 0.75 ± 0.12 Bq/kq and 8.46 ± 1.75 to 41.31 ± 6.63 Bq/kg respectively (Table 28). The activity concentrations of ^{238}U, ^{232}Th and ^{40}K in soil samples are in the range of $4.16 - 10.69$ Bq/kg, $6.22 - 32.24$ Bq/kg and $132 - 354$ Bq/kg respectively and are compared to their respective concentrations in co-located cassava samples in Table 29.

Table 29: Radioactivity intensities (Bqkg^{-1}) of radionuclides ^{238}U, ^{232}Th and ^{40}K in soil and cassava and their corresponding transfer factors. Values for radioactivity intensities are displayed to 3 significant figures. Plus-minus values represent the instrument

Sample	Activity concentration of soil, Bq/kg			Activity concentration of cassava, Bq/kg			Transfer factors		
	^{238}U	^{232}Th	^{40}K	^{238}U	^{232}Th	^{40}K	^{238}U	^{232}Th	^{40}K
CS 1	4.15±0.62	6.22±0.93	132±18.8	0.41±0.10	0.62±0.18	36.9±4.10	0.10	0.10	0.28
CS 2	8.96±1.99	32.2±1.84	340±51.0	0.53±0.08	0.49±0.21	41.3±6.63	0.06	0.02	0.12
CS 3	5.20±0.78	7.43±1.11	189±28.1	0.64±0.21	0.57±0.18	8.46±1.75	0.12	0.08	0.04
CS 4	8.87±1.13	17.1±2.44	354±13.9	0.89±0.43	0.16±0.04	27.2±3.61	0.10	0.01	0.08
CS 5	10.7±0.15	17.7±0.92	213±8.73	1.04±0.44	0.75±0.12	14.3±1.12	0.10	0.04	0.07
Min.	4.15±0.62	6.22±0.93	132±18.8	0.41±0.10	0.16±0.04	8.46±1.75	0.06	0.01	0.04
Max.	10.7±0.15	32.2±1.84	354±13.9	1.04±0.44	0.75±0.12	41.3±6.63	0.12	0.10	0.28
Median	8.87±1.13	17.1±2.44	213±8.73	0.64±0.21	0.57±0.18	27.2±3.61	0.10	0.04	0.08

Source: Laboratory work, 2016

The cassava samples harvested from gardens within the study area were characterised to quantify the activity concentrations of ^{238}U, ^{232}Th and ^{40}K dry weight in Bq/kg. The activity concentrations of ^{238}U, ^{232}Th, and ^{40}K are in the range of 0.41±0.14 to 1.04±0.44 Bq/kq, 0.10±0.004 to 0.75±0.12 Bq/kq and 8.46±1.75 to 41.31±6.63 Bq/kg respectively (Table 29). The activity concentrations of ^{238}U, ^{232}Th and ^{40}K in soil samples are in the range of 4.16 – 10.7 Bq/kg, 6.22 – 32.2 Bq/kg and 132 - 354 Bq/kg respectively and are compared to their respective concentrations in cassava.

The sum of average activity concentrations of 0.70, 52 and 25.63 Bq/kq respectively were used in estimating the average annual effective dose of 38.7 µSv/year (0.0387 mSv/year), based on consumption of 170kg/y. The average activity concentration of ^{40}K is much higher than those of other radionuclides. This is expected, as ^{40}K is an isotope of potassium, an essential macronutrient for plants. Moreover, the addition of potassium to the soil through fertilizer increases its concentration in plants (Santos, Lauria, Amaral & Rochedo, 2002). This radionuclide behaves as an essential nutrient in the human body. Its

behavior resembles that of stable potassium found in muscle tissue. The concentration of stable potassium in muscle tissue is constant due to homeostatic balance (Cardoso, Cardoso, Alhanati, Ciolini, Souza, 2013).

Comparing the results with the exemption levels of ^{238}U (1 Bq/g), Th (1 Bq/g) and ^{40}K (10 Bq/g) (IAEA, 2004), indicate lower values. It implies that the levels of radioactivity in the cassava samples are insignificant and will not pose a significant radiological hazard to human health from ingestion. Similar studies in the oil and gas producing areas in Delta State, Nigeria have been measured using a high purity germanium, (HPGe) detector system in tubers registered 9.58 – 17.78, 6.92 – 16.60 and 49.10 – 202.75 Bq/kg for ^{238}U, ^{232}Th and ^{40}K respectively (Tchokossa, Olomo, Balogun & Adesanmi, 2013). Comparatively, the reported results from Nigeria are far higher than what was obtained for this study, considering similar industrial activity offshore.

Absorbed Dose Rates and Annual Effective Doses and Radiological Risk Assessment

Soil

The estimated radiation dose rates and radiological hazard parameters are presented in Table 30. The absorbed dose ranges from 7.79 to 37.79 nGy/h with an average of 20.48 due to direct gamma exposure to ^{238}U, ^{232}Th and ^{40}K from soil. The annual effective dose is in the range 9.56E+00 to 4.64E+01 µSv/y with an average of 2.51E+01. The Excess Lifetime Cancer Risk (ELCR), internal hazard index (H_{in}), and external hazard index (H_{ex}) were determined to be in the range 35E-05 -1.62E-04, 0.05-0.25 and 0.04-0.22 respectively with average values of 8.80E-05, 0.14 and 0.12 respectively.

Table 30: Radiation Dose Rates and Hazard Parameters in Soil

Community	Absorbed Dose, nGy/h	Annual Effective Dose, µSv/y	ELCR	H_{in}	H_{ex}
ABH	22.09	2.71E+01	9.49E-05	0.15	0.12
ABH 2	24.19	2.97E+01	1.04E-04	0.16	0.14
ABH 3	22.99	2.82E+01	9.87E-05	0.15	0.13
ALIS	11.19	1.37E+01	4.80E-05	0.07	0.06
Axim Castle	25.54	3.13E+01	1.10E-04	0.17	0.14
Krisan 1	7.79	9.56E+00	3.35E-05	0.05	0.04
Krisan 2	27.53	3.38E+01	1.18E-04	0.20	0.17
Krisan 3	16.38	2.01E+01	7.04E-05	0.13	0.09
Beyin 1	31.24	3.83E+01	1.34E-04	0.22	0.19
Beyin 2	8.62	1.06E+01	3.70E-05	0.06	0.05
Ellonyi	31.69	3.89E+01	1.36E-04	0.25	0.19
Kengen 1	17.83	2.19E+01	7.66E-05	0.12	0.10
Kengen 2	11.33	1.39E+01	4.87E-05	0.08	0.06
Twenen	14.78	1.81E+01	6.35E-05	0.10	0.08
Nyale Kplole	37.79	4.64E+01	1.62E-04	0.24	0.22
Nyale Kplole 2	9.82	1.21E+01	4.22E-05	0.07	0.05
Nyale Kplole 3	25.56	3.14E+01	1.10E-04	0.17	0.15
Anokyi 1	29.20	3.58E+01	1.25E-04	0.19	0.16
Anokyi 2	25.77	3.16E+01	1.11E-04	0.16	0.15
Atuabo 2	19.93	2.45E+01	8.56E-05	0.15	0.12
Kikam	24.49	3.01E+01	1.05E-04	0.17	0.14
Half-Assini 1	15.07	1.85E+01	6.47E-05	0.11	0.08
Half-Assini 2	26.26	3.22E+01	1.13E-04	0.15	0.14
Half-Assini 3	13.02	1.60E+01	5.59E-05	0.09	0.08
Half-Assini 4	16.33	2.01E+01	7.02E-05	0.11	0.09
Newtown	15.95	1.96E+01	6.85E-05	0.11	0.09
Range	7.79-37.79	9.56E+00 - 4.64E+01	3.35E-05 1.62E-04	0.05-0.25	0.04-0.22
Mean	20.48	2.51E+01	8.80E-05	0.14	0.12

Source: Laboratory work, 2016

The International Commission on Radiological Protection (ICRP 1993; 2007) has recommended the annual effective dose equivalent limit of 1 mSvy[-1] for the individual members of the public and 20 mSvy[-1] for the radiation workers. The total absorbed dose in the study area ranges from 7.79 to 37.79 nGyh[-1] with an average value of 20.48 nGyh[-1]. The corresponding annual effective doses range from 9.56E+00 to 4.64E+01 mSvy[-1] with an average value of 2.51E+01 mSvy[-1] respectively while the world wide average annual effective dose is approximately 0.5 mSvy[-1] and the results for individual

122

countries being generally within the 0.3- 0.6 mSvy⁻¹ range for indoors. Generally similar type of trend is observed in all the samples and no regular trend in the variation in the annual effective dose and absorbed dose rate is observed from the soil samples. Spatial variations noticed among the values may be due to the physicochemical and geochemical properties of the respective radionuclides along with their presence in the soil samples (El Mamoney & Khater, 2004; Sam, Ahamad, El Khangi, El Nigumi & Holm, 1998).

The results for average annual effective dose are within the range of worldwide average value.   The calculated values of external hazard index, H_{ex} and internal hazard index, H_{in} for the soil samples studied range from 0.04 to 0.22 and 0.05 to 0.25 respectively. Since these values are lower than unity, therefore, according to the Radiation Protection 112 (EC RP, 1999) report, soil from these regions is safe and can be used as construction material without posing any significant radiological threat to population. The Excess Lifetime Cancer Risk confirms this, which is within the accepted limit of 3.35E-05 to 1.62E-04 with an average of 8.80E-05.

The exposure due to γ-radiation is usually defined in terms of radium equivalent activity Ra_{eq} and is given by the Equation:

$$Ra_{eq} = C_U + \frac{10}{7}C_{Th} + \frac{10}{130}C_K$$

The above equation is based on the assumption that 370 Bq kg⁻¹ of ²²⁶Ra, 259 Bq kg⁻¹ of ²³²Th, and 4810 Bq kg⁻¹ of ⁴⁰K produce the same gamma-ray dose rate. The radium equivalent is related to both the external γ-dose and the internal α-dose from radon and its progeny. The permissible maximum value of the radium equivalent activity is 370 Bq kg⁻¹, which corresponds to an effective dose of 1 mSv yr⁻¹ for to the inhabitants of dwellings (UNSCEAR,

1993; 2000). The Ra_{eq} average values for the study area ranged from 15.59 to 81.17 Bqkg^{-1} with an average of 43.37 Bqkg^{-1}. The minimum and the maximum values were as a result of soil samples from Krisan 1 and Nyale Kplole 1 respectively as presented in Table 33. In all of the soil samples, Ra_{eq} values were well below the worldwide value of 370 Bqkg^{-1} recommended under normal circumstances, rendering the sampling areas safe. This has been attributed to the low levels of ^{238}U analysed in the samples and hence should not be attributed to the oil drilling activities offshore.

Table 31 is a presentation of the average activity concentration ratios for soil, radium equivalence and the percentage contributions of [238]U, [232]Th and [40]K to the absorbed dose rate in soil. [238]U contributed an average of 20.14%, [232]Th an average of 34.44% and [40]K contributing the highest average of 45.81%. The radium equivalence Ra_{eq} ranged between 15.58 to 81.17 Bq/kg with an average of 43.37 Bq/kg.

Table 31: Average activity concentration ratios, radium equivalence and percentage contributions of [238]U, [232]Th, [40]K to absorbed dose rate in soil from the study area

Community	Activity concentrations, Bq/kg			Activity concentration ratios			Radium Equivalence (Ra$_{eq}$), Bq/kg	Absorbed Dose Rate, nGy/h	Percentage contribution of radionuclides to absorbed dose rate, %		
	[238]U	[232]Th	[40]K	Th/U	K/U	K/Th			[238]U	[232]Th	[40]K
ABH	8.96	9.12	298.27	1.02	33.29	32.71	44.93	22.09	18.74	24.94	56.32
ABH 2	6.25	19.64	226.41	3.14	36.23	11.53	51.72	24.19	11.94	49.04	39.03
ABH 3	9.32	10.11	301.61	1.08	32.36	29.83	46.96	22.99	18.73	26.56	54.71
ALIS	4.15	6.22	132.15	1.50	31.84	21.25	23.20	11.19	17.14	33.59	49.27
Axim Castle	12.90	8.06	352.87	0.62	27.35	43.78	51.56	25.54	23.33	19.06	57.61
Krisan 1	1.60	3.09	124.43	1.93	77.76	40.26	15.58	7.79	9.49	23.95	66.57
Krisan 2	14.45	16.34	263.41	1.13	18.23	16.12	58.06	27.53	24.25	35.85	39.90
Krisan 3	12.71	8.13	134.26	0.64	10.56	16.51	34.65	16.38	35.85	29.98	34.18
Beyin 1	13.38	29.75	169.99	2.22	12.71	5.71	68.96	31.24	19.79	57.52	22.70
Beyin 2	3.240	3.01	127.28	0.93	39.28	42.29	17.33	8.62	17.36	21.09	61.56

Table 31 (continued)

Ellonyi	21.34	26.03	146.52	1.22	6.87	5.63	69.80	31.69	31.11	49.61	19.28
Kengen 1	5.92	15.16	142.33	2.56	24.04	9.39	38.53	17.83	15.34	51.36	33.30
Kengen 2	7.90	3.81	128.91	0.48	16.32	33.84	23.26	11.33	32.22	20.32	47.46
Twenen	5.20	7.43	189.23	1.43	36.39	25.47	30.37	14.78	16.25	30.36	53.39
Nyale Kplole	8.96	32.24	340.04	3.60	37.95	10.55	81.17	37.79	10.95	51.53	37.52
Nyale Kplole 2	4.62	3.84	128.66	0.83	27.85	33.51	20.00	9.82	21.74	23.62	54.64
Nyale Kplole 3	9.26	19.24	231.70	2.08	25.02	12.04	54.57	25.56	16.74	45.46	37.80
Anokyi 1	8.87	17.12	354	1.93	39.91	20.68	60.56	29.20	14.03	35.41	50.55
Anokyi 2	4.56	20.33	273	4.46	59.87	13.43	54.60	25.77	8.18	47.65	44.18
Atuabo 2	13.95	12.91	136.30	0.93	9.77	10.56	42.88	19.93	32.34	39.13	28.52
Kikam	10.69	17.66	213	1.65	19.93	12.06	52.30	24.49	20.17	43.56	36.27
Half-Assini 1	8.36	6.55	17	0.78	20.81	26.57	31.10	15.07	25.62	26.25	48.13
Half-Assini 2	5.59	2.78	527.63	0.50	94.39	189.80	50.15	26.26	9.83	6.39	83.77
Half-Assini 3	6.08	9.27	110.56	1.53	18.18	11.93	27.83	13.02	21.58	43.01	35.41
Half-Assini 4	9.05	6.01	204.70	0.66	22.62	34.06	33.38	16.33	25.58	22.21	52.22
Newtown	7.45	11.35	135.478	1.52	18.19	11.94	34.09	15.95	21.58	42.99	35.43
Minimum	**1.60**	**2.78**	**110.56**	**0.48**	**6.87**	**5.63**	**15.58**	**7.79**	**8.18**	**6.39**	**19.28**
Maximum	**21.34**	**32.24**	**527.63**	**4.46**	**94.39**	**189.80**	**81.17**	**37.79**	**35.85**	**57.52**	**83.77**
Average	**8.65**	**12.51**	**214.11**	**1.62**	**32.11**	**26.93**	**43.37**	**20.48**	**20.14**	**34.44**	**45.81**

Source: Laboratory work, 2016

The mean excess lifetime cancer risk (ELCR) of 8.8E-05 obtained for soil samples was below the standard value of 0.29 x 10^{-3}. However, average excess lifetime cancer risk (ELCR) for all age brackets in the case of the water samples as contained in Tables 34 - 37 were above the world average value of 10^{-4} (EPA, 2012). The ELCR for babies ranged from 6.90E-03 to 3.28E-02, with an average of 167E-02. Those of children, teenagers and adults are 7.91E-02 to 3.91E-01, 1.15E-01 to 5.56E-01 and 4.55E-01 to 2.28E+00 respectively with their corresponding averages being 1.98E-02, 2.87E-01 and 1.17E+00.

Excess Lifetime Cancer Risk above the recommended limits could have been impacted negatively by activities such as gas flaring as observed during sample collection (Ajibode, Avwiri & Agbalagba, 2013). These areas also show radiological elevation from the percentage risk analysis signifying a radiological burden on the people and the environment of these areas and there is the possibility of one out of a million developing cancer before the age of 70 years by the workers and the people living in the areas. This implies that the chances of having cancer by the general populace are significant. Therefore all the sources of drinking water in these communities of the study area must be treated before consumption to avert the likely health implications.

The significance of exposure from natural radioactivity and the potential risk for causing health detriment, especially cancer, has received considerable attention from some regulatory bodies that use quantitative risk assessment process to determine an excess cancer risk over a lifetime (ELCR). UNSCEAR and BEIR V i.e., Committee on the Biological Effects of Ionizing Radiations, known as the BEIR stated that their risk estimates should be reduced for low dose exposures protracted over several months or years to account for a reduced

effectiveness of the cell damage mechanism Ahier & Tracy, (1995). Using a maximum reduction factor of 2, UNSCEAR, 1993 recommends a lifetime risk estimate of 5% Sv^{-1} for fatal cancer following a protracted whole-body exposure of low dose and low dose rate radiation (Ahier & Tracy, 1995). The International Commission on Radiological Protection, while relying mainly on the assessment of the Japanese survivors by organizations such as UNSCEAR, (1993) & BEIR, (1990), has taken into consideration the entire body of literature in their estimate of risk (Ahier & Tracy, 1995).

The lifetime risk estimate for low-dose exposures as given in the 1990 recommendations of the ICRP is 5% Sv^{-1} for the entire population, based on a linear, no-dose threshold model. On the basis of copious on-going research in human epidemiology, animal studies and cell biology, these organizations concluded that the risk estimates at low doses are likely conservative. Therefore, the need to determine the excess cancer risk over a lifetime (ELCR). This approach mathematically calculates the probability of developing cancer over a lifetime at a given exposure level. It is presented as a value representing the number of extra cancers expected in a given number of people on exposure to a carcinogen at a stated dose.

The radium equivalent activity and the gamma yield from this study are compared to literature and presented in Table 32 and found to be in the range of those from other parts of the world. The average activity concentrations of 8.65 Bq/kq, 12.51 Bq/kq and 214.11 Bq/kq for ^{238}U, ^{232}Th and ^{40}K from the present study are below the world averages of 35 Bq/kq, 30 Bq/kq and 400 Bq/kq respectively reported in UNSCEAR (2000). The average Ra_{eq} of 43.37 Bq/kq from this study is below the recommended world average of 370 Bq/kg.

128

Table 32: Comparison of the average activity concentrations, the radium equivalent Activities (Ra$_{eq}$) of soil of the study area with published data.

Country	Specific activity concentration, Bq/kg			Ra$_{eq}$, Bq/kg	I$_{yr}$	Reference
	^{238}U	^{232}Th	^{40}K			
Ghana	8.65	12.51	214.11	43.37		This study
India	64	93	124	206.5	1.47	Singh, Rani, and Mahajan, 2005
Algeria	47.01	43	329	132	0.95	Wassila and Ahmed, 2011
Brazil	1.69	5.32	34.15	12	0.1	Becegato and Ferreira, 2008
Egypt	13.70	12.30	1233	126.20	1.04	Ahmed and El-Arabi, 2005
Pakistan	27.39	31.16	602.77	142.71	1.02	Akhtar, Tufail, and Ashraf, 2005
Malaysia	12-42.6	19-1377	19-2204	52-2227		Lee et al., 2009
World average	35	30	400	370		UNSCEAR, 2000

Source: Laboratory work, 2016

The summary of statistical analysis of the radiological risk data from soil using SPSS are shown in Table 33.

Table 33: Comparison between mean values of the activity concentrations of ^{238}U, ^{232}Th and ^{40}K as well as the absorbed dose rates and the annual effective doses due to soil samples for the two sets of data.

First and second batch results	^{238}U activity concentration, Bq/kg	^{232}Th activity concentration, Bq/kg	^{40}K activity concentration, Bq/kg	Annual Effective dose, μSv	Absorbed dose rate, nGy/h
Probability value	0.980**	0.956**	0.794**	25.10	20.48

**Correlation is significant at 0.01 level (2-tailed)

Water

The annual Effective dose and Excess Lifetime Cancer Risk due to the exposure to radionuclides in the groundwater sources for adults (17 years and above) is presented in Table 34. The total annual effective dose from the

129

ingestion of groundwater only ranges from 1.30E-01 to 6.50E-01 with an average of 3.28E-01. The Excess Life Cancer Risk due to the ingestion of groundwater is estimated to range from 4.55E-01 to 2.28E+00 with an average of 1.17E+00.

Table 34: Total Annual Effective Dose and Excess Lifetime Cancer Risk in Adults (17 years and above)

Communities	Effective Dose (^{226}Ra,^{228}Ra,^{40}K) mSv/y	Effective Dose (^{222}Rn) mSv/y	Total Annual Effective Dose mSv/y	ELCR
Axim 1	6.47E-05	0.33	3.30E-01	1.16E+00
ABH	6.09E-05	0.30	3.00E-01	1.05E+00
ALIS	1.36E-05	0.48	4.80E-01	1.68E+00
Krisan	1.38E-04	0.63	6.30E-01	2.21E+00
Nyale Kplole 1	1.62E-05	0.32	3.20E-01	1.12E+00
Nyale Kplole 2	1.61E-05	0.20	2.00E-01	7.00E-01
Nyale Kplole 3	3.17E-05	0.27	2.70E-01	9.45E-01
Atuabo 1	9.77E-05	0.13	1.30E-01	4.55E-01
Atuabo 2	9.65E-05	0.16	1.60E-01	5.60E-01
Ekebaku	1.61E-05	0.65	6.50E-01	2.28E+00
Beyin 1	9.47E-05	0.57	5.70E-01	2.00E+00
Beyin 2	1.16E-05	0.43	4.30E-01	1.51E+00
Kikam	2.26E-05	0.24	2.40E-01	8.40E-01
Kengen 1	3.41E-05	0.34	3.40E-01	1.19E+00
Kengen 2	3.15E-05	0.26	2.60E-01	9.10E-01
Anokyi	6.18E-05	0.19	1.90E-01	6.65E-01
Twenen	8.70E-06	0.23	2.30E-01	8.05E-01
Half-Assini 1	1.52E-04	0.29	2.90E-01	1.02E+00
Half-Assini 2	3.86E-05	0.18	1.80E-01	6.30E-01
Half-Assini 3	1.16E-04	0.36	3.60E-01	1.26E+00
Minimum	**2.86E-05**	**0.13**	**1.30E-01**	**4.55E-01**
Maximum	**3.31E-04**	**0.65**	**6.50E-01**	**2.28E+00**
Mean	**1.12E-04**	**0.33**	**3.28E-01**	**1.17E+00**

Source: Laboratory work, 2016

The annual Effective dose and Excess Lifetime Cancer Risk (ELCR) due to the exposure to radionuclides in the groundwater sources for teenagers (13 to 17 years), is presented in Table 35. The total annual effective dose from the ingestion of groundwater only ranges from 1.36E-01 to 6.54E-01 with an average of 3.38E-01. The Excess Life Cancer Risk due to the ingestion of groundwater is in the range of 1.15E-01 to 5.56 with an average of 2.87E-01.

130

Table 35: Total Annual Effective Dose and Excess Lifetime Cancer Risk in Teenagers (13-17 years)

Community	Effective Dose (^{226}Ra, ^{228}Ra, ^{40}K) mSv/y	Effective Dose (^{222}Rn) mSv/y	Total Annual Effective Dose mSv/y	ELCR
Axim 1	2.37E-03	0.33	3.32E-01	2.83E-01
ABH	3.73E-03	0.30	3.04E-01	2.58E-01
ALIS	3.81E-03	0.48	4.84E-01	4.11E-01
Krisan	5.87E-03	0.63	6.36E-01	5.40E-01
Nyale Kplole 1	4.31E-03	0.32	3.24E-01	2.76E-01
Nyale Kplole 2	3.49E-03	0.20	2.03E-01	1.73E-01
Nyale Kplole 3	3.43E-03	0.27	2.73E-01	2.32E-01
Atuabo 1	5.78E-03	0.13	1.36E-01	1.15E-01
Atuabo 2	3.95E-03	0.16	1.64E-01	1.39E-01
Ekebaku	4.13E-03	0.65	6.54E-01	5.56E-01
Beyin 1	5.89E-03	0.57	5.76E-01	4.90E-01
Beyin 2	9.04E-04	0.43	4.31E-01	3.66E-01
Kikam	2.11E-03	0.24	2.42E-01	2.06E-01
Kengen 1	4.30E-03	0.34	3.44E-01	2.93E-01
Kengen 2	1.91E-03	0.26	2.62E-01	2.23E-01
Anokyi	4.60E-03	0.19	1.95E-01	1.65E-01
Twenen	9.29E-04	0.23	2.31E-01	1.96E-01
Half-Assini 1	7.04E-03	0.29	2.97E-01	2.52E-01
Half-Assini 2	3.06E-03	0.18	1.83E-01	1.56E-01
Half-Assini 3	5.78E-03	0.36	3.66E-01	3.11E-01
Min	**9.04E-04**	**0.13**	**1.36E-01**	**1.15E-01**
Max.	**7.04E-03**	**0.65**	**6.54E-01**	**5.56E-01**
Average	**3.87E-03**	**0.33**	**3.38E-01**	**2.87E-01**

Source: Laboratory work, 2016

The annual Effective dose and Excess Lifetime Cancer Risk due to the exposure to radionuclides in the groundwater sources for children (1 to 12 years) is presented in Table 36 and the ELCR is estimated in the range of 7.91E-02 to 3.91E-01 averaging at 1.98E-01. The total annual effective dose from the ingestion of groundwater only ranges from 1.36E-01 to 6.54E-01 with an average of 3.32E-01.

Table 36: Total annual effective dose and excess lifetime cancer risk in
children (1-12 years)

Community	Effective Dose (^{226}Ra, ^{228}Ra, ^{40}K), mSv/y	Effective Dose (^{222}Rn), mSv/y	Total Annual Effective Dose, mSv/y	ELCR
Axim 1	7.52E-04	0.33	3.31E-01	1.98E-01
ABH	1.10E-03	0.30	3.01E-01	1.81E-01
ALIS	1.20E-03	0.48	4.81E-01	2.89E-01
Krisan	1.74E-03	0.63	6.32E-01	3.79E-01
Nyale Kplole 1	1.33E-03	0.32	3.21E-01	1.93E-01
Nyale Kplole 2	1.10E-03	0.20	2.01E-01	1.21E-01
Nyale Kplole 3	1.08E-03	0.27	2.71E-01	1.63E-01
Atuabo 1	1.84E-03	0.13	1.32E-01	7.91E-02
Atuabo 2	1.22E-03	0.16	1.61E-01	9.67E-02
Ekebaku	1.34E-03	0.65	6.51E-01	3.91E-01
Beyin 1	1.87E-03	0.57	5.72E-01	3.43E-01
Beyin 2	2.76E-04	0.43	4.30E-01	2.58E-01
Kikam	6.17E-04	0.24	2.41E-01	1.44E-01
Kengen 1	1.25E-03	0.34	3.41E-01	2.05E-01
Kengen 2	5.90E-04	0.26	2.61E-01	1.56E-01
Anokyi	1.40E-03	0.19	1.91E-01	1.15E-01
Twenen	2.74E-04	0.23	2.30E-01	1.38E-01
Half-Assini 1	2.06E-03	0.29	2.92E-01	1.75E-01
Half-Assini 2	9.84E-04	0.18	1.81E-01	1.09E-01
Half-Assini 3	1.74E-03	0.36	3.62E-01	2.17E-01
Min	**2.74E-04**	**0.13**	**1.36E-01**	**7.91E-02**
Max	**2.06E-03**	**0.65**	**6.54E-01**	**3.91E-01**
Average	**1.19E-03**	**0.33**	**3.32E-01**	**1.98E-01**

Source: Laboratory work, 2016

The annual Effective dose and Excess Lifetime Cancer Risk due to the
exposure to radionuclides in the groundwater sources for babies (<1 year) is
presented in Table 37 and the ELCR is estimated in the range of 6.90E-03 to
3.28E-02 averaging at 1.67E-02. The total annual effective dose from the
ingestion of groundwater only ranges from 1.38E-01 to 6.56E-01 with an
average of 3.33E-01.

Table 37: Total Annual Effective Dose and Excess Lifetime Cancer Risk in BABIES (<1 YEAR)

Communities	Effective Dose (^{226}Ra, ^{228}Ra, ^{40}K), mSv	Effective Dose (^{222}Rn), mSv	Total Annual Effective Dose, mSv	ELCR
Axim 1	3.20E-03	0.33	3.33E-01	1.67E-02
ABH	4.71E-03	0.30	3.05E-01	1.52E-02
ALIS	5.16E-03	0.48	4.85E-01	2.43E-02
Krisan	7.37E-03	0.63	6.37E-01	3.19E-02
Nyale Kplole 1	5.72E-03	0.32	3.26E-01	1.63E-02
Nyale Kplole 2	4.82E-03	0.20	2.05E-01	1.02E-02
Nyale Kplole 3	4.62E-03	0.27	2.75E-01	1.37E-02
Atuabo 1	8.02E-03	0.13	1.38E-01	6.90E-03
Atuabo 2	5.28E-03	0.16	1.65E-01	8.26E-03
Ekebaku	5.77E-03	0.65	6.56E-01	3.28E-02
Beyin 1	8.09E-03	0.57	5.78E-01	2.89E-02
Beyin 2	1.18E-03	0.43	4.31E-01	2.16E-02
Kikam	2.58E-03	0.24	2.43E-01	1.21E-02
Kengen 1	5.31E-03	0.34	3.45E-01	1.73E-02
Kengen 2	2.55E-03	0.26	2.63E-01	1.31E-02
Anokyi	6.02E-03	0.19	1.96E-01	9.80E-03
Twenen	1.17E-03	0.23	2.31E-01	1.16E-02
Half-Assini 1	8.84E-03	0.29	2.99E-01	1.49E-02
Half-Assini 2	4.23E-03	0.18	1.84E-01	9.21E-03
Half-Assini 3	7.47E-03	0.36	3.67E-01	1.84E-02
Minimum	**1.17E-03**	**0.13**	**1.38E-01**	**6.90E-03**
Maximum	**8.84E-03**	**0.65**	**6.56E-01**	**3.28E-02**
Mean	**5.11E-03**	**0.328**	**3.33E-01**	**1.67E-02**

Source: Laboratory work, 2016

To assess public exposure due to intake of radionuclides ^{226}Ra, ^{228}Ra and ^{40}K through water, the annual effective dose received by adults, teenagers, children and infants were estimated (Tables 34 to 37). The recorded effective dose values ranged from 1.20E-04 to 9.50E-04, 9.04E-04 to 7.04E-03, 2.74E-04 to 2.06E-03 and 1.17E-03 to 8.84E-03 μSv/y respectively. The estimated average total annual effective dose from the ingestion of ^{226}Ra, ^{228}Ra, ^{40}K and ^{222}Rn over a year for all age groups are higher than the average value of 0.1mSv/y (100 μSv/y) recommended by the World Health Organisation (WHO) and slightly higher than the average value of 0.29 mSv/y (290 μSv/y) due to ingestion of radionuclides in drinking water and food recommended by

133

UNSCEAR 2000, for public exposure control to natural radiation. From the Radiation Protection point of view, the results revealed that infants and children are most susceptible to high dose related disease through intake of these waters.

Food

The annual effective dose from the ingestion of cassava is 0.0387 mSv/y (Table 38), based on an ingestion rate of 170 kg/y, are far lower than the 1 mSv per year dose limit recommended by the ICRP (2007) for public radiation exposure control. This presents a lower chance for the onset of stochastic effects from these exposures. The highest TF value for ^{238}U was 0.12. For ^{232}Th and ^{40}K, the highest values of transfer factor were 0.10 (CS 1) and 0.28 (CS 1) respectively.

Table 38: Summary of radiological risk assessment from the ingestion of cassava samples

Sample	Individual effective doses, μSv/y			Annual effective doses, μSv/y
	^{238}U	^{232}Th	^{40}K	
CS 1	3.14	7.59	38.9	49.6
CS 2	4.05	6.00	43.5	53.6
CS 3	4.90	6.98	8.92	20.8
CS 4	6.81	1.96	28.7	37.4
CS 5	7.96	9.18	15.0	32.2
Min	3.14	1.96	8.92	20.8
Max	7.96	9.18	43.5	53.6
Mean	5.37	6.34	27.0	38.7
Average annual effective dose				38.7

Source: Laboratory work, 2016

External Gamma Dose Rate at 1m above the Ground

The terrestrial gamma dose rates measured at 1 meter above the ground and their corresponding annual effective dose rate at the sampling points in the study area are shown in Table 39. The annual effective dose from terrestrial

134

gamma dose rate at the soil sampling locations ranged from 83.40 to 137.36 mSv/y and that for the ground water sampling locations is in the range of 66.23 to 143.49 mSv/y with averages of 116.1 and 113.78 mSv/y respectively. The mean absorbed dose rates measured in air at the soil sampling points ranges from 0.07 to 0.11 μSv/h and the water sampling points were 0.05 to 0.12 μSv/h with both averaging at 0.09 μSv/h respectively.

Table 39: Absorbed dose rate levels at 1m above sampling points in the communities and their corresponding calculated annual effective doses

COMMUNITY	Soil Sampling		Water Sampling	
	Annual Effective Dose (mSv/y)	Absorbed Dose Rate (μSv/h)	Annual Effective Dose (mSv/y)	Absorbed Dose Rate (μSv/h)
Axim 1	136.130	0.111	123.866	0.101
ABH	109.1496	0.089	117.734	0.096
ALIS	98.112	0.080	95.659	0.078
Axim Castle	114.055		n.s	n.s
Krisan	137.357	0.112	118.961	0.097
Krisan 2	137.357	0.112	n.s	n.s
Krisan 3	118.961	0.097	n.s	n.s
Nyale Kplole 1	106.697	0.087	122.640	0.10
Nyale Kplole 2	125.093	0.102	114.055	0.093
Nyale Kplole 3	83.395	0.068	111.602	0.091
Anokye	99.338	0.081	131.225	0.107
Anokye 2	133.678	0.109	n.s	n.s
Atuabo 1	91.980	0.075	78.490	0.064
Atuabo 2	101.791	0.083	98.112	0.080
Ekebaku	105.470	0.086	66.226	0.054
Beyin 1	111.602	0.091	143.489	0.117
Beyin 2	126.319	0.103	131.225	0.107
Kikam	127.546	0.104	117.734	0.096
Kengen 1	120.187	0.098	128.772	0.105
Kengen 2	132.451	0.108	133.678	0.109
Twenen	111.602	0.097	127.546	0.104
Half-Assini 1	131.225	0.107	120.187	0.098
Half-Assini 2	109.150	0.089	99.338	0.081
Half-Assini 3	118.961	0.097	112.829	0.092
Half-Assini 4	121.414	0.099	n.s	n.s
Newtown	122.640	0.100	n.s	n.s
Min.	**83.40**	**0.07**	**66.23**	**0.05**
Max.	**137.36**	**0.11**	**143.49**	**0.12**
Average	**116.10**	**0.09**	**113.78**	**0.09**

Source: Laboratory work, 2016   n.s = not sampled

A total of 27 locations for soil and 21 for water were surveyed for background environmental radiation. The dose rate obtained at each point is presented in Table 39. The dose rate varies from 0.07 μSv/hr to 0.11 μSv/hr averaging 0.09 μSv/hr and 83.40 μSv/y to 137.36 μSv/y with an average of 116.10 μSv/y for absorbed dose and annual effective dose respectively at the soil locations. At the water sampling points absorbed dose rates varied in a range of 0.05 μSv/hr to 0.12 μSv/hr with a mean value of 0.09 μSv/h. The corresponding mean annual effective dose was estimated to be 113.78 μSv/y.

Generally, the dose rate levels in each of the locations surveyed are comparable to one another and could simply be attributed to natural sources as there are no radiation generators around them. The total mean dose rate of the surveyed areas is found to be far lower than that of the world average of 56 nSv/hr (UNSCEAR, 2000) and that of other places compared. Assuming the population in the areas surveyed spend 20% of their day in this area, the annual effective dose obtained by using the dose conversion factor of 0.7Sv/ Gy (UNSCEAR, 1993 & 2000) is still lower than the recommended limit of 1mSv/yr by International Commission on Radiation Protection (ICRP, 1991).

Comparisons of the dose obtained at 1m above the ground were made between the values obtained for the present study and published data in Table 40. The value of 0.09 nSv/h is below the world average of 56 nSv/h (UNSCEAR, 1993).

Table 40: Comparison of dose rate at 1m from this work with literature

Country	Dose Rate, nSv/h	Reference
Ghana	0.09	This study
Nigeria	132	Nwakwo and Akoshile, 2005a
Nigeria	134	Nwakwo and Akoshile, 2005b
Spain	56.6	Beaza et al., 1994
India (Bangalore)	117	Shiva et al., 2008
World Average	56	UNSCEAR, 1993
Turkey	253	Merdanoglu and Altinsoy, 2006
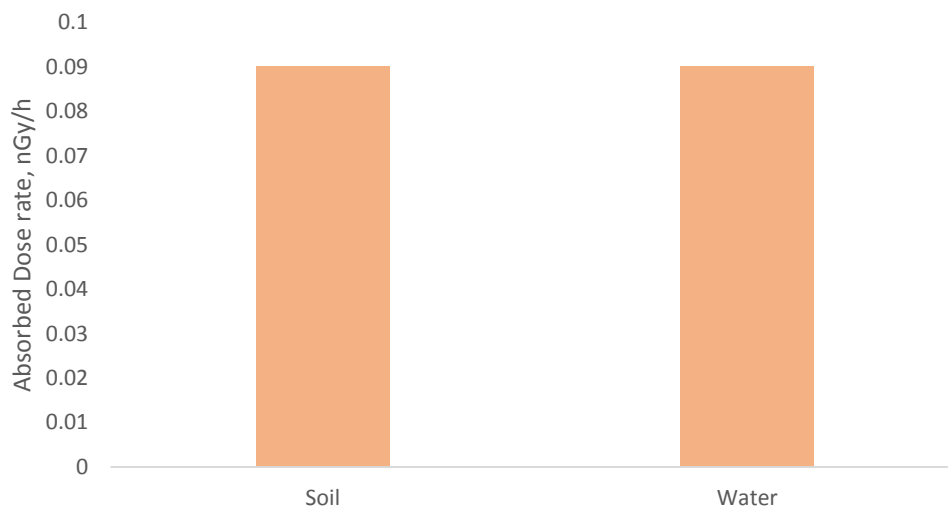
Figure 24: Comparison of absorbed dose rate from direct air measurement at one metre above the ground at soil, water sampling points.

Figure 24 is a comparison of absorbed dose rate from direct air measurement at 1 m the ground at the soil and water sampling points. It is observed that both sampling locations gave the same figure of 0.09 nGy/h.

Figure 25 shows as comparison of average annual effective doses due to soil, water and airborne radon.
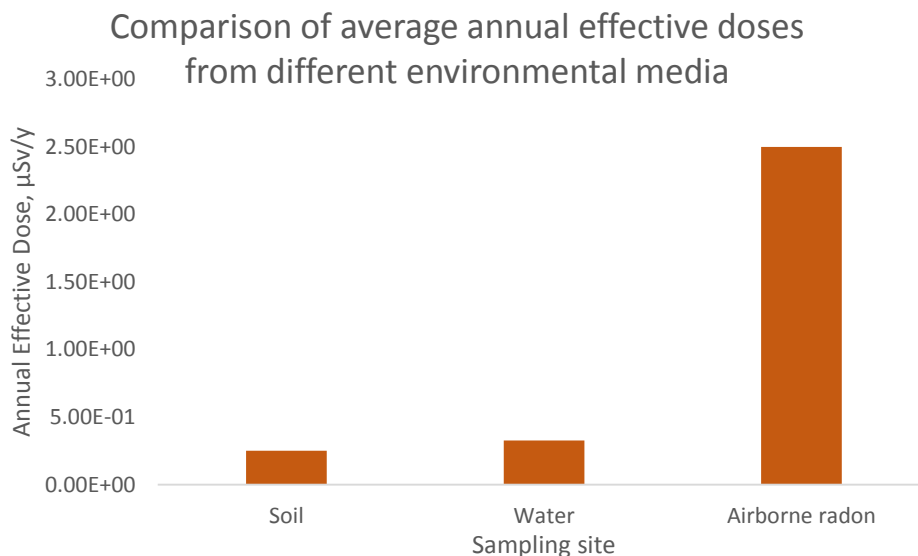
Figure 25: Comparison of average annual effective doses due to soil, water and airborne radon.

Total Annual Effective Dose

A summary of the annual effective doses for the various exposure pathways considered in this study and estimated total annual effective dose are presented in Table 41. The highest contribution of 71.02% to the total annual effective dose is from external irradiation from ^{238}U, ^{232}Th and ^{40}K from soil with least contribution of 0.31% from the ingestion of ^{226}Ra, ^{228}Ra and ^{40}K from groundwater.

Exposure to (TE)NORM will not result in acute and severe effects similar to those effects associated with exposure to high radiation levels, it can however result in delayed effects such as the development of certain forms of cancer such as leukemia, and cancers of the lung, stomach, esophagus, bone, thyroid, and the brain and nervous system. ATSDR, in 1999 stated in its report that increasing the radiation dose does not increase the severity of the cancer; instead it increases the chance of cancer induction. For carcinogens generally, whether chemical or radiological, safety standards are based on a postulated

138

zero threshold. Increasing the size of the dose increases the probability of inducing a cancer with that carcinogen. Cancers that are, in fact, caused by radiation are completely indistinguishable from those that seem to occur spontaneously or are caused by other known or suspected carcinogens (ATSDR, 1999).

Therefore, Ghana like most countries has adopted the recommendations of the ICRP in its publications 60 and 103 (ICRP, 1991 & 2007). The recommendations stipulate that, any exposure to radiation be kept as low as reasonably achievable but below the individual dose limits, which is 20 mSv averaged over 5 years but not exceeding 50 mSv in any single year for occupationally exposed workers and 1 mSv/year for members of the public. Table 41 is a presentation of the total annual effective dose estimated as a summation of equivalent doses from all the potential exposure scenarios of direct external gamma ray exposure from natural radioactivity concentrations in soil, exposure from drinking water containing natural radioactivity, inhalation of airborne radon and ingestion of food (cassava) being 25.10, 0.12, 0.26, and 9.87 nSv respectively. The corresponding total annual effective dose for all the exposure pathways was 35.34 nSv.

The various components contributing to the total effective dose ranged from 0.12 nSv (0.31%) due to the ingestion of water containing radionuclides to 25.10 Sv (39.2%) due to direct gamma ray from natural radionuclide concentrations in soil. The highest contribution to the total effective was due to soil with 71.02% followed by ingestion of food (27.93%), due to inhalation of airborne radon (0.74%) and (0.31%) from ingestion of radionuclides in water respectively. The total annual effective dose of 35.34 nSv/year is also below the

ICRP recommended dose limit of 1 mSv/year for members of the public from

practices. Generally, the annual effective doses calculated from the various

samples are considered insignificant.

Table 41: Summary of annual equivalent doses and the estimated total
effective dose from cassava, water, radon and external gamma dose
rate to each individual member of the public

S/No	Exposure Pathway	Average annual effective dose, µSv/year	Percentage contribution, %
1	External irradiation U, Th and K in soil sample by gamma spectrometry.	25.10	71.02
2	Ingestion ^{226}Ra, ^{228}Ra and ^{40}K in water samples	0.12	0.31
3	Radon measurement in air with Alpha Guard	0.26	0.74
4	Ingestion of U, Th and K in food sample (wet weight)	9.87	27.93
	TOTAL ANNUAL EFFECTIVE DOSE	**35.34**	**100**

Source: Laboratory work, 2016

140
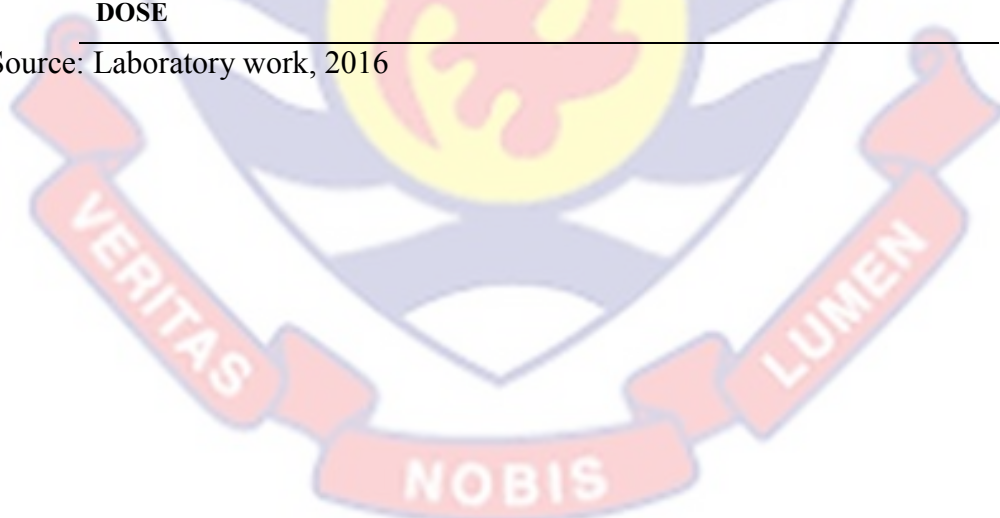
The estimated lifetime fatality cancer risk and hereditary disorders estimated from all the exposure pathways studied are reported in Table 42 with the total Lifetime fatality cancer risks to the population estimated at 1.36.06E-06 and chances of an adult suffering severe hereditary effects being 0.07E-06.

Table 42: Estimated risk components for the various exposure pathways studied.

Exposure pathway	Average Equivalent Dose, μSv/y	Fatality cancer risk to adult per year ($\times10^{-6}$)	Lifetime fatality cancer risk to population ($\times10^{-6}$)	Severe Hereditary Effects to adult per year ($\times10^{-6}$)	Estimated lifetime Hereditary effect in adult workers ($\times10^{-6}$)
External irradiation U, Th and K in soil	25.10	1.38	96.64	0.05	3.51
Ingestion of ^{226}Ra, ^{228}Ra and ^{40}K in water samples	0.12	0.00061	0.42	0.00022	0.0154
Radon measurement in air	0.26	0.014	1.00	0.00052	0.0364
Ingestion of U Th and K in food (wet weight)	9.87	0.54	37.80	0.02	1.38
Total	**35.34**	**1.94**	**136.06**	**0.07**	**4.95**

Source: Laboratory work, 2016

Total trace metals in soil

The results of the geochemical studies carried out on the soil and water samples in the study area are also shown in Tables 43 and 44. The concentrations of the trace metals and major metals in the soil samples determined by Neutron Activation Analysis (NAA) and Atomic Absorption Spectroscopy are presented in Table 30. Mean values of all metals ranged from 0.15 to 2.74 mg/kg.

Table 43: Trace Metals Concentration in Soil Samples

Community	Fe	Pb	Cd	Zn	Cu	Mn	As	Ni
	mg/kg							
ABH	4.43	0.06	0.49	0.30	<0.003	0.41	<0.006	0.01
ABH 2	1.98	0.13	0.96	0.43	<0.003	0.28	<0.006	0.02
ABH 3	1.65	0.11	0.43	0.30	<0.003	0.47	<0.006	0.01
ALIS	7.33	0.08	0.08	2.50	<0.003	0.59	<0.006	0.03
Axim Castle	0.58	0.42	0.62	1.47	<0.003	0.33	<0.006	0.01
Krisan 1	3.68	0.26	1.90	1.46	<0.003	0.25	<0.006	0.02
Krisan 2	5.22	0.38	0.44	0.91	<0.003	0.61	<0.006	0.01
Krisan 3	3.65	0.09	0.61	0.14	<0.003	0.28	<0.006	0.01
Beyin 1	1.46	0.34	0.23	0.32	<0.003	0.25	<0.006	0.02
Beyin 2	3.20	0.17	0.52	0.28	<0.003	0.63	<0.006	0.01
Ellonyi	0.88	0.23	0.56	0.61	<0.003	0.51	<0.006	0.03
Kengen 1	2.01	0.35	0.37	0.11	<0.003	0.17	<0.006	0.01
Kengen 2	1.30	0.51	0.33	0.25	<0.003	0.88	<0.006	0.01
Twenen	3.49	0.42	0.58	0.80	<0.003	0.18	<0.006	0.01
Nyale Kplole	4.99	0.09	0.30	0.30	<0.003	0.36	<0.006	0.02
Nyale Kplole 2	2.91	0.56	0.16	0.46	<0.003	1.31	<0.006	0.02
Nyale Kplole 3	1.46	0.20	0.60	0.49	<0.003	0.27	<0.006	0.01
Anokyi 1	3.27	0.14	0.19	0.60	<0.003	0.14	<0.006	0.02
Anokyi 2	1.91	0.47	0.39	1.51	<0.003	0.09	<0.006	0.02
Atuabo 2	2.45	0.09	0.18	0.08	<0.003	0.22	<0.006	0.01
Kikam	3.41	0.31	0.96	0.16	<0.003	0.51	<0.006	0.02
Half-Assini 1	1.40	0.22	0.21	0.13	<0.003	0.38	<0.006	0.01
Half-Assini 2	1.39	0.19	0.66	0.17	<0.003	0.65	<0.006	0.01
Half-Assini 3	2.01	0.11	0.72	0.34	<0.003	1.02	<0.006	0.01
Half-Assini 4	1.88	0.41	0.35	0.30	<0.003	0.77	<0.006	0.01
Newtown	0.99	0.69	0.51	0.26	<0.003	0.41	<0.006	0.02
Minimum	**0.58**	**0.06**	**0.08**	**0.08**		**0.09**		**0.01**
Maximum	**7.33**	**0.69**	**1.90**	**2.50**		**1.31**		**0.03**
Mean	**2.74**	**0.28**	**0.55**	**0.62**		**0.48**		**0.15**

Source: Laboratory work, 2016

Comparing the results with standard range, shows that the concentrations of all the heavy metals in exception of Cd in the studied area are lower than standards. Summary statistics for the analyzed elements in all the studied samples are presented in Table 43. Though, cadmium has a low mean concentration (0.55 mg/kg), it is well above the maximum permissible limits given by all WHO standards (Table 44). This should be a source of concern as Cd has no biological function. The average concentration of the studied metals are in the order of Fe > Zn > Cd > Mn> Pb>Ni. Copper and arsenic were not registered at their respective minimum detection levels.

The level of these metals in the soils are from communities which are rural except Axim and Half-Assini, are within similar range suggesting they might be derived from common input. Lead and Cd are anthropogenic metals and they are normally not abundant in upper layer soils (Al-Turki & Helal, 2004; Ren, Wang & Zhang, 2005). The low concentration of lead can also be attributed to the sparse use of leaded gasoline and also may be air borne.

Table 44: Standards for Metal Concentrations in Soil (mg/kg)

Standard	Fe	Pb	Cd	Zn	Cu	Mn	As	Ni
USEPA	NR	10	-	NR	30			40
GLC	NR	20	-	NR	NR			20
WHO	47200	20	0.3	50	4			68

An important component of the present study is the source apportionment of the metals in sediments using Principal Component Analysis (PCA) and Cluster Analysis (CA). The principal component loadings of the heavy metals in soil is presented in Table 45 whereas the corresponding CA is shown in Figure 26. Two principal components (PCs) were extracted with the eigenvalues of the two extracted components greater than the ones before and

143

after the matrix rotation and are more than 1 accounting for 66.67% of all the data variation. PC1 included Mn, Cd and Zn and show good similarity and are therefore clustered in one group while PC 2 was constituted by Fe showing less similarity but still correlated with the other elements.

Two components extracted for this analysis for soil samples as presented in Table 45.

Table 45: Principal Component Loadings of Trace Metals in Soil

Trace metal	Component	
	1	2
Fe	0.745	-0.122
Pb	-0.317	0.782
Cd	0.158	-0.264
Zn	0.802	0.297
Mn	-0.232	0.560
Ni	0.680	0.401

Extraction Method: Principal Component Analysis
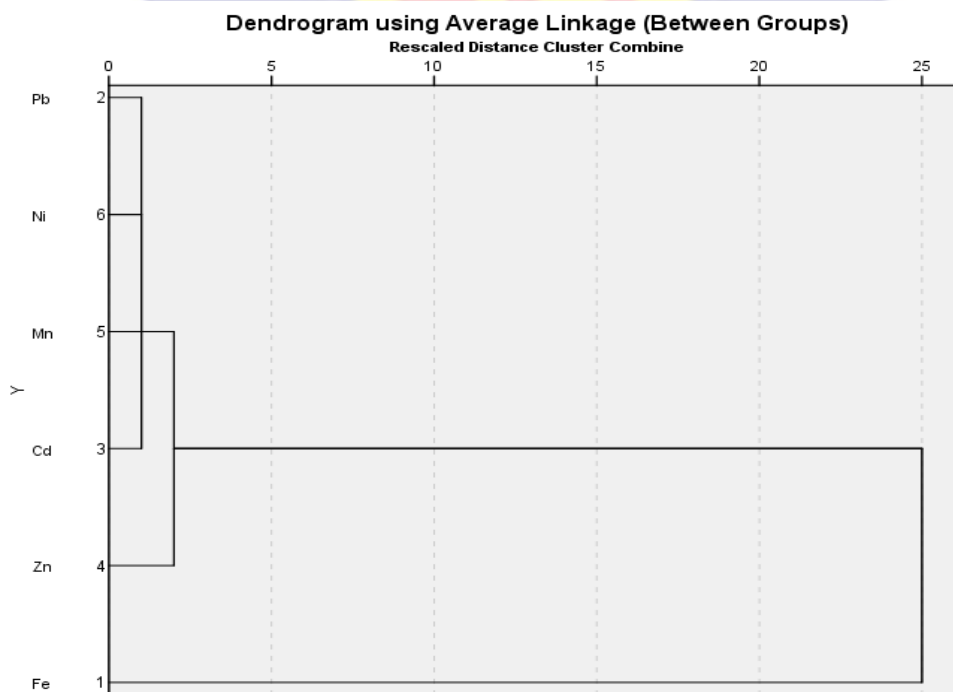
Figure 26: Dendrogram analysis mean of metal elements in soil samples

The strong similarity between Mn, Cd, and Zn shows that these metals come from the same source. Micó, Recatalá, Peris, & Sánchez, (2006) reported that Mn and Ni appeared to be associated with the lithosphere whereas Cu and Pb constituted an anthropogenic components. Facchinelli, Sacchi & Mallen, (2001) also concluded that Ni was controlled by parent rocks, on the other hand, Cu and Zn were associated with specific agronomic practices, and Pb derived from car exhausts and all three metals were related to anthropogenic activities. From these analyses, it is reasonable to conclude that Mn, Cd, Zn and Ni are associated with the lithosphere or parent rocks from sampling points whereas Fe and Pb are anthropogenic.
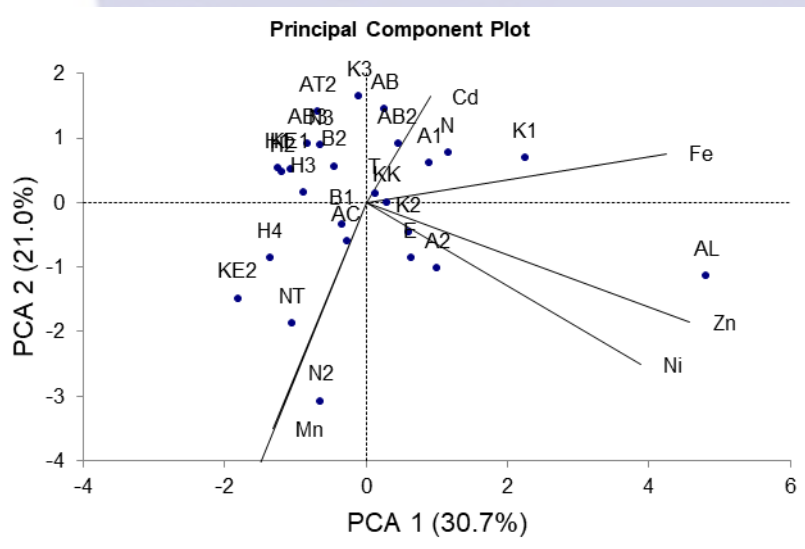
Figure 27: PCA biplot for PC1 and PC2 soil samples

The resultant biplots of the 26x6 data matrix PCA analysis without pre-treatment are shown in Fig. 27. From the scree plot and results of analysis, three principal components (PC) are considered significant with an Eigen value ≥ 1 (Kaiser & Hunka, 1973) and contributing 71% of the variance in the data. PC1 and PC2 contributed 51% of the variance. Ni and Zn are highly positively

145

correlated with PC1, indicating a potential common source most probably lithosphere or parent rocks. Cd and Fe are also relatively correlated whilst Fe and Ni are orthogonal implying they have independent sources. Cd and Mn are negatively correlated. Object AL and N2 exhibit significant variance in the heavy metals estimated and are highly correlated with Zn and Mn respectively.

Micó et al., (2006) reported that Mn and Ni appeared to be associated with the lithosphere whereas Cu and Pb constituted anthropogenic components. Facchinelli et al., (2001) also concluded that Ni was controlled by parent rocks, on the other hand, Cu and Zn were associated with specific agronomic practices, and Pb derived from car exhausts and all three metals were related to anthropogenic activities. With the exception of few objects such as AL, N2 and K1 most of the objects form clusters. For instance, H4, KE2 and NT can be considered a cluster. This high level of cluster in the data can be considered highly beneficial for future monitoring of communities in assessing the potential impact of the oil and gas industry on the soil ecosystem since few of those highly correlated objects can be randomly selected to represent that cluster. The largest cluster of objects is highly correlated with Cd implying these communities are more susceptible to Cd pollution. Considering the deleterious ecological and human health risk posed by Cd in the environment, future monitoring of the randomly selected objects might be crucial.

The contour plot for heavy metals in soil as shown by Fig. 28 indicates significant levels of Pb and Cd in soil of Kikam (KK) area. Considering the deleterious nature of Pb and Cd to the ecosystem KK requires regular monitoring and assessment of these critical metals. Additionally, T, KE1, KE2 and E also exhibit potentially high concentrations of Pb.
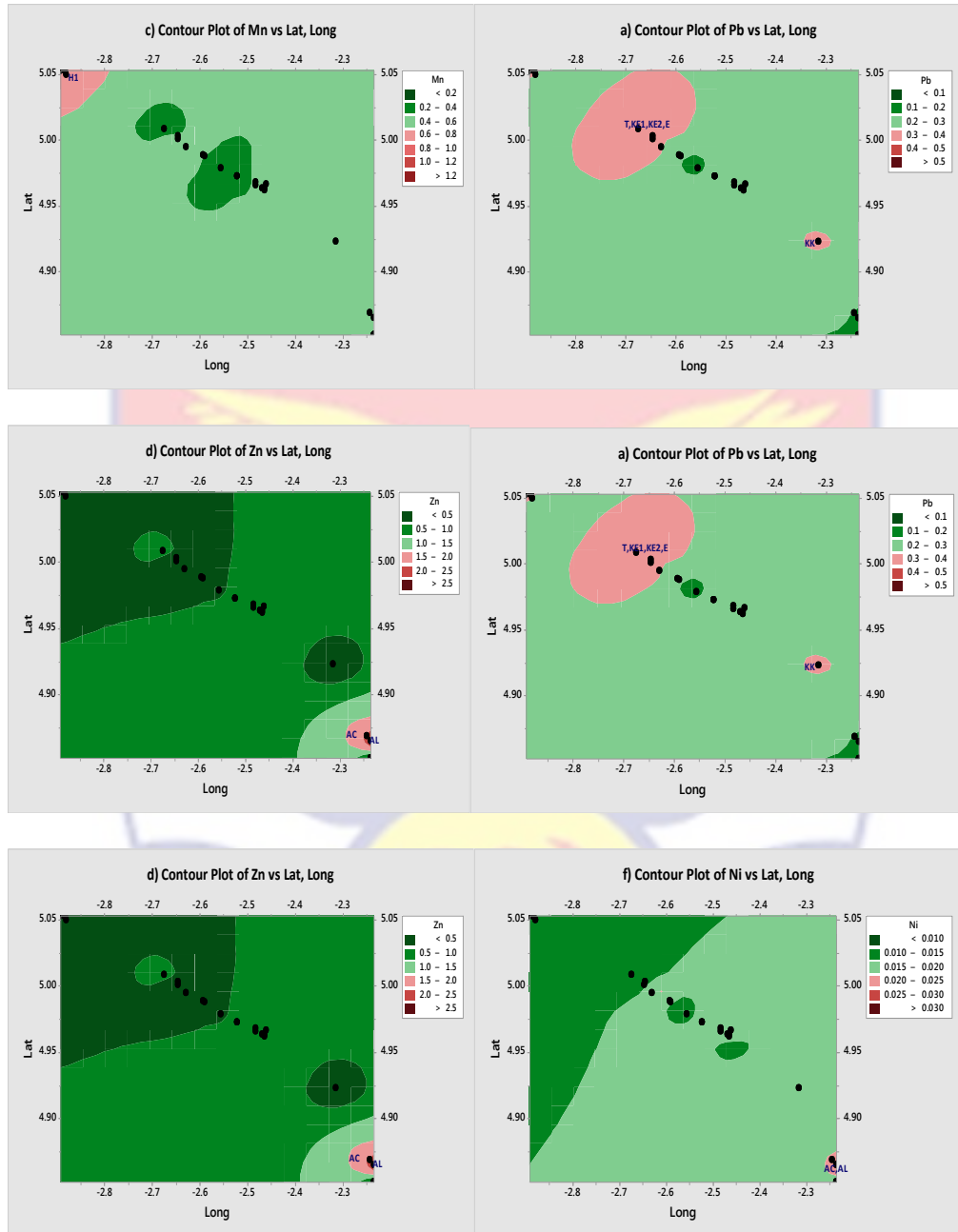
Figure 28: Contour plot of trace metals in soil

Non- Carcinogenic Hazard Index and Cumulative Carcinogenic Lifetime Risks for Adults

The results for non-carcinogenic hazard index and carcinogenic lifetime risk for individual elements and cumulative risk for different exposure pathways for individual elements as determined for adults are presented in Table 46.

147

Table 46 is a summary of average non-carcinogenic hazard index and carcinogenic lifetime risk for individual elements and cumulative risk for different exposure pathways for individual elements as determined for adults. Total lifetime carcinogenic risk recorded a low 3.24E-09 to a high of 1.04E-06.

Table 46: Average non-carcinogenic hazard index and carcinogenic lifetime risk for individual elements and cumulative risk for different exposure pathways for individual elements as determined for adults

Element	RfD_{ing} CSF_{ing}	RfD_{inh} CSF_{inh}	RfD_{dermal} CSF_{dermal}	HQ_{ing}	HQ_{inh}	HQ_{dermal}	$HI= \sum HQ$	$Risk_{(ing)}$	$Risk_{(inh)}$	$Risk_{(dermal)}$	Total Risk
Fe-non cancer	7.00E-01			5.37E-06			5.37E-06				
Pb-non cancer	3.50E-03		5.25E-04	1.09E-04		2.89E-05	1.38E-04				
Pb-cancer	8.5E-03	1.20E-05						3.24E-09	1.01E-12		3.24E-09
Cd-non cancer	1.00E-03	8.00E-04	1.00E-05	7.50E-04	3.31E-06	2.99E-04	1.05E-03				
Cd-cancer		6.30E+00							1.04E-06		1.04E-06
Zn-non cancer			1.23E-04	2.81E-06		5.62E-08	2.87E-06				
Mn-non cancer	4.60E-02	1.40E-05	1.80E-03	1.42E-05	1.65E-04	1.45E-06	1.81E-04				
Ni-non cancer	2.00E-02	2.00E-03	8.00E-04	1.05E-06	3.71E-08	1.55E-08	1.10E-06				
Ni-cancer		8.40E-01							3.90E-09		3.90E-09

Source: Laboratory work, 2016

The concentrations of Pb, Cd, Zn and Mn were quite low but the concentrations of Ni are comparable to the levels found in soil from the central zone of Belgrade (Grzertic & Ghariani, 2008). Despite its low concentrations, Cd appeared as the single largest contributor to the overall risk. This is critical as Cd is a known carcinogen capable of causing increased lung cancer mortality through inhalation and dermal contact and several internal organ cancers through ingestion (USEPA, 2005). The investigations show that the concentrations of Pb, Cd and Ni which are known carcinogens presents no significant carcinogenic lifetime risk due to ingestion, inhalation and/or dermal contact with soil. No matter how small the probability is, a carcinogenic risk exists and varies from the maximum value of 3.9E-09 in case of Ni to the minimum value of 1.04E-06 for Cd. On the other hand, the non-carcinogenic risk, expressed as the hazardous index *(HI)*, is not so benevolent; even though the cumulative index for all elements are less than 1. As a rule, the greater the value of CDI/RfD above unity, the greater is the level of concern.

Trace Metals in Water Samples

The concentrations of heavy metals Fe, Pb, Cd, Zn, Cu, Mn, As, and Ni, in the drinking water samples were analyzed and presented in Table 47. Highest heavy metal concentration was found for iron. Levels of copper, and arsenic were below the detection limit in all the samples. All of the samples contained Fe, Zn, Mn and Ni at values complying with specified WHO 2008 maximum contaminant levels (MCLs). In contrast, in 100.0% and 59.0% of the samples registered Cd and Pb, respectively above WHO MCLs. This is of concern because cadmium has carcinogenic properties as well as a long biological half-life leading to chronic effects as a result of accumulation in liver and renal

cortex. It can also cause kidney damage as well as producing acute health effects resulting from over exposure to high concentrations (Momodu & Anyakora, 2010). Cadmium at higher concentrations, it is known to have a toxic potential.

The main sources of cadmium are industrial activities; the metal is widely used in electroplating, pigments, plastics, stabilizers and battery industries (Nassef, Hannigan, El Sayed & Tahawy, 2006). Cadmium is highly toxic and responsible for several cases of poisoning through food. Small quantities of cadmium cause adverse changes in the arteries of human kidney. It replaces zinc biochemically and causes high blood pressures, kidney damage etc (Rajappa, Manjappa & Puttaiah, 2010). It interferes with enzymes and causes a painful disease called Itai-itai. Concentration of cadmium in water samples ranged between 0.006 to 0.072 mg/L (Table 47) all above the WHO, 2008 recommended value (3µg/L). Due to possible long term effects of chronic exposure, the presence of lead in drinking water is crucially important for public concern.

WHO permissible limit of lead in water is 0.05mg/L. Concentration of lead in the water samples ranged between 0.008 to 0.170 mg/L. 59% of the water samples had their concentration above the WHO permissible limit. Lead as a contaminant is a widespread issue; It accumulates with age in bones, the aorta, and kidneys, the liver and the spleen. It can enter the human body through uptake of food (65%), water (20%) and air (15%). Overall average concentration of heavy metals in water samples varies as Fe > Pb > Cd > Ni > Zn > Mn. The results reveal that the amount of heavy metals depends on the sampling locations

The physical parameters and chemical parameters of the water samples such as pH, temperature, salinity, conductivity, total dissolved solid (TDS), and metals which are shown in Table 32 for the groundwater sample.

Table 47: Summary of Groundwater Chemistry

COMMUNITY	T/^{O}C	Cond./μScm^{-1}	Sal.	pH	TDS mg/L	Fe	Pb	Cd	Zn	Cu	Mn	As	Ni
Axim 1	29.2	137.5	0.0	5.8	83	0.038	0.008	0.013	0.012	<0.003	0.003	<0.006	0.023
ABH	32.3	420	0.1	6.9	252	0.099	0.061	0.072	0.007	<0.003	0.010	<0.006	0.015
ALIS	29.5	120.9	0.0	5.5	73	0.004	0.042	0.006	0.003	<0.003	0.008	<0.006	0.010
Krisan	32.9	181.5	0.0	5.7	109	0.120	0.053	0.041	0.017	<0.003	0.016	<0.006	0.019
Nyale Kplole 1	32	216	0.0	5.5	129	0.074	0.170	0.005	0.005	<0.003	0.005	<0.006	0.031
Nyale Kplole 2	30.2	51.4	0.0	5.7	31	0.218	0.028	0.045	0.008	<0.003	0.004	<0.006	0.024
Atuabo 1	29.7	238	0.0	6.8	143	0.162	0.122	0.063	0.006	<0.003	0.006	<0.006	0.011
Ekebaku	35.1	104.6	0.0	5.5	63	0.083	0.034	0.071	0.021	<0.003	0.006	<0.006	0.016
Beyin 1	29.1	399	0.1	7.2	239	0.110	0.030	0.052	0.009	<0.003	0.007	<0.006	0.021
Beyin 2	30.4	263	0.0	6.7	158	0.060	0.062	0.009	0.011	<0.003	0.023	<0.006	0.011
Kikam	28.6	207	0.0	6.6	103	0.152	0.038	0.030	0.006	<0.003	0.007	<0.006	0.036
Kengen 1	29.6	99.4	0.0	6.0	60	0.285	0.051	0.065	0.006	<0.003	0.005	<0.006	0.023
Kengen 2	29.5	416	0.1	6.1	250	0.330	0.093	0.028	0.040	<0.003	0.004	<0.006	0.010
Twenen	29.0	148.4	0.0	4.8	89	0.090	0.047	0.025	0.003	<0.003	0.005	<0.006	0.016
Half-Assini 1	29.9	238	0.0	6.1	143	0.431	0.134	0.040	0.007	<0.003	0.008	<0.006	0.013
Half-Assini 2	32.5	141.2	0.0	4.4	84	0.103	0.062	0.039	0.003	<0.003	0.010	<0.006	0.022
Half-Assini 3	29.2	234	0.0	7.2	140	0.211	0.071	0.042	0.005	<0.003	0.009	<0.006	0.010

Source: Laboratory work, 2016

Table 48: Principal Component Loadings of Trace Metals in Groundwater

Trace metal	Component	
	1	2
Fe	0.851	0.169
Pb	0.438	-0.092
Cd	0.467	0.279
Zn	0.550	-0.250
Mn	-0.260	-0.799
Ni	0.421	0.723

Extraction Method: Principal Component Analysis
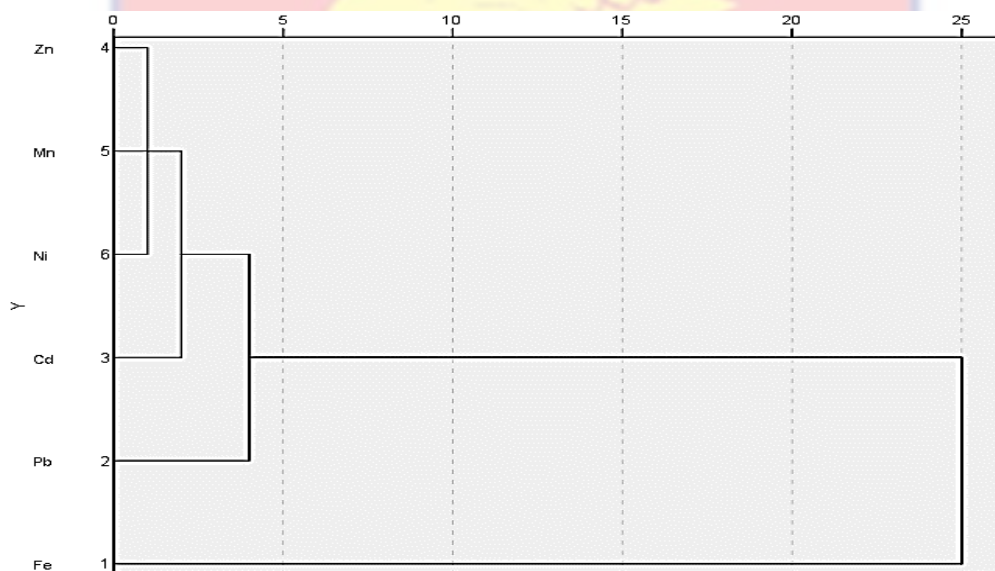
Figure 29: Dendrogram analysis mean of metal elements in ground water samples.

The principal component loadings of the heavy metals in water is presented in Table 48 whereas the corresponding cluster analysis is shown in Figure 29. Two components were extracted accounting for 87.50% of all the data variation. PC1 included Mn, Ni and Cd and show good similarity and are therefore clustered in one group while PC 2 was constituted by Fe and Pb. The strong similarity between Mn, Ni and Cd shows that these metals come from the same source. From the earlier references made to Micó et al., 2006 reporting

152

that Mn and Ni appeared to be associated with the lithosphere whereas Cu and Pb constituted anthropogenic components. Facchinelli et al., (2001) also concluding that Ni was controlled by parent rocks, whilst Cu and Zn were associated with specific agronomic practices, and Pb derived from car exhausts. The analysis from the present study suggests that Mn, Ni and Cd are controlled by the geology of the groundwater sources whereas Pb and Fe may be anthropogenic.
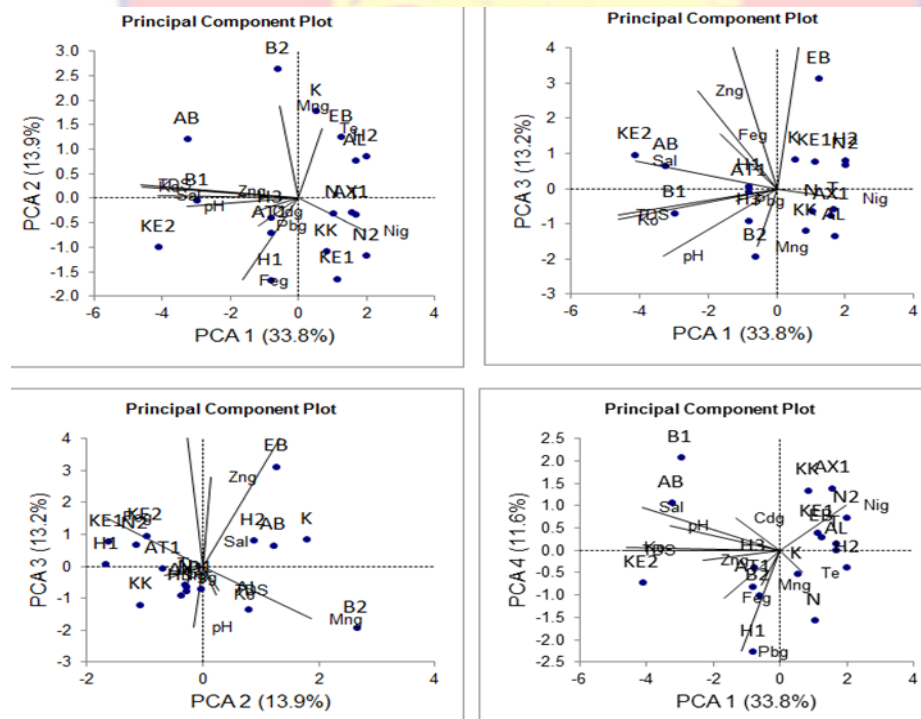
Figure 30: PCA biplot for PC1 & PC2, PC1 & PC3, PC2 & PC3, PC1 & PC4 groundwater.

A 17x11 data matrix was used for the PCA analysis. The data was subjected to pre-treatment using standardization prior to analysis. The results of the analysis are shown on Table 48 and Fig. 30. Using an Eigenvalue ≥ 1, five principal components have been determined as significant as indicated by the biplots in Fig. 30 and Fig. 42 (Appendix II). These five PCs contributed 82% of

153

the total variance in the observed data with approximately 48% contribution by PC1 and PC2. From Fig. 30 and Fig. 42 biplots, and Table 47, TDS, Ko, Sal, pH and Zng are highly positively correlated and they exert significant influence on the groundwater at B1. Cd_g, Pb_g and Fe_g are also highly correlated positively but with higher variance in Fe_g and may be originating from the same source. Moreover, Cd_g, Pb_g and Fe_g exert enormous influence on the groundwater at H3 and AT1.

Considering the significant ecological and health impact of cadmium and lead in the environment, H3 and AT1 need to be on the monitoring radar in the immediate future in assessing the potential impact of the oil and gas industry in the release of these critical trace metals in those communities. Temperature, Te correlates with Mn_g whilst independent with Ni_g and inversely correlated with Cd_g, Pb_g and Fe_g heavy metals as well as TDS, Ko, Sal, and pH. Relatively few objects form clusters with a maximum of six. The groundwater from N, AX1, T, N2, KE1 and KK are very similar thus can be considered as a cluster and highly influenced by Ni_g.

The contour plot for trace metals in groundwater as indicated by Fig. 31 shows minimal levels of Pb in groundwater of the study area (Fig. 31a). EB and AT1 however exhibit appreciable level of Cd in groundwater as indicated by Fig. 31b and therefore requires constant monitoring and assessment of Cd especially AT1 where the presence of a gas processing factory might play significant role in future release of trace metals.
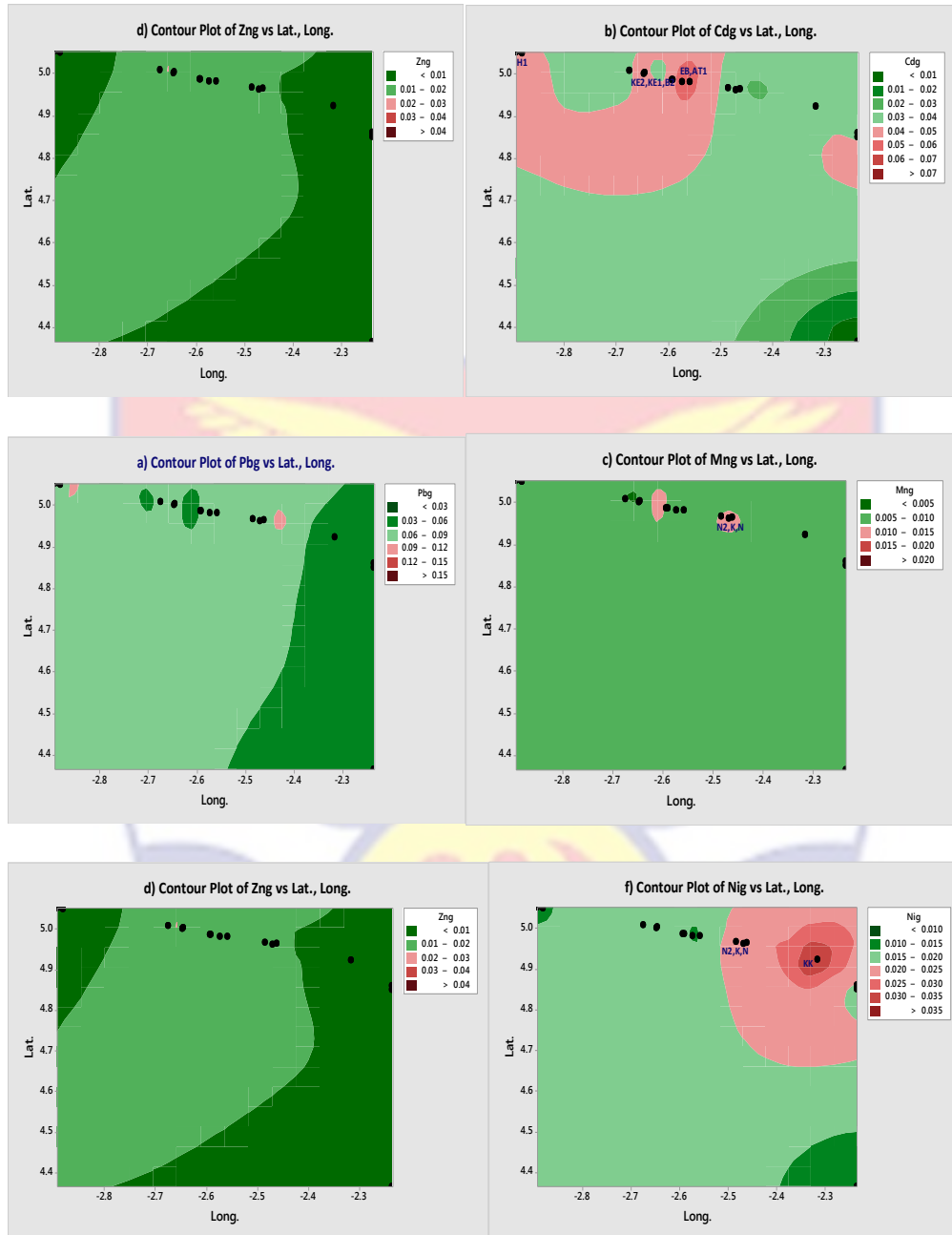
Figure 31: Contour Plot of Heavy Metals in Groundwater.

Soil and Groundwater

A 14x12 data matrix consisting of 14 actions and 12 criteria was subjected to PROMETHEE-GAIA analysis using two modelling scenarios. In the first modelling scenario, all the criteria was maximized, assigned equal weighting and subjected to V-shaped preference function. Moreover, to prioritize the selection of communities in assessing the potential impact of the

155

oil and gas operations in the Tano Basin on the neighbouring onshore communities, PROMETHEE-II was used and Fig. 33 depicts the resultant GAIA. The GAIA was interpreted according to the guidelines published by Espinasse et al., 1997. The GAIA biplot represented 46.8% of the information in the data.
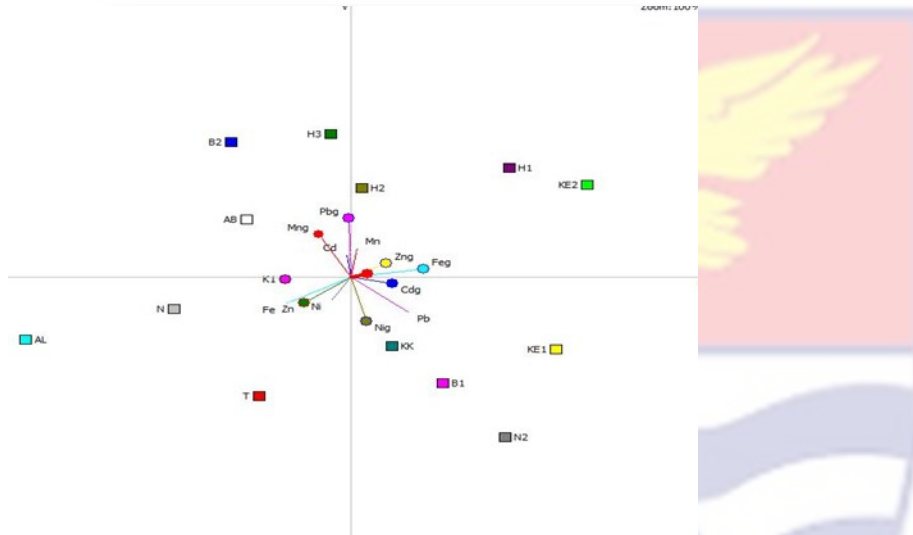
Figure 32: The GAIA biplot for Soil and Groundwater Samples Scenario 1.

Rank	action		Phi	Phi+	Phi-
1	K1	●	0,3429	0,6378	0,2949
2	N2	■	0,1795	0,5481	0,3686
3	H3	■	0,1058	0,4968	0,3910
4	KK	■	0,0897	0,5000	0,4103
5	AB	□	0,0577	0,4776	0,4199
6	KE2	■	0,0160	0,4615	0,4455
7	B1	■	-0,0256	0,4455	0,4712
8	B2	■	-0,0353	0,4423	0,4776
9	H2	■	-0,0577	0,4167	0,4744
10	KE1	□	-0,0865	0,3974	0,4840
11	H1	■	-0,0897	0,4038	0,4936
12	N	■	-0,0994	0,4006	0,5000
13	T	■	-0,1699	0,3654	0,5353
14	AL	■	-0,2276	0,3526	0,5801
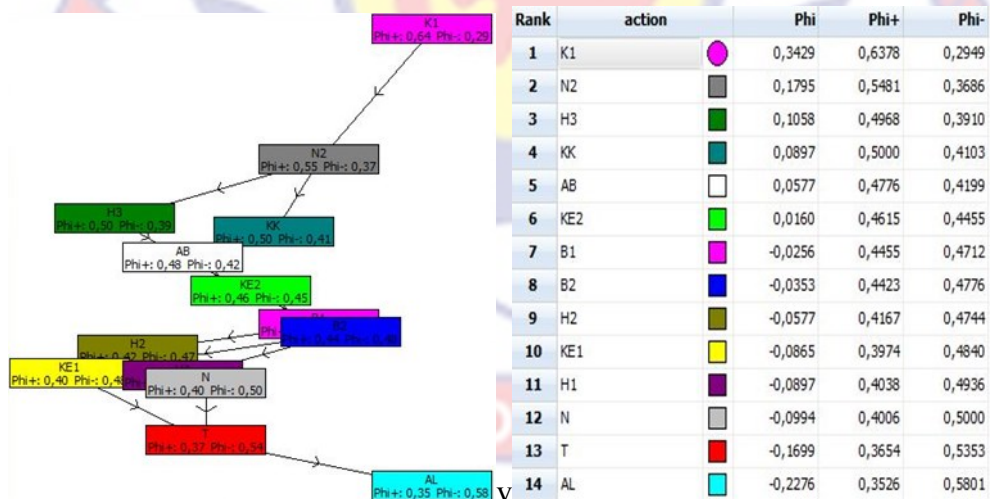
Figure 33: PROMETHEE IIrankingfor soil and Groundwater Samples Scenario 1.

The following observations have been made from the Fig. 33, Zn_g, Fe_g, Cd_g and Mn may play significant role in the ranking of the studied communities

156

due to their relative proximity to pi (π), the decision axis. From the PROMETHEE-II results as shown on Fig. 30, the communities can be ranked as K1 > N2 > H3…T > AL. Fe, Pb, Pb_g, Mn_g, Fe_g and Ni_g criteria have higher variance compared to others. Fe, Zn and Ni are highly correlated likewise Cd, Mn_g and Pb_g, and Ni_g, Pb and Cd_g. This may be an indication of similar sources from the environment. However, Fe and Zn in soil are opposite to Fe_g and Zn_g in groundwater. This may be a possible indication of leaching of iron and zinc from the soil to the groundwater in AL, T, N and K1 communities.

The same argument holds true for Pb and Pbg, and Cd and Cdg. However, Ni and Nig, and Mn and Mng are correlated positively a possible indication of similar sources of these heavy metals in soil and groundwater respectively. Furthermore, four clusters of communities is observed as follows. H1 and KE2 form a cluster and are strongly influenced by Zng and Feg. AL, T, N and K1 can also be considered a cluster and is impacted mostly by Fe, Zn and Ni. Thirdly, AB, B2, H3 and H2 form another cluster and are highly influenced by Cd, Mn_g and Pb_g. Finally, N2, KK and KE1 also form a cluster and are strongly influenced by Pb, Ni_g and Cd_g.

Considering the critical deleterious fate of Cd and Pb on the environment, the latter two clusters may require constant monitoring in the near future to determine the impact of oil and gas exploration and drilling activities on future pollution of soil and groundwater in these communities. Moreover, the groundwater resources in these communities are very essential to the daily life of the residents, thus deleterious pollutants such as Cd and Pb likely to impede the sustainable use of this vital natural resource needs to be regularly monitored to guarantee public health and safety.
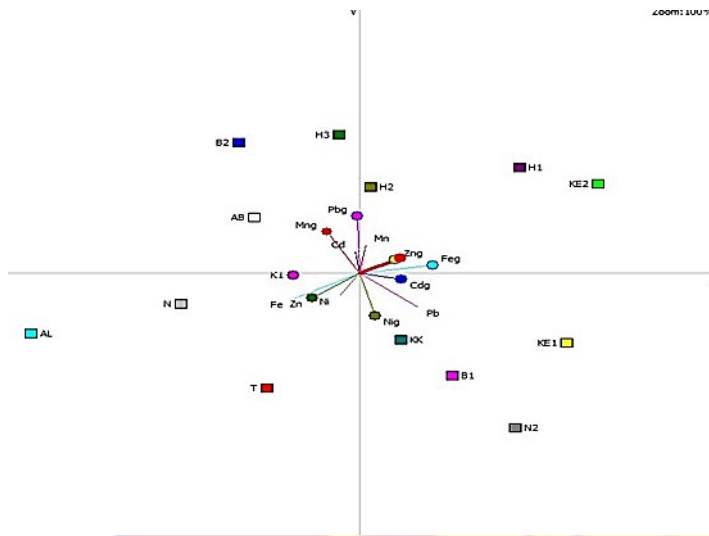
Figure 34: The GAIA biplot for Soil and Groundwater Samples Scenario 2.

Rank	action		Phi	Phi+	Phi-
1	K1		0,3253	0,6410	0,3157
2	H3		0,1827	0,5609	0,3782
3	KE2		0,1234	0,5385	0,4151
4	KE1		0,0865	0,5112	0,4247
5	KK		0,0641	0,5096	0,4455
6	AB		0,0577	0,4984	0,4407
7	N2		0,0513	0,5048	0,4535
8	H2		0,0385	0,4824	0,4439
9	H1		-0,0256	0,4567	0,4824
10	B1		-0,0465	0,4535	0,5000
11	T		-0,0657	0,4423	0,5080
12	B2		-0,0897	0,4279	0,5176
13	N		-0,1843	0,3782	0,5625
14	AL		-0,5176	0,2196	0,7372
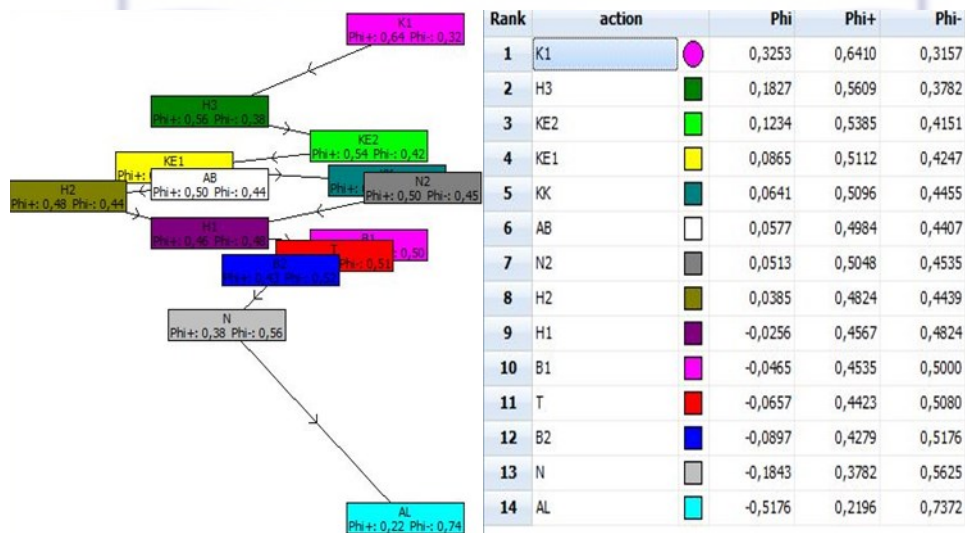
Figure 35: PROMETHEE II ranking for Soil and Groundwater Samples
Scenario 2.

In the second modelling scenario, all the criteria was maximized and subjected to V-shaped preference function. However, cadmium and lead were given a weighting of 4 due to the critical deleterious nature of these two heavy metals on human health and the ecology at large. There was no significant alteration in the GAIA biplot as shown on Fig. 34 except that π decision became comparatively longer but in the same direction as the previous Scenario 1. There

158

was however, a relative change in the PROMETHEE-II ranking as indicated on Fig. 35 in the order K1 > H3 > KE2 > KE1 >… > N > AL. To reduce the cost and time associated with such future monitoring of soil and groundwater for possible contamination by heavy metals, this study has successfully prioritized areas that may require immediate future monitoring as well those areas that may exhibit similar heavy metal pollution risk by virtue of their clustering. In this regard, randomly selected communities from each cluster may be sampled and analysed for heavy metals in soil and groundwater.

Physico-Chemical Parameters of Groundwater

Physical parameters studied in this research include temperature and color of water while chemical parameters include pH, dissolved oxygen contents, alkalinity, hardness and electrical conductivity. Table 47 shows the results for pH, electrical conductivity, salinity, total dissolved solids and heavy metal concentrations in groundwater samples (Table 47). WHO normal range for pH is 6.5 - 8.5. The pH of the water samples were recorded in the range of 4.4 – 7.2. This suggest that the analysed water samples were more acidic than the WHO standard.

Acid pH of water may be due to dissolved carbon dioxide and organic acids such as fulvic and humic acids which are derived from decay and subsequent leaching of plant materials (De, 2000; Langmuir, 1997). pH is mainly influenced by volume of water, soil type. Low pH of groundwater can cause gastrointestinal disorders especially hyperacidity, ulcers and burning sensation (Laluraj & Gopinath, 2006). Water having pH below 6.5, causes corrosion of metal pipes, resulting in the release of toxic metals such as zinc, lead, cadmium, copper etc. Higher values of pH hasten scale formation in water

heating apparatus and decrease germicidal potential of chlorine. None of the samples had pH exceeding the recommended upper limit value which suggested that the water can allow effective disinfection with chlorine. The low pH probably is derived from carbonic acid due to the dissolution of atmospheric CO_2 or CO_2 generated in the soil zone as a result of the oxidation of soil organic matter

The temperature of water samples varied from 28.6°C to 35.1°C, the variation of the water temperature having more effect directly or indirectly on all life processes. WHO normal range for electrical conductivity of water is 400-600 µS/cm. The electrical conductivity values for the present study recorded relatively low values in the range of 51.4 – 420 µS/cm

TDS is an important parameter which imparts a peculiar taste to water and reduce its potability. Desirable limit of TDS is 500mg/L (IS: 10500 standards) and maximum allowable limit is 1500 mg/L. The value of TDS of studied ground water samples ranged between 31 to 252 ppm with all the values obtained are much lower than the limits.

Soil-to-Cassava Transfer Factor

The highest TF value for [238]U was 0.553. For [232]Th and [40]K, the highest values of transfer factor were 0.078 (CS 5) and 0.057 (CS 1) respectively (Table 29). The soil-to-plant transfer factor (TF) is an important parameter used as measure transfer of radionuclides from soil to the food chain and modelling the behavior of radionuclides in the food chain. Differences in TF may occur even for the same plant species as having been reported (Vandenhove, Olyslaegers, Sanzharova, Shubina, Reed, Shang & Velasco, 2009). For instance, for grass, the [238]U transfer factor has a range over more than 4 orders of magnitude, [230]Th

over 3 orders of magnitude and ^{226}Ra over 3 orders of magnitude (Vandenhove et al., 2009). These variations occur because the transfer of radionuclides to plants is complex, depending on the chemistry of the specific radionuclide, soil type, pH, solid/liquid distribution coefficient, exchangeable K$^+$, organic matter (Chakraborty, Azim, Rahman & Sarker, 2013) and type of plant (WHO & FAO, 2011). Variations in radionuclides TF values also occur for different plant species due to the different characteristics of the plants.

The soil-to-plant transfer factor (TF) is an important parameter used as measure transfer of radionuclides from soil to the food chain and modelling the behavior of radionuclides in the food chain. Differences in TF may occur even for the same plant species as having been reported (Vandenhove et al., 2009). For instance, for grass, the ^{238}U TF has a range over more than 4 orders of magnitude, ^{230}Th over 3 orders of magnitude and ^{226}Ra over 3 orders of magnitude (Vandenhove et al., 2009). These variations occur because the transfer of radionuclides to plants is complex, depending on the chemistry of the specific radionuclide, soil type, pH, solid/liquid distribution coefficient, exchangeable K$^+$, organic matter (Chakraborty et al., 2013) and type of plant (WHO & FAO, 2011). Variations in radionuclides TF values also occur for different plant species due to the different characteristics of the plants.

The comparative uptake of ^{238}U, ^{232}Th and ^{40}K by different plants is affected by geologic, chemical and biological conditions of the soil. These effects and the individual chemical properties of the nuclides, tend to affect its uptake by plants (Jazzar & Thabayneh, 2014). For example, retention of radionuclides onto the soil particles will affect their availability for plant uptake. Uranium exhibits much higher mobility than thorium (Martinez-Aguirre,

Garcia-Leo´n, & Ivanovich, 1995), which is consistent with the observation in this study that ^{232}Th has smaller average TF than ^{238}U. The magnitude and range of TF of ^{238}U and ^{232}Th found in this study appeared to be generally similar to values obtained in other studies where radionuclides uptake was the primary point of focus (Frissel & Koster 1988; IAEA-TECDOC-1616, 2009) and with root uptake considered as the primary mechanism of accumulation. ^{40}K is an essential element for plant growth, it was expected that ^{40}K would register the highest TF. ^{238}U, however, had the highest transfer factor in sharp contrast to a report where soil-to-cassava and soil-to-sweet potato TFs (geometric mean) for ^{40}K were found to be significantly higher than that for the other nuclides in almost all locations (Asaduzzaman et al. 2014).

The observed values of TFs are however above the range reported by the IAEA for ^{232}Th in root crops (roots) of 9.0×10^{-6} to 3.9×10^{-5}, and root crops (tubers), of 2.9×10^{-6} to 3.5×10^{-5}, (IAEA-TECDOC-1616, 2009). As earlier stated, these variations are as a result of soil type and properties such as pH, solid/liquid distribution coefficient, exchangeable K^+, organic matter (Chakraborty et al., 2013) and type of food (WHO & FAO, 2011). TFs on dry weight basis (soil depth considered is upper 20 cm) by compiling data from six different countries having tropical environments (Australia, Brazil, India, Indonesia, Marshall Islands and Vietnam) (IAEATECDOC-1616; Velasco et al. 2009). Vandenhove et al. (2009) also published a similar report in Journal of Environmental Radioactivity.

Computational Activity Concentration Assessment

Figures 49 to 53 shows the simulation of the decay of the radionuclides ^{238}U, ^{232}Th and ^{40}K from 100 years to 10^8 years. It is observed that the decay curve of the radionuclides tend to became more significant and to approaches exponential decay graph as the years increase.
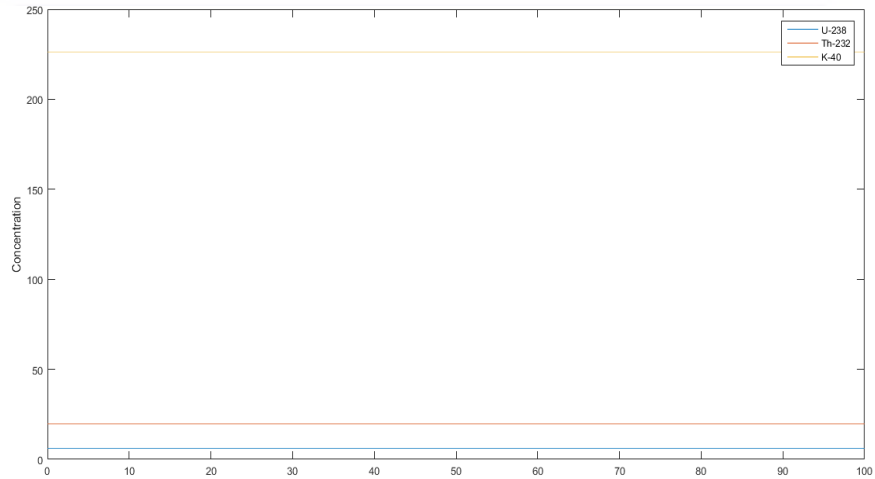
Figure 36: Simulation of the decay of the radionuclides ^{238}U, ^{232}Th and ^{40}K in 100 years.
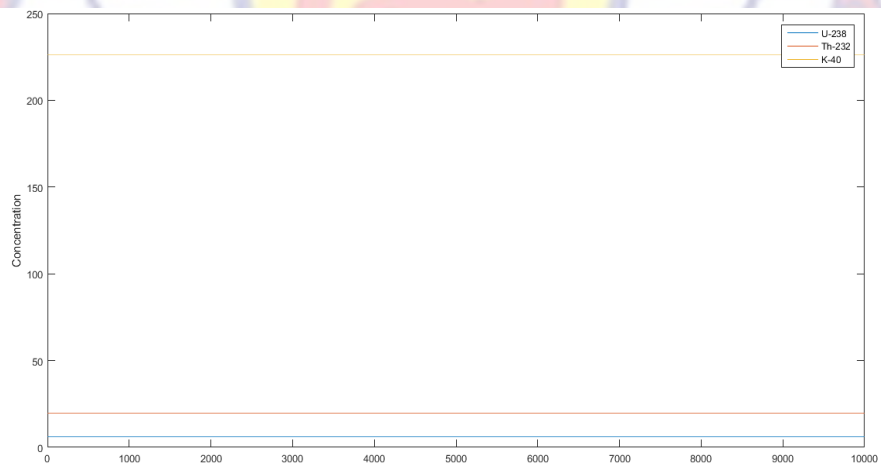
Figure 37: Simulation of the decay of the radionuclides ^{238}U, ^{232}Th and ^{40}K in 10000 years.
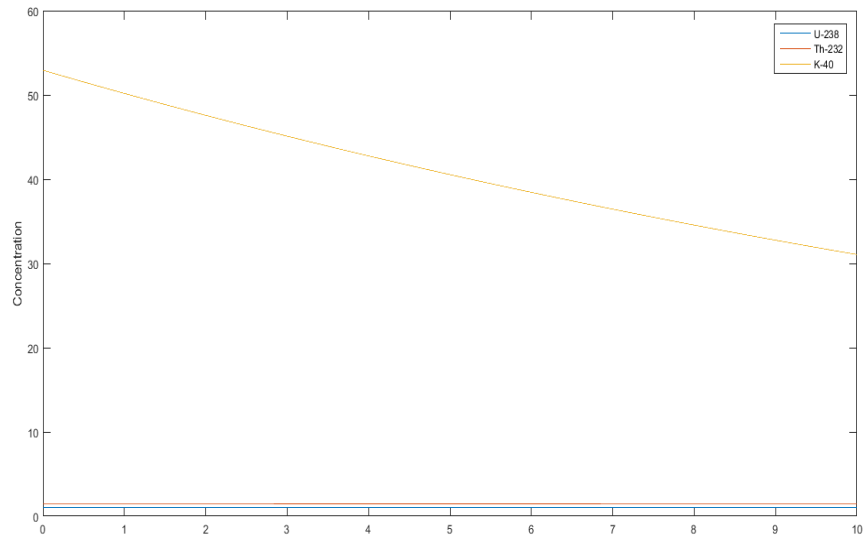
Figure 38: Simulation of the decay of the radionuclides ^{238}U, ^{232}Th and ^{40}K for $\times 10^8$ years.
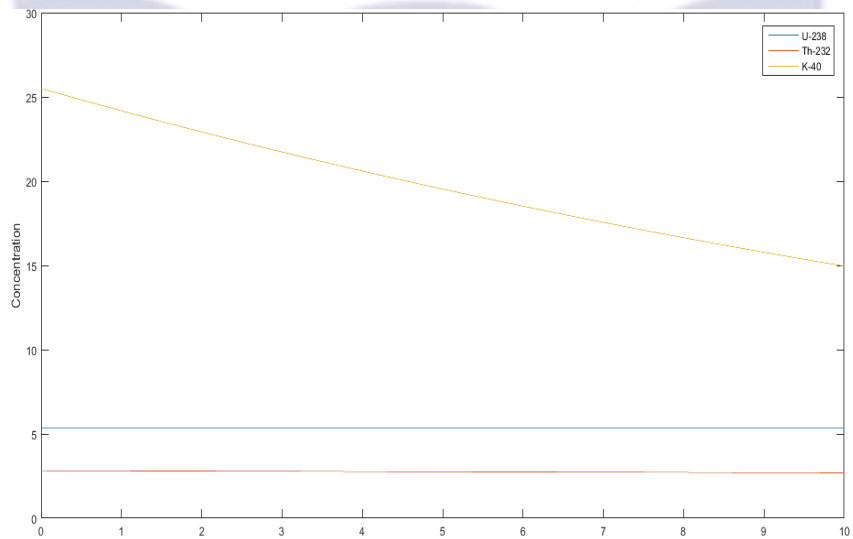
Figure 39: Simulation of the decay of the radionuclides ^{238}U, ^{232}Th and ^{40}K for $\times 10^8$ years.
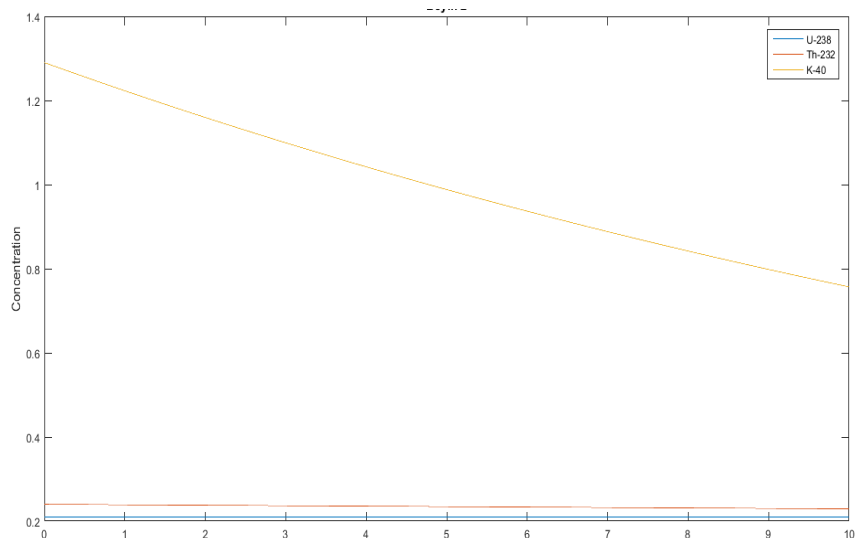
Figure 40: Simulation of the decay of the radionuclides ^{238}U, ^{232}Th and ^{40}K for $\times 10^8$ years.

The activity concentrations of the radionuclides were predicted using the Forward Differential Approach and a written MATLAB R13 script as presented in Appendix III, based on their current measured concentrations. Different year considerations were chosen to estimate the extent of decay. From the predicted results, it was observed that there was no significant variance in the predicted activity concentrations from the measured or experimental activity concentrations for ^{238}U and ^{232}Th whilst the activity concentration of ^{40}K showed variation from the measured activity concentrations that were quite significant. From the decay equation

$$A = A_0 e^{-\lambda t}$$

A plot of A against t was expected to give an exponential decay graph, and if the background radiation were ignored, the line would tend toward A = 0 as time goes by. This was not observed in the sample graphs presented in Figures 49 and 50. This is explained by the long half-lives of the radionuclides of concern. ^{238}U has a half-life of 4×10^9 years with that of ^{232}Th being 1.4×10^{10}

165

years and ^{40}K being 1.25×10^9 years. With these half-lives, the decay that these radionuclides will undergo in 100 years will be insignificant. As the years were increased, the decay plot of the respective radionuclides became more significant and tend to approach an exponential decay graph, particularly for ^{40}K as presented in Figures 51 to 53.

The minor decrease in the activity concentrations of ^{238}U and ^{232}Th will translate into minor decrease exposure to the public expressed as the effective dose. This supposes that the impact of the radionuclides on the public will remain fairly constant for the next several years.

Summary

The results obatained for radionuclide activity and trace metal concentration and their potential human health risks were presented in this chapter. It was estimated that 1 out of 10,000 may suffer from some form of cancer fatality and for the lifetime hereditary effect approximately 5 out of 1,000.000 may suffer some hereditary effect due to exoosure to radionuclides. The cancer fatality risk value from trace metals was considered negligible.

CHAPTER FIVE

SUMMARY, CONCLUSIONS AND RECOMMENDATIONS

Summary

This research work was conducted with the aim to assess the risks to members of the public in the study area from exposure to natural sources of radiation as a consequence of oil and gas drilling activities. The exposure pathways considered for the study were; direct external gamma ray exposure from natural radioactivity concentrations in soil, internal exposure from drinking water containing natural radioactivity, ingestion of food (cassava), and inhalation of radon gas. The study covered the major communities bordering the Tano Basin, starting from Axim to New Town.

This current study on natural radioactivity established baseline data on the activity concentrations of ^{238}U, ^{232}Th and ^{40}K in soil and food samples and ^{226}Ra, ^{228}Ra and ^{40}K in water samples as well as radiation doses and risks. The activity concentrations of all radionuclides in different media for all the potential pathways through which members of the public are most likely to be exposed were quantified using direct gamma spectroscopic analysis.

The mean activity concentrations of ^{238}U, ^{232}Th and ^{40}K in soil were found to be 8.65±1.17, 12.51±1.25 and 214.11±24.34 Bqkg^{-1}, respectively. The mean activity concentration of ^{226}Ra, ^{228}Ra and ^{40}K in water samples were 0.58±0.06, 0.84±0.09 and 2.51±0.15 Bq/L respectively. For the fresh weight food samples the mean activity concentrations of ^{238}U, ^{232}Th and ^{40}K were 0.20±0.03, 0.16±0.05 and 6.08±1.22 Bq/kg respectively and airborne ^{222}Rn averaging 20.30±2.85 Bq/m^3. Despite the fluctuation in the measurements of the activity concentrations of each natural radionuclide ^{238}U/^{226}Ra, ^{232}Th/^{228}Ra,

^{40}K and ^{222}Rn from one sampling location to the other, the data are found to be normal in comparison to the worldwide standards in other countries as presented in UNSCEAR, (2000).

The potential exposure of the public in the study area was assessed by estimating the annual effective doses in various media and the total annual effective dose was determined from the sum of all the mean annual effective doses from all the exposure pathways considered for purposes of comparison with recommended dose limits. The total annual effective dose for all the exposure pathways was 35.34 μSv/y, far lower than the 1 mSv per year dose limit recommended by the ICRP for public radiation exposure control. This presents a lower chance for the onset of carcinogesis from these exposures.

The radiological hazards to the population in the study area were assessed based on the calculation of radium equivalent activity (Ra_{eq}) and hazard indices (external and internal). The average Ra_{eq} of 43.37 Bq/kg was found to be less than the recommended maximum value of 370 Bq/kg, and the external and internal hazard indices had values less than unity. It can be concluded that soil may be used for construction of buildings may not pose any significant radiological hazards.

ICRP risk assessment methodology for fatal cancer risk and hereditary effects was used estimate the risks to members of the public. The lifetime fatality cancer risks from the exposure pathways considered varied from 4.2 x 10^{-7} to 9.66 x 10^{-5} from the ingestion of ^{226}Ra, ^{228}Ra and ^{40}K in groundwater and external irradiation from ^{238}U, ^{232}Th and ^{40}K respectively. Lifetime hereditary effects were estimated to be in the range of 1.5 x 10^{-8} from the ingestion of ^{226}Ra, ^{228}Ra and ^{40}K and 3.5 x 10^{-6} from external irradiation due to ^{238}U, ^{232}Th

and ^{40}K. The total lifetime cancer and total lifetime hereditary effects were estimated to be 1.36 x 10^{-4} and 4.95 x 10^{-6} respectively. This means that in terms of the lifetime fatality cancer risk approximately 1 out of 10,000 may suffer from some form of cancer fatality and for the lifetime hereditary effect approximately 5 out of 1,000.000 may suffer some hereditary effect. The negligible cancer fatality risk value recommended by USEPA is in the range of 1 x 10^{-6} to 1 x 10^{-4} (i.e. 1 person out of 1 million or 10,000 suffering from some form of cancer fatality). The total lifetime risk estimated was within acceptable range recommended by the USEPA.

The results from this study will serve as baseline data for any future referencing and comparison and also add up to the national database on TE(NORM) required to help develop guidelines for the regulation of NORM in Ghana for radiation protection workers and the public. The results which have also been published in peer reviewed journals for the reading public will help create awareness on NORM to individuals, policy makers and academia.

The physical parameters such as pH, temperature, conductivity and total dissolved solids (TDS) of the water samples were also assessed. The conductivity and TDS were all within the acceptable limits recommended by the WHO in drinking water (WHO, 2004). In the case of the pH of the water samples, the recommended range in drinking water is 6.5-8.5, but in this study some of the water samples had pH values falling as low as 4.8. 88% of the water samples studied had pH less than 7, making them acidic. Considering that these water samples are used for domestic or consumption purposes the pH values may have significant health hazard to the public. For the heavy metals namely; Fe, Pb, Cd, Zn, Mn and Ni their concentrations were variable from one location

to another with Cu and As below detection limit. 100% and 59% of the water samples had their Cd and Pb concentrations above the WHO permissible limit.

For the concentrations of metals determined in the soil samples, it was found that all the concentrations of trace metals except Fe were below the recommended levels.

As shown from the results, agricultural soils in the study communities have low Transfer Factors of radionuclides which compared well with studies in other countries. It is therefore safe for farmers, and the general population and can be used as a raw building materials or other human activities without any radiological risk. The results would be useful for establishing of the database in the area under consideration and represent a basis to assess any future changes in the radioactivity background levels due to any artificial influences and various geological processes in or around the area.

Recommendations

The following recommendations are outlined for future research

- Determination of activity concentrations of ^{238}U, ^{232}Th and ^{40}K by gamma spectrometry activity concentrations in other crops from the study area.

- Studies on the fate and transport of radionuclides in groundwater systems as a case study of the Tano Basin are also recommended.

- Speciation studies on the metals present in groundwater as in most cases, speciation of these metals determines their toxicity.

- The determination of the Transfer Factors (TF) of other crops that are widely grown and consumed in the study communities is recommended.

- Mathematical models suitable for making accurate computerized projections into the long term movement of radionuclides into the roots of plants under different circumstances are needed.

REFERENCES

A. N. L. (2005). *Natural Decay Series: Uranium, Radium, and Thorium*. Human Health Fact Sheet, Argonne National Laboratory, EVS

Abo-Emagd, M., Soliman, H. A., Salman Kh. A., & El-Masry, N. M. (2010). *Radiological hazards of TENORM in the wasted petroleum pipes*. Journal of Environmental Radioactivity 101, 51 – 54.

Adda, W. G. (2013). *The Petroleum Geology and Prospectivity of the Neo-Proterozoic, Paleozoic and Cretaceous Sedimentary Basins in Ghana*: Search and Discovery Article #10544 http://www.searchanddiscovery.com/documents/2013/10544adda/ndx_adda.pdf. Accessed May 13, 2015.

Ademola, J. A. (2011). *Occupational Exposure Due To Naturally Occurring Radionuclide Material in Granite Quarry Industry*. Radiat Prot Dosimetry 148(3), 297 – 300.

Adriano D. C. (2003). *Trace Elements in Terrestrial Environments: Biogeochemistry, Bioavailability and Risks of Metals*. Springer, New York, NY, USA, 2nd edition.

Agbalagba, E. O., Avwiri, G. O., & Chadumoren, Y. E. (2013). *Radiological impact of oil and Gas Activities in selected oil fields in Production Land Area of Delta State, Nigeria*. J. Appl. Sci. Environ. Manage. 17(2), 279 – 288.

Ahier, B. A. & Tracy, B. L. (1995). *Radionuclides in the Great Lakes basin*. Environ. Health Perspect. 103, 89 – 101.

Ahmed, N. K., & El-Arabi, A. G. M. (2005). *Natural radioactivity in farm soil and phosphate fertilizer and its environmental implications in Qena Governorate, Upper Egypt.* Journal of Environmental Radioactivity 84, 51 – 64.

Ajibode, M. O., Awviri, G. O., & Agbalagba, E. O. (2013). *Evaluation of radiation hazard indices in an oil mineral lease (oil block) in Delta State, Nigeria.* International Journal of Engineering and Applied Sciences 4(2), 104 – 121.

Ajugwo, O. A. (2013). *Negative Effects of Gas Flaring: the Nigerian Experience.* Journal of Environmental Pollution and Human Health 1(1): 6 – 8.

Akar, T. U., Gurler, O., Akkaya, G., Kilic, N., Yalcin, S., Kaynak, G., & Gundogdu, O. (2012). *Evaluation of radon concentration in well and tap waters in Bursa, Turkey.* Radiat. Prot. Dosim. *150*, 207 – 212.

Akhtar, N., Tufail, M., & Ashraf, M. (2005). *Natural environmental radioactivity and estimation of radiation exposure from saline soils.* International Journal of Environmental Science & Technology 1, 279 – 285.

Al-Turki, A. I & Helal, M. I. D. (2004). *Mobilization of Pb, Zn, Cu and Cd, in Polluted Soil, Pakistan.* Journal of Biological Sciences A 7, 1972 – 1980.

Ansre C. Y., Miyittah M. K., Andam A. B., & Dodor D. E. (2017). *Risk assessment of radon in the South Dayi District of the Volta Region, Ghana.* Journal of Radiation Research and Applied Sciences xxx, 1 – 8.

173

Asaduzzaman K., Khandaker M. U., Amin, Y.M., Bradley, D.A., Mahat, R.H., & Nor, R.M. (2014). *Soil-to-root vegetable transfer factors for ^{226}Ra, ^{232}Th, ^{40}K and ^{88}Y in Malaysia.* Journal of Environmental Radioactivity 135, 120 – 127.

ASTM (American Society for testing and Materials) (2005). *C1402-04 Standard Guide for High Resolution Gamma –Ray Spectrometry of Soil Samples*. Annual Book Standard Vol. 12.01. Nuclear Energy (I), ASTM International Standard Worldwide, Philadelphia, U.S.A

Asumadu-Sakyi A. B., Oppon O. C., Quashie F. K., Adjei C. A., Akortia E., Nsiah-Akoto I., & Appiah K. (2012). *Levels and potential effect of radon gas in groundwater of some communities in the Kassena Nankenna district of the Upper East region of Ghana.* Proceedings of the International Academy of Ecology and Environmental Sciences 2(4), 223 – 233.

ATSDR (1999). *Toxicological profile for ionizing radiation*. U. S. Department of Health and Human Services, Public Health Service, Agency for Toxic Substances and Disease Registry.

ATSDR (2011). *Substance priority list*. U. S. Department of Health and Human Services, Public Health Service, Agency for Toxic Substances and Disease Registry.

ATSDR (2012). *Toxicological profile for radon*. U. S. Department of Health and Human Services, Public Health Service, Agency for Toxic Substances and Disease Registry. Availablble at https://www.atsdr.cdc.gov/toxprofiles/tp145-c3.pdf. Accessed 14th January, 2015.

Attallah, M. F., Awwad, N. S. & Aly, H. F. (2012*). Environmental Radioactivity of TENORM Waste Produced from Petroleum Industry in Egypt: Review on Characterization and Treatment, Natural Gas-Extraction to End Use*. InTech, chapter 4, 75-98

Atta-Peters, D. & Garrey, P. (2014*). Source rock evaluation and hydrocarbon potential in the Tano basin, South Western Ghana, West Africa*. International Journal of Oil, Gas and Coal Engineering 2(5), 66 – 77.

Atwood David A. (2013). *Radionuclides in the Environment*. Google Books Result, https://books.google.com.gh/books. Retrieved 8th September, 2015.

Auvinen, A., Salomen, L., Pekkanen, J., Pukkala, E., Ilus T., & Kurttio P. (2005). *Radon and other natural radionuclides in drinking water and risk of stomach cancer: a case-cohort study in Finland*. Int J Cancer 114, 109 – 113.

Avivar C. J. (2012). *Automated flow systems for total and isotopic analysis of thorium and uranium in samples of environmental interest*. Doctoral thesis, Department of Chemistry, Universitat de les Illes Balears, page 14.

Avwiri, G. O, Ononugbo, C. P, & Nwokeoji, I. E (2014*). Radiation Hazard Indices and Excess Lifetime cancer risk in soil, sediment and water around mini-okoro/oginigba creek, Port Harcourt, Rivers State, Nigeria*. Comprehensive Journal of Environment and Earth Sciences 3(1), 38 – 50.

Ayoko, G. A., Bonire, J. J., Abdulkadir, S. S., Olurinola, P. F., Ehinmidu, J. O., Kokot, S. & Yiasel, S. (2003). *A multicriteria ranking of organotin (IV) compounds with fungicidal properties*. Applied Organometallic Chemistry 17(10), 749 – 758.

Azeri, Chirac & Gunashili (2004). *Full field Development phase 3.* Environmental and Socio-economic Impact Assessment 31648 – 046, Appendix 10

Badham, K., Mehra, K., & Sonkawade, R. G. (2010). *Measurement of radon concentration in groundwater using RAD 7 and assessment of average annual dose in the environs of NITJ, Punjab, India*. Indian Journal of Pure and Applied Physics 48: 508 – 511.

Beaza, A., dei Rio M., Miro, C. & Paniagua, J. (1994). *Natural radionuclide distribution in soils of Caceres (Spain): dosimetry implications*. J. Environ. Radioactivity 23, 19 – 37.

Becegato, V. A., Ferreira, F. J. F., & Machado, W. C. P. (2008). *Concentration of radioactivity elements derived from phosphate fertilizers in cultivated soils*. Brazilian Archives of Biology and Technology 51: 1255 – 1266.

Behzadian, M., Kazemzadeh, R. B., Albadvi, A. & Aghdasi, M. (2010). *PROMETHEE: A comprehensive literature review on methodologies and applications*. European Journal of Operational Research 200(1), 198 – 215.

BEIR V. (1990). *Health Effects of Exposure to Low Levels of Ionizing Radiation*. National Academy Press, Washington, DC.

BEIR VI (1999). *Health effects of exposure to indoor radon*. BEIR, National Academy Press, Washington D.C.

Bem, H., Plota, U., Staniszewska, M., Bem, E. M. & Mazurek, D. (2013). *Radon (²²²Rn) in underground drinking water supplies of the southern greater Poland region.* J. Radioanal. Nucl. Chem. 299, 1307 – 1312.

Blantz, R. C., Pelayo, J. C., Gushwa, L.C., Myers, R., & Evan, A. P. (1985). *Functional basis for glomerular alterations in uranyl nitrate acute renal failure*. Kidney Int. 228, 733 – 743.

Bou-Rabee, F., Al-Zamel, A. Z., Al-Fares, R. A., & Bem, H. (2009). *Technologically enhanced naturally occurring radionuclide materials in the oil and gas industry (TENORM). A review*. NUKLEONIKA 54(1), 3 – 9.

Capone, D. W., Chatterjee, S., Cleland, T., Fortunato, D. Roehrig, G., Walker, H. H., & Bush, T. O. (1997). *Results of Bench Scale of Mobile On-Site NORM Treatment System in Texas and New Mexico*. In proceedings of U. S Department of Energy's Natural gas Conference, Houston, TX, March 24-27

Cardoso, L. X., Cardoso, S. N. M., Alhanati, C. E., Ciolini, R., & Souza S. O. (2013*). Assessment of Environmental radioactivity in soil, water and foods consumed in Northeastern State of Sergipe, Brazil*. Int. Nuclear Atlantic Conf. – INAC, Recife, Brazil, Nov. 24 – 29.

Caussy, D., Gochfeld, M., Gurzau, E., Neagu, C., & Ruedel, H. (2003). *Lessons from case studies of metals: investigating exposure, bioavailability, and risk*. Ecotoxicol Environ Saf 56, 45 – 51.

177

CDC (Center for Disease Control and Prevention), ATSDR (Agency for Toxic Substances and Disease Registry). (2010). *Case studies in environmental medicine. Radon Toxicity*. U. S. Department of Health and Human Services, Public Health Service, Agency for Toxic Substances and Disease Registry

Cember, H. (1996). *Introduction to Health Physics*. 3rd Edition, McGraw-Hill, New York

Cevik, U., Damla, N., & Karahan, G. (2006). *Natural radioactivity in tap waters of eastern black sea region of Turkey*. Radiation Protection Dosimetry 118, 88 – 92.

CGG. (2012). Tano Basin 3D, Multi-Client Data Library-Marine, Ghana. www.cggveritas.com/.../2532_13F-DM-110-V1_150dpi_Ghana. Retrieved 21/10/2015.

Chakraborty, S. R., Azim, R., Rahman, A. K. M., & Sarker, R. (2013*). Radioactivity concentrations in soil and transfer factors of radionuclides from soil to grass and plants in the Chattagong City of Bangladesh.* Journal of Physical Sciences 24(1), 95 – 113.

Christie, C., 2012. *Disposal of Produced Water from Oil & Gas Exploration: Environmental Impacts on Waterways in Western Pennsylvania*. Masters project submitted in partial fulfillment of the requirements for the Master of Environmental Management degree in the Nicholas School of the Environment of Duke University

Colgan, P. A., Organo, C., Hone, C. & Fenton, D. (2008). *Radiation dose received by the Irish population.* RPII 08/01. Dublin: Radiological Protection Institute of Ireland.

Cosma, C., Moldovan, M., Dicu, T., & Kovacs, T. (2000). *Radon in water from Transylvania (Romania)*. Radiation Measurements 43, 1423 – 1428.

Cothern, C. R., Lappenbusch, W. L., & Michel, J. (1986). *Drinking-water contribution to natural background radiation*. Health Phys *50*(1), 33 – 47.

CRPC. (2000). *Canadian guidelines for the management of naturally occurring radioactive materials (NORM)*. 1st edition; Canadian NORM working group of federal provincial territorial Radiation Protection Committee (CPRC), published by authority of the Minister of Health

Dailly, P., Henderson, T., Hudgens, E., Kanschat, K., & Lowry, P. (2013). Exploration for Cretaceous stratigraphic traps in the Gulf of Guinea, West Africa and the discovery of the Jubilee Field: a play opening discovery in the Tano Basin, Offshore Ghana. *Geological Society, London, Special Publications*, *369*(1), 235 – 248.

Darko, E. O, Tetteh, G. K. & Akaho, E. H. K. (2005). *Occupational radiation exposure to norms in a gold mine*. Radiat Prot Dosimetry 114(4), 538 – 545.

Darko, E. O., Faanu, A., Razak, A., Emi-Reynolds, G., Yeboah, J., Oppon, O. C. & Akaho, E. H. K. (2010). *Public exposure hazards associated with natural radioactivity in open-pit mining in Ghana*. Rad. Prot. Dosim. 138, 45 – 51.

De Miguel, E., Iribarren, I., Chacon, E., Ordonez, A., & Charlesworth, S. (2007*). Risk-based evaluation of the exposure of children to trace elements in playgrounds in Madrid Spain*. Chemosphere 66, 505 – 513.

De, A. K. (2000). *Environmental Chemistry*. 4th Edn. New Age international publishers' P. Ltd., New Delhi.

Doyi, I., Oppon, O. C., Glover, E. T., Gbeddy, G., & Kokroko, W. (2013). *Assessment of occupational radiation exposure in underground artisanal gold mines*, Upper East Region of Ghana. Journal of Environmental Radioactivity 126, 77 – 82.

Duggal, V., Mehra, R., & Rani, A. (2013*). Determination of ^{222}Rn level in groundwater using a RAD7 detector in the Bathinda district of Punjab, India*. Radiat. Prot. Dosim. *156*, 239 – 245.

Egidi, P., & Hull, C. (1999). *NORM and TENORM: procedures, users and proposed regulations.* In: Health Physics Society, 32nd Midyear Topical Meeting, Albuquerque, New Mexico, USA, January 24-27, 25 – 30.

Ehsanpour E, Abdi M. R., Mojtaba M., & Hashem B. (2014). *^{226}Ra, ^{232}Th and ^{40}K contents in water samples in part of central deserts in Iran and their potential radiological risk to human population*. Journal of Environmental Health Science & Engineering 12, 80

Eisenbud, M. (1987). *Environmental radioactivity from natural, industrial and military sources*. Third edition. Academic Press, 84-104.

El Afifi, E. M., & Awwad, N. S. (2005). *Characterization of TENORM waste associated with oil and natural gas production in Abu Reis, Egypt*. Journal of Environmental Radioactivity 82, 7 – 19.

El Afifi, E. M., Awwad, N. S., & Hilal, M. A. (2009). *Sequential chemical treatment of radium species in TENORM waste sludge produced from oil and natural gas production*. Journal of Hazardous Materials 161, 907 – 912.

El Mamoney, M., & Khater, A. E. (2004). *Environmental characterization and radio-ecological impacts of non-nuclear industries on the Red Sea coast*. *J Environ Radioact* 73(2), 151–168.

EPA. (1999). Final draft for the drinking water criteria document on radium, US Environmental Protection Agency, Washington, Dc, 1999 Tr-1241-85

EPA. (2003). EPA assessment of risks from radon in homes. U.S. Environmental Protection Agency. EPA402R03003. http://www.epa.gov/radiation/docs/assessment/402-r-03-003.pdf.

EPA. (2004). *Understanding Variation in Partition Coefficient, Kd, Values*. Volume III: Review of Geochemistry and Available Kd Values for Americium, Arsenic, Curium, Iodine, Neptunium, Radium, and Technetium. Office of Air and Radiation. July 2004 (EPA 402-R-04-002C)

Escott, P. (1984). The Occurrence of Radioactive Contamination on Offshore Installations. NRPB report for the Department of Energy, London.

Espinasse, B., Picolet, G., & Chouraqi, E. (1997). *Negotiation support systems: a multi-criteria and multi-agent approach*. European Journal of Operational Research 103(2): 389 – 409.

European Commission (EC). 1999. *European Commission Report on Radiological Protection Principles Concerning the Natural Radioactivity of Building Materials* .Radiation Protection No. 112, Luxembourg.

Evens, A., Hryhorczuk, D., Lanphear, B., Rankin, K., Lewis, D., Forst, L., & Rosenberg, D. (2015). *The effect of childhood lead exposure on school performance in Chicago public schools: A population-based retrospective cohort study*. Environ Health 14: 21.

Faanu, A., (2011). *Assessment of Public Exposure to Naturally Occurring Radioactive Materials from Mining and Mineral Processing Activities of Tarkwa Goldmine in Ghana*. PhD thesis, Department of Chemistry, Kwame Nkrumah University of Science and Technology, Kumasi.

Facchinelli, A., Sacchi, E., & Mallen, L. (2001). *Multivariate statistical and GIS-based approach toidentify heavy metal sources in soils*, Environmental Pollution 114: 313–324.

Fadol, N., Salih, J., Idriss, H., Elfaki, A., & Sam, A. (2015). *Investigation of Natural Radioactivity levels in soil samples from North Korfodan State, Sudan*. Res J. of Physical Sci. 3(7), 1 – 7.

Fasasi, M. K., Oyawale A. A., Mokobia C. E., Tchokossa P, & Ajayi T. R. (2003). *Natural radioactivity of the tar-sand deposits of Ondo State, Southwestern Nigeria*. Nuclear Instruments and Methods in Physics Research Section A 505, 449 – 453.

Focazio, J. M., Szabo, Z., Kraemer, F. T., Mullin, H. A., Barringer, T. H., & DePaul T. V. (1998). *Occurrence of Selected Radionuclides in Ground Water Used for Drinking Water in the United States: A Targeted Reconnaissance Survey*. U.S. GEOLOGICAL SURVEY, Water-Resources Investigations Report 00-4273, http://pubs.usgs.gov/wri/wri004273/pdf/wri004273.pdf Retrieved 03/08/2016.

Frame, P. (2006). *Radium equivalent*. Health Physics Society: http//hps.org/.

Frissel M. J., & Koster J. (1988). *The IUR project on soil-to-plant transfer factor of radionuclides expected values and uncertainties*. In: Desmet, G. (Ed.), Realiability of radioactive transfer models. Elsevier Applied Science, London.

Gaisser, T. K., & Stanev, T. (2007). *Cosmic rays*. http://pdg.lbl.gov/. Retrieved 06/08/2014

Gascoyne, M. (1989). *High levels of uranium and radium in groundwater at Canada's Underground*. Appl. Geochem. 4, 557 – 591.

Gazineu, M. H. P., de Araujo, A. A., Brandao, Y. B., Hazin, C. A., & Godoy, J. M. (2005). *Radioactivity concentration in liquid and solid phases of scale and sludge generated in the petroleum industry*. J Environ Radioact 81, 47 – 54.

Gessel, T. F. (1975). *Occupational Radiation Exposures due to ^{222}Rn in natural gas and natural gas products*. Health Phys 29, 681 – 687.

Ghoose, S. & Heaton, B. (2005). *The release of radium from scales produced in the North Sea oilfields*. Radioactivity in the Environment 7, 1081 – 1089.

Gould, E. (2009). *Childhood lead poisoning: conservative estimates of the social and economic benefits of lead hazard control*. Environ. Health Perspect. 117(7), 1162 – 1167.

Gray, P. R. (1993). *Regulations for control of NORM*. SPE paper 26272, presented at the SPE/EPA Exploration and Production Environmental Conf., San Antonio, TX, http://www.ead.anl.gov/pub/doc/normbibi.pdf

Greenwood, N. N., & Earnshaw, A. (1984). *Chemistry of the elements*. Pergamon Press, London, p.1542.

Gregoric, A., Zmazek, B., & Vaupotic, J. (2008). *Radon concentration in thermal water as an indicator of seismic activity.* Coll Antropol. 32 (Suppl 2), 95 – 98.

Gržetić, I., & Ghariani, R. H. A. (2008). *Potential health risk assessment for soil heavy metal contamination in the central zone of Belgrade (Serbia).* J. Serb. Chem. Soc. 73(8–9), 923 – 934. JSCS–3773

GWRTAC. (1997). *Remediation of metals-contaminated soils and groundwater.* Tech. Rep. TE-97-01, GWRTAC, Pittsburgh, Pa, USA, GWRTAC-E Series.

Hamidatou, L., Slamene, H., Akhal, T. & Zouranen, B. (2013). *Concept, Instrumentation and Techniques of Neutron Activation Analysis.* Imaging and Radioanalytical Techniques in Interdisciplinary Research, INTECH chapter 6, 141 – 178.

Harb, S., El-Kamel, A. H., Zahran, A. M., Abbady, A., & Ahmed, F. A. (2014). *Assessment of Natural Radioactivity in Soil and Water Samples from Aden Governorate South Of Yemen Region.* International Journal of Recent Research in Physics and Chemical Sciences 1(1), 1 – 7.

Hegazy, A. K., & Emam, M. H. (2010). *Accumulation and soil-to-plant transfer of Radionuclides in the Nile Delta Coastal Black Sand Habitats. International Journal of Phytoremediation* 13(2), 140 – 155.

Hivert, G., Coquet, S., Glorennec, P., & Bard, D. (2002). *Is compliance to current lead regulations safe enough for infants and toddlers?* Rev Epidemiol Sante Publique 50, 297 – 305.

184

Hrichi, H., Baccouche, S., & Belgaied, J. (2013). *Evaluation of radiological impacts of tenorm in the Tunisian petroleum industry*. Journal of Environmental Radioactivity, 115, 107–113. http://www-pub.iaea.org/MTCD/publications/PDF/Pub1202_web.pdf. Accessed 22/09/2017

IAEA. (1996). *International Basic Safety Standards for Protection against Ionizing Radiation and for the Safety of Radiation Sources*. International Atomic Energy Agency, Vienna, pp. 353

IAEA. (2003). *Extent of Environmental Contamination by Naturally Occurring Radioactive Material (NORM) and Technological Options for Mitigation*. Technical Report Series no. 419, 12-21

IAEA. (2004). *Quatifying Uncertainty in Nuclear Analytical Measurements*. International Atomic Energy Agency, IAEA-TECDOC-1401.

IAEA. (2007). *IAEA safety glossary: terminology used in nuclear safety and radiation protection*. 2007 edition. Vienna: International Atomic Energy Agency.

IAEA-tecdoc-1616 (International Atomic Energy Agency). (2009). *Quantification of Radionuclide Transfer in Terrestrial and Freshwater Environments for Radiological Assessments*. IAEA, Vienna, Austria, 216 – 218.

IAEA-TECDOC-564. (1990). *Practical Aspect of Operating a Neutron Activation Analysis Laboratory*. IAEA-TECDOC-564, IAEA, Vienna.

ICRP. (1991). *1990 Recommendations of the International Commission on Radiological Protection*. ICRP Publication 60, International Commission on Radiological Protection (ICRP). http://www.icrp.org/publication.asp?id=ICRP+Publication+60.

ICRP. (1993*). Protection against Radon-222 at Home and at Work*. ICRP Publication 65. Ann. ICRP 23 (2), Pergamon Press, Oxford.

ICRP. (2007). *2006 Recommendations of the International Commission on Radiological Protection*. Annals of the ICRP PUBLICATION 103 Pergamon Press, Oxford.

Isam, S. M. M., Pettersson, H. B. L., & Lund, E. (2002). *Uranium and thorium series radionuclides in drinking water from drilled bedrock wells: Correlation to geology and bedrock radioactivity and dose estimation*. Radiation Protection Dosimetry 102, 249 – 258.

Jaishankar, M., Tseten, T., Anbalagan, N., Mathew, B. B., & Beeregowda, K. N. (2014). *Toxicity, mechanism and health effects of some heavy metals*. Interdiscip Toxicol. 7(2), 60 – 72.

Jazzar, M. M., & Thabayneh, K. M. (2014). Transfer of natural radionuclides from soil to plants and grass in the western north of West Bank environment- Palestine. *International Journal of Environmental Monitoring and Analysis* 2(5): 252 – 258.

Johnson, S. S. (1991). *Annual report*. Virginia minerals 37 (2): 9 – 16.

Kaiser, H. F., & Hunka, S. (1973). *Some empirical results with Guttman's stronger lower bound for the number of common factors. Educational and Psychological Measurement* 33(1), 99 – 102.

Karpinska M., Kapala J., Mnich Z., & Szpak A. (2010). *Radon in drinking water in the Bialystok region of Poland*. NUKLEONIKA 55(2), 177 – 180.

Karsten, L. (2007). *Chemical types of bounding of natural radionuclides in TENORM*. Doctoral thesis, Department of Biology and Geography, University of Duisburg-Essen

Kastning, T. (2011). *Basic Overview of Ghana's Emerging Oil Industry*. Friedrich Ebert Stiftung, Ghana. www.fesghana.org/Basic Overview_ Oil Economy-Ghana. Retrieved 30/10/2014.

Khalil, WA-S, Goonetilleke, A, Kokot, S & Carrol, S. (2004). *Use of chemometrics methods and multicriterion decision –making for site selection for sustainable on-site sewage effluent disposal*. Analytica Chimica Acta 506(1), 41 – 56.

Khan, S., Rehman, S., Khan, A. Z., Khan, M. A., & Shah, M. T. (2010). *Soil and vegetables enrichment with heavy metals from geological sources in Gilgit, Northern Pakistan*. Ecotoxicology and Environmental Safety 73, 1820 – 1827.

Kirpichtchikova, T. A., Manceau, L., Spadini, L., Panfili, F., Marcus, M. A., & Jacquet, T. (2006). *Speciation and solubility of heavy metals in contaminated soil using X-ray microfluorescence, EXAFS spectroscopy, chemical extraction, and thermodynamic modeling*. Geochimica et Cosmochimica Acta 70(9), 2163 – 2190.

Knutsson, G., & Olofsson, B. (2002). *Radon content in groundwater from drilled wells in Stockholm region of Sweden*. Norges geologiske undersokelse Bulletin 439, 79 – 85.

Kpeglo, O. D. (2015). *Radiation Exposure to Natural Radioactivity in Crude Oil and Petroleum Waste from Oil Fields in Ghana: Modelling, Risk Assessment and regulatory Control*. Doctoral thesis, Department of Nuclear Safety and Security, School of Nuclear and Allied Sciences, University of Ghana, Legon-Accra

Laluraj, C. M, & Gopinath, G. (2006). *Assessment on seasonal variation of groundwater quality of phreatic aquifers - a river basin system*. Environ Monit Assess 117, 45 – 57.

Landsberger, S. (1994). *Delayed Instrumental Neutron Activation Analysis.* In: Chemical Analysis by Nuclear Methods, Chapter 6, (Alfassi, Z. B., ed.), John Wiley & Sons, 121 – 139.

Langmuir, D. (1997). *Aqueous Environmental Chemistry*. Prentice-Hall. Inc., New Jersey, 600.

Lee, S. K., Wagiran, H., Ramli, A.T., Apriantoro, N. H., & Wood, A. K. (2009). *Radiological monitoring: terrestrial natural radionuclides in Kinta district, Perak, Malaysia*. Journal of Environmental Radioactivity 100, 368 – 374.

Lin W., Xiao T., Wu Y., Ao Z., & Ning Z. (2012*). Hyperaccumulation of zinc by Corydalis davidii in Zn polluted soils*. Chemosphere 86(8), 837 – 842.

Ling, W., Shen, Q., Gao, Y., Gu, X., & Yang, Z. (2007). *Use of bentonite to control the release of copper from contaminated soils*. Australian Journal of Soil Research 45(8), 618 – 623.

Lokeshwari, H., & Chandrappa, G. T. (2006). *Heavy metals content in water, water hyacinth and sediments of Lalbagh tank, Bangalore (India)*. J. Environ. Sci. Eng. 48(3), 183 – 188.

Mahmood, Z. U. W., & Mohamed, C. A. R. (2010). Thorium in radionuclides in the environment, D. A. Atwood (Ed.), Wiley and sons, chapter 24, 247 – 253.

Martinez-Aguirre, A., Garcia-Leo´n, M., & Ivanovich, M. (1995). *U and Th speciation in river sediments*. Sci. Total Environ 173, 203 – 209.

Mazzilli, B. P., & Saueia, C. H. R. (2011). *Radiological impact of the application of phosphogypsum in agriculture*. INIS Repository. Retrieved from http://www.iaea.org/inis/collection/NCLCollection Store/Public/42/093/42093176.pdf. March 2, 2016.

McArthur, A., Major, M., and Lowe, D. J. (1995). "NORM Disposal in Class II Wells." SPE paper 29713, presented at the Society of Petroleum Engineers/Environmental Protection Agency Exploration and Production Environmental Conference, Houston, TX, March 27-29

McLaine, P., Navas-Acien, A., Lee, R., Simon, P., Diener-West, M., & Agnew, J. (2013). *Elevated blood lead levels and reading readiness at the start of kindergarten*. Pediatrics 131, 1081 – 1089.

McLaughlin, M. J., Hamon, R. E., McLaren, R. G., Speir, T. W., & Rogers, S. L. (2000b). *Review: a bioavailability-based rationale for controlling metal and metalloid contamination of agricultural land in Australia and New Zealand*. Australian Journal of Soil Research 38(6), 1037 – 1086.

McLaughlin, M. J., Zarcinas, B. A., Stevens, D. P, & Cook, N. (2000a). *Soil testing for heavy metals*. Communications in Soil Science and Plant Analysis 31(11–14), 1661 – 1700.

Mehra, R., Badhan, K., Sonkawade, R. G, Kansal, S., & Singh, S. (2010). *Analysis of terrestrial natural radionuclides in soil samples and assessment of average effective dose*. Indian Journal of Pure and Applied Physics 48, 805 – 808.

Mehrdadi, N., Nabi, B. G. R., Nasrabadi, T., Hoveidi, H., Amjadi, M., & Shojaee, M. A. (2009*). Monitoring the arsenic concentration in groundwater resources, case study: Ghezel ozan water basin, Kurdistan, Iran*. Asian J. Chem. 21(1), 446 – 450.

Merdanoglu, B. & Altinsoy, N. (2006). *Radioactivity concentrations and dose assessment for soil samples from Kestanbol granite area, Turkey*. Radiation Protection Dosimetry 121, 59 – 62.

Micó, C., Recatalá, L., Peris, M, & Sánchez, J. (2006). *Assessing heavy metal sources in agricultural soils of a European Mediterranean area by multivariate analysis*. Chemosphere 65, 863 – 872.

Miller, J. N. & Miller, J. C. (2010). *Statistics and chemometrics for analytical chemistry*. Sixth edition. *Pearson Education Limited*, England.

Miranda, M. L, Kim, D., Reiter J., Overstreet Galeano, M. A., & Maxson P. (2009). *Environmental contributors to the achievement gap*. Neurotoxicology 30(6), 1019 – 1024.

Mitchel, N., Perez-Sanchez, D., & Thorne, M. C. (2013). *A review of the behavior of U-238 series radionuclides in soils and plants*. J. Radio. Prot. 33, R17 - R48.

Momodu M. A., & Anyakora C. A. (2010). *Heavy metal contamination of groundwater: the Surulere case study*. Res J Environ Earth Sci 2, 39 – 43.

Nassef, M., Hannigan, R., EL Sayed, K. A., & Tahawy, M.S.E. (2006). *Determination of some heavy metals in the environment of Sadat industrial city*. Proceeding of the 2nd Environmental Physics Conference, Cairo University, Egypt, 145 – 152.

NCHH. (2015). *Issue Brief: childhood lead and educational outcomes*. National Center for Healthy Housing. www.nchh.org/Portals/0/Contents/ Childhood_Lead_Exposure.pdf Accessed: 14/02/2017

NCRP. (1984). *National Council on Radiation Protection and Measurements*. Exposures from the Uranium Series with Emphasis on Radon and Its Daughters, NCRP Report No. 77 (National Council on Radiation Protection and Measurements, Bethesda, Maryland)

Nguelem, E. J. M., Darko, E. O., Ndontchueng, M. M., Schandorf, M. M., Akiti, T. T., Muhulo, A. P., & Dogbey, R. O. G. (2013). *Assessment of Natural Radioactivity level in Groundwater from selected areas in Accra Metropolis*. Research Journal of Environmental and Earth Sciences 5(2), 85 – 93.

NRC. (1999). *Evaluation of guidelines for exposure to Technologically Enhanced Naturally Occurring Radioactive Materials*. National Research Council, Washington DC.

Nwankwo, L. I. (2012). *Study of Natural Radioactivity of Groundwater in Sango-Ilorin, Nigeria*. Journal of Physical Science and Applications 2(8), 289 – 295.

Nwankwo, L. I. (2013*). Determination of Nutural Radioactivity in Groundwater in Tanke-Ilorin, Nigeria*. West Africa Journal of Applied Ecology 21(1), 111 – 119.

Nwankwo, L. I., & Akoshile, C. O. (2005a). *Background radiation study of Offa industrial area of Kwara State, Nigeria*. J. Appl. Sci. Environ. Manage. 9(3), 95 – 98.

Nwankwo, L. I., Akoshile, C. O. (2005b). *Monitoring of external background radiation level in Asa Dam Industrial area of Ilorin, Kwara State, Nigeria*. J. Appl. Sci. Environ. Manage. 9(3), 91 – 94.

O'brien, R. S. & Copper, M. B. (1998). *Technologically Enhanced Naturally Occurring Radioactive Material (NORM): Pathway Analysis and Radiological Impact.* Appl. Radiat. Isot. 49, 227 – 239.

Offshore-Technology.com (2011). Jubilee Field, Ghana. http://www.offshoretechnology.com/projects/jubilee field. Accessed 30/10/2014.

OGP. (2008). *Guidelines for the management of Naturally Occuring radioactive Materials in the oil and gas industry*. International Association of Oil & Gas Producers, Report No. 412

Ogunbanjo, O., Onawumi, O., Gbadamosi, M., Adejoke, O., & Anselm, O. (2016). *Chemical speciation of some heavy metals and human health risk assessment in soil around two municipal dumpsites in Sagamu, Ogun State, Nigeria*. Chem Spec Bioavailab 28(S. 1–4), 142 – 151.

O'Neil, M. J., Heckelman, P. E., & Koch C. B. (2006). *The Merck index*. 14th ed. Whitehouse Station, NJ: Merck & Co., Inc., 1393-1394

Ononugbo, C. P., Avwiri, G. O., & Egieya, J. M. (2013*). Evaluation of Natural Radionuclide Content in surface and groundwater and Excess Lifetime Cancer Risk due to Gamma Radioactivity*. Academic Research International 4(6), 636 – 647.

Osae, E.K. (1988). *Principles of Neutron Activation Analysis*. Technical Report, GAEC, 1988.

Osei, B. (2002). *Neutron Activation Analysis of Soils*. M.Phil thesis, Department of Physics, University of Ghana, Legon-Accra. Available at http://ugspace.ug.edu.gh. Accessed 30-01-2018

Penfold, T. S. S., Degrange, J. P., Mobbs, S. F. & Schneider, T. (1999). *Establisment of reference levels for regulatory control of workplaces where materials are processed which contain enhanced levels of naturally occurring radionuclides*. Radiation Protection 107, European Commission, Luxemboug.

Peroni, M., Mulas V., Betti E., Patata L., & Ambrosini P. (2012). *Decommissioning and Remediation of NORM/TENORM Contaminated Sites in Oil and Gas*. *Chemical* Engineering Transaction 28, 181 – 186.

Petroleum Commission of Ghana. (2014). The Tano-Cape Three Points Basin/Western Basin. www.petrocom.gov.gh/index.php/resource-brief

Priest, N. D., (2001). *Toxicity of depleted uranium*. Lancet 357, 244 – 245.

Raabe, O. G. (1996). *Studies of the solubility of naturally occurring radionuclides in petroleum scale*. NORM/NARM: Regulation and Risk Assessment (Proc. 29th Midyear Top Mtg Scottsdale), Health Physics Society, Scottsdale, AZ, 121-128, http://www.ead.anl.gov/pub/doc/ normbibl.pdf

Rajappa, B., Manjappa, S., & Puttaiah, E.T. (2010). *Monitoring of heavy metal concentration in groundwater of Hakinaka Taluk, India*. Contemporary Engineering Science*s* 3(4), 183 – 190.

Rajaretnam, G., & Spitz, H. B. (2000). *Effect of leachability on environmental risk assessment for naturally occurring radioactive materials in petroleum oil fields*. Health Physics 78 (2), 191 – 198.

Rania, M. S. (2014*). Environmental Radiological Study in um Bogma Formation of AL-Ramsy Mines, East Abu-Zeneima area – Southwestern Sinai, Egypt*. MSc Thesis, Department of Physics, Ain Shams University, Egypt

Rector, D., Allard, D., Jones, D., Hyland, J., Lopez, B., Mitchell, J., Nickel, B., Opila, J., Sandhu, M., & Whitfall, D. (2011). *Incidental TENORM: A Guidance for State Solid Waste Managers*. Association of State and Territorial Solid Waste Management Officials, 444 North Capital Street N. W., Suite 315, Washington D.C. 20001.

Ren, H. M., Wang, J. D. & Zhang, X. L. (2005). *Assessment of soil lead exposure in children in Shenyang, China*. Environmental Pollution. 144, 327 – 335.

Reuben, A., Caspi, A., Belsky, D. W., Broadbent, J., Harrington, H., Sugden, K., Houts, R. M., Ramrakha, S., Poulton, R., & Moffitt, T. E. (2017). *Association of childhood blood lead levels with cognitive function and socioeconomic status at age 38 years and with IQ change and socioeconomic mobility between childhood and adulthood* JAMA 317(12), 1244 – 1251.

Rich, A. L & Crosby, E. C. (2013). *Analysis of reserve pit sludge from unconventional natural gas hydraulic fracturing and drilling operations for the presence of Technologically Enhanced Naturally Occurring Radioactive Material (TENORM)*. New Solutions 23(1), 117 – 153.

Ripa, N.A. (2010). *Analysis of Newton's Forward Interpolation Formula*. International Journal of Computer Science & Emerging Technologies 1, 12 – 16.

Rood, A. S. (1998). In: 29th Midyear Topical Meeting of the Health Physics Society, Scottsdale, Arizona, USA, January 7-10, p 10.

Sam, A. K, Ahamed, M. M, El Khangi, F., El Nigumi, Y., & Holm, E. (1998). *Radioactivity levels in the Red Sea coastal environment of Sudan*. Mar Pollut Bull 36(1), 19 – 26.

Santos, E. E., Lauria, D. C., Amaral, E. C. S., & Rochedo, E. R. (2002). *Daily ingestion of Th-232, U-238, Ra-226, Ra-228 and Pb-210 in vegetables by inhabitants of Rio de Janeiro city*. J. Environ. Radioact. 62, 75 – 86.

Scaife, W.W., Mueller, S. G & Young, D. R. (1994). *Downhole Disposal of NORM Wastes in an Offshore Setting: Lessons Learned*. In Proceedings of the International Petroleum Environmental Conference, Houston, TX, March 2-4.

Semlali, R., Dessogne, J. B., Monna F, Bolte, J., Azimi, S, Navarro, N., Denaix, L., Loubet, M., Chateau, C., & van Oort, F. (2004). *Modeling lead input and output in soils using lead isotopic geochemistry*. Environmental Science & Technology 38, 1513 – 1521.

Serfor-Armah, Y., Nyarko, B. J. B., Carboo, D., Osae, E. K., Anim-Sampong, S., & Akaho, E. H. K. (2000). *Instrumetal neutron activation analysis of iodine levels in fourteen seaweed species from the coastal belt of Ghana*. Journal of Radioanalytical and Nuclear Chemistry 245(2), 443 – 446.

Shapiro, J. (1990). *Ionizing radiation and public health*. In: Shapiro J, ed. Protection: A guide for scientists and physicians, 3rd edition. Cambridge MA: Harvard University Press, 334 – 429.

Shawky, S., Amer, H., Nada, A. A., El-Maksoud, T. M. A., & Ibrahiem, N. M. (2001). *Characteristics of NORM in the oil industry from Eastern and Western deserts of Egypt*. Applied Radiation and Isotopes 55, 135 – 139.

Shiva, P. N. G., Nagaiah, N., Ashok, G. V., & Karunakara, N. (2008). *Concentration of ^{226}Ra, ^{232}Th, and ^{40}K in the soils of Bangalore region, India*. Health Phys. 94 (3), 264 – 271.

Siegel, F. R. (2002). *Environmental geochemistry of potentially toxic metals*. Springer-Verlag Berlin Heidelberg, eBook: 978-3-662-04739-2., Germany

Singh, S., Kumar, A., Singh, B., Mahajan, S., Kumar, V., & Dhar, D. (2010). *Radon monitoring in soil gas and ground water for earthquake prediction studies in North West Himalayas, India*. Terr Atmos Ocean Sci. 21, 685 – 695.

Singh, S., Rani, A., & Mahajan, R. K. (2005). *^{226}Ra, ^{232}Th and ^{40}K analysis in soil samples from some areas of Punjab and Himachal Pradesh, India using gamma ray spectrometry*. Radiation Measurements 39, 431 – 439.

Sipple-Srinivasan, M., Bruno, M. S., Bilak, R. A., & Danyluk, P. G. (1997). *Field Experiences with Oilfield Waste Disposal through slurry Fracture Injection*. SPE paper 38254 presented at 67th Annual Western Regional Meeting of the Society of Petroleum Engineers, Long Beach, CA, June 23-27

Somlai, J., Jobbagy, V., Somlai, K., Kovacs, J., Nemeth, C., & Kovacs, T. (2008). *Connection between radon emanation and some structural properties of coal-slag as building material*. Radiation Measurements 43, 72 – 76.

Spaite, P. W., & Smithson, G. R. (1992). *Technical and Regulatory Issues Associated with Naturally Occurring Radioactive Materials (NORM) in the Gas and Oil Industry*. Rep. GRI – 92/0178, Gas Research Institute, Chicago, IL.

Steck, D. J., Field, R. W., & Lynch, C. F. (1999). *Exposure to atmospheric radon*. Environ Health Perspect 107(2), 123 – 127.

Taapopi, E. E. (2015). *Assessment of naturally occurring radionuclide materials and trace elements in playgrounds of selected Basic Schools in the Ga East Municipal District, Accra, Ghana*. M.Phil thesis. Department of Nuclear Sciences and Applications, University of Ghana, Legon-Accra.

Taskin, H., Karavus, M., Topuzoglu, A., Hindiroglu, S., & Karahan, G. (2009). *Radionuclide concentrations in soil and Lifetime cancer risk due to the gamma radioactivity in Kirklareli, Turkey*. J. Environmental Radioactivity 100, 49 – 53.

Tchokossa, P., Olomo, J. B., Balogun, F. A., & Adesanmi, C. A. (2013). *Assessment of Radioactivity Contents of Food in the Oil and Gas Producing Areas in Delta State, Nigeria*. International Journal of Science and Technology 3(4), 245 – 250.

Tchounwou, P. B., Yedjou, C. G., Patlolla, A. K., & Sutton, D. J. (2012). *Heavy Metals Toxicity and the Environment. Molecular, Clinical and Environmental Toxicology* 101 of the series Experientia Supplementum, 133 – 164.

Testa, C., Desideri, D., Guerra, F., Meli, M. A., & Roselli, C. (1998). Proc. Of the Int. Solv. Extraction Symp. Moscow, Russia, June 21-27, 416.

Testa, C., Desideri, D., Meli, M. A., Roselli, C., Bassignani, A., Colombo, G., & Fantoni, R. F. (1994). *Radiation protection and radioactive scales in oil and gas production*. Health Phys 71, 34 – 38.

Thabayneh, K. M., & Jazzar, M. M. (2012). *Natural Radioactivity Levels and Estimation of Radiation Exposure in Environmental Soil Samples from Tulkarem Province-Palestine*. Open Journal of Soil Science 2, 7 – 16.

Tome, F. V., Rodriguez, M. P. B., & Lozano J. C. (2003*). Soil-to-plant transfer for natural radionuclides and stable elements in a Mediterranean area*. Journal of Environmental Radioactivity 65(2), 161 – 175.

Tufail, M., Ahmad, N., Khan, M. A., Zafar, M. S., & Khan, H. A. (1992). *Effective dose equivalent rate for the respiratory tract from daughter products of radon*. J. Islamic Acad. Sci. 5(2), 136 – 141.

Tufail, M., Iqbal, M. & Mirza, S. (2000). *Radiation doses due to the natural radioactivity in Pakistan Marble*. Radioprotection 35, 299 – 310.

Tullow Ghana Limited. (2009). *Jubilee Field*. Draft Environmental Impact Assessment, Environmental Resources Management, chapter 4_6, pp 4-4 – 4-6.

United States Environmental Protection Agency (2006). *Radon*. Environmental Protection Agency (Washington DC) [*http://www.epa.gov/radon/ aboutus.html*] Accessed March 1, 2016,

United States Environmental Protection Agency (2012). Edition of the Drinking water Standards and Health Advisories, Environmental Protection Agency (Washington DC).

United States Environmental Protection Agency, 2013. Basic radon facts, U. E. P. A Publication 402-F-12-005. Retrieved 16th July, 2015.

UNSCEAR (1996). Source and Effects of Ionizing Radiation, 1996 Report to the General Assembly with scientific annex, United Nations, New York

UNSCEAR (2012). *Biological Mechanisms of Radiation Actions at low doses*. Report to the general assembly with scientific annexes. United Nations, New York, United States.

UNSCEAR (United Nation Scientific Committee on the Effects of Atomic Radiation) (1993). *Sources and Effects of Ionizing radiation*. Report to the general assembly with scientific annexes. United Nations; New York

UNSCEAR (United Nation Scientific Committee on the Effects of Atomic Radiation). (2000). *Sources and effect of Ionizing radiation*. Report to the general assembly with scientific annexes. United Nations; New York.

US EPA (US Environmental Protection Agency). (2005). Integrated Risk Information System (IRIS). http://www.epa.gov/iris/subst/0278.htm#carc. Accessed 24/04/2015.

US EPA, (1993). United States Environmental Protection Agency, Office of Radiation and Indoor Air, Diffuse NORM Wastes – Waste Characterization and Preliminary Risk Assessment

USNRC (2014). *Biological Effects of Radiation*. Reactor Concepts Manual, 9-20, 0603

USNRC Technical Training Center (2014). *Natural and Man-made Radiation Sources.* Reactor Concepts Manual, 6-5, 0703.

Vandenhove, H., Olyslaegers, G., Sanzharova, N., Shubina, O., Reed, E., Shang, Z., & Velasco, H. (2009). *Proposal for new best estimates of the soil to plant transfer factor of U, Th, Ra, Pb and Po*. J. Environ. Radioact. 100, 721 – 732.

Vázquez-López, C., Zendejas-Leal, B. E., Golzarri, J. I., & Espinosa, G. (2011). *A survey of ^{222}Rn in drinking water in Mexico City*. Radiat. Prot. Dosim. *145*, 320 – 324.

Veil, A. J, Smith, K. P., Tamasko, D., Elcock, D., Blunt, D. L. & Gustavious, P. W. (1998). *Disposal of NORM Contaminated Oil Field Wastes in Salt Caverns*. US department of energy, Office of Fossil Energy, Natural Petroleum Technology Office under contract W – 31 – 109 – Eng -38.

Velasco, H., Juri Ayub, J., & Sansone, U. (2009). *Influence of crop types and soil properties on radionuclide soil-to-plant transfer factors in tropical and subtropical environments*. Journal of Environmental Radioactivity 100 (9), 733 – 738.

Wassila, B., & Ahmed, B. (2011). The radioactivity measurements in soils and fertilizers using gamma spectrometry technique. Journal of Environmental Radioactivity 102, 336 – 339.

Water Quality Association. (2005). *Radium*. Technical Application Bulletin, Water Quality Association, National Headquarters & Laboratory, USA.

White G. J. (1992). *Naturally Occurring Radioactive Materials (NORM) in Oil and Gas Industry Equipment and Wastes – A Literature Review*. Rep. DOE/ID/01570-T158, prepared by Idaho National Engineering Laboratory for US Department of Energy, Bartleville, OK

WHO (2008). *Guidelines for drinking water quality*. Third Edition Incorporating The First And Second Addenda Volume 1 Recommendations. World Health Organization, Geneva. Retrieved from http://www.bibme.org/citation-guide/apa/book/ Accessed 20/03/ 2016.

WHO (World Health Organization) & FAO (Food and Agricultural Organization). (2011). Nuclear accidents and radioactive contamination of foods. Available at: www.who.int/foodsafety/fsmanagement/ radionuclidesand_food_300311.pdf?ua Accessed 1/06/2017.

Wu, Y-Y., Ma, Y-Z., Cui, H-X., Liu, J-X, Shang, B., & Su, X. (2014*). Radon Concentrations in Drinking Water in Beijing City, China and Contribution to Radiation Dose*. Int. J. Environ. Res. Public Health 11, 11121 – 11131.

Wuana, R. A. & Okieimen F. E. (2011). *Heavy metals in contaminated soils: a review of sources, chemistry, risks and best available strategies for remediation*. International Research Notices www.saber.ula.ve/imagen ologia/chapter2%20biological%20effects.pdf

Yasir, M., Ab Majid, A. & Yahaya, R. (2007). *Study of natural radionuclides and its radiation hazard index in Malaysia building materials*. Radioanalytical and Nuclear Chemistry 273, 539 – 541.

Yousef, M. I., Abu, El-Ela, A., & Yousef, H. A. (2007). *Natural Radioactivity Levels in Surface Soil of Kitchener drain in the Nile Delta of Egypt*. Journal of Nuclear and Radiation Physics 2(1), 61 – 68.

Yuce, G., Didem, U., Alimeju, T. D., Turgay, E., Muset, S., Mert D., & Sakir, O. F. A. (2009). *The effects of lithology on water pollution: Natural radioactivity and trace elements in water resources of Eskisehir region (Turkey)*. Water Air Soil Pollut. 202, 69 – 89.

Zaidan, J. A. R. (2010). *Natural Occurring Radioactive Materials (NORM) in the oil and gas industry*. Journal of Petroleum Researches and Studies 1(1), 4 – 21.

Zavodska, L., Kosorinova, E., Scerbakova, L., & Juraj, L. (2008). *Environmental Chemistry of uranium*. HU ISSN 1418-7108: HEJ Manuscript number: ENV-081221-A.

Zhang, N., Baker, H. W., Tufts, M., Raymond, R. E., Salihu, H., & Elliott, M. R. (2013). *Early childhood lead exposure and academic achievement: evidence from Detroit public schools, 2008–2010*. Am J Public Health 113, 72 – 77.

Zovko, M., & Romić, M. (2011). *Soil Contamination by Trace Metals: geocgemical Behaviour as an Element of Risk management*. In: Environmental Sciences, Earth and Environmental Sciences. Ed. Imran A. Dar and Mithas A. Dar. Available at: https://www.intechopen.com/books/earth-and-environmental-sciences/soil-contamination-by-trace-metals-geochemical-behaviour-as-an-element-of-risk-assessment. Accessed 07/02/1018.

APPENDICES

APPENDIX A – TABLES
Appendix A1
Gamma dose rates at 1m above ground level for soil sample locations.

Community	Axim 1	ABH	ABL	Axim Castle	Krisan	Krisan 2	Krisan 3	Nyale Kplole 1	Nyale Kplole 2	Nyale Kplole 3	Anokye 1	Anokye 2	Atuabo
Gamma	0.09	0.09	0.07	0.1	0.1	0.11	0.1	0.08	0.1	0.09	0.09	0.11	0.08
dose rates	0.1	0.09	0.09	0.08	0.09	0.1	0.11	0.09	0.11	0.07	0.07	0.11	0.07
(μSv/h)	0.12	0.09	0.09	0.09	0.11	0.11	0.1	0.08	0.1	0.06	0.07	0.11	0.08
	0.11	0.09	0.08	0.09	0.12	0.12	0.11	0.09	0.11	0.07	0.08	0.1	0.07
	0.1	0.09	0.09	0.09	0.12	0.12	0.1	0.09	0.1	0.06	0.09	0.1	0.08
	0.11	0.08	0.09	0.09	0.12	0.12	0.1	0.09	0.1	0.06	0.09	0.11	0.07
	0.13	0.09	0.07	0.1	0.12	0.11	0.1	0.08	0.1	0.06	0.09	0.1	0.07
	0.12	0.08	0.07	0.09	0.11	0.12	0.09	0.09	0.1	0.07	0.08	0.11	0.07
	0.12	0.09	0.08	0.1	0.12	0.1	0.08	0.09	0.1	0.07	0.07	0.12	0.08
	0.11	0.1	0.07	0.1	0.11	0.11	0.08	0.09	0.1	0.07	0.08	0.12	0.08
Average	0.111	0.089	0.08	0.093	0.112	0.112	0.097	0.087	0.102	0.068	0.081	0.109	0.075
Min.	0.09	0.08	0.07	0.08	0.09	0.1	0.08	0.08	0.1	0.06	0.07	0.1	0.07
Max	0.13	0.1	0.09	0.1	0.12	0.12	0.11	0.09	0.11	0.09	0.09	0.12	0.08

Appendix A2
Gamma dose rates at 1m above ground level for soil sample locations.

Community	Ekebaku	Beyin 1	Beyin 2	Ellonyi	Kengen 1	Kengen 2	Twenen	Half-Assini 1	Half-Assini 2	Half-Assini 3	Half-Assini 4	Newtown
Gamma	0.09	0.09	0.08	0.09	0.09	0.1	0.09	0.11	0.09	0.09	0.09	0.08
dose rates	0.1	0.1	0.08	0.1	0.1	0.1	0.08	0.12	0.09	0.1	0.1	0.1
(μSv/h)	0.1	0.09	0.1	0.09	0.09	0.11	0.09	0.11	0.08	0.1	0.09	0.1
	0.09	0.09	0.09	0.09	0.1	0.1	0.1	0.11	0.09	0.1	0.09	0.11
	0.09	0.1	0.1	0.09	0.1	0.12	0.1	0.11	0.08	0.09	0.1	0.09
	0.08	0.09	0.1	0.08	0.1	0.11	0.09	0.11	0.09	0.1	0.11	0.09
	0.08	0.09	0.11	0.08	0.11	0.1	0.09	0.1	0.1	0.09	0.1	0.1
	0.08	0.09	0.12	0.07	0.1	0.12	0.09	0.1	0.09	0.1	0.11	0.1
	0.07	0.09	0.12	0.07	0.1	0.1	0.09	0.1	0.09	0.1	0.1	0.11
	0.08	0.08	0.13	0.08	0.09	0.12	0.09	0.1	0.09	0.1	0.1	0.12
Average	0.086	0.091	0.103	0.084	0.098	0.108	0.091	0.107	0.089	0.097	0.099	0.1
Min.	0.07	0.08	0.08	0.07	0.09	0.1	0.08	0.1	0.08	0.09	0.09	0.08
Max.	0.1	0.1	0.13	0.1	0.11	0.12	0.1	0.12	0.1	0.1	0.11	0.12

Appendix A3
Gamma dose rates at 1m above ground level for water sample locations.

Community	Axim 1	ABH	ALIS	Krisan	Nyale Kplole	Nyale Kplole 2	Atuabo	Ekebaku	Beyin	Beyin 2	Kengen
	0.1	0.09	0.07	0.08	0.1	0.09	0.05	0.06	0.12	0.09	0.1
	0.09	0.1	0.08	0.08	0.11	0.09	0.05	0.05	0.13	0.12	0.11
	0.09	0.1	0.08	0.09	0.1	0.1	0.05	0.06	0.12	0.12	0.11
	0.1	0.1	0.08	0.1	0.11	0.09	0.08	0.06	0.12	0.1	0.1
	0.1	0.1	0.09	0.1	0.1	0.09	0.08	0.05	0.11	0.1	0.1
	0.1	0.09	0.08	0.11	0.1	0.1	0.08	0.04	0.12	0.13	0.1
	0.1	0.1	0.07	0.1	0.1	0.09	0.07	0.05	0.12	0.1	0.11
	0.1	0.09	0.08	0.11	0.1	0.11	0.08	0.05	0.12	0.11	0.12
	0.11	0.09	0.08	0.1	0.09	0.08	0.05	0.06	0.11	0.1	0.1
	0.12	0.1	0.07	0.1	0.09	0.09	0.05	0.06	0.1	0.1	0.1
Average	**0.101**	**0.096**	**0.078**	**0.097**	**0.1**	**0.093**	**0.064**	**0.054**	**0.117**	**0.107**	**0.105**
Min.	**0.09**	**0.09**	**0.07**	**0.08**	**0.09**	**0.08**	**0.05**	**0.04**	**0.1**	**0.09**	**0.1**
Max.	**0.12**	**0.1**	**0.09**	**0.11**	**0.11**	**0.11**	**0.08**	**0.06**	**0.13**	**0.13**	**0.12**

Appendix A4
Gamma dose rates at 1m above ground level for water sample locations.

Community	Kengen 2	Twenen	Half-Assini 1	Half-Assini 2	Half-Assini 3
Gamma dose	0.11	0.11	0.11	0.08	0.1
rates (μSv/h)	0.1	0.12	0.1	0.09	0.11
	0.11	0.11	0.11	0.09	0.09
	0.11	0.1	0.09	0.08	0.09
	0.12	0.11	0.1	0.08	0.09
	0.11	0.1	0.1	0.09	0.08
	0.12	0.09	0.09	0.09	0.09
	0.1	0.1	0.09	0.07	0.09
	0.1	0.1	0.09	0.07	0.09
	0.11	0.1	0.1	0.07	0.09
Average	**0.109**	**0.104**	**0.098**	**0.081**	**0.092**
Min.	**0.1**	**0.09**	**0.09**	**0.07**	**0.08**
Max.	**0.12**	**0.12**	**0.11**	**0.09**	**0.11**
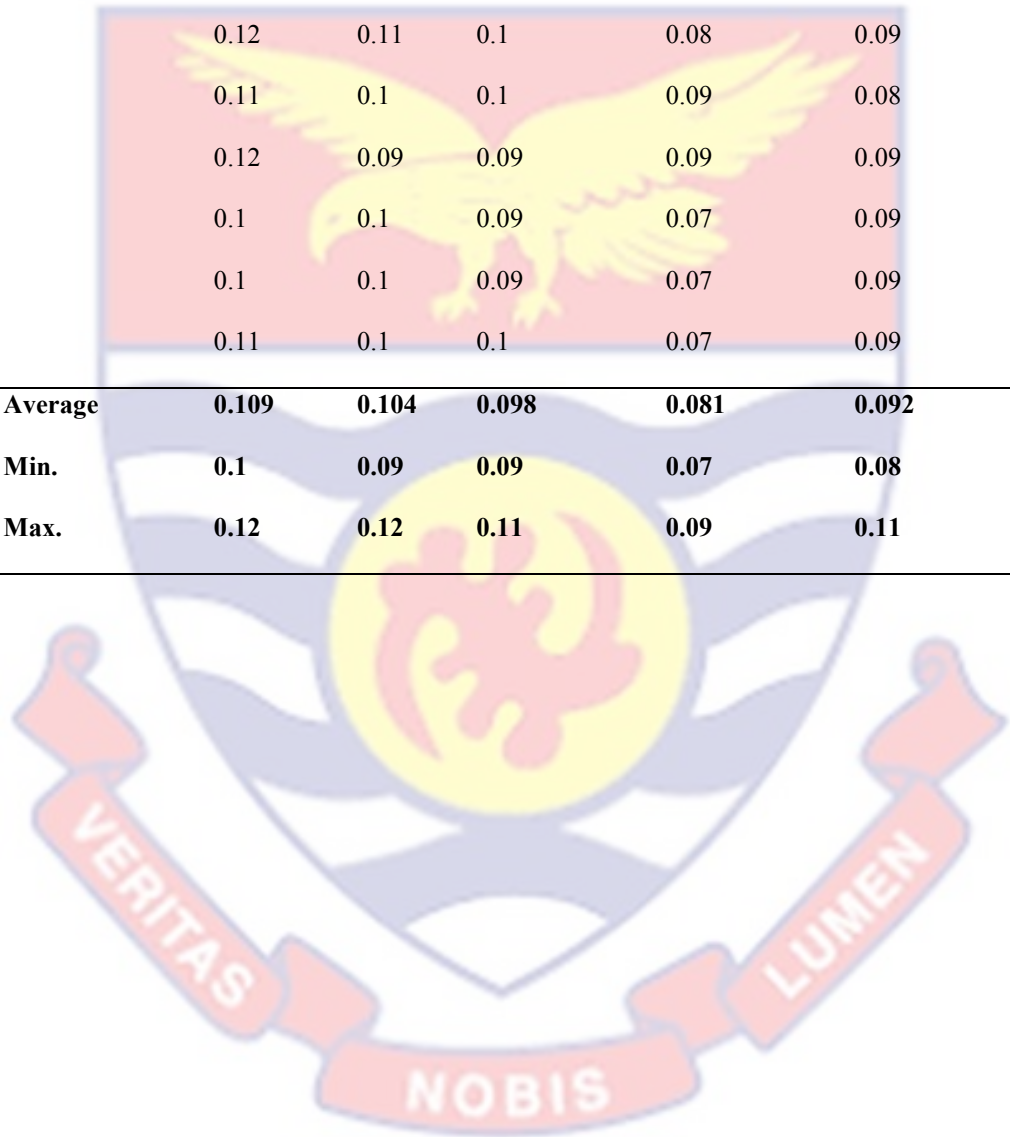
Appendix A5
Activity concentration of ^{238}U in soil.

COMMUNITY	SAMPLE		AVERAGE
	1ST	2ND	
ABH	8.99 ± 1.61	8.93 ± 1.48	8.96 ± 1.54
ABH 2	7.01 ± 0.42	5.49 ± 0.36	6.25 ± 0.39
ABH 3	9.11 ± 1.45	9.53 ± 1.35	9.32 ± 1.40
ALIS	4.52 ± 0.66	3.78 ± 0.38	4.15 ± 0.62
Axim Castle	13.41 ± 1.10	12.39 ± 1.04	12.90 ±1.07
Krisan 1	1.52 ± 0.30	1.68 ± 0.42	1.60 ± 0.36
Krisan 2	14.01 ± 1.90	14.46 ± 2.37	14.45 ± 2.17
Krisan 3	12.84 ± 1.79	12.58 ± 2.03	12.71 ± 1.91
Beyin 1	12.96 ± 4.31	13.80 ± 6.61	13.38 ±5.36
Beyin 2	3.11 ± 0.19	3.37 ± 0.23	3.24 ± 0.21
Ellonyi	23.10 ± 1.52	19.58 ± 1.38	21.34 ± 1.40
Kengen 1	5.86 ± 0.90	5.98 ± 0.72	5.92 ± 0.81
Kengen 2	8.12 ± 0.40	7.68 ± 0.30	7.90 ± 0.35
Twenen	5.31 ± 0.77	5.09 ± 0.79	5.20 ± 0.78
Nyale Kplole	8.83 ± 1.97	9.09 ± 2.01	8.96 ±1.99
Nyale Kplole 2	4.40 ± 0.28	4.84 ± 0.34	4.62 ± 0.31
Nyale Kplole 3	9.46 ± 2.50	9.06 ± 2.16	9.26 ± 2.33
Anokyi 1	8.63 ± 1.02	9.11 ± 1.24	8.87 ± 1.13
Anokyi 2	4.40 ±0.63	4.72 ± 0.59	4.56 ± 0.61
Atuabo 2	13.24 ± 0.19	14.66 ± 0.29	13.95 ± 0.24
Kikam	10.81 ± 0.17	10.57 ± 0.13	10.69 ± 0.15
Half-Assini 1	8.24 ± 0.75	8.48 ±0.87	8.36 ± 0.81
Half-Assini 2	5.49 ± 0.83	5.69 ± 0.85	5.59 ± 0.84
Half-Assini 3	5.81 ± 0.87	6.35 ± 0.95	6.08 ± 0.91
Half-Assini 4	8.86 ± 2.19	9.24 ± 2.45	9.05 ± 2.32
Newtown	7.71 ± 0.44	7.19 ± 0.30	7.45 ± 0.37

Appendix A6
Activity concentration of ^{232}Th in soil.

COMMUNITY	SAMPLE		AVERAGE
	1ST	2ND	
ABH	10.04 ± 1.20	8.20 ± 1.12	9.12 ±1.16
ABH 2	17.51 ± 1.48	21.77 ± 1.64	19.64 ±1.56
ABH 3	10.24 ± 1.49	9.98 ± 1.55	10.11±1.52
ALIS	6.45 ± 0.87	5.99 ± 0.99	6.22 ± 0.93
Axim Castle	7.81 ± 1.65	8.31 ± 1.35	8.06 ± 1.50
Krisan 1	2.93 ± 0.20	3.25 ± 0.40	3.09 ± 0.30
Krisan 2	16.11 ± 2.22	16.47 ± 2.78	16.34 ± 2.45
Krisan 3	9.01 ± 1.19	7.25 ± 1.25	8.13 ± 1.22
Beyin 1	28.37 ± 2.61	31.13 ± 3.03	29.75 ± 2.82
Beyin 2	2.90 ± 0.25	3.12 ± 0.23	3.01 ± 0.24
Ellonyi	24.70 1.10	27.36 ± 0.86	26.03 ±0.98
Kengen 1	16.32 ± 2.07	14.00 ± 1.69	15.16 ± 1.88
Kengen 2	3.57 ± 0.28	4.05 ± 0.44	3.81 ± 0.36
Twenen	7.51 ± 1.10	7.35 ± 1.12	7.43 ± 1.11
Nyale Kplole	34.18 ± 2.26	31.16 ± 1.52	32.24 ± 1.84
Nyale Kplole 2	4.13 ± 0.38	3.55 ± 0.24	3.84 ± 0.31
Nyale Kplole 3	18.06 ± 1.17	20.42 ± 1.23	19.24 ±1.20
Anokyi 1	19.13 ± 2.75	15.11 ± 2.13	17.12 ± 2.44
Anokyi 2	23.31 ± 1.69	17.02 ± 1.55	20.33± 1.62
Atuabo 2	11.98 ± 0.31	13.84 ± 0.19	12.91 ± 0.25
Kikam	16.04 ± 1.21	19.28 ± 0.63	17.66 ± 0.92
Half-Assini 1	6.38 ± 0.64	6.72 ± 0.90	6.55 ± 0.77
Half-Assini 2	2.56 ± 0.44	3.00 ± 0.40	2.78 ± 0.42
Half-Assini 3	7.84 ± 1.37	10.70 ± 1.41	9.27 ± 1.39
Half-Assini 4	4.57 ± 1.76	7.45 ± 2.14	6.01 ±1.95
Newtown	12.79 ± 1.30	9.91 ± 1.60	11.35 ± 1.45

Appendix A7
Activity concentration of ^{40}K in soil

COMMUNITY	SAMPLE		
	1ST	2ND	AVERAGE
ABH	275. 08 ± 41.	321.46 ± 47.81	298.27 ± 44.74
ABH 2	242.72 ± 39.21	210.62 ± 28.71	226.41 ± 33.96
ABH 3	313.10 ± 43.78	290.12 ± 46.70	301.61 ± 45.24
ALIS	115.24 ± 17.54	149.06 ± 20.10	132.15 ± 18.82
Axim Castle	361.43 ± 60.14	344.31 ± 45.71	352.87 ± 52.93
Krisan 1	109.66 ± 1.73	139.20 ± 1.23	124.43 +1.48
Krisan 2	251.82 ± 41.29	275.00 ± 37.01	263.41 ± 39.15
Krisan 3	126.05 ± 17.92	142.47 ± 22.36	134.26 ± 20.14
Beyin 1	182.43 ± 27.20	157.55 ± 23.80	169.99 ± 25.50
Beyin 2	136.24 ± 1.61	118.32 ± 0.97	127.28 ± 1.29
Ellonyi	138.71 ± 25.49	154.33 ± 18.47	146.52 ± 21.98
Kengen 1	154.80 ± 4.50	129.86 ± 3.92	142.33 ± 4.21
Kengen 2	117.67 ± 1.62	140.15 ± 1.04	128.91 ± 1.33
Twenen	204.13 ± 31.47	174.33 ± 24.81	189.23 ± 28.14
Nyale Kplole	326.92 ± 46.28	353.16 ± 55.74	340.04 ± 51.01
Nyale Kplole 2	147.75 ± 70.13	109.57 ± 52.65	128.66 ± 61.39
Nyale Kplole 3	251.48 ± 37.39	211.92 ± 32.13	231.70 ± 34.76
Anokyi 1	339.67 ± 17.15	368.33 ± 10.65	354 ± 13.90
Anokyi 2	284.93 ± 10.02	261.07 ± 4.80	273 ± 7.41
Atuabo 2	139.01 ± 0.48	133.59 ± 0.36	136.30 ± 0.42
Kikam	187.82 ± 10.12	238.18 ± 7.34	213 ± 8.73
Half-Assini 1	162.36 ± 3.49	185.64 ± 3.45	174 ± 3.47
Half-Assini 2	541.77 ± 84.36	513.49 ± 73.92	527.63 ± 79.14
Half-Assini 3	99.86 ± 2.02	121.26 ± 1.06	110.56 ± 1.54
Half-Assini 4	187.25 ± 27.84	222.15 ± 33.58	204.70 ± 30.71
Newtown	131.41 ± 1.19	139.55 ± 1.75	135.478 ± 1.47

209

Appendix A8
Activity concentration of ^{222}Rn in groundwater samples.

COMMUNITY	SAMPLE		AVERAGE
	1ST	2ND	
Axim 1	86 ± 9	95 ± 7	91 ± 8
ABH	85 ±12	81 ± 10	83 ± 11
ALIS	130 ± 15	134 ± 15	132 ± 15
Krisan	161 ± 12	185 ± 20	173 ± 17
Nyale Kplole 1	94 ± 10	82 ± 12	88 ± 11
Nyale Kplole 2	60 ± 11	52 ± 13	56 ± 12
Nyale Kplole 3	68 ±5	82 ± 9	75 ± 7
Atuabo 1	30 ± 4	40 ± 6	35 ± 5
Atuabo 2	39 ± 5	47 ± 9	43 ± 7
Ekebaku	190 ± 27	164 ± 17	177 ± 22
Beyin 1	149 ± 15	162 ± 13	156 ± 14
Beyin 2	115 ± 14	121 ± 16	118 ± 15
Kikam	62 ± 3	72 ± 9	67 ± 6
Kengen 1	90 ± 10	98 ± 15	94 ± 13
Kengen 2	73 ± 5	69 ± 5	71 ± 5
Anokyi	58 ± 8	46 ± 4	52 ± 6
Twenen	57 ± 6	67 ± 8	62 ± 7
Half-Assini 1	76 ± 10	82 ± 14	79 ± 12
Half-Assini 2	43 ± 7	57 ± 15	50 ± 11
Half-Assini 3	91 ± 5	107 ± 11	99 ± 8

Appendix A9
Activity concentration of ^{226}Ra in groundwater samples.

COMMUNITY	SAMPLE		AVERAGE
	1ST	2ND	
Axim 1	0.21 ± 0.05	0.27 ± 0.07	0.24 ± 0.06
ABH	0.76 ± 0.03	0.88 ± 0.03	0.82 ± 0.03
ALIS	0.28 ± 0.01	0.42 ± 0.03	0.35 ± 0.02
Krisan	1.40 ± 0.20	1.36 ± 0.24	1.38 ± 0.22
Nyale Kplole 1	0.62 ± 0.04	0.50 ± 0.01	0.56 ± 0.03
Nyale Kplole 2	0.15 ± 0.01	0.21 ± 0.01	0.18 ± 0.01
Nyale Kplole 3	0.33 ± 0.01	0.39 ± 0.03	0.36 ± 0.02
Atuabo 1	0.23 ± 0.01	0.27 ± 0.01	0.25 ± 0.01
Atuabo 2	0.40 ± 0.05	0.52 ± 0.09	0.46 ± 0.07
Ekebaku	0.12 ± 0.01	0.16 ± 0.01	0.14 ± 0.01
Beyin 1	0.36 ± 0.05	0.38 ± 0.07	0.37 ± 0.06
Beyin 2	0.17 ± 0.01	0.13 ± 0.01	0.15 ± 0.01
Kikam	0.67 ± 0.02	0.56 ± 0.02	0.61 ± 0.02
Kengen 1	1.08 ± 0.09	1.17 ± 0.15	1.13 ± 0.12
Kengen 2	0.25 ± 0.03	0.19 ± 0.05	0.22 ± 0.04
Anokyi	0.70 ± 0.06	0.76 ± 0.11	0.73 ± 0.08
Twenen	0.22 ± 0.02	0.20 ± 0.02	0.21 ± 0.02
Half-Assini 1	1.61 ± 0.34	1.63 ± 0.26	1.62 ± 0.30
Half-Assini 2	0.13 ± 0.01	0.19 ± 0.01	0.16 ± 0.01
Half-Assini 3	0.99 ± 0.07	1.07 ± 0.09	1.03 ± 0.08

Appendix A10
Activity concentration of ^{228}Ra in groundwater samples

COMMUNITY	SAMPLE		AVERAGE
	1ST	2ND	
Axim 1	0.57 ± 0.09	0.51 ± 0.13	0.54 ± 0.11
ABH	0.66 ± 0.02	0.80 ± 0.02	0.73 ± 0.02
ALIS	0.84 ± 0.02	0.92 ± 0.02	0.88 ± 0.02
Krisan	1.09 ± 0.17	1.15 ± 0.23	1.12 ± 0.20
Nyale Kplole 1	0.90 ± 0.02	1.00 ± 0.02	0.95 ± 0.02
Nyale Kplole 2	0.79 ± 0.02	0.91 ± 0.04	0.85 ± 0.03
Nyale Kplole 3	0.81 ± 0.05	0.75 ± 0.07	0.78 ± 0.06
Atuabo 1	1.36 ± 0.20	1. 48 ± 0.22	1.42 ± 0.21
Atuabo 2	0.83 ± 0.16	0.95 ± 0.20	0.89 ± 0.18
Ekebaku	1.10 ± 0.04	0.94 ± 0.02	1.02 ± 0.03
Beyin 1	1.35 ± 0.15	1.51 ± 0.21	1.41 ± 0.18
Beyin 2	0.16 ± 0.01	0.22 ± 0.03	0.19 ± 0.02
Kikam	0.34 ± 0.03	0.40 ± 0.05	0.37 ± 0.04
Kengen 1	0.73 ± 0.02	0.85 ± 0.02	0.79 ± 0.02
Kengen 2	0.40 ± 0.06	0.46 ± 0.04	0.43 ± 0.05
Anokyi	1.03 ± 0.11	0.93 ± 0.09	0.98 ± 0.10
Twenen	0.17 ± 0.01	0.19 ± 0.01	0.18 ± 0.01
Half-Assini 1	1.29 ± 0.16	1.43 ± 0.24	1.36 ± 0.20
Half-Assini 2	0.72 ± 0.07	0.76 ± 0.09	0.74 ± 0.08
Half-Assini 3	1.26 ± 0.25	1.14 ± 0.19	1.20 ± 0.22

Appendix A11
Activity concentration of ^{40}K in groundwater samples.

COMMUNITY	SAMPLE		AVERAGE
	1ST	2ND	
Axim 1	3.36 ± 0.56	3.74 ± 0.60	3.55 ± 0.58
ABH	1.14 ± 0.12	0.90 ± 0.08	1.02 ± 0.10
ALIS	3.84 ± 0.11	4.00 ± 0.09	3.92 ± 0.10
Krisan	4.67 ± 0.49	4.81 ± 0.55	4.74 ± 0.52
Nyale Kplole 1	2.91 ± 0.23	3.15 ± 0.21	3.03 ± 0.22
Nyale Kplole 2	0.98 ± 0.12	0.86 ± 0.08	0.92 ± 0.10
Nyale Kplole 3	3.80 ± 0.10	3.96 ± 0.08	3.88 ± 0.09
Atuabo 1	2.30 ± 0.18	2.34 ± 0.10	2.32 ± 0.14
Atuabo 2	1.45 ± 0.19	1.39 ± 0.11	1.42 ± 0.15
Ekebaku	5.83 ± 0.06	6.11 ± 0.14	5.92 ± 0.10
Beyin 1	4.70 ± 0.24	4.58 ± 0.17	4.64 ± 0.21
Beyin 2	0.90 ± 0.15	0.66 ± 0.09	0.78 ± 0.12
Kikam	2.54 ± 0.10	2.68 ± 0.08	2.61 ± 0.09
Kengen 1	1.33 ± 0.10	1.41 ± 0.12	1.37 ± 0.11
Kengen 2	0.93 ± 0.20	0.75 ± 0.10	0.84 ± 0.15
Anokyi	2.19 ± 0.03	2.47 ± 0.07	2.33 ± 0.05
Twenen	0.50 ± 0.03	0.42 ± 0.01	0.46 ± 0.02
Half-Assini 1	0.59 ± 0.02	0.77 ± 0.02	0.68 ± 0.02
Half-Assini 2	4.02 ± 0.09	3.68 ± 0.07	3.85 ± 0.08
Half-Assini 3	1.77 ± 0.03	1.91 ± 0.07	1.84 ± 0.05

Appendix A12
Certificate of Standards used for Calibration of Gamma Spectrometry System
(Geometry Reference Source).

Source no. :   NW 146

Drawing: VZ – 1520/20

Volume: approximately 1000ml

Density: approximately $1.0g/cm^3$

Construction: The radionuclide mixture is homogeneously

incorporated in the matrix of the source.

Nuclide	Gamma-ray energy (MeV)	Activity	Emission rate (s^{-1})
Americium-241	0.060	2.97E03	1.06E03
Cadmiun-109	0.088	1.69E04	6.14E03
Cobalt-57	0.122	8.84E02	7.57E02
Cerium-139	0.166	9.66E02	7.71E02
Mercury-203	0.279	2.56E03	2.09E03
Tin-113	0.392	3.18E03	2.07E03
Strontium-85	0.514	3.89E03	3.83E03
Caecium-137	0.662	2.78E03	2.36E03
Yitrium-88	0.898	6.62E03	6.22E03
Cobalt-60	1.173	3.40E03	3.40E03
Cobalt-60	1.333	3.40E03	3.40E03
Yitrium-88	1.836	6.62E03	6.57E03

Reference date: 1st February, 2006 at 12.00 GMT

214

Appendix A13

Correlation matrix for the physicochemical parameters in groundwater.

	Te	Ko	Sal	pH	TDS	Feg	Pbg	Cdg	Zng	Mng	Nig
Te	1.000										
Ko	-0.132	1.000									
Sal	-0.056	0.853	1.000								
pH	-0.348	0.616	0.422	1.000							
TDS	-0.112	0.997	0.859	0.600	1.000						
Feg	-0.254	0.168	0.121	0.193	0.168	1.000					
Pbg	0.081	0.280	-0.042	0.047	0.290	0.373	1.000				
Cdg	0.335	0.117	0.274	0.278	0.124	0.307	-0.120	1.000			
Zng	0.190	0.360	0.454	0.052	0.370	0.280	-0.016	0.045	1.000		
Mng	0.240	0.172	-0.096	0.197	0.175	-0.226	-0.011	-0.152	-0.051	1.000	
Nig	0.012	-0.273	-0.185	-0.189	-0.320	-0.145	-0.102	-0.108	-0.258	-0.282	1.000

APPENDIX B

FIGURES

Appendix B1
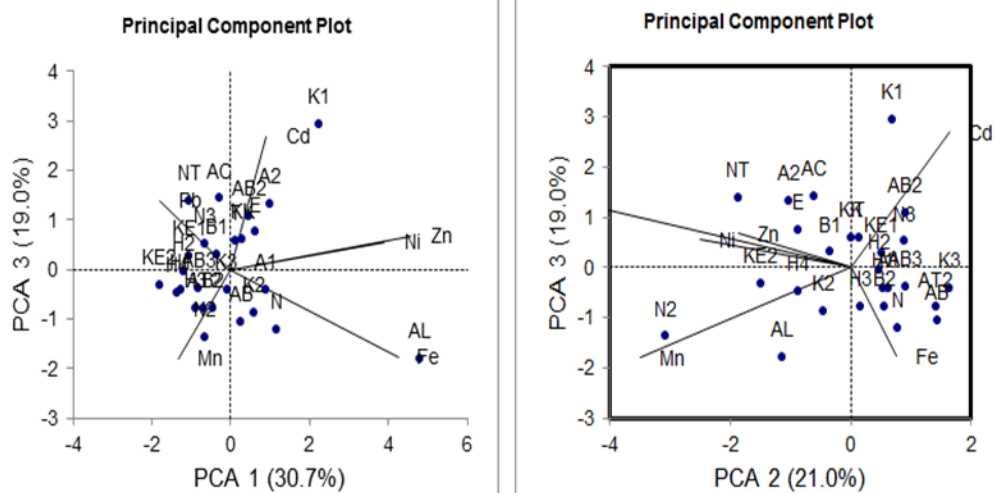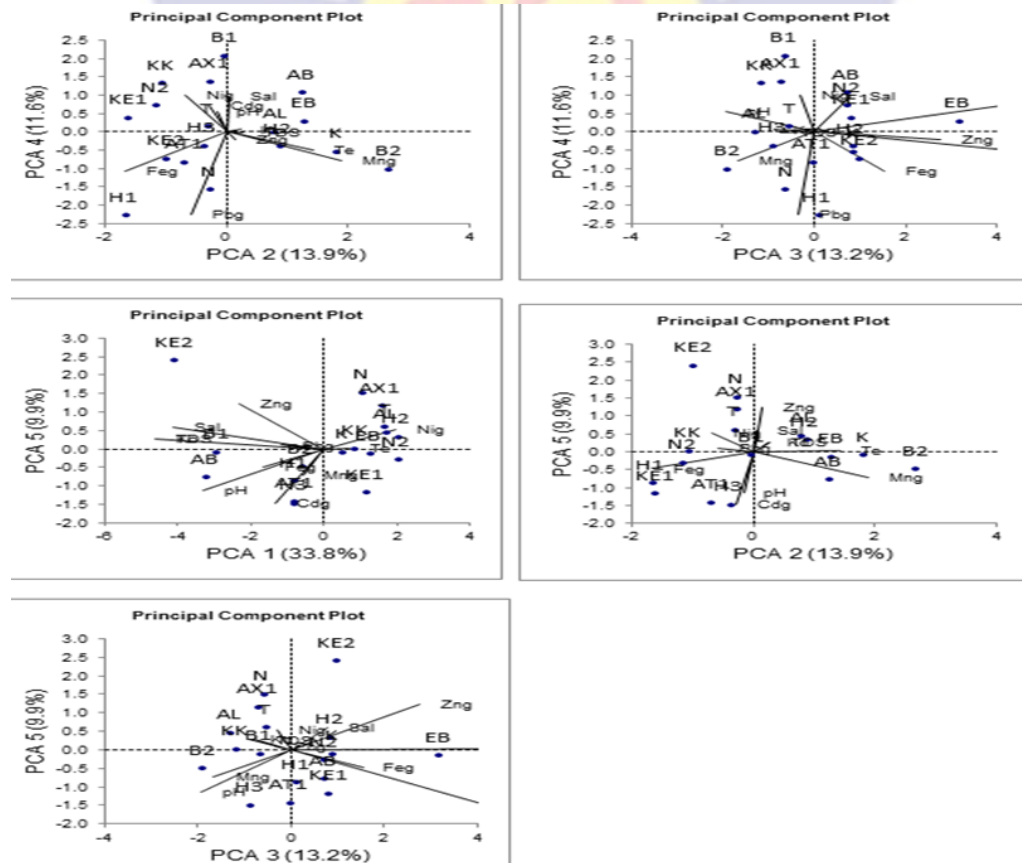PCA biplot for PC1 & PC3, and PC2 & PC3 soil samples

Figure 41: PCA biplot for PC2&PC4, PC3&PC4, PC1&PC5, PC2&PC5 and PC3&PC5 groundwater

APPENDIX C

```
classdef ActivitySim < handle
   %ActivitySim Simulates concentrations of radio nuclides
   %   This script gives a graphical simulation of three radio nuclides:
   %   U-238, Th-232, and K-40.
   %   over variable length of years


   % UI Properties
   properties(Access = 'private')
      wndMainDialog;
      hFigure;
   end

   % User Properties
   properties(Access = 'private')
      file;
      idxU     = 1;
      idxTh    = 2;
      idxK     = 3;

      tStart   = 0;
      tEnd     = 0;
      tStep    = 0;

      cDecay   = [
               .000000000000000049160
               .000000000046056
               .00000000053319
               ];

      selections = [];
   end

   methods
      function obj = ActivitySim
         createGUI(obj);
         if nargout == 0
            clear obj;
         end
      end

      function delete(obj)
         %delete(obj.hFigure);
         delete(obj.wndMainDialog);
      end
   end


   methods(Access = 'private')
      function createGUI(obj)
         obj.wndMainDialog = dialog;
         obj.wndMainDialog.Name = 'Activity Graph';
         obj.wndMainDialog.WindowStyle = 'Normal';
         obj.wndMainDialog.Position = [0 0 700 450];
         obj.wndMainDialog.Visible = 'off';

         %[+]   Major container in figure
```

217

```matlab
tp = uitabgroup(obj.wndMainDialog, 'Units', 'pixels');
tp.Position = [15 60 670 375];
   %[+]    General
   tabGen = uitab(tp, 'Title', 'General');

     %[+]    Group left
     gPan = uipanel(tabGen, 'Units', 'pixels');
     gPan.BorderType = 'etchedout';
     gPan.Position = [10 10 200 325];

        %[+]    File
        uipf = uipanel(gPan);
        uipf.Units = 'pixels';
        uipf.Title = 'Data File';
        uipf.Position = [10 260 180 60];

           %[-]    ...
           uicontrol(uipf, ...
           'Style','edit',...
           'Enable', 'off', ...
           'Tag', 'lblFileDisp', ...
           'HorizontalAlignment','left',...
           'Position',  [8 10 125 25]);

           %[-]    ...
           uicontrol(uipf, ...
           'Style', 'pushbutton', ...
           'String', '...', ...
           'Tag', 'btnOpenFile', ...
           'Callback', @obj.onFileSearch,...
           'Position', [140 10 30 25]);

        %[+]    Map file columns
        uimf = uipanel(gPan);
        uimf.Units = 'pixels';
        uimf.Tag = 'fileColumn';
        uimf.Position = [10 142 180 120];

           %[-]    ...
           uicontrol(uimf,...
           'Style', 'checkbox',...
           'String','Set data column indices',...
           'Tag','rbnEnableIdx',...
           'Callback', @obj.onchangeidx,...
           'Position', [10 90 180 25]);

           %[-]    ...
           uicontrol(uimf,...
           'Style','text',...
           'String', 'Uranium-238',...
           'Enable','off',...
           'Tag','lblUranium',...
           'HorizontalAlignment', 'right',...
           'Position', [5 55 100 25]);

           %[-]    ...
           uicontrol(uimf,...
           'Style','text',...
           'String','Thorium-232',...
```

218

```
'Enable', 'off',...
'Tag','lblThorium',...
'HorizontalAlignment','right',...
'Position',[5 30 100 25]);

%[-]    ...
uicontrol(uimf,...
'Style', 'text',...
'String', 'Potasium-40',...
'Enable', 'off',...
'Tag', 'lblPotasium',...
'HorizontalAlignment', 'right',...
'Position', [5 5 100 25]);

%[-]    /...
uicontrol(uimf,...
'Style','edit',...
'String', obj.idxU,...
'Tag', 'txfUranium',...
'Enable', 'off',...
'Callback', @obj.u238,...
'HorizontalAlignment', 'right',...
'Position', [120 55 50 25]);

%[-]    /...
uicontrol(uimf,...
'Style','edit',...
'String', obj.idxTh,...
'Tag', 'txfThorium',...
'Enable', 'off',...
'Callback', @obj.th232,...
'HorizontalAlignment', 'right',...
'Position', [120 30 50 25]);

%[-]    /...
uicontrol(uimf,...
'Style', 'edit',...
'String', obj.idxK,...
'Tag', 'txfPotasium',...
'Enable', 'off',...
'Callback', @obj.k40,...
'HorizontalAlignment', 'right',...
'Position',[120 5 50 25]);

%[+]    Period
uipp = uipanel(gPan);
uipp.Units = 'pixels';
uipp.Title = 'Period';
uipp.Position = [10 8 180 135];

%[-]    >
%uicontrol(uipp,...
%'String','Unit',...
%'HorizontalAlignment','right',...
%'Position',[10 90 20 25]);

%[-]    <
uicontrol(uipp,...
'Style', 'popup',...
```

219

```
            'Tag','popunit',...
            'String',{'Seconds','Minutes','Hours',...
            'Days','Months','Years'},...
            'Callback',@obj.changeformat,...
            'Position',[80 90 90 25]);

            %[-]    ...
            uicontrol(uipp,...
            'Style','text',...
            'String','Start',...
            'Tag','lblStartPeriod',...
            'HorizontalAlignment','right',...
            'Position',[5 55 100 25]);

            %[-]    ...
            uicontrol(uipp,...
            'Style','text',...
            'String', 'End',...
            'Tag','lblEndPeriod',...
            'HorizontalAlignment','right',...
            'Position',[5 30 100 25]);

            %[-]    ...
            uicontrol(uipp,...
            'Style','text',...
            'String','Step',...
            'Tag', 'lblStepPeriod',...
            'HorizontalAlignment', 'right',...
            'Position',[5 5 100 25]);

            %[-]   /...
            uicontrol(uipp,...
            'Style','edit',...
            'String',obj.tStart,...
            'Tag','txfStartPeriod',...
            'HorizontalAlignment','right',...
            'Callback', @obj.onStartFieldSet,...
            'Position',[120 55 50 25]);

            %[-]   /...
            uicontrol(uipp,...
            'Style','edit',...
            'String',obj.tEnd,...
            'Tag','txfEndPeriod',...
            'HorizontalAlignment', 'right',...
            'Callback', @obj.onEndFieldSet,...
            'Position',[120 30 50 25]);

            %[-]   /...
            uicontrol(uipp,...
            'Style', 'edit',...
            'String', obj.tStep,...
            'Tag','txfStepPeriod',...
            'HorizontalAlignment', 'right',...
            'Callback', @obj.onStepFieldSet,...
            'Position',[120 5 50 25]);

        %[+]    Group right
        oPan = uipanel(tabGen, 'Unit', 'pixels');
```

220

```
            oPan.BorderType = 'etchedout';
            oPan.Position = [220 10 435 325];

                %[-]    Table
                uitable(oPan, 'Unit', 'pixels',...
                'Enable', 'off',...
                'Tag','tblData',...
                'CellSelectionCallback', @obj.onTblItemSelected,...
                'Position',[10 10 415 305]);

            %[+]    Options
            %uitab(tp, 'Title', 'Options');

            %[-]    ?
            uicontrol(obj.wndMainDialog,...
            'Style','pushbutton',...
            'Enable','off',...
            'Tag','btnPlotGraph',...
            'String','Plot',...
            'Callback',@obj.onPlotBtn,...
            'Position',[475 15 100 30]);

            %[-]    ?
            uicontrol(obj.wndMainDialog,...
            'Style','pushbutton',...
            'Enable','off',...
            'Tag','btnClearSelection',...
            'String','Clear',...
            'Callback',@obj.onClearBtn,...
            'Position',[585 15 100 30]);

        obj.hFigure = figure;
        obj.hFigure.Visible = 'off';

        movegui(obj.wndMainDialog, 'center');
        obj.wndMainDialog.Visible = 'on';
    end
end

methods(Access = 'private')

    function is = paramsset(obj)
        is = obj.tStep > 0 && (obj.tEnd - obj.tStart)/obj.tStep >= 1;
    end

    function onFileSearch(obj, ~, ~)
        [f, p] = uigetfile(...
                {'*.xls; *.xlsx; *.xlsm; *.xltx; *.xltm', ...
                'Excel Files (.xls, .xlsx, .xlsm, .xltx, .xltm)'}, ...
                'Select Data File', obj.file);
        if isequal(p, 0) && isequal(f, 0)
            return;
        end
        obj.file = fullfile(p, f);
        try
            [dat, tx]= xlsread(obj.file);

            if ~isequal(dat,0)
```

221

```
            table = findobj(obj.wndMainDialog, 'Tag','tblData');
            table.Data = [dat(:, obj.idxU) dat(:, obj.idxTh) dat(:, obj.idxK)];
            %table.Position(3) = table.Extent(3);
            %table.Position(4) = table.Extent(4);
            table.Enable = 'on';

            lblFileName = findobj(obj.wndMainDialog, 'Tag','lblFileDisp');
            lblFileName.String = ['.../' f];

            if ~isequal(tx, 0)
                row = tx(:, 1); row = row(2:end);
                table.RowName = row;

                col = tx(1, :); col = col(2:end);
                table.ColumnName = col;
            end
        end
    catch ME
        errordlg(['Error: ' ME.message], 'File Error');
        return;
    end
end

function onTblItemSelected(obj, ~, eventdata)
    bclear = findobj(obj.wndMainDialog, 'Tag', 'btnClearSelection');
    bplot = findobj(obj.wndMainDialog, 'Tag', 'btnPlotGraph');
    sel = eventdata.Indices;
    obj.selections = unique(sel(:,1));
    if isempty(obj.selections)
        bplot.Enable = 'off';
        bclear.Enable = 'off';
    else
        bclear.Enable = 'on';

        if paramsset(obj)
            bplot.Enable = 'on';
        end
    end
end

function onStartFieldSet(obj, hHandle,~)
    input = str2double(hHandle.String);
    if isnan(input)
        hHandle.String = obj.tStart;
    else
        obj.tStart = input;
        bplot = findobj(obj.wndMainDialog, 'Tag', 'btnPlotGraph');
        if paramsset(obj) && ~isempty(obj.selections)
            bplot.Enable = 'on';
        else
            bplot.Enable = 'off';
        end
    end
end

function onEndFieldSet(obj, hHandle,~)
    input = str2double(hHandle.String);
    if isnan(input)
        hHandle.String = obj.tEnd;
```

222

```
      else
         obj.tEnd = input;
         bplot = findobj(obj.wndMainDialog, 'Tag', 'btnPlotGraph');
         if paramsset(obj) && ~isempty(obj.selections)
            bplot.Enable = 'on';
         else
            bplot.Enable = 'off';
         end
      end
end

function onStepFieldSet(obj, hHandle,~)
   input = str2double(hHandle.String);
   if isnan(input)
      hHandle.String = obj.tStep;
   else
      obj.tStep = input;
      bplot = findobj(obj.wndMainDialog, 'Tag', 'btnPlotGraph');
      if paramsset(obj) && ~isempty(obj.selections)
         bplot.Enable = 'on';
      else
         bplot.Enable = 'off';
      end
   end
end

function u238(obj, hHandle,~)
   input = str2double(hHandle.String);
   if isnan(input)
      hHandle.String = obj.idxU;
   else
      obj.idxU = input;
   end
end

function th232(obj, hHandle,~)
   input = str2double(hHandle.String);
   if isnan(input)
      hHandle.String = obj.idxTh;
   else
      obj.idxTh = input;
   end
end

function k40(obj, hHandle,~)
   input = str2double(hHandle.String);
   if isnan(input)
      hHandle.String = obj.idxK;
   else
      obj.idxK = input;
   end
end

function onchangeidx(obj, hHndl, ~)
   uip = findobj(obj.wndMainDialog,'Tag','fileColumn');
   c = setdiff(uip.Children,hHndl);

   if hHndl.Value == hHndl.Max
      for i=1:length(c)
```

223

```
          c(i).Enable = 'on';
      end
   else
      for i=1:length(c)
          c(i).Enable = 'off';
      end
   end
end

function onClearBtn(obj, ~, ~)
   tbl = findobj(obj.wndMainDialog,'Tag','tblData');
   obj.selections = [];
   dat = tbl.Data;
   tbl.Data = [];
   tbl.Data = dat;
end

function changeformat(~,~,~)
   %{
   str = hHndl.String;

   switch str{hHndl.Value}
      %u238 = 4.51x10^9
      %th232 = 1.41x10^10
      %k40 = 1.251x10^9
      case 'Seconds'
          obj.cDecay(1) = 1;
          obj.cDecay(2) = 2;
          obj.cDecay(3) = 1;

      case 'Minutes'
          obj.cDecay(1) = 1;
          obj.cDecay(2) = 2;
          obj.cDecay(3) = 1;

      case 'Hours'
          obj.cDecay(1) = 1;
          obj.cDecay(2) = 2;
          obj.cDecay(3) = 1;

      case 'Days'
          obj.cDecay(1) = 1;
          obj.cDecay(2) = 2;
          obj.cDecay(3) = 1;

      case 'Months'
          obj.cDecay(1) = 1;
          obj.cDecay(2) = 2;
          obj.cDecay(3) = 1;

      case 'Years'
          obj.cDecay(1) = 1;
          obj.cDecay(2) = 2;
          obj.cDecay(3) = 1;

   end
   %}
end
```
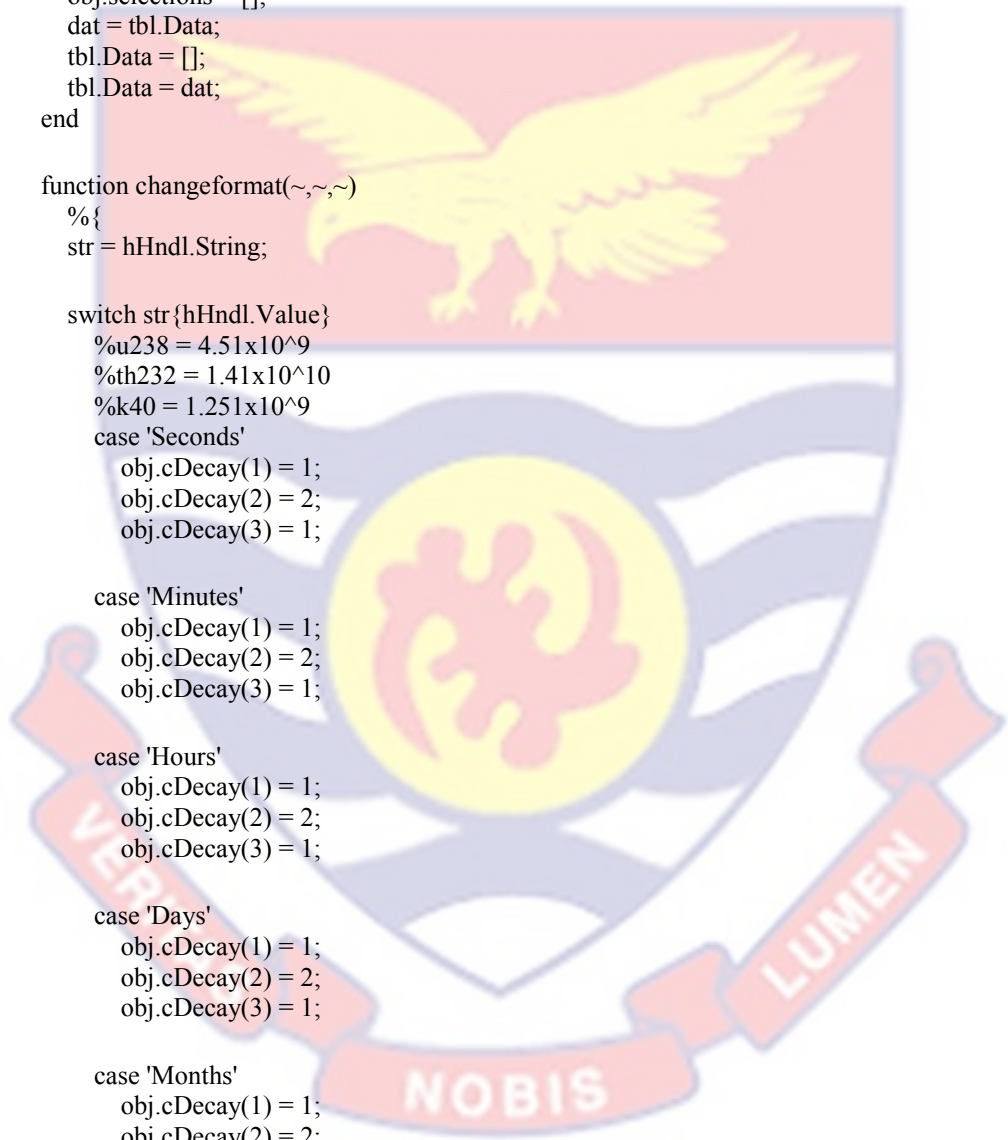
224

```matlab
function onPlotBtn(obj, ~, ~)
    % assumed that the condition below is met, since the 'Plot'
    % button is only enabled to receive inputs when these
    % conditions are met.
    %{
    if isempty(obj.selections) || ...
            ~paramsset(obj)
        return;
    end
    %}
    time = obj.tStart:obj.tStep:obj.tEnd;
    tbl = findobj('Tag','tblData');
    wData = tbl.Data;

    data = wData(obj.selections,:);

    [r,~] = size(data);
    if r == 1
        fu238  = expxxx(obj.cDecay(1)).*data(1,obj.idxU);
        fth232 = expxxx(obj.cDecay(2)).*data(1,obj.idxTh);
        fk40   = expxxx(obj.cDecay(3)).*data(1,obj.idxK);
        %{
        if ~isempty(obj.hFigure)
            close(obj.hFigure(1));
        end
        %}
        obj.hFigure = 1;
        figure(obj.hFigure);
        fig = gcf;
        fig.NumberTitle = 'off';

        plot(time, fu238, time, fth232, time, fk40);
        meas = findobj('Tag','popunit');
        str = meas.String;

        rn = tbl.RowName;
        if ~isempty(rn)
            if ~isempty(rn(1))
                title(['Simulation of Concentrations '...
                    'of U238, Th-232 and K-40 for' rn(obj.selections(1))]);
            end
        end

        legend('U-238','Th-232','K-40');
        xlabel(['Time (' str{meas.Value} ')']);
        ylabel('Concentration');

    else
        msgbox('Request is yet to be implemented');
    end


    function e = expxxx(hlf)
        x = time.*hlf;
        e = exp(-x);
    end
    end
  end
end
```

225

APPENDIX D

PUBLICATIONS

ELSEVIER

Spatial distribution, accumulation and human health risk assessment of heavy metals in soil and groundwater of the Tano Basin, Ghana

Israel Doyi[a,b,c], David Essumang[b], Gustav Gbeddy[c,d,*], Samuel Dampare[c], Elliot Kumassah[e], David Saka[c]

[a] Department of Environmental Sciences, Faculty of Science and Engineering, Macquarie University, Sydney, NSW 2109, Australia
[b] Department of Chemistry, School of Physical Sciences, University of Cape Coast, Ghana
[c] Ghana Atomic Energy Commission, P. O. Box LG 80, Kwabenya, Accra, Ghana
[d] Civil Engineering and Built Environment (CEBE), Queensland University of Technology (QUT), GPO Box 2434, Brisbane 4001, Queensland, Australia
[e] Department of Teacher Education, P. O. Box 1181, University of Ghana, Legon, Accra, Ghana

ARTICLE INFO

ABSTRACT

Soil serves as a vast matrix for heavy metal accumulation and subsequent redistribution to critical aspects of the environment such as groundwater. Soil pollution study is essential for sustainable human health and ecosystem protection. This study provides vital insight into the fate, accumulation, interactions, and health risk posed by heavy metals in soil and groundwater by employing geochemical accumulation index (Igeo), risk assessment models and multivariate data analysis techniques such as principal component analysis (PCA), preference ranking organisation method for enrichment evaluation (PROMETHEE) and geometrical analysis for interactive aid (GAIA). The median I_{geo} estimates show moderate to strong Pb accumulation levels whilst all the other metals indicate uncontaminated to moderate levels. The PCA output point to anthropogenic origin of Pb and Cd in the Tano Basin and surrounding communities. PROMETHEE-GAIA results indicate that Pb, Cd, Zn and Fe accumulated in the soil matrix may potentially leach into the groundwater resources. The carcinogenic lifetime risks posed by Pb, Cd, and Ni metals to adults are within the tolerable acceptable risk and thus do not present an immediate danger in the study area. Due to the significant toxicity, bioaccumulation and biomagnification properties of Pb and Cd in the environment, areas associated with significant anthropogenic activities require regular monitoring and evaluation in order to ensure that these metals are consistently below the regulatory limits. This study has further elucidated the subject of heavy metal pollution and is therefore expected to enhance sustainable protection of the environment and human health.

1. Introduction

Soil is a critical repository for numerous deleterious pollutants thereby serving as a good matrix for assessing the status quo of environmental pollution. These accumulated pollutants can then be redistributed to other compartments of the environment via the influence of anthropogenic and natural factors such as wind, vehicular movement and gravity (Gbeddy et al., 2018). Organisms especially human beings are subsequently exposed to the pollutants through dermal contact, inhalation and ingestion processes. In this context, heavy metals laden in soil pose significant health challenges due to their high toxicity, bioaccumulation and biomagnification properties (Lin et al., 2012; Wuana and Okieimen, 2011). Heavy metals may percolate into the underlining groundwater resources (Ghosh and Singh, 2005) thereby

creating further challenges to water quality and sustainable water supply. Accordingly, Lin et al. (2012) noted that heavy metal pollution is a crucial global problem and therefore, merits continuous investigation in order to provide an up-to-date information required for successful risk mitigation.

Heavy metals emanate from myriad of sources in the environment including industrial waste, spillage of petrochemicals, fertilizer application, atmospheric deposition and mine tailings (Wuana and Okieimen, 2011). Areas associated with significant oil and gas exploration and drilling activities are therefore, most likely to experience challenges with heavy metals due to the generation and release of produced water and solid wastes contaminated with heavy metals (Christie, 2012; Namdari et al., 2017). The Tano Basin in Ghana is one such area with high level of commercial oil and gas industry since 2007

226

Soil-to-cassava transfer of naturally occurring radionuclides from communities along Ghana's oil and gas rich Tano Basin

Israel Nutifafa Yawo Doyi[a,c,*], David Kofi Essumang[b], Asare Kwaku Agyapong[b], Samuel Asumadu-Sarkodie[c]

[a] Radioactive Waste Management Centre, Ghana Atomic Energy Commission, P. O. Box LG 80, Legon, Accra, Ghana
[b] Department of Chemistry, School of Physical Sciences, University of Cape Coast, Ghana
[c] Department of Environmental Sciences, Faculty of Science and Engineering, Macquarie University, Sydney, NSW 2109, Australia

ARTICLE INFO

ABSTRACT

Soil-to-plant transfer factor (TF) is widely used to assess the impact of soil radioactivity on agricultural crops. The root crop cassava (*Manihot esculenta*) provides 30%–50% of the calories consumed in Sub-Saharan Africa and is widely used in South America. γ-ray analysis was used to measure activity concentrations of ^{238}U, ^{232}Th, and ^{40}K in cassava root and soil. The TF values for ^{238}U, ^{232}Th, and ^{40}K were in the range 0.06–0.12, 0.01–0.10 and 0.04–0.28 respectively. The median transfer factors were 0.10 (^{238}U), 0.04 (^{232}Th) and 0.08 (^{40}K). For ^{238}U and ^{232}Th, the highest TF values were 0.12 and 0.10 respectively.

1. Introduction

Naturally occurring radioactive materials (NORMs) are found everywhere in the earth's crust and are present in very low concentrations (Doyi et al., 2013; UNSCEAR, 2000). Humans are continually being exposed to NORMs mainly through activities such as burning of fossil fuels, metal refining, manufacture and use of fertilizer (UNSCEAR, 2000) and natural processes like exhalation of radon gas to the atmosphere or by dissolving in groundwater (IAEA, 1999) or through the food chain (NRC, 1999).

Uptake of radionuclides by plants occurs both via the root system and from atmospheric deposition through activity trapping onto external plant surfaces (Vandenhove et al., 2009). The bioavailability of radionuclides in soils and hence their transfer to plants are rather complex, depending on several factors. These factors include the chemistry of the specific radionuclide, soil type and climatic conditions, soil pH, solid/liquid distribution coefficient, organic matter, plant genotype, and agronomic management (Chakraborty et al., 2013; Kabata-Pendias and Pendias, 1984; WHO & FAO, 2011; Malik et al., 2010). Some radionuclides mimic essential elements of plants such as potassium and calcium (James et al., 2011). Cassava, a root crop, exhibits greater root absorption of radioactivity than through the trapping onto external plant surfaces though there is some level of atmospheric capture (Asaduzzaman et al., 2014).

Cassava (*Manihot esculenta*) is native to South America and represents 30%–50% of all calories consumed in Sub-Saharan Africa (Long et al., 2017) and is the third most important source of calories in the tropics (FAO, 2008). There is a considerable range of soil types on which cassava

is grown worldwide. In Ghana, cassava production is estimated to exceed 15,000,000 Mt by 2015. Estimates put the yield of the crop at 48.7MT per hectare under rain-fed conditions. The edible root varies significantly in size from 15 to 100 cm as well as in weight from 0.5 to 2.0 kg (Amponsah, 2016). In addition to being the most consumed staple crop in the study area and several other communities, cassava is also used as raw material for the production of industrial starch, ethanol (biofuel) and animal feed (Adjei-Nsiah & Sakyi-Dawson, 2012).

The transfer factor (TF) expresses the plant's intake of radionuclides from the soil, and is commonly used in environmental transfer models estimating dose impact on humans (Chakraborty et al., 2013).

Studies of the soil-to-cassava TF of radionuclides are limited. These few studies were done in Australia, Brazil, India, Indonesia, Marshal Islands and Vietnam (IAEA-TECDOC-1616, 2009; Velasco et al., 2009) and Malaysia (Asaduzzaman et al., 2014). There has been no study on the characterization of TFs for the Ghanaian ecosystem for any crop. This study TFs of naturally occurring radionuclides from soil-to-cassava as an important tool for future modelling of the accumulation of ^{238}U, ^{232}Th and ^{40}K by the root crop.

2. Methodology

2.1. Study area

The coastal communities bordering the Tano Basin in Ghana were selected for this study due to the offshore oil and gas activities. Ghana is

227

SCIENTIFIC REPORTS

OPEN

Evaluation of radionuclides and decay simulation in a terrestrial environment for health risk assessment

I. N. Doyi[1,4], D. K. Essumang[2], S. B. Dampare[3], D. Duah[3] & A. F. Ahwireng[3]

This study is to assess the natural radioactivity level in soil samples in communities bordering the Tano Basin in Ghana. The radioactivity concentration of ^{238}U, ^{232}Th and ^{40}K have been determined using γ-ray spectrometry, moreover, the absorbed dose rates and annual effective dose were calculated. MATLAB R2013 script was written to simulate the decay of the radionuclides ^{238}U, ^{232}Th and ^{40}K using their respective half-lives. This is to determine the future impact of natural radionuclides and estimate future anthropogenic inputs. The level ^{238}U, ^{232}Th, and ^{40}K ranged from (1.60 to 21.3), (2.78 to 32.2) and (111 to 528) with average values of be 8.65 $Bqkg^{-1}$, 12.5 $Bqkg^{-1}$ and 214 $Bqkg^{-1}$ respectively in soil. The activity concentrations were lower than United Nations Scientific Committee on the Effects of Atomic Radiation guidelines for ^{238}U, ^{232}Th and ^{40}K. The absorbed dose rates and annual effective dose were found to be in range of 7.79 to 37.8 nGy h^{-1} and 9.56E + 00 to 4.64E + 01 μSvy^{-1} respectively. The overall annual effective dose was lower than the allowable limit of $1mSvy^{-1}$ set by International Commission on Radiological Protection H_{ex}, H_{in} and excess lifetime cancer risk (ELCR) were calculated and found to be within internationally recommended values.

Soil is not only a source of continuous radiation exposure to humans[1], it is also a medium of migration and transfer of radionuclides to biological systems[1,2]. Subsequently, soil can provide an indication of anthropogenic radiological contamination in the environment[1,3]. Soil radioactivity is also affected by man-made activities[4]. The evaluation of the radioactive components in soil is critical in understanding the behavior of radioactivity in the ecosystem, due to its impact on the total absorbed dose via ingestion, inhalation and external irradiation[5,6]. Yet, soil radioactivity studies largely focus on radiation protection and establishing baseline data for future radiation impact assessments[7]. They also estimate changes in environmental radioactivity caused by nuclear, industrial, and other human activities[8].

Natural radioactivity arises mainly from primordial radionuclides, such as potassium-40 (^{40}K) and the radionuclides from uranium-238 (^{238}U), thorium-232 (^{232}Th) series and their decay products, which are present at trace levels in all ground formations[9]. The amount of radioactivity in soil varies widely and significantly affects gamma radiation levels, which in turn can be used for the assessment of terrestrial gamma dose rates[10,11]. Natural radiation is the main source of radiation exposure in humans[12] and has led to studies of radiation levels, doses from natural radiation sources and its effects on health. Further, studying the distribution of radionuclides in the environment improves our understanding of radiation damage, and, therefore, is of great importance as a reference when standards and regulatory control actions on radiation protection are established[5,13,14].

The twelfth United Nations Development Programme Sustainable Development Goal (SDG) aims to achieve responsible consumption and production[15]. The SDG identifies proper disposal of toxic wastes and pollutants as a critical priority in achieving this overarching goal[15]. For instance, the disposal of toxic wastes from oil and gas drilling activities that contain radionuclides and trace metals should be an important target in achieving this goal

[1]National Radioactive Waste Management Centre, Ghana Atomic Energy Commission, P. O., Box LG 80, Legon-Accra, Ghana. [2]Department of Chemistry, School of Physical Sciences, University of Cape Coast, Cape Coast, Ghana. [3]Graduate School of Nuclear & Allied Sciences, Ghana Atomic Energy Commission, P. O. Box AE 1, Kwabenya-Accra, Ghana. [4]Department of Environmental Sciences, Faculty of Science and Engineering, Macquarie University, Sydney, NSW, 2109, Australia. Correspondence and requests for materials should be addressed to I.N.D. (email: i.doyi@gaecgh.org)

Technologically Enhanced Naturally Occurring Radioactive Materials (TENORM) in the Oil and Gas Industry: A Review

Israel Doyi, David Kofi Essumang, Samuel Dampare, and Eric Tetteh Glover

Contents

1   Introduction

Radiation is part of the natural environment: it is estimated that approximately 80 % of all human exposure comes from naturally occurring or background radiation. Certain extractive industries such as mining and oil logging have the potential to increase the risk of radiation exposure to the environment and humans by

I. Doyi (✉) • S. Dampare
National Radioactive Waste Management Centre, National Nuclear Research Institute, Ghana Atomic Energy Commission, Accra, Ghana
e-mail: i.doyi@gaecgh.org; dampee_2000@yahoo.com

D.K. Essumang
Graduate School of Nuclear and Allied Sciences, Ghana Atomic Energy Commission, Accra, Ghana
e-mail: kofiessumang@yahoo.com; dessumang@ucc.edu.gh

E.T. Glover
Department of Chemistry, University of Cape Coast, Cape Coast, Ghana
e-mail: e.glover@gaecgh.org